



PARIS
REINFORCE



PARIS
REINFORCE

20/09/2022

D4.4 Stakeholder-driven comparisons of national/sectoral strategies

WP4 – Robustification & Socio-Technical Analysis
Toolbox
Version: 1.00

www.paris-reinforce.eu



Disclaimer

The sole responsibility for the content of this publication lies with the authors. It does not necessarily reflect the opinion of the European Union. Neither the EASME nor the European Commission is responsible for any use that may be made of the information contained therein.

Copyright Message

This report, if not confidential, is licensed under a Creative Commons Attribution 4.0 International License (CC BY 4.0); a copy is available here: <https://creativecommons.org/licenses/by/4.0/>. You are free to share (copy and redistribute the material in any medium or format) and adapt (remix, transform, and build upon the material for any purpose, even commercially) under the following terms: (i) attribution (you must give appropriate credit, provide a link to the license, and indicate if changes were made; you may do so in any reasonable manner, but not in any way that suggests the licensor endorses you or your use); (ii) no additional restrictions (you may not apply legal terms or technological measures that legally restrict others from doing anything the license permits).

Grant Agreement Number	820846		Acronym	Paris Reinforce
Full Title	Delivering on the Paris Agreement: A demand-driven, integrated assessment modelling approach			
Topic	LC-CLA-01-2018			
Funding scheme	Horizon 2020, RIA – Research and Innovation Action			
Start Date	June 2019	Duration	42 Months	
Project URL	https://www.paris-reinforce.eu/			
EU Project Officer	Frederik Accoe			
Project Coordinator	National Technical University of Athens – NTUA			
Deliverable	D4.4 Stakeholder-driven comparisons of national/sectoral strategies			
Work Package	WP4			
Date of Delivery	Contractual	30/09/2022	Actual	20/09/2022
Nature	Report	Dissemination Level	Public	
Lead Beneficiary				
Responsible Author	Alexandros Nikas	Email	anikas@epu.ntua.gr	
	NTUA	Phone	+30 210 772 3612	
Contributors	Anastasios Karamaneas, Natasha Frilingou, Haris Doukas (NTUA); Georgios Xexakis (HOLISTIC)			
Reviewer(s):	Ben McWilliams (Bruegel); Lorenza Campagnolo (CMCC)			
Keywords	Fuzzy cognitive maps; co-creation; stakeholder-informed modelling; national mitigation pathways; Greece; Italy; Sustainable Development Goals			



EC Summary Requirements

1. Changes with respect to the DoA

No changes with respect to the work described in the DoA.

2. Dissemination and uptake

This deliverable is released publicly, available on the project website. It is intended as a reference point for the research community engaged in fuzzy modelling, featuring the documentation of the methodological novelties in the Fuzzy Cognitive Mapping (FCM) approach as well as of the In-Cognitive FCM design and simulation tool. It also aims to inform science and policy on climate change mitigation pathways for Greece and Italy that contribute to energy-sector sustainability in the light of the 2022 global energy crisis. Finally, it also aims to inform Integrated Assessment Modelling (IAM) scientists on gaps in model representation of Sustainable Development Goals (SDGs) and the added value of stakeholder insights for future model enhancements.

3. Short summary of results (<250 words)

This report first advances the theoretical background of FCMs, via methodological novelties that both ensure FCM model solution and integrate Monte Carlo for parametric uncertainty analysis (Section 1), and documents a new open-source FCM simulation tool (Appendix 5). The enhanced framework is then used in three case studies. The first study assesses the impact of selected strategies and important uncertainties on Italy's progress to energy-sector sustainability: experts appear to favour renewables over new gas infrastructure, finding them more robust against uncertainties, including regulatory/political instabilities (Section 2). The second study takes a broader view of the multi-faceted emergencies of our time (recession, pandemics, international conflict), aiming to capture modellers' and experts' perceptions of the impacts of such crises on SDG progress, considering models' existing/planned capacity and parametric uncertainty; we find that progress in SDGs 7, 8, 13 appears most prone to such emergencies and that expert perceptions of bigger and wider crisis propagation can meaningfully inform model developments, while modellers' perceptions may be biased based on their models' existing capacities (Section 3). The final application in Greece couples two energy system models to explore where Greece is headed given its current policies and uses FCMs to elicit critical bottlenecks from stakeholders; we project that the current framework can double gas use between 2022 and 2030, while an alternative, ambitious renewables and energy efficiency strategy can lead to zero Russian gas imports by 2026, highlighting however the need for an overall diversified supply mix and investments in new, costlier technologies (Section 4).









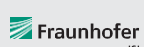









4. Evidence of accomplishment

This report, along with the five accompanying papers, published or currently under review (as reported in each Section), and the In-Cognitive tool that is available online on Github ([link](#)).



Preface

PARIS REINFORCE will develop a novel, demand-driven, IAM-oriented assessment framework for effectively supporting the design and assessment of climate policies in the European Union as well as in other major emitters and selected less emitting countries, in respect to the Paris Agreement. By engaging policymakers and scientists/modellers, PARIS REINFORCE will create the open-access and transparent data exchange platform I²AM PARIS, in order to support the effective implementation of Nationally Determined Contributions, the preparation of future action pledges, the development of 2050 decarbonisation strategies, and the reinforcement of the 2023 Global Stocktake. Finally, PARIS REINFORCE will introduce innovative integrative processes, in which IAMs are further coupled with well-established methodological frameworks, in order to improve the robustness of modelling outcomes against different types of uncertainties.

NTUA - National Technical University of Athens	GR	
BC3 - Basque Centre for Climate Change	ES	
Bruegel - Bruegel AISBL	BE	
Cambridge - University of Cambridge	UK	
CICERO - Cicero Senter Klimaforskning Stiftelse	NO	
CMCC - Fondazione Centro Euro-Mediterraneo sui Cambiamenti Climatici	IT	
E4SMA - Energy, Engineering, Economic and Environment Systems Modelling Analysis	IT	
EPFL - École polytechnique fédérale de Lausanne	CH	
Fraunhofer ISI - Fraunhofer Institute for Systems and Innovation Research	DE	
Grantham - Imperial College of Science Technology and Medicine - Grantham Institute	UK	
HOLISTIC - Holistic P.C.	GR	
IEECP - Institute for European Energy and Climate Policy Stichting	NL	
SEURECO - Société Européenne d'Economie SARL	FR	
CDS/UnB - Centre for Sustainable Development of the University of Brasilia	BR	
CUP - China University of Petroleum-Beijing	CN	
IEF-RAS - Institute of Economic Forecasting - Russian Academy of Sciences	RU	
IGES - Institute for Global Environmental Strategies	JP	
TERI - The Energy and Resources Institute	IN	



Executive Summary

Fuzzy Cognitive Maps (FCM) have recently gained ground in many engineering applications, mainly because they allow stakeholder engagement in reduced-form complex systems representation and modelling. They provide a pictorial form of systems, consisting of nodes (concepts) and node interconnections (weights), and perform system simulations for various input combinations. Due to their simplicity and quasi-quantitative nature, they can be easily used with and by non-experts. However, these features come with the price of ambiguity in output: recent literature indicates that changes in selected FCM parameters yield considerably different outcomes. Furthermore, it is not a priori known whether an FCM simulation would reach a fixed, unique final state (fixed point). There are cases where infinite, chaotic, or cyclic behaviour (non-convergence) hinders the inference process, and literature shows that the primary culprit lies in a parameter determining the steepness of the most common transfer functions, which determine the state vector of the system during FCM simulations. To address ambiguity in FCM outcomes, in Section 1 we propose a certain range for the value of this parameter, λ , which is dependent on the FCM layout, for the case of the log-sigmoid and hyperbolic tangent transfer functions. The analysis of this study is illustrated through a novel software application, *In-Cognitive* (see detailed documentation in Appendix 5), which allows non-experts to define the FCM layout via a Graphical User Interface and then perform FCM simulations given various inputs. The proposed methodology and developed software are validated against a real-world energy policy-related problem in Greece, drawn from the literature.

The new framework and tool are then used in three case studies.

1. Following Russia's invasion of Ukraine and amidst COVID-19 recovery efforts, the energy crisis has put enormous pressure to policymakers to balance climate action, sustainable development, and the need to mitigate the impacts of fuel supply disruptions and price shocks. Policy and market responses, such as liquefied natural gas infrastructure investments and use of every available fossil-fuel lever to make up for Russian gas supply cuts, are much debated and feared to trigger new lock-ins, jeopardising decarbonisation. This is also the case in Italy, which is highly dependent on Russia-imported gas. Quantitative systems modelling tools typically used to support such decisions take time to produce meaningful scenarios and, in times of crisis, are largely driven by highly uncertain parameters. In Section 2, PARIS REINFORCE turns to experts' knowledge and perceptions and employs fuzzy cognitive maps, to qualitatively assess the impact of selected strategies and important uncertainties on the three pillars of Italy's progress to energy-sector sustainability: decarbonisation, affordability, and reliability. In a framework of deliberation and simulation, experts display strong preference for renewable energy sources, compared to new gas infrastructure. Renewables are notably deemed to have positive impacts across all three sustainability dimensions and are found more robust against uncertainties, such as regulatory and political instability, which is highlighted as the biggest risk. Critically, despite their expectedly positive impact, demand-side transformations including demand reductions and broader behavioural shifts—a core component of the EU's current approach—may prove inadequate, should large system pressures from negative socio- and techno-economic developments persist.
2. The multi-faceted emergencies of our time (recession, pandemics, and international conflict) can disrupt progress towards sustainable development goals (SDGs). While climate-economy models can show pathways out of these disruptions, numerous stakeholder-informed enhancements are required to navigate through the interconnected SDG landscape. Section 3 introduces a Monte Carlo Fuzzy Cognitive Mapping (MCFCM) approach to capture, and understand the differences among, modellers' and experts' perceptions of the impacts of such crises on broader sustainability, considering models' existing/planned capacity and uncertainty over perceived magnitude of impacts and propagation across SDGs. Expert



stakeholders appeared more concerned over the implications of these crises for sustainable development than modellers, but expectations were considerably constrained by model capabilities. SDGs 8 (growth), 7 (energy-sector sustainability), and 13 (climate action) were robustly found as most prone to examined shocks. The MCFCM approach highlighted potentially critical propagation effects and gaps in IAM capabilities to holistically study the SDG action space.

3. While fossil fuel prices soar during the 2022 global energy crisis, the European Union is looking to activate all available fossil-fuel levers and Greece still plans to use natural gas as a transition fuel for delignitisation, with strong concerns over potential exacerbation of energy poverty and hurdles to progress in climate action. Section 4 assesses the trajectory of the Greek electricity mix and its reliance on natural gas under the current policy framework on the one hand, and an ambitious scenario aiming for complete decarbonisation by 2035 on the other. We model these scenarios using an energy system modelling framework, comprising LEAP and OSeMOSYS model implementations for Greece, and use a stakeholder-informed fuzzy cognitive mapping exercise to uncover transition uncertainties. While power generation from natural gas is projected to almost double between 2022 and 2030 under existing policies, the proposed decarbonisation scenario has the potential to achieve complete independence from Russian gas by 2026 while also leading to a cleaner and considerably cheaper power sector. This 'higher climate ambition' scenario is shown to be more robust in case high fossil fuel prices persist post-2022, even if bottlenecks stressed by stakeholders such as community acceptance or technological constraints emerge and potentially constrain the expansion of certain renewable energy technologies. Apart from the added value of stakeholder input in modelling science, as reflected in the impact of barriers Greek stakeholders critically highlighted, our results emphasise that a diversified energy-supply mix alongside bold energy efficiency strategies are key to rapid and feasible decarbonisation in the country.



Contents

1	Introduction to, and upgrade of, Fuzzy Cognitive Maps.....	11
1.1	Introduction.....	11
1.2	FCM background and layout notations	12
1.3	FCM equilibrium analysis with no steady nodes	13
1.3.1	State-of-the-art bounds of parameter λ of transfer functions	14
1.3.2	Remarks on transfer functions	15
1.3.3	Proposed bounds for parameter λ	16
1.4	FCM equilibrium analysis with steady nodes	20
1.4.1	Bounds of λ parameter when there are steady/input FCM nodes	20
1.5	Normalisation of final state values	21
1.5.1	Normalisation in the case of the Sigmoid Transfer function	21
1.5.2	Normalisation in the case of the Hyperbolic Tangent transfer function	24
1.6	Software implementation: the “In-Cognitive” tool	25
1.7	Case study validation of the proposed framework and software	27
1.7.1	Hyperbolic tangent FCM for different parameter λ values	30
1.7.2	Proposed parameter λ values with normalised final output vector	33
1.8	Remarks and conclusions	33
2	Navigating through an energy crisis: challenges and progress towards electricity decarbonisation, reliability, and affordability in Italy.....	35
2.1	Introduction.....	35
2.2	Methods & Tools	36
2.3	Designing the FCM for the Italian power sector.....	38
2.3.1	Policy nodes.....	38
2.3.2	System nodes.....	40
2.3.3	Uncertainty nodes	43
2.4	Eliciting and quantifying experts’ perspectives	44
2.5	Simulation results and analysis.....	47
2.6	Conclusions.....	53
3	Expectations from and capabilities of climate-economy models for measuring the impact of crises on sustainability.....	55
3.1	Introduction.....	55
3.2	Methods and tools.....	57
3.2.1	Fuzzy cognitive maps: concepts and mathematical formulation	57
3.2.2	Integrating Monte Carlo simulations into FCMs.....	58
3.2.3	Map construction and scenario design.....	59
3.3	Results	61
3.3.1	No-crisis baseline.....	61
3.3.2	Crisis propagation without uncertainty	63
3.3.3	Crisis propagation under uncertainty	66
3.4	Discussion	69



3.5	Conclusions.....	71
4	Enabling an energy transition in Greece following the Ukraine 2022 invasion	73
4.1	Introduction.....	73
4.2	Methods & Tools	74
4.2.1	The energy system modelling framework	74
4.2.2	Scenario design.....	76
4.2.3	Fuzzy cognitive mapping.....	78
4.3	Initial energy-system modelling analysis.....	79
4.3.1	Energy demand.....	79
4.3.2	Electricity Generation	84
4.4	Considerable risks from the stakeholders' perspective.....	91
4.5	Stakeholder-informed sensitivity analysis	95
4.5.1	Persistent price shocks from today's energy crisis.....	95
4.5.2	The impact of underexplored technical constraints to the High Ambition scenario.....	97
4.5.3	What happens if all goes sideways?	97
4.6	Conclusions.....	98
5	Key Takeaways.....	100
	Appendix 1: Weight node interconnections	101
	Appendix 2: Workshop questionnaire (in printed format)	102
	Appendix 3: Mathematical framework of FCM simulations	104
	Appendix 4: Additional Material for Chapter 3.....	105
	Appendix 5: In-Cognitive: a Python framework for Monte Carlo Fuzzy Cognitive Maps	106
	References	116

Table of Figures

Figure 1: A node and its interconnections.....	13
Figure 2: Example of a small FCM, with steady nodes (C_1 and C_4) represented by solid-border circles and intermediate nodes (C_2 , C_3 , and C_5) represented by dotted-border circles	13
Figure 3: Plot of (a) a log-sigmoid function and (b) a hyperbolic tangent function.....	16
Figure 4: The almost linear region of (a) a log-sigmoid function and (b) a hyperbolic tangent function	17
Figure 5: Comparison of lambda parameter bounds for two different weight matrices (log-sigmoid transfer function)	19
Figure 6: Sigmoid functions f_s and their corresponding y_s , when $\lambda_s=0.5$ (red lines) and $\lambda_s1=4.5579$ (green lines)	22
Figure 7: Second step of linear transformation of sigmoid transfer function	23
Figure 8: Sigmoid functions f_s and their corresponding y_s when $\lambda_s=0.5$ (red lines) and $\lambda_s1=4.5579$ (green lines).25	25
Figure 9: Description of In-Cognitive Python web application.....	26
Figure 10: The In-Cognitive GUI.....	27
Figure 11: Hyperbolic tangent FCM with $\lambda=0.1$, SP: middle of the road, policy: P3 (SP2_P3).....	31
Figure 12: Hyperbolic tangent FCM with $\lambda=0.421$, SP: middle of the road, policy: P3 (SP2_P3).....	31
Figure 13: Hyperbolic tangent FCM with $\lambda=1$, SP: middle of the road, policy: P3 (SP2_P3)	31
Figure 14: Hyperbolic tangent FCM with $\lambda=10$, SP: middle of the road, policy: P3 (SP2_P3).....	32



Figure 15: Hyperbolic tangent FCM with $\lambda=50$, SP: middle of the road, policy: P3 (SP2_P3).....	32
Figure 16: All iterations of hyperbolic tangent FCM with $\lambda=0.421$ and normalised final values, SP: middle of the road, policy: P3 (SP2_P3).....	33
Figure 17: Employed FCM methodological framework.....	37
Figure 18: Illustrative example of the FCM design process, for P1 (increasing solar and wind capacity).	42
Figure 19: The original FCM designed for the Italian power sector	44
Figure 20: A simplified representation of the final FCM, as adapted from Figure 19 and populated to include the experts' assessed weights of interactions.....	46
Figure 21: FCM results for the performance of the four policy strategies on the three key dimensions of SDG7 progress in Italy	48
Figure 22: FCM results for the implications of the four uncertainties on wholesale electricity prices, behavioural changes, share of natural gas in the electricity mix, and progress on SDG7.....	50
Figure 23: FCM results for the implementation of each policy strategy under uncertainty relative to a no policy – no uncertainty scenario.....	52
Figure 24: The proposed Monte Carlo FCM (MCFCM) method.....	59
Figure 25: FCM typology forming the basis for the construction of the four maps used.....	60
Figure 26: Causal Relationship Importance of each SDG in the “no-crisis” baseline scenario.....	63
Figure 27: Impact of the crises on each SDG in the “fixed level of crisis” scenario expressed as a difference compared to the baseline (%) in each map	64
Figure 28: Impact of the crises on each SDG in the “fixed level of crisis” scenario expressed as absolute scores per crisis on each map.....	65
Figure 29: Impact of crises on SDG13 in the “fixed level of crisis” scenario.....	66
Figure 30: Impact of the crises on each SDG in the “crisis under uncertainty” scenario assuming uncertainty on inputs.....	67
Figure 31: Impact of the crises on each SDG in the “crisis under uncertainty” scenario assuming uncertainty on weights.....	67
Figure 32: Impact of the crises on each SDG in the “crisis under uncertainty” scenario uncertainty on inputs and weights at the same time	69
Figure 33: Projected energy demand (TWh) in Greece for the NECP, Climate Law, and High Ambition scenarios: (a) total demand (includes industry and agriculture), (b) the transport sector, (c) the household sector, and (d) the tertiary sector.	81
Figure 34: Transport energy demand per fuel (in TWh) for the: (a) Greek NECP, (b) Climate Law, and (c) High Ambition scenarios.....	83
Figure 35: Household energy demand per fuel (in TWh) for the: (a) Greek NECP, (b) Climate Law, and (c) High Ambition scenarios.....	84
Figure 36: Electricity generation per technology (in TWh) for the: (a) Greek NECP, (b) Climate Law, and (c) High Ambition scenarios.....	87
Figure 37: Power generation capacity installed per technology (in GW) for the: (a) Greek NECP, (b) Climate Law, and (c) High Ambition scenarios.	89
Figure 38: Electricity generation costs (in €/MWh) for the: (a) Greek NECP, (b) Climate Law, and (c) High Ambition scenarios.....	90
Figure 39: Electricity generation emissions (in Mtn CO ₂) per scenario.	91
Figure 40: The resulting FCM for the Greek power sector, including the experts' assessed weights of interconnections.....	93
Figure 41: FCM results for the implications of each uncertainty (U _x) on Greek power sector decarbonisation (S17).	



.....	94
Figure 42: Electricity per technology (in TWh) in the High Ambition Scenario if current prices gradually align with IEA's 2021 World Energy Outlook (IEA, 2021) projections (a) in 2023-2030 (fossil-fuel price projection 1) and (b) in 2025-2035 (fossil-fuel price projection 2).....	96

Table of Tables

Table 1: Node descriptions	28
Table 2: Socio-economic risk scenarios	29
Table 3: Policies and corresponding input nodes.....	29
Table 4: FCM output node values for different parameters λ	32
Table 5: Ordering of FCM output node values for different parameters λ	33
Table 6: Key policy targets stemming from the INECP	38
Table 7: FCM nodes, including policies (Px), system components (Sx), and uncertainties (Ux)	39
Table 8: Input assumptions for LEAP and OSeMOSYS.....	75
Table 9: Core policy assumptions across the three scenarios.....	77
Table 10: System components of the Greek power sector FCM, as designed with the stakeholders	92
Table 11: Barriers/bottlenecks and/or uncertainties raised and discussed by the stakeholders	92



1 Introduction to, and upgrade of, Fuzzy Cognitive Maps

This section has been published in Operational Research:

- Koutsellis, T., Xexakis, G., Koasidis, K., Nikas, A., & Doukas, H. (2022). Parameter analysis for sigmoid and hyperbolic transfer functions of fuzzy cognitive maps. *Operational Research*, in press. <https://doi.org/10.1007/s12351-022-00717-x>

1.1 Introduction

Fuzzy Cognitive Maps (FCMs) (Kosko, 1986) have been used to model systems in many scientific areas, such as in social and political science (Craigier and Coover, 1994; Tsadiras and Kouskouvelis, 2005; Axelrod, 2015) as well as in economics (Koulouriotis et al., 2001; Carvalho and Tomé, 2004; Koulouriotis, 2004; Penn et al., 2013; Azevedo and Ferreira, 2019). They have also been used in the presentation of social scientific knowledge and description in various decision-making methods (Zhang et al., 1989, 1992; Georgopoulos et al., 2003). Other notable applications include geographical information systems (Liu and Satur, 1999; Satur and Liu, 1999b, a), pattern-recognition applications (Papakostas et al., 2006, 2008), numerical and linguistic prediction of time-series functions (Silva 1995; Stach et al., 2008), technological (Stylios and Groumpos, 2004), industrial (Abbaspour Onari and Jahangoshai Rezaee, 2020; Markaki and Askounis, 2021) and medical applications (Foelich et al., 2012; Amirkhani et al., 2017, 2018; Apostolopoulos et al., 2017; Bevilacqua et al., 2018; Puerto et al., 2019).

Several other studies have also employed FCMs in environmental and ecological problems (Hobbs et al., 2002; Fons et al., 2004; Xirogiannis et al., 2004; Çelik et al., 2005; Mendoza and Prabhu, 2006; Kok, 2009; Ceccato, 2012; Soler et al., 2012; Cakmak et al., 2013; Gray et al., 2014a) or energy policy and efficiency projects (Ghaderi et al., 2012; Kyriakarakos et al., 2012; Huang et al., 2013; Reckien, 2014; Hsueh, 2015; Karavas et al., 2015; Amer et al., 2016; Olazabal and Pascual, 2016; Nikas and Doukas, 2016; Nikas et al., 2020c, 2019; Antosiewicz et al., 2020; Doukas and Nikas, 2020). As a policy support tool, FCMs have particularly gained ground in such energy and climate policy applications, partly due to stakeholders encountering difficulties in understanding, or being excluded from, state-of-the-art policy support frameworks, like energy- and climate-economic modelling tools (Nikas and Doukas, 2016). Due to limited model complexity and reliance on quantitative data, FCMs have proliferated as a policy support tool, especially at the local level, allowing policymakers to reflect their understanding of a problem domain in a structured manner and act based on it (Özesmi and Özesmi, 2004). They have also been proposed as an effective way to bridge the science-policy gap and engage stakeholders in environmental modelling processes (van Vliet et al., 2010).

Broadly speaking, however, the simplicity and attractiveness of FCMs across application areas and domains lies in their ability to capture the perception of a system in graphical representations consisting of concepts (nodes) and interconnections (weights) among these nodes, which are characterised by transfer functions determining the state vector of the system in simulation (Tsadiras, 2008). However, the topology of nodes and weights, on the one hand, and the transfer function, on the other, are formulated differently: the former are typically defined by the non-expert decision makers (stakeholders) of the case study, while the latter are selected by the analysts. In essence, like stakeholders, the analysts are required to take decisions, which are both relevant to the analysis and critical to its results.

However, despite the plethora of applications, the FCM theory is still inconsistently applied in the literature (Felix et al., 2019). Notably, there seems not to exist a common ground among researchers regarding one of its core features, the type of transfer function used to drive simulations. Various monotonic functions have been used in literature, such as step, sigmoidal, ramp, and linear functions (e.g. (Hobbs et al., 2002; Mendoza and Prabhu, 2006)



and (Soler et al., 2012)), with each one potentially yielding markedly different results. This diversity in FCM outcomes imposes barriers to the final inference procedure. In the absence of common criteria on selecting the transfer function, analysts should carefully justify their choice based on the physical interpretation of each application, which however is not common practice (Nápoles et al., 2018).

In this study, we propose the use of two transfer functions, namely the log-normal (sigmoid) and hyperbolic tangent functions. We also introduce a criterion to define their parameter λ —i.e., their steepness—toward standardising the selection of the FCM transfer function. The observations and analysis in this study build on previous studies (Boutalis et al., 2008; Kottas et al., 2010; Lee and Kwon, 2010; Knight et al., 2014; Harmati and Kóczy, 2018; Harmati et al., 2018), which provided bounds for parameter λ . Depending on the λ value, the sigmoid and hyperbolic tangent functions yield a unique final state of nodes for a given set of input values (i.e., a fixed state vector). However, by providing a domain of parameter λ , they only restrict λ values so they do not yield chaotic, ambiguous FCM responses. The selection of parameter λ is thus still subject to the subjective selection of the analyst within the provided bounds.

Despite providing final node values with clear ordering, the linear transfer function suffers from the undesired condition of chaotic final states (Knight et al., 2014). Additionally, although the sigmoid and hyperbolic tangent functions—given parameters λ within specific bounds provided in the literature—do not exhibit such behaviour, they often result in final node values close to one another, thereby hindering clear inference. To tackle these barriers, we propose an improved version of sigmoid and hyperbolic tangent transfer functions, which is active within an almost-linear region. We illustrate this methodology through a Python web software application “In-Cognitive” that we developed in the context of this study. This novel application features a user-friendly Graphical User Interface (GUI) that allows various stakeholders to define the FCM layout (e.g., nodes, weight interconnections, input/initial state vector, etc.), and execute scenario simulations before reaching a final state vector. The value of parameter λ is calculated endogenously, based on the proposed analysis.

Section 1.2 provides a theoretical background (notations and definition) of fuzzy cognitive mapping. In Section 1.3, we provide an FCM analysis without considering input nodes (all nodes may change throughout the simulation iterations): we first present and discuss the state-of-the-art bounds of parameter λ , before introducing a framework to define bounds/value of λ parameter. Section 1.4 performs similar analysis for the case of FCMs with given input nodes that remain steady and unaffected by other nodes throughout the simulation. Section 1.5 focuses on the normalisation of final state values. The “In-Cognitive” software application is presented in Section 1.6 and then validated in Section 1.7 in a case study drawn from the literature. Section 1.8 finally concludes the research, highlighting key takeaways and discussing prospects.

1.2 FCM background and layout notations

An FCM consists of n concepts (nodes), $C_i: i = 1, 2, \dots, n$, linked to one another through a weight, w_{ij} , which describes the degree of influence of C_j over C_i within $[-1, 1]$. When $w_{ij} < 0$ (negative causality), C_i decreases for an increase in C_j . When $w_{ij} > 0$ (positive causality), C_i increases for an increase in C_j . Finally, when $w_{ij} = 0$ there is no relationship (nor adjacency) between C_j and C_i . Figure 1 illustrates how node C_i is connected through weights with all the other nodes.



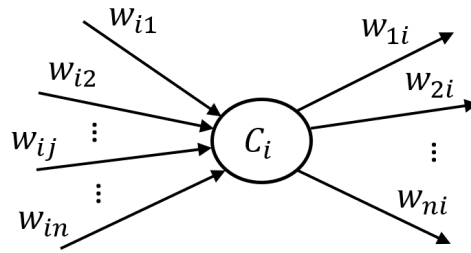


Figure 1: A node and its interconnections

Input or steady nodes, steady nodes hereafter, influence but are not influenced by other nodes (i.e., they have outbound but no inbound links). The nodes which are neither steady nodes nor output nodes are called intermediate nodes. In Figure 2, an FCM of 5 nodes is presented: nodes C_1 and C_4 (solid circles) are steady nodes, while nodes C_2 , C_3 and C_5 (dotted circles) are intermediate nodes. For a real-world example, the reader is referred to Section 1.7.

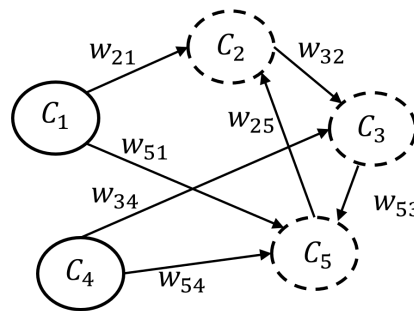


Figure 2: Example of a small FCM, with steady nodes (C_1 and C_4) represented by solid-border circles and intermediate nodes (C_2 , C_3 , and C_5) represented by dotted-border circles

The matrix consisting of all FCM weights w_{ij} is called the weight matrix, W . Eq. (1) shows the weight matrix of the FCM illustrated in Figure 2.

$$W = \begin{bmatrix} w_{1,1} & w_{1,2} & w_{1,3} & w_{1,4} & w_{1,5} \\ w_{2,1} & w_{2,2} & w_{2,3} & w_{2,4} & w_{2,5} \\ w_{3,1} & w_{3,2} & w_{3,3} & w_{3,4} & w_{3,5} \\ w_{4,1} & w_{4,2} & w_{4,3} & w_{4,4} & w_{4,5} \\ w_{5,1} & w_{5,2} & w_{5,3} & w_{5,4} & w_{5,5} \end{bmatrix} = \begin{bmatrix} 0 & 0 & 0 & 0 & 0 \\ w_{2,1} & 0 & 0 & 0 & w_{2,5} \\ 0 & w_{3,2} & 0 & w_{3,4} & 0 \\ 0 & 0 & 0 & 0 & 0 \\ w_{5,1} & 0 & w_{5,3} & w_{5,4} & 0 \end{bmatrix} \quad (1)$$

1.3 FCM equilibrium analysis with no steady nodes

To analyse FCM outcomes, we express node interactions using a mathematical formulation that should be iterative through time. If A_i^k is the value of node i at time instance k , the iterative interconnection expression for each node is

$$A_i^{k+1} = f \left(\sum_{j=1, j \neq i}^n (w_{ij} A_j^k + d_i A_i^k) \right) \quad (2)$$

where $f(\cdot)$ is the transfer function and d_i the feedback coefficient $\in [0,1]$. The latter indicates the dependency of node C_i on its starting value in each iteration. The transfer function could be any function. However, to avoid chaotic FCM behaviours, the transfer function values should be bounded. Usually, the *log-sigmoid* and *hyperbolic tangent* functions are used. The values of the former span within $[0,1]$ and of the latter within $[-1,1]$. The general form of the log-sigmoid function is

$$f_s = \frac{1}{1 + \exp(-\lambda x)} \quad (3)$$

whereas the corresponding one of the hyperbolic tangent is

$$f_h = \frac{\exp(\lambda x) - \exp(-\lambda x)}{\exp(\lambda x) + \exp(-\lambda x)} = \frac{\exp(2\lambda x) - 1}{\exp(2\lambda x) + 1} \quad (4)$$

As discussed in (Knight et al., 2014), the selection of the transfer function should be justified based on the given application and, therefore, there is no standard criterion to yield the best fitted transfer function; Knight et al., also show that different types of transfer functions yield different FCM final states and thus different inferences. To tackle this issue, Knight et al., proposed the execution of various simulations, with each one having different transfer functions. They then compared results to identify common patterns: nodes, whose final values are relatively high (low) for all executions are considered the most (least) important FCM concepts.

1.3.1 State-of-the-art bounds of parameter λ of transfer functions

Different types of transfer functions yield different inferences for the iterative function of Eq. (2)—similarly, different λ parameters of the same transfer function (see Eq. (3) and (4)) may yield different FCM final states and therefore different inferences. Some of the various final states of Eq. (2) might be chaotic, infinite, or periodic (Knight et al., 2014). These states are not fit for any kind of inferences. Therefore, it is necessary to ensure the FCM converges and explore whether a given layout can be stabilised around a final steady state after several iterations of Eq. (2).

Under certain conditions and a given combination of (a) the weight matrix, (b) the number of nodes, and (c) the parameters of the transfer function, it is possible to reach a final, unique fixed vector regardless of the initial values $A_i^0, \forall i \in [0, n]$. It should be noted that, for any of these combinations, the final state is not necessarily the same.

It should be noted that, in previous research (Boutalis et al., 2008; Kottas et al., 2010; Lee and Kwon, 2010; Knight et al., 2014; Harmati and Kóczy, 2018; Harmati et al., 2018), the authors provided conditions under which the existence and uniqueness of solutions of concept values (see Eq. (2)) are guaranteed. In Knight et al. (2014), the authors provided a maximum bound of λ parameter for the log-sigmoid transfer function (see Eq. (3)), regardless of the structure and contents of the weight matrix; they also showed that, when the FCM is equipped with a step function (i.e., the limit state of log-sigmoid function when $\lambda \rightarrow \infty$), the uniqueness and existence of a fixed solution is not guaranteed as well as that, as the examined FCM grows in size ($n \rightarrow \infty$, where n the number of FCM nodes), the λ parameter to guarantee the existence and the uniqueness of a final fixed solution gets smaller ($\lambda \rightarrow 0$). However, the provided upper bounds of λ parameter were strict enough, rendering unnecessary the consideration of the layout of a given FCM (i.e., the weight matrix). In Kottas et al., (2010), the authors provided a less strict upper bound conditions, under which there is a fixed-point solution when $\lambda = 1$, for both Eq. (3) and (4), depending also on the weight matrix/structure. Consequently, the conditions discussed in Knight et al. (2014) are less restrictive in case $\lambda = 1$. In Harmati et al. (2018), the authors extended the results of Kottas et al., (2010) for all $\lambda > 0$ and finally reached a bound of λ for all log-sigmoid and hyperbolic tangent-equipped FCM implementations.

In the case of the log-sigmoid transfer function, the bound guaranteeing the existence and uniqueness of FCM final state is found to be (Harmati et al., 2018):

$$\lambda_s < \lambda'_s = \frac{4}{\|W\|_F} \quad (5)$$

Whilst, in the case of the hyperbolic tangent transfer function, the bound is:

$$\lambda_h < \lambda'_h = \frac{1}{\|W\|_F} \quad (6)$$



where \mathbf{W} is the weight matrix and $\|\cdot\|_F$ the Frobenius norm, such that:

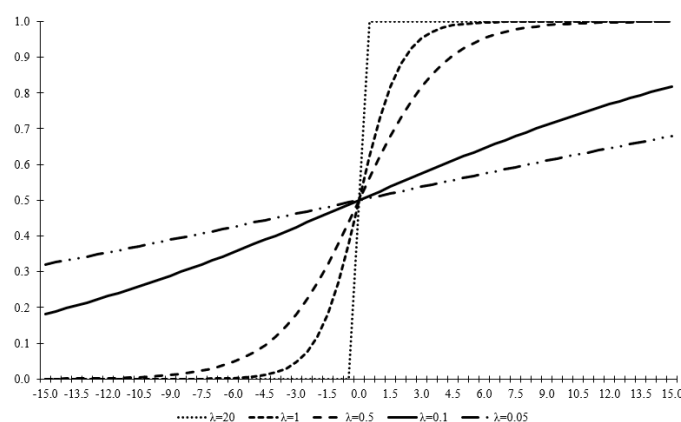
$$\|\mathbf{W}\|_F = \sqrt{\sum_{i=1}^n \sum_{j=1}^n (w_{ij}^2)} \quad (7)$$

It should be noted that the above conditions are sufficient, but not necessary for an FCM to have one and only one fixed point for a given parameter λ : there could be cases where an FCM has a unique fixed-point solution if λ is greater than the above upper bounds (see Eq. (5) and (6)).

Lee and Kwon (2010) reached similar conclusions for the log-sigmoid transfer function, by using a different approach (Lyapunov criteria).

1.3.2 Remarks on transfer functions

Among many transfer functions, the linear function—more specifically the identity function—yields lucid inferences, because the distance among outcomes is clearer than other transfer functions (Knight et al., 2014). Based on the structure of Eq. (2), the linear function features no distortion during the calculation of A_i^{k+1} from previous iterative values A_j^k . The value of the transfer function is always proportional to the argument of Eq. (2) through all iterations. This property of linear functions gives room to lucid inferences; the distance among the final node values is sufficient to distinguish each node final state from the others. However, the linear transfer function comes with certain caveats. Often, during iterations, the A_i^{k+1} values are constantly increasing (decreasing) reaching infinite (minus infinite) values. Despite FCMs equipped with linear transfer functions exhibiting a closer-to-reality increment (decrement), the above extreme case behaviour is restrictive for the execution of the iterative procedure (Eq. (2)). For this reason, the analysts tend to impose restrictions on A_i^{k+1} values by using bounded transfer functions—i.e., the log-sigmoid and hyperbolic tangent function. Both are odd functions around the $y = 0.5$ and $y = 0$ axis, respectively, and exhibit an *almost-linear* behaviour in a region close to these axes. This linearity gives them resemblance to a linear transfer function for a sufficient interval. The non-linear regions on the tails of these functions are used to represent the large A_j^{k+1} values. The $y = 0$ and $y = 1$ bounds ($y \pm 1$ bounds) are used to represent the infinite (or close to infinity) A_j^{k+1} values for the case of the log-sigmoid (hyperbolic tangent) transfer function (see Figure 3). The heavy curved regions close to these bounds are mainly responsible for the distortion (non-proportionality) of A_j^{k+1} values; arguments close to infinite tend to map to almost the same A_j^{k+1} values (i.e., no sufficient distance among nodes' final values).



(a)



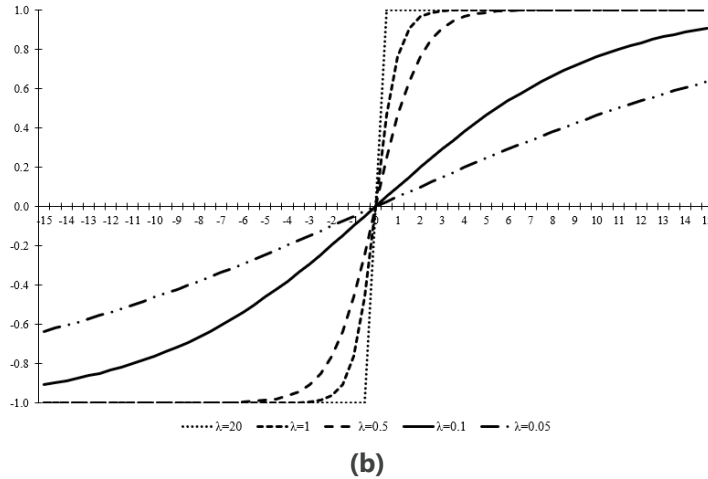


Figure 3: Plot of (a) a log-sigmoid function and (b) a hyperbolic tangent function

However, bounded transfer functions exhibit shortcomings as well. Not only do the non-linear regions introduce distortion, but the existence of bounds ($y = 0$ and $y = 1$, or $y \pm 1$) could yield final states that are either chaotic or limit cycles (i.e., a period function of A_i). This could happen when the x_i^k arguments of Eq. (2)

$$x_i^{k+1} = \sum_{j=1, i \neq j}^n (w_{ij}A_j^k + d_iA_i^k) \quad (8)$$

exhibit prolonged stay in the area where $f_s \rightarrow +1$ or $f_s \rightarrow 0$ (log-sigmoid case), or $f_h \rightarrow \pm 1$ (hyperbolic tangent case) during the iterative procedure of Eq. (2). In this case, it is more likely for the FCM simulation to conclude to a state where all final A_i values are close to 0 or 1 (log-sigmoid) or ± 1 (hyperbolic tangent) making the ordering of final A_i values obscure. From Figure 3, we can conclude that this undesired behaviour happens when parameter λ exhibits large values (i.e., f is almost a step function). Knight et al., (2014) reached the same conclusion by using a different approach. Similarly, another case yielding cyclic behaviour happens when the x_i^k values are perpetually changing sign through iterations and parameter λ is simultaneously large enough (i.e., the transfer function is almost a step function). In that case, the A_i values are more likely to oscillate with an amplitude having extreme values close to the bounds of the transfer function. Such oscillations in node values are almost chaotic and insufficient for inferences. As a rule of thumb, the FCM analyst should therefore avoid large values of the λ parameter.

Another undesirable condition occurs when parameter λ is too small (almost zero). When $\lambda \rightarrow 0$, the transfer function is almost flat (see Figure 3) in all ranges of x_i^k values and, therefore, all A_i values conclude to almost the same value. This state is stable; however, it cannot reach a conclusion because there is no lucid ordering among A_i values. Concluding, FCM analysts should avoid both small and large values of parameter λ . Below we propose an upper bound of parameter λ based on the above remarks. These bounds can thereafter be combined with the bounds of Eq. (5) and (6).

1.3.3 Proposed bounds for parameter λ

The proposed methodology refers to FCMs equipped with the log-sigmoid or hyperbolic tangent transfer function. It is based on the conclusion that $\lambda \rightarrow 0$ and $\lambda \rightarrow \infty$ are two undesired regions of parameter λ and the assertion that linear transfer functions are preferable, if they do not yield chaotic, cyclic, or infinite final states (see Section 3.2). The main idea behind the proposed methodology is that both log-sigmoid and hyperbolic tangent transfer functions have a region that is almost linear (desired region). We provide certain conditions, under which all A_i^{k+1} values fall within that region. These conditions are then used to provide bounds of parameter λ . By operating in



the almost linear region, we get a combination of benefits of both linear and bounded transfer functions (see Section 1.3.2); mainly, we avoid the distortion that the curved segments in the tails of the bounded transfer functions introduce (Figure 4).

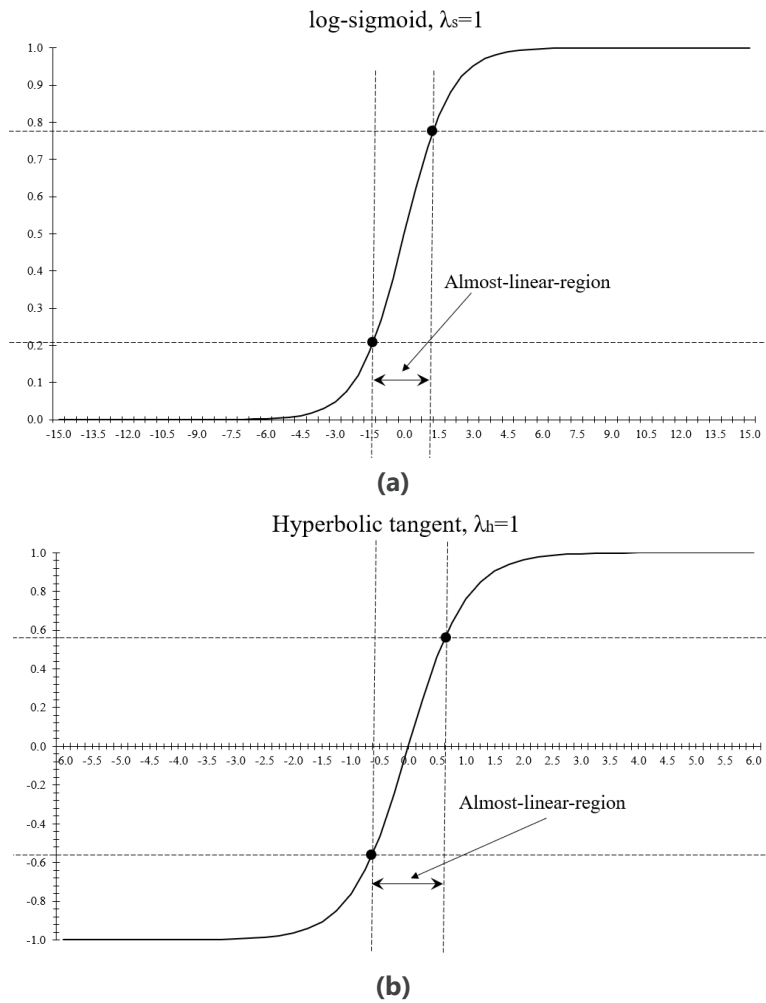


Figure 4: The almost linear region of (a) a log-sigmoid function and (b) a hyperbolic tangent function

However, working in the almost linear region comes at a cost. This region is not as large as the interval between the bounds of the log-sigmoid or hyperbolic tangent function; therefore, the final A_i^{k+1} values are usually close to one another. To avoid this, we propose a normalisation procedure (see Section 1.3.4).

1.3.3.1 The almost linear region of the log-sigmoid and hyperbolic tangent functions

For the almost linear region to be 'active' for all nodes during all FCM iterations, all arguments x_i^k 's (Eq. (8)) must not lie in the region of the transfer function tails. The desired region where x_i^k values lie on is hereafter called '*almost linear region*' (see Figure 4); all x values bounded by $-x^*$, $+x^*$, where $f'''(\pm x^*) = 0$, which is where the f'' has local maxima (see Figure 4). We call $-x^*$ and $+x^*$ "turning points," hereafter.

The third derivative of log-sigmoid (Eq. (3)) is

$$f_s'''(x) = \lambda^2 f_s'(x) \{ (1 - f_s(x))(1 - 2f_s(x)) - f_s(x)(1 - 2f_s(x)) - 2f_s(x)(1 - f_s(x)) \} \quad (9)$$

The third derivative of hyperbolic tangent (Eq. (4)) is:

$$f_h'''(x) = -2\lambda f_h''(x) (f_h(x) + f_h''(x)) \quad (10)$$



The λ parameter is always positive, as well as $f_s'(x)$ (Kottas et al., 2010). Then, after equating the $\{\cdot\}$ factor of Eq.(9) with zero, we conclude to $(f_s(x))^2 - f_s(x) + (1/8) = 0$, which is true if $f_s(x) \approx 0.789$ or $f_s(x) \approx 0.211$. Therefore, $0.211 \leq f_s(x) \leq 0.789$ (see Figure 4a). After using Eq. (3), we finally get $0.211 \leq \frac{1}{1+\exp(-\lambda_s x)} \leq 0.789$, which is equivalent to:

$$-1.317 \leq \lambda_s \cdot x \leq 1.317 \quad (11)$$

where λ_s is parameter λ of the log-sigmoid transfer function.

Similarly, from Eq. (10) we get that

$$-0.658 \leq \lambda_h \cdot x \leq 0.658 \quad (12)$$

where λ_h is parameter λ of the hyperbolic tangent transfer function.

The almost linear region is odd with respect to the $x = 0$ axis and parameter λ is always positive; therefore, we can rewrite Eq. (11) and (12) as

$$0 \leq \lambda_s \cdot |x| \leq 1.317, \quad \forall x \quad (13)$$

And

$$0 \leq \lambda_h \cdot |x| \leq 0.658, \quad \forall x \quad (14)$$

1.3.3.2 Bounds of parameter λ with quarantine that the almost linear region is always "active"

Equations (13) and (14) indicate that all absolute argument values multiplied by parameter λ (i.e., $\lambda \cdot |x_i^k|$) should lie in intervals $[0, 1.317]$ or $[0, 0.658]$, respectively. This is satisfied if the largest argument $\lambda \cdot |x_i^k|_{max}$ is smaller or equal to the upper bound of each interval. Substituting the argument of Eq. (8) to $|x_i^k|_{max}$ we get $|\sum_{j=1, i \neq j}^n (w_{ij} A_j^k + d_i A_i^k)|_{max}$.

When the transfer function is log-sigmoid, all state values are positive, that is $0 < A_j^k < 1$. If we need to restrict the A_j^k values to the "almost linear region" (see Figure 4), then $0.211 \leq A_j^k \leq 0.789$. In contrast, the w_{ij} values could be positive or negative. Given the maximum values of A_j^k and w'_{ij} values for a specific i node, the maximum value $|x_i^k|$ is equal to

$$|x_i^k|_{max} = \max \left(\left| 0.211 \cdot \sum_{i=1}^p w_{ij}^+ + 0.789 \cdot \sum_{i=1}^q w_{ij}^- \right|, \left| 0.211 \cdot \sum_{i=1}^p w_{ij}^- + 0.789 \cdot \sum_{i=1}^q w_{ij}^+ \right| \right) \quad (15)$$

where w_{ij}^+ 's and w_{ij}^- 's are all positive and negative input weights, respectively, which end up to the i^{th} node.

We define as s -norm of matrix \mathbf{W} , $\|\mathbf{W}\|_s$, the following

$$\|\mathbf{W}\|_s = \max_i \left(m |x_i^k|_{max} \right) \quad (16)$$

From Eq. (16) we can see that the maximum value the absolute arguments $|x_i^k|$ could get is

$$|x|_{max} = \|\mathbf{W}\|_s \quad (17)$$

Therefore, from Eq. (13) and (17) we finally conclude

$$\lambda_s \leq \lambda_s^* = \frac{1.317}{\|\mathbf{W}\|_s} \quad (18)$$

For an FCM equipped with the hyperbolic tangent transfer function, the maximum value the absolute arguments $|x_i^k|$ could get through all iterations is different because $-1 < A_j^k < 1$. The A_j^k will fall in the 'almost linear region'



when $-0.577 \leq A_j^k \leq 0.577$. Therefore, the possible maximum value for node C_i could be achieved if all w_{ij}^+ are multiplied by $+0.577$ (-0.577) and all w_{ij}^- by -0.577 ($+0.577$). Equivalently, the maximum value of $|x_i^k|$ could be achieved when $|x_i^k| = 0.577 \cdot (\sum_{i=1}^n |w_{ij}|)$. The latter factor is equal to the infinite norm of the weight matrix, \mathbf{W} , which is equal to the maximum absolute row sum of \mathbf{W} . Therefore,

$$|x|_{\max} = 0.577 \cdot \|\mathbf{W}\|_{\infty} \quad (19)$$

where $\|\mathbf{W}\|_{\infty} = \max_i \sum_{j=1}^n |w_{ij}|$, the infinite norm of \mathbf{W} matrix. From Eq. (14) we conclude

$$\lambda_h \leq \lambda_h^* = \frac{1.14}{\|\mathbf{W}\|_{\infty}} \quad (20)$$

The ordering among parameters λ'_s , λ^*_s and λ'_h , λ^*_h is not constant for all applications. As such, we cannot a priori conclude to the existence and uniqueness of the FCM fixed-point if $\lambda < \lambda^*_s$ or $\lambda < \lambda^*_h$. Figure 5 illustrates the bounds λ'_s and λ^*_s for weight matrices $\mathbf{W}_{1(n \times n)} = \mathbf{J}_n$ and $\mathbf{W}_{2(n \times n)}$, where \mathbf{W}_1 is a matrix of ones and \mathbf{W}_2 is a square matrix having three elements per row, all of which are equal to one and aligned around its diagonal. \mathbf{W}_2 could represent an FCM whose nodes are only connected with their three adjacent nodes ($\mathbf{W}_{2(1 \times 1)}$ and $\mathbf{W}_{2(2 \times 2)}$ are equal to matrices of ones because their size is smaller than three). From Figure 5 it can be shown that the ordering of bounds λ'_s and λ^*_s changes depending on the size (the number of nodes) and type (e.g., \mathbf{W}_1 or \mathbf{W}_2) of the weight matrix. Similar conclusions can be drawn for λ'_h and λ^*_h .

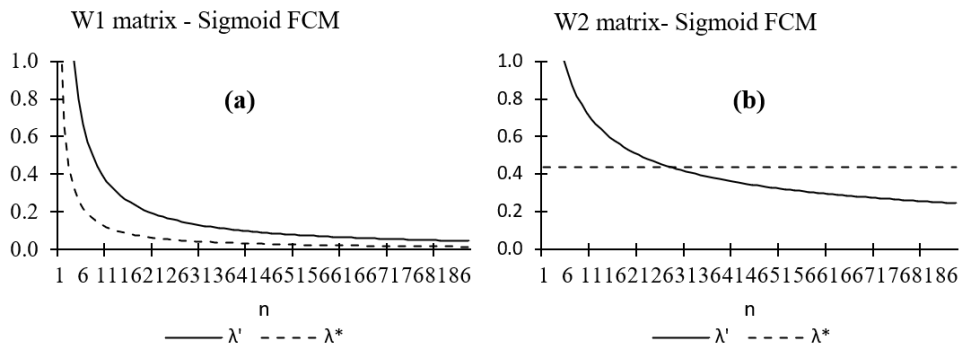


Figure 5: Comparison of lambda parameter bounds for two different weight matrices (log-sigmoid transfer function)

Based on the above remarks, when λ'_s (λ'_h) is greater than λ^*_s (λ^*_h), the FCM analysts should choose the λ^*_s (λ^*_h). By doing so, they can guarantee that there would be a fixed final point due to $\lambda < \lambda'_s$ ($\lambda < \lambda'_h$) and that this fixed point would consist of A_i values lying in the 'almost linear region' of the transfer function. On the other hand, if λ^*_s (λ^*_h) is greater than λ'_s (λ'_h), the λ'_s (λ'_h) should be preferred to guarantee that there would be a unique fixed point. These remarks can be formulated as follows:

$$\lambda_s < \min(\lambda'_s, \lambda^*_s) \quad (21)$$

for the log-sigmoid transfer function, and

$$\lambda_h < \min(\lambda'_h, \lambda^*_h) \quad (22)$$

for the hyperbolic tangent transfer function.

Once the final bound is estimated (Eq. (21) or Eq. (22)), we should choose a parameter λ that is as close to the final bound as possible, because parameter λ must not get extremely low values, $\lambda \rightarrow 0$ (see Section 1.3.2). This value is the infimum value of bounds in Eq. (21) and Eq. (22). For the sake of simplicity, we propose as close to infimum λ value, which is derived after rounding the final bound of Eq. (21) or Eq. (22) at the third decimal digit.



1.4 FCM equilibrium analysis with steady nodes

In Section 1.3, we presented conditions, under which an FCM with no input/steady nodes has a unique solution ($\lambda < \lambda'_s$) consisting of final A_i values distinct enough ($\lambda < \lambda'_s$) to yield lucid inferences. In case of FCM with steady nodes though, which is the case for scenario analysis (Nikas et al., 2019b, 2020c; Antosiewicz et al., 2020) the unique equilibrium does not depend solely on the weight matrix and parameter λ , as it does in the case of FCMs with no input nodes; it also depends on the values of the steady nodes (external excitations). Therefore, we can achieve a variation of equilibria/responses by changing the excitation of steady nodes and simultaneously reassuring that we will not get a chaotic final state if we choose certain values of parameter λ similarly to Eq. (21) and Eq. (22). To do so, we must express parameter λ with respect to the weight set of the non-steady nodes (Kottas et al., 2010).

1.4.1 Bounds of λ parameter when there are steady/input FCM nodes

Based on Kottas et al., (2010), the existence of equilibrium is guaranteed if Eq. (5) and Eq. (6) are valid for the weight set of the non-steady nodes. First, we need to reconstruct the extended weight matrix, \mathbf{W} , so that the first rows correspond to the steady-nodes and the end rows to the non-steady nodes. That is

$$\mathbf{W} = \begin{bmatrix} w_{11} & 0 & \cdots & 0 & 0 \\ 0 & w_{22} & \cdots & 0 & 0 \\ \vdots & \vdots & \vdots & \vdots & \vdots \\ \hline & & & \mathbf{W}^* & \end{bmatrix} \quad (23)$$

The FCM illustrated in Figure 2 with

$$\mathbf{W} = \begin{bmatrix} 0 & 0 & 0 & 0 & 0 \\ 0 & 0 & 0 & 0 & 0 \\ w_{2,1} & 0 & 0 & 0 & w_{2,5} \\ 0 & w_{3,2} & 0 & w_{3,4} & 0 \\ w_{5,1} & 0 & w_{5,3} & w_{5,4} & 0 \end{bmatrix} \quad (24)$$

has now the following reconstructed extended weight matrix

$$\mathbf{W}^* = \begin{bmatrix} w_{2,1} & 0 & 0 & 0 & w_{2,5} \\ 0 & w_{3,2} & 0 & w_{3,4} & 0 \\ w_{5,1} & 0 & w_{5,3} & w_{5,4} & 0 \end{bmatrix}. \quad (25)$$

To identify the conditions, under which an FCM with steady nodes has equilibrium, Kottas et al., (2010) considered the case where $\lambda = 1$. In this research, we propose the corresponding inequality $\forall \lambda \in \mathbb{R}$. The mathematical proof follows similar steps as described in Harmati et al. (2018). Eq. (26) corresponds to an FCM equipped with log-sigmoid whereas Eq. (27) with a hyperbolic tangent transfer function.

$$\lambda_s < \lambda'_s = \frac{4}{\|\mathbf{W}^*\|_F} \quad (26)$$

$$\lambda_h < \lambda'_h = \frac{1}{\|\mathbf{W}^*\|_F} \quad (27)$$

Similarly, the λ_s^* and λ_h^* bounds, when the FCM has steady nodes, are

$$\lambda_s^* = \frac{1.317}{\|\mathbf{W}^*\|_s} \quad (28)$$

And

$$\lambda_h^* = \frac{1.14}{\|\mathbf{W}^*\|_\infty} \quad (29)$$



Finally, as in the case of non-steady nodes, Eq. (21) and (22) must be satisfied.

As in Section 1.3.3.2., we propose that the final λ would be derived by the final bound of Eq. (21) or Eq. (22) rounded at the third decimal digits.

1.5 Normalisation of final state values

The proposed λ bounds squash all concept values during all iterations within $[0.211, 0.789]$ and $[-0.577, 0.577]$ for log-sigmoid and hyperbolic tangent transfer functions, respectively. This may end up to final output values close to one another. Consequently, the relative distance among these values might be unclear. To return to the $[0, 1]$ or $[-1, 1]$ interval for log-sigmoid and hyperbolic tangent, respectively (normalised intervals, hereafter), we need to multiply all these values with a factor so that the A_j^k values are within these normalised intervals.

All concept values, during all iterations, lie in the almost linear region and are, therefore, within the following intervals:

$$0.211 \leq A_j^k \leq 0.789 \quad (30)$$

And

$$-0.577 \leq A_j^k \leq 0.577 \quad (31)$$

for log-sigmoid and hyperbolic tangent, respectively. For the case of a log-sigmoid FCM, to normalise A_j^k we should express them in terms of the $y = 0.5$ line. Recall that the log-sigmoid function is an odd function with respect to $y = 0.5$. After subtracting 0.5 from Eq. (30) we get $-0.289 \leq A_j^k - 0.5 \leq 0.289$. Equivalently, $\frac{-0.289}{2 \cdot 0.289} = -0.5 \leq \frac{A_j^k - 0.5}{2 \cdot 0.289} \leq \frac{0.289}{2 \cdot 0.289} = 0.5 \Leftrightarrow 0 \leq \frac{A_j^k - 0.5}{2 \cdot 0.289} + 0.5 \leq 1$. We conclude:

$$0 \leq \frac{A_j^k - 0.211}{0.578} \leq 1 \quad (32)$$

Therefore, to normalise the final values of all FCM nodes, we need to subtract -0.211 for any of them and then divide them with 0.578.

Similarly, for hyperbolic tangent FCMs, the necessary transformation to normalise the final values of FCM nodes is the multiplication with 1.733:

$$-1 \leq 1.733 \cdot A_j^k \leq 1 \quad (33)$$

1.5.1 Normalisation in the case of the Sigmoid Transfer function

To normalise the FCM results back to the domain of $[0,1]$, we express the almost linear region of the sigmoid function in terms of the $[0,1]$ interval. This is done through a two-step linear transformation.

To identify the almost linear region, the knee points of $f(\cdot)$ are needed, which are provided after solving the following equation:

$$f_s'''(x_i; \lambda_s) = 0$$

Using linear algebra, the knee points are:

$$K_1 = \left(x_{k1} = \frac{1.317}{\lambda_s}, y_{k1} = 0.789 \right) \quad (34a)$$



$$K_2 = \left(x_{k2} = \frac{-1.317}{\lambda_s}, y_{k2} = 0.219 \right) \quad (34b)$$

The straight line passing through points K_1 and K_2 is:

$$y_s = (0.2195 \cdot \lambda_s) \cdot x + 0.5 \quad (35)$$

It should be noted that y_s always passes through $(0, 0.5) \forall \lambda_s$. The slope of y_s is equal to one (see Eq. (5)) when

$$\begin{aligned} 0.2195 \cdot \lambda_s^1 &= 1 \Leftrightarrow \\ \lambda_s^1 &\approx 4.5579 \end{aligned} \quad (36)$$

1.5.1.1 First stage of the linear transformation

Figure. 6 illustrates the pair of f_s, y_s and the knee points for $\lambda_s = 0.5$ and $\lambda_s^1 = 4.5579$. It also depicts the first step of the linear transformation.

During the first step, the A_i^f values, which lie within the almost linear region of $f_s(\cdot; \lambda_s)$, are mapped onto the almost linear region of $f_s(\cdot; \lambda_s^1)$. The range of $f(\cdot; \lambda_s^1)$ values lies in $[0.289, 0.789]$ (y-axis) and its domain is in $[-\frac{1.317}{\lambda_s^1} = -0.289, 0.289]$ (x-axis) (see Eq. (34)).

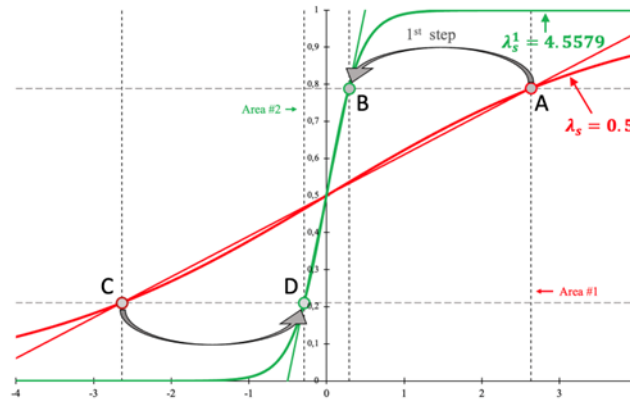


Figure 6: Sigmoid functions f_s and their corresponding y_s , when $\lambda_s = 0.5$ (red lines) and $\lambda_s^1 = 4.5579$ (green lines)

This means that the linear transformation (see Eq. (37)) should perform the interpretation of points A to B and C to D (see Eq. (38)).

$$\begin{Bmatrix} \hat{x}_i^f \\ \hat{A}_i^f \end{Bmatrix} = [T_{s_1}] \cdot \begin{Bmatrix} x_i^f \\ A_i^f \end{Bmatrix} = \begin{bmatrix} a & b \\ c & d \end{bmatrix} \cdot \begin{Bmatrix} x_i^f \\ A_i^f \end{Bmatrix} \quad (37)$$

$$A = \left(\frac{2.279}{\lambda_s}, 0.789 \right) \quad (38a)$$

$$B = (0.289, 0.789) \quad (38b)$$

$$C = \left(\frac{-2.279}{\lambda_s}, 0.211 \right) \quad (38c)$$

$$D=(-0.289,0.211) \quad (38d)$$

After substituting the points of Eq. (38) to Eq. (37) the following hold for parameters a, b of Eq. (38):

$$0.289=a \cdot \left(\frac{2.279}{\lambda_s}\right) + 0.789 \cdot b \quad (39a)$$

$$-0.289=-a \cdot \left(\frac{2.279}{\lambda_s}\right) + 0.211 \cdot b \quad (39b)$$

Similarly, for c and d parameters:

$$0.789=c \cdot \left(\frac{2.279}{\lambda_s}\right) + 0.789 \cdot d \quad (40a)$$

$$0.211=-c \cdot \left(\frac{2.279}{\lambda_s}\right) + 0.211 \cdot d \quad (40b)$$

After solving the system of equations of (Eq. (39) and Eq. (40)) we get: $a=0.1268 \cdot \lambda_s$, $b=0$, $c=0$, $d=1$. Therefore, the transformation matrix of the first step is:

$$[T_{s1}] = \begin{bmatrix} 0.1268 \cdot \lambda_s & 0 \\ 0 & 1 \end{bmatrix} \quad (41)$$

1.5.1.2 Second stage of the linear transformation

The scope of this second step of the linear transformation is to transfer the FCM results from the area of ABCD (see Eq. (36)) back into the range of [0,1] for y-axis (FCM domain). Figure. 7 illustrates this transformation.

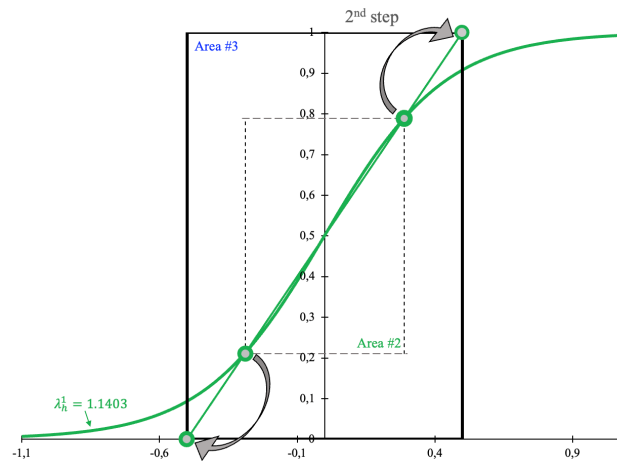


Figure 7: Second step of linear transformation of sigmoid transfer function

Like in the previous section, the linear transformation is of the form:

$$\begin{Bmatrix} \hat{x}_i^f \\ \hat{A}_i^f \end{Bmatrix} = [T_{s2}] \cdot \begin{Bmatrix} x_i^f \\ A_i^f \end{Bmatrix} = \begin{bmatrix} a & b \\ c & d \end{bmatrix} \cdot \begin{Bmatrix} x_i^f \\ A_i^f \end{Bmatrix} \quad (42)$$

and performs the transition from B to B' and D to D' (see Eq. (43)).

$$B=(0.289,0.789), \quad (43a)$$

$$B'=(0.5,1), \quad (43b)$$



$$D=(-0.289,0.211), \quad (43c)$$

$$D'=(-0.5,0) \quad (43d)$$

All the above yield the second transformation matrix:

$$[T_{s_2}] = \begin{bmatrix} 1.73 & 0 \\ 0.73 & 1 \end{bmatrix} \quad (44)$$

After combining Eq. (41) with Eq. (44), the global transformation matrix is:

$$\begin{aligned} [T_s] &= [T_{s_2}] \cdot [T_{s_1}] = \begin{bmatrix} 1.73 & 0 \\ 0.73 & 1 \end{bmatrix} \cdot \begin{bmatrix} 0.1268 \cdot \lambda_s & 0 \\ 0 & 1 \end{bmatrix} \Rightarrow \\ [T_s] &= \begin{bmatrix} 0.219 \cdot \lambda_s & 0 \\ 0.09 \cdot \lambda_s & 1 \end{bmatrix} \end{aligned} \quad (45)$$

Concluding,

$$\begin{aligned} \begin{Bmatrix} \hat{x}_i^f \\ \hat{A}_i^f \end{Bmatrix} &= \begin{bmatrix} 0.219 \cdot \lambda_s & 0 \\ 0.09 \cdot \lambda_s & 1 \end{bmatrix} \cdot \begin{Bmatrix} x_i^f \\ A_i^f \end{Bmatrix} \Rightarrow \\ \hat{A}_i^f &= A_i^f + (0.09 \cdot \lambda_s) \cdot x_i^f \end{aligned} \quad (46)$$

The corresponding transformation in Doukas and Nikas (2020) is:

$$\hat{A}_i^f = 1.73 \cdot A_i^f - 0.365 \quad (47)$$

Equations (46) and (47) vary significantly. The proposed transformation additionally depends on the selected " λ " " s " based on the proposed bounds calculated in sections 1.3.3 and 1.4.1, and the input influences, x_i^f , of C_i node as well. Various simulations show that the proposed transformation gives smaller \hat{A}_i^f values compared to Koutsellis et al. (2022b). However, the ordering and span among \hat{A}_i^f values are proportional to that study and well distinguished. The fact that the \hat{A}_i^f values are smaller gives similar results when λ_s varies, which is important in FCM analysis. That, combined with the fact that the novel transformation interprets the results back to the FCM domain, provides a significant improvement.

1.5.2 Normalisation in the case of the Hyperbolic Tangent transfer function

Following a similar procedure as in Section 1.5.1, the corresponding straight line passing through the knee points of the hyperbolic tangent function is:

$$y_h = (0.877 \cdot \lambda_h) \cdot x \quad (48)$$

The knee points are:

$$K_1 = \left(x_{k1} = \frac{0.658}{\lambda_h}, y_{k1} = 0.577 \right), \quad (49a)$$

$$K_2 = \left(x_{k2} = \frac{-0.658}{\lambda_h}, y_{k2} = -0.577 \right) \quad (49b)$$

It should be noted that y_h always passes through $(0,0) \forall \lambda_h$.

The slope of y_h is equal to one (see Eq. (48)) when

$$0.877 \cdot \lambda_h^1 = 1 \Leftrightarrow,$$



$$\lambda_h^1 \approx 1.1403 \tag{50}$$

Figure 8 illustrates all these points for the cases of $\lambda_s=0.5$ (red lines) and $\lambda_s^1=4.5579$ (green lines).

The linear transformation is like Eq. (37):

$$\begin{Bmatrix} \hat{x}_i^k \\ \hat{A}_i^{k+1} \end{Bmatrix} = [T_h] \cdot \begin{Bmatrix} x_i^k \\ A_i^{k+1} \end{Bmatrix} = \begin{bmatrix} a & b \\ c & d \end{bmatrix} \cdot \begin{Bmatrix} x_i^k \\ A_i^{k+1} \end{Bmatrix} \tag{51}$$

It should be noted that the final transformation (green line on Figure 8) is on the $y=x$ line. Therefore, variables $\Delta y = \hat{A}_i^{k+1} - A_i^{k+1}$ and $\Delta x = \hat{x}_i^k - x_i^k$ are independent of each other. This means that $b=c=0$ (see Eq. (51)). The rest of the variables (i.e., a and d) can be found after using the following points:

$$\left(\frac{0.658}{\lambda_h}, 0.577 \right), \tag{52a}$$

$$A'' = (1,1) \tag{52b}$$

Substituting Eq. (22) to Eq. (51) we finally get:

$$[T_h] = \begin{bmatrix} 1.52 \cdot \lambda_h & 0 \\ 0 & 1.733 \end{bmatrix} \tag{53}$$

Eq. (53) means that

$$\hat{A}_i^f = 1.733 \cdot A_i^f \tag{54}$$

which is identical to the transformation introduced in Koutsellis et al. (2022b) for the case of the hyperbolic tangent transfer function.

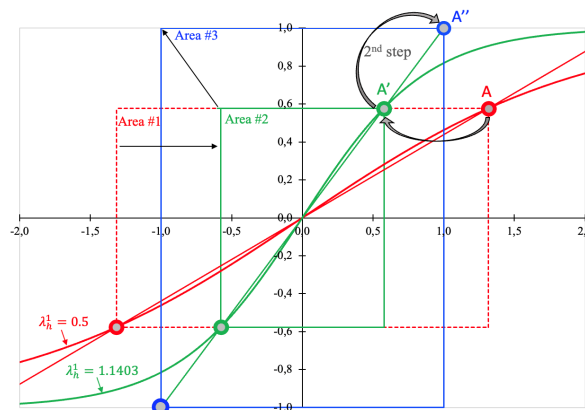


Figure 8: Sigmoid functions f_s and their corresponding y_s when $\lambda_s=0.5$ (red lines) and $\lambda_s^1=4.5579$ (green lines)

1.6 Software implementation: the “In-Cognitive” tool

There exist several software solutions for FCM design and simulation (see Nikas et al., (2019) and Tsadiras et al., (2021) for detailed accounts). The In-Cognitive software tool¹ is a web-based interactive application for the creation, visualisation, and simulation of FCMs, featuring the methodology presented in Sections 1.3-1.4. It is

¹ <https://github.com/ThemisKoutsellis/InCognitiveApp>

written in the Python programming language (Python 3.7.3) and based on the Bokeh Python library (Bokeh 2.4.0). It consists of a client-side web GUI (front-end) and a web server (back-end), with the former exchanging information and queries with Python code/modules stored in the latter. The front-end uses the JavaScript and HTML/CSS technologies to implement the interaction procedure with the end-user (analyst or otherwise). Both JavaScript and HTML/CSS codes are automatically created by the Python Bokeh framework driven by Python scripts. The back-end is built on top of a Tornado Python web framework. In Figure 9, we briefly illustrate the interaction between the front-end and back-end parts of the In-Cognitive application. As a main functionality, browsers request documents (contents of the web pages) and the server's Python code provides them. The user interacts with the content of documents and ask for services. The document catches these events and afterwards send out feedbacks to the server that listens to these request events.

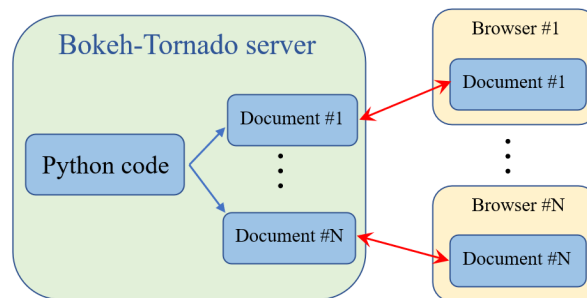


Figure 9: Description of In-Cognitive Python web application

Figure 10 illustrates the developed GUI. It is divided into two subsections: the (a) FCM editor and display layout, and (b) the simulation outcome subsection. The end-user can easily interact with the FCM editor in order to introduce the FCM layout or edit an existing one and configure the FCM by defining the structure and parameters (i.e., node interconnections, weights, input node values/excitations, transfer function). Parameter λ is automatically calculated based on the analysis in Sections 1.3-1.4 and, thus, the end-user need not insert any specific value for this parameter. Finally, the end-user can also alter the format (e.g., size, colour, etc.) of the introduced FCM components (e.g., nodes, edges, etc.) to a preferable format and save afterwards the figure of the introduced FCM layout. In the GUI subsection (b), the outcomes of the FCM simulation executed on the server-side are presented in a user-friendly visualisation. There is also an integrated console, which displays useful information regarding the execution of the corresponding iterative FCM simulation (e.g., warnings, FCM layout information, etc.).

INCOGNITIVE

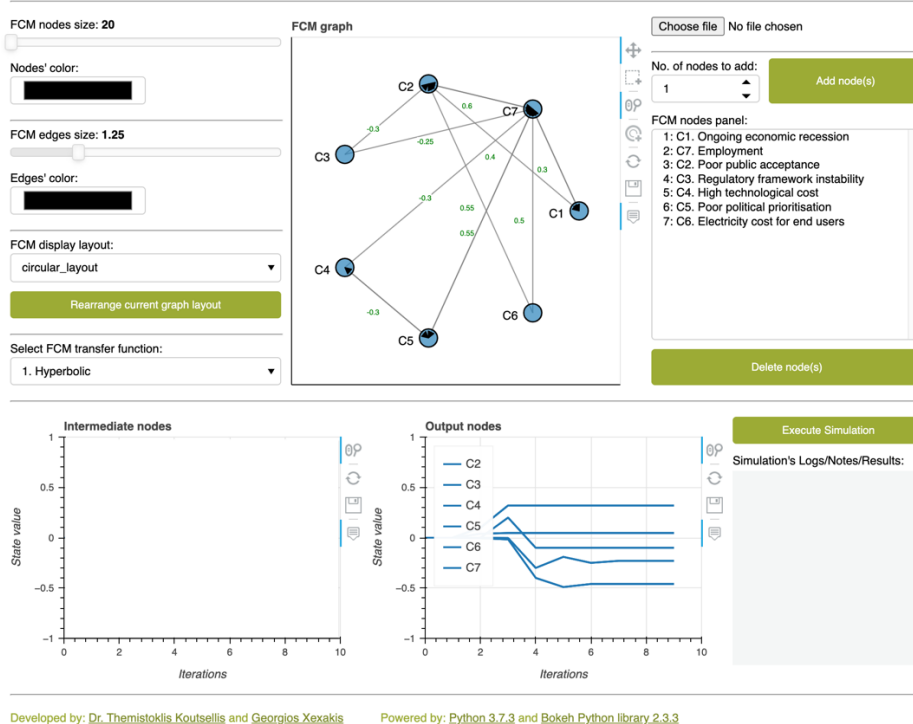


Figure 10: The In-Cognitive GUI

The main contribution of the In-Cognitive web application is the implementation of the methodology of selecting parameter λ as presented in this study (Section 1.3 and 1.4). To our knowledge, all FCM software tools (e.g., Mohr, 1997; Margaritis et al., 2002; Aguilar and Contreras, 2010; Papaioannou et al., 2010; Cheah et al., 2011; Gray et al., 2013; De Franciscis, 2014; Poczęta et al., 2015; Nápoles et al., 2017; Nikas et al., 2017, 2019b; Tsadiras et al., 2021) do not contain any software module to select λ based on the FCM layout. Instead, parameter λ is considered a constant parameter usually equal to one (Nikas et al., 2019b).

For more information on In-Cognitive and the theoretical background, please see Appendix 5)

1.7 Case study validation of the proposed framework and software

There is a plethora of studies applying the FCM theory in energy/climate policy (e.g., Nikas and Doukas, 2016; Nikas et al., 2018, 2019b, 2020a; Doukas and Nikas, 2020). In Nikas et al. (2020a), the authors proposed an FCM layout to identify the most pertinent implementation risks to the diffusion of new solar power before calculating the long-term socioeconomic impacts of wide-scale solar PV deployment in an energy system and macroeconomic analysis in Greece, building on the uncertainty space associated with the identified implementation risks.

Table 1 briefly describes each node/concept of the FCM, while Appendix 1 presents the FCM layout in tabular format. Nodes C_1 to C_9 are the steady nodes. Nodes C_1 to C_5 correspond to the barriers of solar-based energy transition in Greece as suggested by the stakeholders (uncertainty drivers). Nodes C_6 to C_9 correspond to various policies (policy drivers). C_{26} to C_{30} are the output nodes (concepts under examination) and C_{10} to C_{25} are the intermediate nodes that change their values through iterations. Various value combinations of C_1 to C_5 are illustrated in Table 2, representing different socio-economic risk scenarios—i.e., socioeconomic paths (SP), hereafter. We adapt the following abbreviations regarding the various SPs (see Table 2): SP1: Sustainability, SP2: Middle of the road, SP3: Regional rivalry, SP4: Inequality and SP5: Fossil fuelled development. For each SP, four policies, P_1 , P_2 , P_3 and P_4 (see Table 3) are applied to explore their effect on the output nodes. Therefore, the



following input combinations are applied to the introduced FCM: SP1_P1 to SP1_P4, SP2_P1 to SP2_P4, SP3_P1 to SP3_P4, SP4_P1 to SP4_P4 and SP5_P1 to SP5_P4.

Table 1: Node descriptions

Node	Description	Operation
C1	B1. Ongoing economic recession	Input node
C2	B2. Poor public acceptance	Input node
C3	B3. Regulatory framework instability	Input node
C4	B4. High technological cost	Input node
C5	B5. Poor political prioritisation	Input node
C6	P1. Financial incentives for large-scale projects	Input node
C7	P2. Enhanced land-use planning	Input node
C8	P3. Wide-scale deployment of smart meters	Input node
C9	P4. Financial incentives for storage units and devices	Input node
C10	S1. Monitoring capacity for energy consumption	Intermediate node
C11	S2. Control of utility bills	Intermediate node
C12	S3. Privacy invasion concerns	Intermediate node
C13	S4. Demand flexibility	Intermediate node
C14	S5. Trust in institutions	Intermediate node
C15	S6. Development of large-scale solar projects	Intermediate node
C16	S7. Technological lock-ins	Intermediate node
C17	S8. Share of lignite in the energy mix	Intermediate node
C18	S9. Share of RES in the power generation mix	Intermediate node
C19	S10. Grid stability	Intermediate node
C20	S11. Wholesale electricity prices	Intermediate node
C21	S12. Energy security	Intermediate node
C22	S13. Coal mining jobs	Intermediate node
C23	S14. Small-scale energy storage	Intermediate node
C24	S15. 'Green' engineering and consulting jobs	Intermediate



		node
C25	S16. Not-In-My-Backyard complaints	Intermediate node
C26	C1. Electricity costs for end-users	Output node
C27	C2. Economic growth in the long-term	Output node
C28	C3. Investments	Output node
C29	C4. Employment	Output node
C30	C5. Tariff deficits	Output node

Table 2: Socio-economic risk scenarios

Node	Node values				
	Sustainability	Middle of the road	Regional rivalry	Inequality	Fossil-fuelled development
C1	-0.5	0.1	-0.2	0.6	-0.7
C2	-0.7	-0.1	0.65	0.75	-0.7
C3	-0.8	-0.1	0.6	0.8	-0.8
C4	-0.7	0.2	-0.1	-0.35	-0.7
C5	-0.6	0.2	0.6	0.9	0.15

Table 3: Policies and corresponding input nodes

Nodes	Policies			
	Policy 1 (P1)	Policy 2 (P2)	Policy 3 (P3)	Policy 4 (P4)
C6	1	0	0	0
C7	0	1	0	0
C8	0	0	1	0
C9	0	0	0	1

After applying the analysis of Section 1.4, the norms of matrix \mathbf{W}^* of FCM layout of Appendix 1 are:

$$\|\mathbf{W}^*\|_F \approx 1.522, \quad (55)$$

$$\|\mathbf{W}^*\|_\infty \approx 2.708\lambda_h^1 \approx 1.1403 \quad (56)$$

And

$$\|\mathbf{W}^*\|_s \approx 1.421 \quad (57)$$

From Eq. (26) to (29)

$$\lambda'_s = \frac{4}{\|\mathbf{W}^*\|_F} = \frac{4}{1.522} \approx 2.628, \quad (58)$$

$$\lambda'_h = \frac{1}{\|\mathbf{W}^*\|_F} = \frac{1}{1.522} \approx 0.657, \quad (59)$$

$$\lambda_s^* = \frac{1.317}{\|\mathbf{W}^*\|_s} = \frac{1.317}{1.421} \approx 0.927, \quad (60)$$

$$\lambda_h^* = \frac{1.14}{\|\mathbf{W}^*\|_\infty} = \frac{1.14}{2.708} \approx 0.421 \quad (61)$$

Finally, from Eq. (21) and (22)



$$\lambda_s < \min(2.628, 0.927) = 0.927 \quad (62)$$

And

$$\lambda_h < \min(0.657, 0.421) = 0.421 \quad (63)$$

In this example the smallest bounds for both λ_s and λ_h are equal to the proposed ones (see Section 1.3.3.2).

All simulations are performed and visualised in the “In-Cognitive” software application in the sub-sections below. In Section 1.6.1, we illustrate the results of FCM simulations for S2_P3 (S2: Middle of the road, P3: Wide-scale deployment of smart meters) when the FCM is equipped with hyperbolic tangent transfer function. The values of parameters λ vary so that we can reach to useful conclusion regarding the analysis of Sections 1.3 and 1.4 (we include the proposed bound $\lambda_h = 0.421$ as well). Moreover, the final concept values, A_i^k , is not normalised so that we can compare the results for various λ values. The normalisation procedure described in Sections 1.3.3.3 and 1.4.2 is only applied to lambdas smaller than the proposed bounds, λ_s^* and λ_h^* . In contrast, the normalisation procedure and the proposed $\lambda_h = 0.421$ are only applied in Section 1.7.2.

1.7.1 Hyperbolic tangent FCM for different parameter λ values

Figures 11-15 present the distributions of arguments x_i^k 's of Eq. (8) for all intermediate and output nodes through all iterations. For all $\lambda_h \leq 0.421$ the arguments do not exceed the turning points (Figures 11 and 12); the arguments always lie in the almost-linear region. For $\lambda = 1$ (Figure 13), a commonly used value in FCM simulations, the arguments are already out of the turning points and the A_i^k 's values have distortion due to the curved regions of the transfer function. We also observe that the greater the lambda parameter, the more arguments fall within the tails of the transfer function; consequently more A_i^k receive ± 1 value (see Figures 14 and 15). Due to this effect, the final output vector is dense around the ± 1 region, making the inferences ambiguous (see Table 4 for $\lambda = 10$ to $\lambda = 100$). This observation is in accordance with the analysis in Section 1.3.2 where we concluded that the greater the lambda parameter ($\lambda \rightarrow \infty$), the closer to the step function the transfer function gets, and the final node values get close to ± 1 (undesired condition). In this specific application, for $\lambda_h > \lambda'_h = 0.657$ (i.e., Table 4 for $\lambda = 1$ to $\lambda = 100$) the FCM concludes to a fixed-point despite, according to Axelrod et al., (2015), the existence of a fixed point not being guaranteed for $\lambda_h > \lambda'_h$. This means that, if we try different excitations (other than S2_P3), we may get chaotic FCM behaviour when $\lambda_h > \lambda'_h = 0.657$. Finally, it is worth pointing out that the ordering of final output values is different when λ varies (Table 5), as expected by the analysis in Section 1.3—the variation refers to the stage before normalisation.



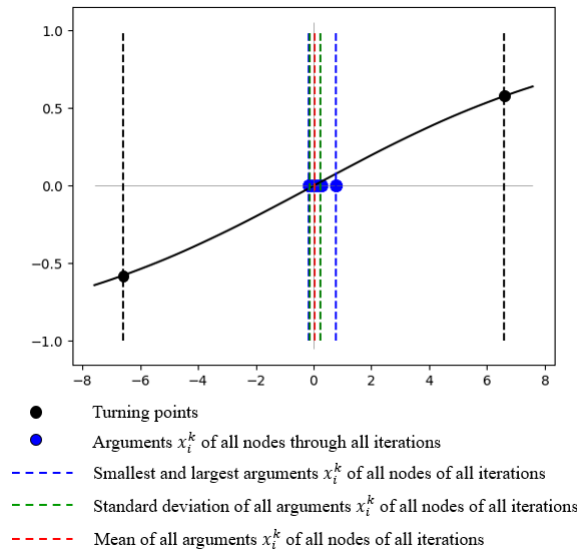


Figure 11: Hyperbolic tangent FCM with $\lambda=0.1$, SP: middle of the road, policy: P3 (SP2_P3)

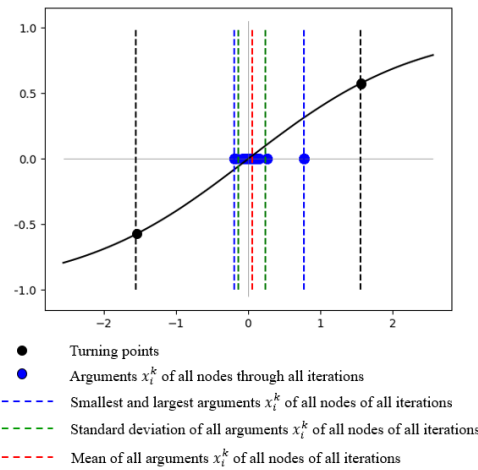


Figure 12: Hyperbolic tangent FCM with $\lambda=0.421$, SP: middle of the road, policy: P3 (SP2_P3)

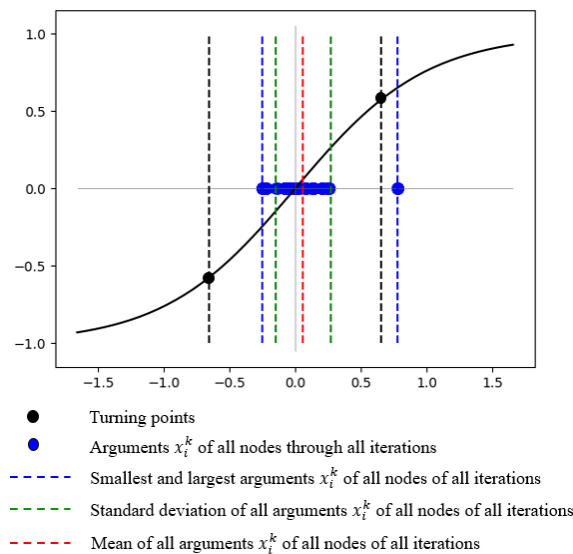


Figure 13: Hyperbolic tangent FCM with $\lambda=1$, SP: middle of the road, policy: P3 (SP2_P3)



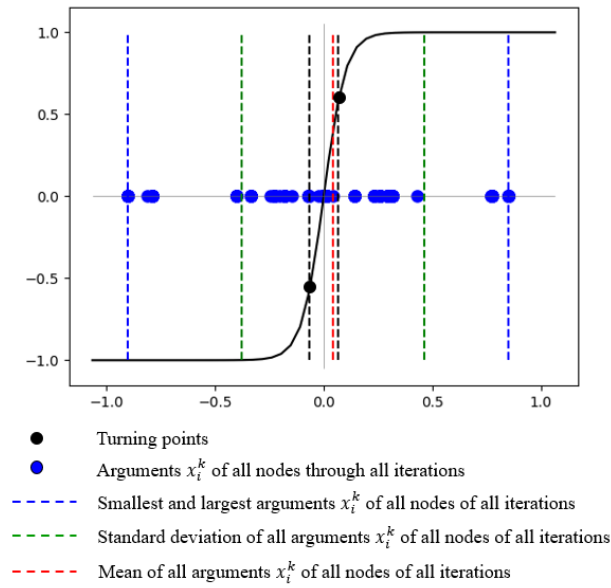


Figure 14: Hyperbolic tangent FCM with $\lambda=10$, SP: middle of the road, policy: P3 (SP2_P3)

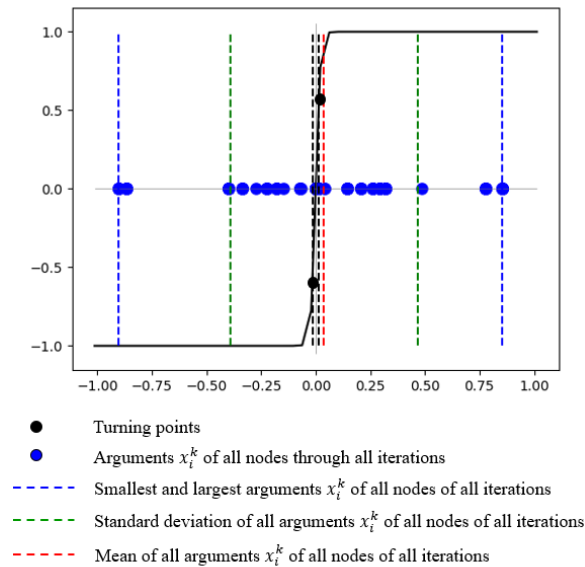


Figure 15: Hyperbolic tangent FCM with $\lambda=50$, SP: middle of the road, policy: P3 (SP2_P3)

Table 4: FCM output node values for different parameters λ

		Node final values					
		Node	$\lambda=0.1$	$\lambda=0.421$	$\lambda=1$	$\lambda=10$	$\lambda=50$
Output nodes	C26	-9.9313E-05	-0.00717	-0.08205	-0.99934	-1	-1
	C27	0	0	0	0	0	0
	C28	-2.4574E-04	0.00356	0.07818	0.98154	1	1
	C29	0	0	0	0	0	0
	C30	1.3504E-03	0.02886	0.20616	1.00000	1	1

Table 5: Ordering of FCM output node values for different parameters λ

		Nodes/Concepts					
		$\lambda=0.1$	$\lambda=0.421$	$\lambda=1$	$\lambda=10$	$\lambda=50$	$\lambda=100$
Ascending ordering		C28	C26	C26	C26	C26	C26
		C26	C27	C27	C27	C27	C27
		C27	C29	C29	C29	C29	C29
		C29	C28	C28	C28	C28	C28
		C30	C30	C30	C30	C30	C30

1.7.2 Proposed parameter λ values with normalised final output vector

Figure 16 illustrates the values of all intermediate and output nodes during all iterations when the excitation is S2_P3 and $\lambda_h = 0.421$. All of them are normalised based on Eq. (33). The distribution of all arguments (Eq. (8)) through all iterations are as in Figure 12. We can see that, for all x_i^k and their corresponding A_i^k values, the almost linear region is much larger. This happens due to the given SP2_P3 excitation. Different excitation would yield different distribution of x_i^k values but all these distributions would fall within the almost linear region because $\lambda_h = 0.421 < \lambda_h^* \approx 0.4211$. Finally, it should be noted that values do not fall within a narrow band region and therefore their ordering is clear and closer to a realistic representation of relative values of each node's deviation. This happens because, in the almost linear region, the deviations of A_i^k values are proportional to the deviations of x_i^k values (see Section 1.3.2).

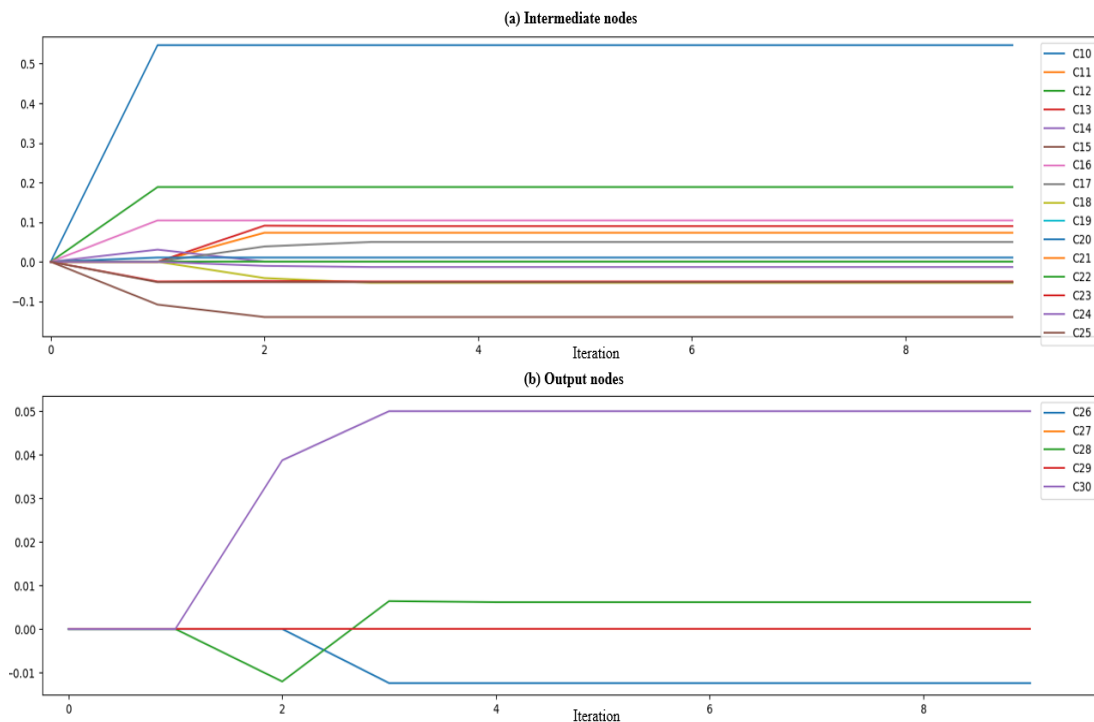


Figure 16: All iterations of hyperbolic tangent FCM with $\lambda=0.421$ and normalised final values, SP: middle of the road, policy: P3 (SP2_P3)

1.8 Remarks and conclusions

We have proposed a framework for identifying a value for parameter λ for both log-sigmoid and hyperbolic



tangent FCM transfer functions. With the previous state-of-the-art λ values, the transfer function was active for all possible f values. Given that both transfer functions have a curved region close to their tails (see Figure 4) thereby creating distortion, final node values usually concluded to an overcrowded region (close to 0 and 1 or ± 1 , respectively), hence unclear inference. To tackle this barrier, we proposed that transfer functions should operate in the almost linear region (see Figure 4). The latter requirement yielded a certain bound for parameter λ . We also demonstrated why parameter λ should not be excessively large or small (see Section 1.3.2). Therefore, we reached the conclusion that parameter λ must be as close to the proposed bounds in Eq. (21) and Eq. (22). The analysis was performed for FCMs with or without steady nodes. We also proposed a normalisation procedure so that outcomes are clear, distinct, and sufficient for inferences.

Based on the proposed methodology, we furthermore developed a web software application written in Python, called "In-Cognitive", containing a user-friendly GUI that allows non-expert users to connect to the server, define the FCM layout (e.g., nodes, their weight interconnection, input state vector if any, etc.) and then request the results. The choice of parameter λ is taken endogenously based on Sections 1.3 and 1.4.

Finally, by using the "In-Cognitive" software application, we ran a simulation of an FCM layout drawn from a real-world application in the literature (Nikas et al., 2020c), validating the methodological takeaways of Sections 1.3 and 1.4.

The parameter λ bounds that are proposed in this research aim to contribute to the hitherto ambiguity of FCM implementation and results, since different parameters λ yield different FCM outcomes and therefore different inferences. By providing an objective criterion to select a unique parameter λ we hope to contribute to further exploitation of FCM theory in research and policy-/decision-making.

A caveat of this study is that it focuses on a parameter of the transfer function that is defined by the analyst. On one hand, this means that other parameters defined by the analyst have not been touched. For example, as a prospect of our research, the impact of the choice of transfer function (among sigmoid and hyperbolic tangent) on the robustness of the inference/results must be thoroughly examined. This also applies for parameter d_i of the driver function (Eq. 2) and the extent to which it can retain its physical meaning in the FCM model simulation. On the other hand, this caveat also means that the impact of aspects of the FCM model that are (largely) defined by the decision-makers, such as the FCM layout and the weight matrix, must also be further explored. On the latter, much research has been carried out in the form of learning algorithms; however, the extent to which the simulation outcomes change with regard to input data uncertainty (e.g., via Monte Carlo analysis in the weight matrix) is largely understudied. Future research should finally focus on improving the proposed normalisation procedure, which squashes node values to a smaller range based on the presented example, thereby rendering differences within the final state vector less distinct and therefore any conclusion harder.



2 Navigating through an energy crisis: challenges and progress towards electricity decarbonisation, reliability, and affordability in Italy

This section has been submitted and is currently under review in *Energy Research & Social Science*:

- Frilingou, N., Xexakis, G., Koasidis, K., Nikas, A., Campagnolo, L., Delpiazzi, E., Chiodi, A., Gargiulo, M., McWilliams, B., Koutsellis, T., & Doukas, H. (2022). Navigating through an energy crisis: challenges and progress towards electricity decarbonisation, reliability, and affordability in Italy. *Energy Research & Social Science*, under review.

2.1 Introduction

Halfway through 2022, the global economy has been witnessing rising inflation and a growing crisis in both food and energy markets, alongside a slower-than-expected recovery from COVID-19 and Russia's invasion of Ukraine in February 2022 (IMF, 2022). In this troubling context, the European Union (EU) is facing an additional challenge: a potential disruption of natural gas imports from Russia, the Union's biggest importer of natural gas (42% in 2020 (Eurostat, 2022b)). Such disruption presents a significant threat to the bloc's energy security and affordability, prompting Member States to plan for rapid reduction of their gas demand towards late 2022 (Council of the EU, 2022).

Among Member States, Italy can be particularly vulnerable by such potential disruption of gas supply. Natural gas dominates the Italian power market, making up almost half its electricity mix (Ritchie et al., 2020); in 2020, 92.8% of this gas was imported, with 43% of these imports coming from Russia (Eurostat, 2020b). At the same time, Italy is facing multiple socio-political challenges, including political instability and a sprawling bureaucracy (Gratton et al., 2021) as well as steadily increasing poverty, unemployment, and net income inequality (ASviS, 2021). This suggests that a sustainable solution to the current energy crisis for Italy need not only achieve energy security and decrease resource dependency, but also avoid exacerbating existing problems by achieving *inter alia* political consensus, administrative effectiveness, and reduced economic burden to the most vulnerable.

The multi-faceted challenge of the current crisis may be, at least partly, addressed by diversifying the EU's natural gas supplies, as suggested in the recent REPowerEU plan for limiting the bloc's reliance on Russian fossil fuels (European Commission, 2022a). Such diversification necessitates additional fossil-fuel infrastructure around Europe, such as liquified natural gas (LNG) terminals, thereby raising stark warnings that this route may jeopardise the EU's net-zero transition (Höhne et al., 2022). On the other hand, ramping up the rollout of renewable energy and heat pumps to reduce reliance on Russian gas while achieving EU climate targets may also require high investment costs and rapid build-up (Pedersen et al., 2022). It is thus evident that navigating through the current energy crisis requires effective and acceptable trade-offs between different energy dimensions.

Based on the United Nations' Sustainable Development Goals (SDGs) for 2030, three core dimensions are assumed for a sustainable energy system (SDG7): affordability, reliability, and provision of clean—and, especially for developing nations, modern—energy services (UN, 2015). All three are relevant in the Italian context, considering the role of natural gas in the country's energy mix and its contribution in power system flexibility (Papaefthymiou et al., 2018), as well as the high share of nation-wide energy poverty, estimated at 8-11% in 2016 (Faiella and Lavecchia, 2021) notably with significant regional disparities (Bardazzi et al., 2021). While the EU has adopted the SDG framework as part of its sustainability policies (European Commission, 2021), progress has been slow in terms of producing tangible domestic political outcomes across Member States (Biermann et al., 2022), as well as within



countries (e.g., unequal North-South progress in Italy (D'Adamo et al., 2021)). As this progress may be even further slowed down by the current energy crisis, domestic decarbonisation pathways must consider new energy supply chains and geopolitical concerns as well as an enhanced role for energy security and affordability.

Energy-sector transformation is scientifically studied and quantitatively assessed in science and practice using energy-system (Chiodi et al., 2015) and/or integrated assessment models (Nikas et al., 2019a)—this is also the case for Italy's roadmap to a low-carbon/net-zero future (e.g., Deane et al., 2015; Borasio and Moret, 2022; Gaeta et al., 2022). Considering the firm links between energy transitions and SDGs (Von Stechow et al., 2016) and the capacity of these tools to explore several aspects of sustainable development outside climate action (van Soest et al., 2019), integrated assessment models can also be used to delve into co-benefits and trade-offs of energy-sector transformations with other SDGs (Soergel et al., 2021b). Nonetheless, such modelling studies typically take time to conduct, which renders them detached from real-time energy decision-making support in emergencies, including international conflicts with large implications for energy trade, security of supply, availability, and prices. This is especially relevant for Russia's invasion of Ukraine and the energy policy/market responses to it, which altogether may critically disrupt energy transitions and sustainability (Kemfert et al., 2022). A vital consideration for modelling scientists, before setting out to timely assess current energy geopolitics and implications for Europe's path to net-zero under these circumstances, lies in today's highly uncertain market and policy environment. For example, fossil fuel price projections constitute a key input into models and an important driver of their cost-optimisation process—and, currently, there is no up-to-date authoritative outlook for future fossil fuel prices (Doukas and Nikas, 2022).

This research thus turns to experts, whose perceptions have been found critical in supporting and/or guiding the 'best available science' of quantitative systems modelling (Peters, 2016), for example by highlighting hidden risks (van Vliet et al., 2020) or prioritising technological solutions (Wilson et al., 2019) that are relevant and must be considered in energy research and policy. Towards eliciting Italian experts' perspectives of how the country can achieve energy-sector broad sustainability amidst a crisis of energy supply and price spikes fuelled by international conflict, here we employ fuzzy cognitive maps (FCMs) (Kosko, 1986). These have been widely established as a stakeholder-driven decision-making methodology in the energy (Nikas et al., 2019b), climate (Doukas and Nikas, 2020), and environmental (Mourhir, 2021; Castro, 2022) problem domains, notably for linking expert knowledge and modelling work (van Vliet et al., 2010; Nikas et al., 2020a). Since the adoption of the SDG agenda, FCMs have also been used to assess a diversity of dimensions of the entire SDG spectrum (e.g., Nikas et al., 2020a; Nasirzadeh et al., 2020), including issues of relevance to SDG7, such as power-sector decarbonisation (Antosiewicz et al., 2020) and energy affordability (Papada et al., 2019).

Section 2.2 introduces the adapted FCM methodological framework employed. Section 2.3 delves into the problem domain, offering an overview of the Italian context for energy-system decarbonisation, attempting to establish the links between selected policy instruments and current uncertainties on the one hand, and the power sector, energy market, citizens, and national SDG7 progress on the other. Section 2.4 discusses the insights gained in an expert workshop held in Venice, Italy in July 2022, focusing on broader energy sustainability in Italy in light of Russia's invasion of Ukraine, and quantifies these insights for the purposes of the FCM exercise. Section 2.5 presents the simulation analysis and discusses the results, while Section 3.6 summarises key takeaways for research and policy.

2.2 Methods & Tools

This research employs FCMs to extract stakeholders' knowledge towards understanding—and helping them understand—how they perceive the Italian electricity generation system, as well as the impact of different strategies and uncertainties on it. The FCM methodology builds on the cognitive mapping approach to graphically



representing and qualitatively assessing system causality and dynamics (Huff, 1990), by employing fuzzy logic and computational processes used in artificial neural networks (Papageorgiou et al., 2004). Our framework is broken down into three steps (Figure 17).

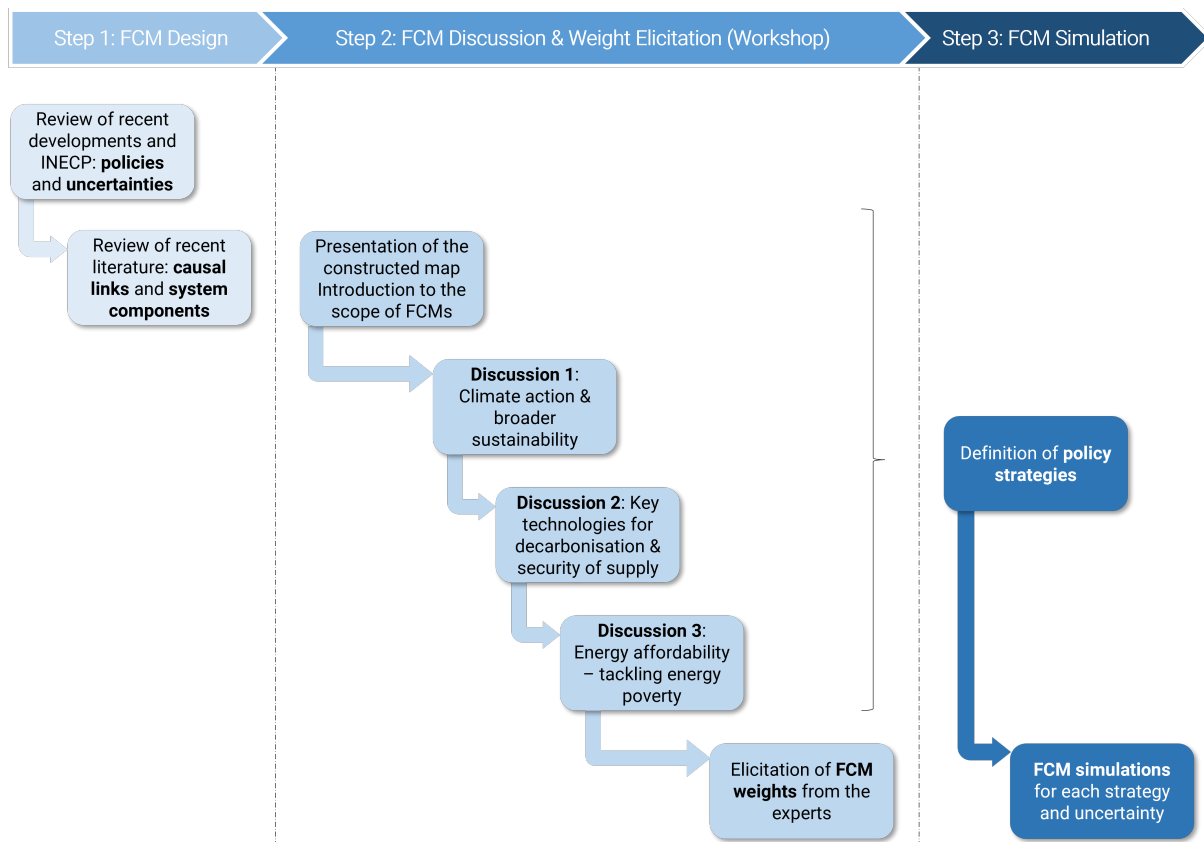


Figure 17: Employed FCM methodological framework

The first step entails the design of the map (Section 2.3). Contrary to most stakeholder-driven FCM studies in this domain (e.g., Papageorgiou et al., 2004; Özemi and Özemi, 2004; Gray et al., 2014a), our study differs in that the map is designed *a priori*, based on desk research on the Italian power sector, which includes review of recent literature, current developments, and latest national legislation. Considering the time requirements of the FCM design process *per se*, our approach allows us to invest more time in discussing with experts the SDG7 dimensions for Italy (affordability, decarbonisation, reliability).

The stakeholder workshop constitutes the second step and entails introducing the designed map as well as the FCM background and scope to experts in the country, discussing with them all dimensions relevant to energy-sector sustainability as reflected and represented in the map, and eliciting from them the importance of the interconnections among the FCM concepts (Section 2.4) in a structured approach. For the purposes of this research, we used a Google survey² that experts were asked to fill in electronically. To facilitate participants without access to a smartphone/computer at the time, the questionnaire was also handed out as a printed table (Appendix 2).

The final step is map simulation (Section 2.5). Mimicking that of an artificial neural network, the FCM simulation

² <https://forms.gle/tcPi552wGUBf3uuOA>

process attempts to capture the perceived causal propagation within a system, by understanding the impact of an exogenous shock on the concepts comprising the system. We use In-Cognitive, an open-source tool for FCM illustration and simulation (Koutsellis et al., 2022b), for which more information and its theoretical background, can be seen in Appendix 5. The mathematical framework of the FCM simulation is detailed in Appendix 3.

2.3 Designing the FCM for the Italian power sector

Generally, FCMs comprise three types of nodes/concepts (Kokkinos et al., 2018): (a) drivers, which only influence other nodes and are typically used to induce system shocks; (b) receiver(s), which are only influenced by other nodes and are typically used to represent the objective(s) of the application; and (c) ordinary nodes, which both influence and are influenced by other nodes and are typically used to represent components of the system, via which drivers' influence propagates to the receivers. Here, we distinguish two types of driver nodes: policies and uncertainties. We first dive into Italy's most recent energy and climate strategy vis-à-vis the EU's updated objectives and energy response to the Ukraine conflict, towards fleshing out broad policy nodes (Section 2.3.1). With progress to SDG7 being the main objective (i.e., receiver node), Section 2.3.2 then documents insights from the literature into how the selected policy nodes may enable this progress, leading to the identification of the map's system (ordinary) nodes. Finally, Section 2.3.3 extracts transition-related concerns from the literature, while considering the current energy crisis, to define relevant important uncertainties, negative developments about which may hinder SDG7 progress.

2.3.1 Policy nodes

The 2019 Italian National Energy and Climate Plan (INECP) sets binding targets, contributions, and policies for decarbonising the economy, promoting energy efficiency, securing energy supply, transforming domestic energy market and interconnectivity, as well as prioritising research and innovation (R&I) in clean energy (Ministry of Economic Development, 2019) (Table 6).

Table 6: Key policy targets stemming from the INECP

Focus area	Key takeaways
Whole-system decarbonisation	The INECP commits to a 30% contribution of renewable energy sources (RES) to gross final energy consumption by 2030, which constitutes a big leap from current levels (20.4%), despite previous overperformance in the country's 2020 target of 17% (Eurostat, 2020c). More importantly, however, this points to a large ambition gap from EU targets, which were set at 40% in the 'Fit for 55' package (European Commission, 2021) and then further upgraded in July 2022 to 45% in the EU's REPowerEU plan setting out how to eliminate its dependency on Russian fossil fuels (European Commission, 2022a).
Energy efficiency	The INECP indicates a ~10% drop in final energy consumption by 2030, compared to 2020 levels, mostly to be achieved in the residential and transport sectors and much less in the commercial and industrial sectors. This is supported by obligation schemes and policies, such as Conto Termico (Thermal Account), and tax reduction schemes like Ecobonus that aim to speed up the energy efficiency uptake and protect vulnerable households.
Energy security	The INECP underlines that phasing out imported coal by 2025 must be supported by widespread use of renewable energy. With the electricity sector being key, the country aims for a 55% share of RES in power generation by 2030, primarily through solar and wind energy. The increase of renewables in the power sector must be underpinned by significant investments (€46 billion by 2030) for upgrading and digitalising network infrastructure, with a focus on strengthening smart grids in large municipalities, and by new storage systems aiming to add 10GW of storage capacity by 2030. Additionally, a



	series of economic and fiscal instruments are proposed, including <i>inter alia</i> support of distributed storage systems installations, tax deductions and incentives for stimulating private R&I investments, exemptions from self-consumption charges for small units, promotion of power purchase agreements for large RES plants, and doubling the budget share for public research into clean energy.
Regulatory reforms	The INECP explicitly targets the regulatory framework towards facilitating investments, streamlining authorisation procedures for new plants and energy communities, and protecting consumers facing energy poverty (Shyu, 2021), which are key towards clean and affordable energy. In particular, the plan calls for removing administrative barriers and introducing automated tools for granting financial support to energy-poor households. Furthermore, it supports the construction of small-scale RES plants by merging authorisation, network connection, and support mechanisms into a single process, while recognising the role of energy communities in reaching consensus over authorisation of new plants at the local level. The FER 1 Decree provides support to the most mature large-scale RES plants through a feed-in tariff or a two-way sliding feed-in premium (Ministry of Economic Development, 2019). Both small- and large-scale renewables can benefit from a stable regulatory framework that is streamlined across regions. Guidelines on suitable areas for RES plants are set in Legislative Decree 17/2022, where regions are referenced when identifying areas within their territory (Ministry for Ecological Transition, 2022).
Citizen engagement	The INECP clearly acknowledges that, despite primarily entailing a shift in terms of fuels and technologies, energy transition in Italy would also heavily rely upon sociopolitical aspects. Given the large land and sea surface needed as well as the different levels of governance involved in the decision-making process, stakeholder engagement throughout the selection and construction process of renewable plants is imperative to reach consensus. Citizen participation is also envisaged through information programs aiming to increase awareness on how to achieve energy savings and promote behavioural change.

In this context, we identify eight broad policy instruments and initiatives currently in place and/or debated for achieving progress towards a clean, reliable, and secure Italian energy power sector—see policies (P_x) in Table 7.

Table 7: FCM nodes, including policies (P_x), system components (S_x), and uncertainties (U_x)

ID	Short description
P1.	Increased solar and wind capacity
P2.	Modernisation of the electricity grid
P3.	Financing R&I
P4.	Regulatory reform and economic incentives for RES
P5.	Provision of information and technical assistance to citizens
P6.	Support of the digitalisation of energy supply and demand
P7.	Investments in new natural gas infrastructure, with or without CCS
P8.	Promotion of energy efficiency measures
S1.	Natural gas imports
S2.	Carbon lock-in effects
S3.	Land loss & devaluation
S4.	Deployment of digital technologies



S5.	Multi-level governance
S6.	Wholesale electricity prices
S7.	Public-private partnership for RES
S8.	Electricity system decarbonisation
S9.	Energy storage
S10.	R&I in energy
S11.	Energy sector employment
S12.	Electricity demand
S13.	Electricity system affordability
S14.	Decentralisation of energy
S15.	Energy communities
S16.	Societal acceptance/behavioural changes
S17.	Share of natural gas in the electricity mix
S18.	Electricity system reliability
S19.	Share of renewables in the electricity mix
S20.	Progress in SDG 7
U1.	Regulatory and political environment stability
U2.	Technological costs
U3.	Citizen awareness & engagement
U4.	International conflict & price shocks

2.3.2 System nodes

Having defined the policy nodes, we then explore how these can promote energy-sector sustainability by reviewing the literature and determining the chains of linear cause-and-effect relationships between each policy and SDG7. Following the approach outlined in (Song et al., 2020), we identify 20 system components (S_x)—see Table 7.

Starting from P1, a policy framework increasing solar and wind capacity in line with the INECP primarily aims to boost the share of RES in the electricity mix (S19). This, however, also entails strengthening administrative decentralisation; Decrees No. 387/2003 and No. 28/2011 render Italian regions and municipalities responsible for all but offshore wind RES installations, thereby fostering energy decentralisation (S14) (Di Nucci and Prontera, 2021). At the same time, as the INECP promotes self-consumption and small-scale renewable installations that already make up a large chunk of RES in Italy (Pierro et al., 2021), a decentralised power system (S14) can foster the development of initiatives from energy communities (S15), by enabling distributed renewable production (Lowitzsch et al., 2020) and increasing grid reliability (S18), through improved load balancing of growing intermittent sources. A more reliable electricity system (S18) can then drive reductions in wholesale electricity prices (S6), by integrating new resources at lower costs (Hsieh and Anderson, 2017).

Energy communities (S15) play another vital role in the transition, by directly increasing the share of renewables in the electricity mix (S19), as well as promoting a transition to prosumerism, thereby also encouraging patterns of behavioural change (S16) and enhancing citizen agency in the transition (Di Silvestre et al., 2019). Their participatory processes can potentially increase societal acceptance (S16) (Spandagos et al., 2022) of energy saving



practices and/or adoption of energy-sufficient profiles, by co-designing and supporting local energy efficiency measures (Gjorgievski et al., 2021) and therefore contributing to lower electricity demand (S12).

Apart from advancing decarbonisation of the electricity system (S8) (Borasio and Moret, 2022), a larger share of renewables (S19) will require considerable investments in energy storage (S9) to account for intermittency and load balancing effects (Pierro et al., 2021; (Domínguez-Garabitos et al., 2022; Ministry of Development et al., 2019); improving energy storage capacity can provide grid flexibility (S18) and help tackle the asynchronous power generation (Al Kez et al., 2020). Lower costs of intermittent RES, compared to those of natural gas-powered electricity in the country, may also enhance affordability (S13) (Antweiler and Muesgens, 2021; Bompard et al., 2020), which can in turn help reduce energy poverty (Siksnyte-Butkiene, 2022). On the other hand, renewable energy technologies such as onshore wind and open-field solar photovoltaics require many acres of land to develop at-scale; this may prove detrimental to landscape and property values in concerned areas (S3) (Betakova et al., 2015; Karimi and Rodi, 2022; Yenneti et al., 2016). The potential impact of increasing solar and wind power on landscapes and seaside in Italy (S3) has in the past given rise to social opposition and NIMBYism within the communities involved—it can, therefore, hinder the development of RES facilities (S16) (Leiren et al., 2020; O' Neil, 2020).

Eventually, a growing share of renewables will shrink natural gas (S17) in the Italian electricity mix, possibly affecting energy-sector employment (S11). Assuming that the RES sector can be more labour-intensive than the fossil fuel-based power sector in fossil-fuel importing countries like Italy, the net effect of RES expansion may be positive, provided however that this is supported with re-skilling initiatives (Pierro et al., 2021; Fragkos and Paroussos, 2018), to ensure a just transition and opportunities for vulnerable and marginalised communities (boyle et al., 2021). Decreasing natural gas in the Italian electricity mix (S17) will also drive down gas imports (S1) and, considering the current energy prices crisis, this may lead to decreased wholesale electricity prices (S6), as demand in the long run will be compensated by RES supply.

Being one of its core pillars, increased affordability (S13) can help Italy make progress in SDG7 (S20) (Villavicencio Calzadilla and Mauger, 2018) and increase public acceptance of RES uptake (S16). However, affordable electricity may also increase demand (S12) (Sorrell, 2015), as lower prices may encourage increased consumption unless mitigated by behavioural changes. Considering that the current electricity mix is ~60% reliant on fossil fuels (Ritchie et al., 2020), additional demand in the near-term may hinder decarbonisation of the electricity sector (S8) in the longer run and, in turn, progress towards SDG7 (S20) (IEA et al., 2022).

Figure 18 provides an indicative example of how the FCM was built for P1.



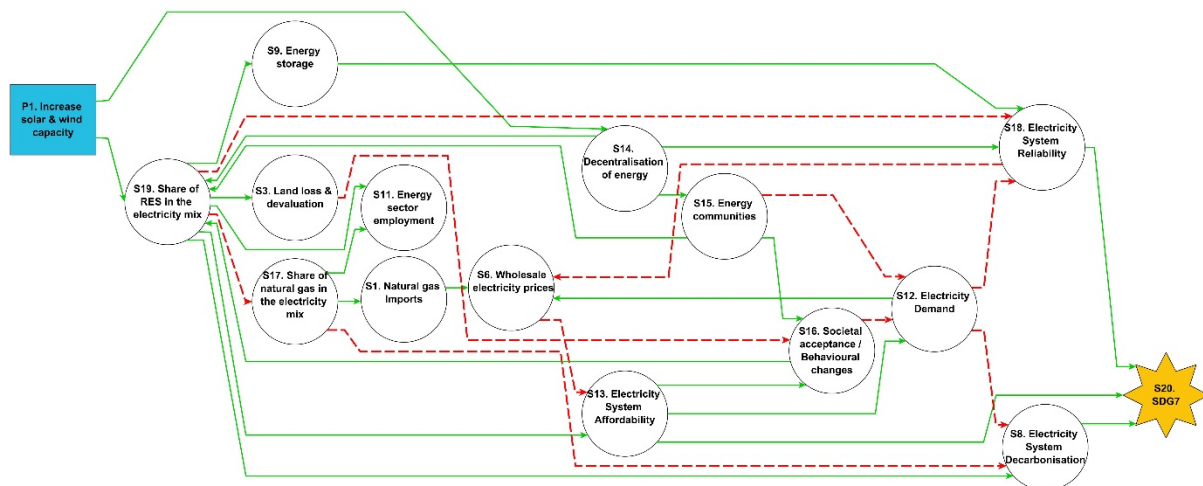


Figure 18: Illustrative example of the FCM design process, for P1 (increasing solar and wind capacity).

The blue square represents the policy (P1), and white ovals represent system components. Green (red) arrows show a positive (negative) relationship—i.e., an increase in the start concept will lead to an increase (reduction) to the end concept.

Policy instruments aiming to drive the modernisation of the electricity grid (P2), as outlined in the INECP and relevant legislation, will enhance grid flexibility and reliability (S18) via upgrades to transmission capacity, promoting the development of smart grids and increasing interconnections both within Italy and with other countries (France, Switzerland, Austria, Slovenia, Greece). The planned high RES capacity, along with Italy's geographical constraints (sea and mountainous regions), render interconnection a key challenge with a 2030 target for capacity to transfer electricity produced to neighbouring countries set at 10%, which is lower than the EU's overall objective of minimum 15% (European Commission, 2018).

A carefully designed investment- and innovation-friendly policy framework (P3) will increase overall R&I in the power sector (S10). R&I in storage technologies, in particular, can enhance technological maturity and improve technical parameters, such as energy density and degradation rates, and thus increase energy storage deployment (S9) (IRENA, 2020a). R&I can also foster the development of power-to-hydrogen projects as long-term storage options (S9), which will help maintain energy-supply stability (S18) (Hu et al., 2020). On the other hand, increasing R&I in carbon capture and storage (CCS) technologies may lead to carbon lock-in effects (Unruh and Carrillo-Hermosilla, 2004) and hence increase the electricity share of natural gas, since CCS-powered natural gas is viewed as consistent with Italy's strategy for decarbonisation (Thimet and Mavromatidis, 2022). R&I can finally lower technological costs for RES (Dinica, 2008; IRENA, 2020b) and thus support public-private partnerships (PPP) for renewables (S7), which will contribute to increasing the share of RES in the power generation mix (S19), while boosting energy-sector employment (S11) (Fragkos and Paroussos, 2018).

Nevertheless, a policy framework providing tax reliefs and incentives for RES as well as simplifying the regulatory framework (P4) can also facilitate PPP for renewables (S7) (Akintoye et al., 2020; Vagliasindi, 2012) by monetising benefits among owners and stakeholders (IRENA, 2020a). Incentives for PVs were introduced in Italy in 2005 through feed-in tariffs and green certificates and resulted in rapid growth of new installations (Antonelli et al., 2018). However, as of 2013, the feed-in benefits are no longer available, and there is now stagnation of new projects. A public investment portfolio that includes regional development of renewables and promotes strengthened partnership across government layers can enhance multi-level governance (S5) (Mizell and Allain-Dupré, 2013), which may in turn promote a decentralised power system (S14) and support energy communities (S15) (Brisbois, 2020) by easing planning and authorisation procedures, engaging with local actors, and promoting knowledge transfer via one stop-shops (Krug et al., 2022). From a regulatory reform perspective, such a strategy can also enhance capacity for multi-level governance (S5) (De Laurentis and Cowell, 2021) and align targets and

actions across regions (Hofbauer et al., 2022). A simplified regulatory framework can also tackle red-tape barriers for RES, thereby increasing their (S19) by lessening administrative constraints or planning and licensing complexities faced by new RES installations (Di Nucci and Prontera, 2021).

From a societal perspective, providing citizens with information and technical assistance (P5) can help them make informed decisions throughout the energy transition, shifting their energy-related behaviours (S16) and increasing their participation in energy efficiency and self-consuming schemes (Caporale and De Lucia, 2015; Sarica et al., 2018).

Digitalisation of electricity supply and demand (P6) through Internet-of-Things (IoT) schemes, smart metering, and smart grids will foster wider deployment of digital technologies (S4) and interconnections within the power system, further supporting its decentralisation (S14) (Wagner and Götz, 2021). Digital technologies (S4) may also bring a shift in behaviour (S16), by helping consumers become self-consumers and prosumers, and allowing them to monitor their electricity demand (Sareen, 2021).

Critically, natural gas is used not only in the power sector but also in industry and the built environment; LNG infrastructure is, thus, very central in the current policy agenda, indicatively with Italian energy infrastructure company SNAM recently acquiring two new floating regasification units. However, policies promoting investments in new gas infrastructure (P7) in the coming years—e.g., (LNG Prime, 2022)—will inevitably lead to strong carbon lock-in (S2) (Brauers et al., 2021). Similar issues may arise from recent plans to reopen closed coal plants in response to the current energy crisis (Nature, 2022).

Finally, policy measures that support energy efficiency schemes (P8), in line with the ‘energy efficiency first’ principle, can contribute to energy demand cuts (Brugger et al., 2021). Here, the focus is on electricity demand and market, although we acknowledge that such measures can strongly impact natural gas demand and market alike, as over half of residential heating is gas-powered (Eurostat, 2020a).

2.3.3 Uncertainty nodes

In light of well-established areas of concern surrounding the energy transition, as reflected in the literature, and the current energy crisis, we finally identify four critical uncertainties (U_x) that could significantly impact Italy’s progress in SDG7 (Table 7). A stable regulatory framework (U1) with favourable policies towards renewables and political stability throughout its deployment may facilitate R&I (S10) in energy by lowering investment risks. Additionally, framework stability can directly promote renewables (S19) and thus decrease the share of natural gas (S17) (Bellantuono, 2018). In contrast, high RES technological costs (U2) may decrease confidence and pose hurdles to creating partnerships for renewables (S7), thereby potentially increasing wholesale electricity prices (S6) (Polzin et al., 2021). Higher levels of citizen awareness and engagement (U3) in local RES generation, trading, and storage can directly support energy communities (Reis et al., 2021; Mihailova et al., 2022). By exemplifying citizens’ contribution in the energy transition and providing clear, transparent, and localised information on renewable energy projects, their benefits and externalities can help increase citizen acceptance (Pellizzone et al., 2015). Additionally, participatory design through local energy communities can also foster acceptance through the realised gains and integration of local needs and concerns (Gjorgievski et al., 2021; Leiren et al., 2020; Caporale and De Lucia, 2015). Finally, the current conflict in Ukraine (U4) increases the need for diversifying natural gas supply, as also stated explicitly in REPowerEU. New LNG terminals (Offshore Technology, 2022) or even new natural gas pipelines are long-lived capital assets that can lead to considerable carbon lock-ins (S2) (Bertram, 2013; Fisch-Romito et al., 2021), while price shocks (U4) such as those observed in 2021-2022 will considerably affect wholesale electricity prices (S6) in the absence of price caps (Gencer and Akcura, 2022; Sgaravatti et al., 2021).

The resulting FCM is presented in Figure 19.



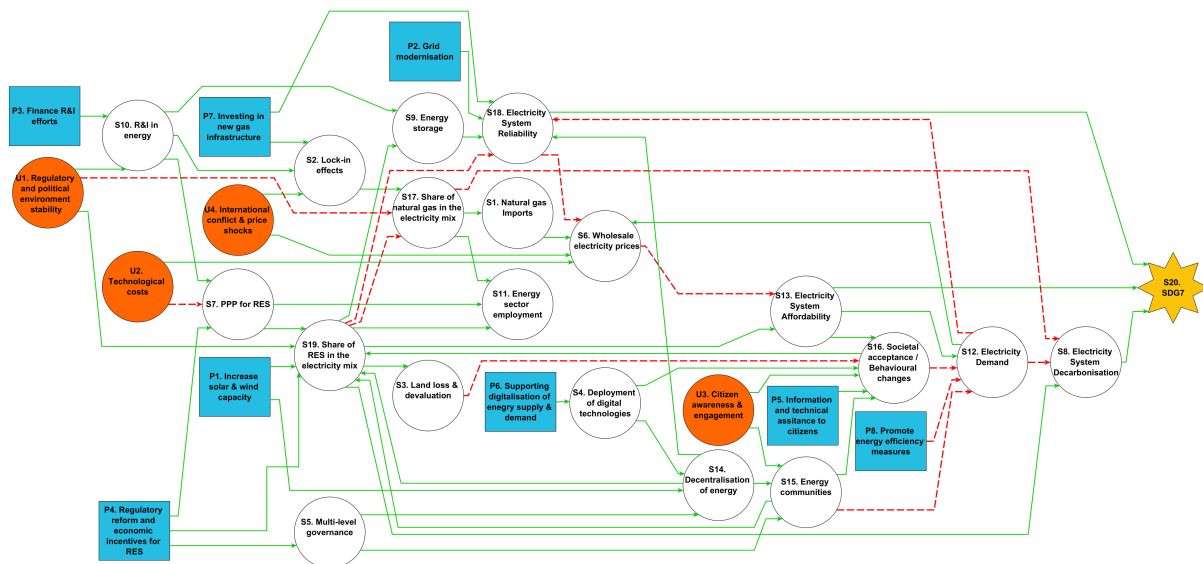


Figure 19: The original FCM designed for the Italian power sector

Blue squares are used for policy concepts (P_x), orange ovals for uncertainty concept (U_x), and white ovals for system components. Green (red) arrows show a positive (negative) relationship—i.e., an increase in the start concept will lead to an increase (reduction) to the end concept; assessment of positive vs. negative interactions is based on the original design process of Section 2.3 – to be validated or contested by stakeholders in Section 2.4.

2.4 Eliciting and quantifying experts' perspectives

An expert workshop was held in Venice, Italy, on 5 July 2022, at the premises of the Ca' Foscari University, aiming to engage with experts to elicit their knowledge, views, and perceptions of Italy's challenges and opportunities emerging from the current energy crisis towards net-zero and progress in SDG7, in both an open discussion and a semi-structured setting using FCMs. The workshop was carried out physically, although the event was also livestreamed to allow as large and diversified an audience as possible, considering COVID-imposed difficulties to join in-person. Experts were identified and invited from contacts of the host university; to ensure objective selection, the initial contact database was screened to identify experts that meet the following criteria: (i) appropriate level of professional knowledge and skills in relevance to Italy's energy-sector decarbonisation and sustainability; and (ii) knowledge of the English language. Eventually, 25 experts joined from four universities, seven research institutes, one economic thinktank, one association, two industries, and one energy poverty NGO. The intention was not to recruit vast numbers, but rather a variety of backgrounds and areas of expertise, to examine the broad possibility space. Ethical standards were put in place, and the workshop was conducted after the approval of the Data Protection Officer of NTUA. Participants were informed that their responses would be anonymous and that Chatham House rules would apply throughout.

Initially, the scope and objectives of the workshop were presented to the participants; this was followed by an introduction to the FCM exercise, including its purpose and methodological framework, as well as a presentation and brief discussion of the designed map (Figure 19).

During the first session of the workshop, experts discussed the interplay between climate mitigation and broader sustainability from both an Italian and an EU perspective. This was kicked off by a presentation on current trends and progress of Italy across SDGs. A more forward-looking study of climate policy implications for EU progress in several SDGs followed, drawing from recent modelling work (Sognaes et al., 2021; Nikas et al., 2021a). Experts highlighted hurdles and delays: notably, poverty in the country is on the rise, agriculture-related pollution remains a challenge despite recent sectoral progress, considerable diffusion of renewables must be realised to double their



share in final energy consumption by 2030, and there is significant ground to cover in terms of unemployment and net-income inequality. Experts indicated that—apart from positive signs in SDGs 7 (clean, reliable, and affordable energy), 13 (climate action), and 16 (peace, justice, and strong institutions) as well as relative stability in SDGs 2 (hunger elimination), 6 (clean water and sanitation), and 9 (innovation)—Italy has been displaying negative trends across the sustainability spectrum. This was deemed to be notably the case for social and human development targets (poverty, equalities, growth and employment, etc.). Other insights stemming from this session include the need to holistically address the SDG spectrum, lack of political will to implement existing measures, limited national stakeholder ownership of EU-level decisions, and the need to restructure schemes to support energy efficiency such as the Ecobonus—whose budget has run dry.

The second session offered a deep dive into the role of key energy technologies, starting with a brief presentation on the various shades (green, blue, grey) of hydrogen and the question mark for CCS, as well as their rollout outside power generation. We also delved into the national energy scenarios currently developed for the Italian government (Gaeta et al., 2022; Kemfert et al., 2022), with a focus on renewables, energy efficiency, and greenhouse gas emissions, as well as a technological discussion of the role of natural gas. The latter was primarily targeted as part of the broader discussion on Italy's near- and longer-term fossil-fuel dependence. In the subsequent discussion, experts noted that the 'Fit for 55' package and the more concrete strategies stemming from REPowerEU are deemed to considerably contribute to reducing reliance on Russia. Nonetheless, RES expansion should also ramp up, with the assumed growth rate (6-7%) being questioned as unrealistic. One concern expressed was the exclusion of behavioural changes and circularity performance from the core national energy scenarios. Although all presentations highlighted CCS use, expectedly taking off post-2030 and making a big chunk of emissions cuts in 2050, experts stressed that Italian policymakers appear not to favour this technology (especially blue hydrogen, from CCS-powered gas). Despite heavy LNG investments widely seen as an unfavourable route, experts also agreed on the need for diversification of fossil gas imports as total gas phase-out by 2050 was contested. There was consensus on the potential of small-scale/rooftop solar installations, and the big role offshore wind can play in energy-system decarbonisation. Finally, nuclear was disregarded as a possible option for the Italian context, and experts clearly saw possible trade-offs emerging among security of supply and emissions reductions, at least in the near-term.

In the third session, the focus shifted from technological and security-of-supply aspects of the energy transition towards the affordability component of SDG7. The session started with a presentation on energy poverty, which offered various definitions and criteria for energy poverty (expenditure-based observations or theoretical modelling, self-reported assessments, or direct smart-meter measurements) that Member States are flexible to establish and use when reporting to the Commission. In Italy, in particular, an alternative Low-Income, High-Cost approach was recently used in the INECP (Camboni et al., 2021), accounting for household income, housing conditions, energy tariffs, behaviours, and special needs. Experts highlighted that Italy has several contrasting policies, including discounts on energy bills per household income/wealth and other subsidies for tax exemptions and regional heating price discounts, which are not well-targeted to address affordability issues. Indicatively, Ecobonus was argued to yield unequal average tax rebates among household income levels, underestimating the needs for the poorest, most vulnerable households. This is in line with previous insights into the effectiveness of longstanding energy schemes for households, such as Bonus Elettrico—in 2012, only 16% of energy-poor households received this bonus and about 80% of awarded households were not *de facto* energy-poor (Miniaci et al., 2014). Insufficiently targeting energy-poor households, coupled with bold tax exemptions stemming from existing policies, led to considerable losses in public revenue flows. Another discussed paradox was the performance of regulated prices during the Ukraine conflict and in the light of the sharp energy price shocks: according to the participants, compared to regulated price contracts based on spot prices, free-market contracts yielded lower utility costs, due to free markets hedging against the price increases and absorbed these shocks in



wholesale electricity. Experts observed that, in the first half of 2022 that was overshadowed by Russia’s invasion of Ukraine and energy price-related implications of associated responses, bold electricity demand cuts among households were inadequate to counterbalance the price shocks, which anyway led to considerably costlier utility bills. Experts, thus, concluded that there is considerable need to rethink how to define and measure energy poverty, as well as to avoid rolling out contrasting policies and to better target redistributive effects, citizen behaviours, policy integration, and fiscal viability. Participants, finally, discussed energy poverty from a macroeconomic perspective (financial system sustainability and broader economic independence, as well as caps on global-level financial speculations on energy and material supply), before notably linking affordability to the supply side. For example, the pressing need to invest in interconnections and concretely defining the role of hydrogen was emphasised to address energy price volatility both in the near-term and in the longer run; moreover, large electricity market reforms were not seen favourably, while experts also discussed the challenges for winter 2022-2023, when scarcities in the European supply system may result in uneven races for fossil-fuel imports and require activating as many system flexibilities and readily available fossil-fuel levers as possible.

Finally, considering all presentations and points raised, experts were asked to populate the FCM in a structured approach. In total, 16 responses were collected from the experts, which were aggregated by calculating the average of all responses (Figure 20).

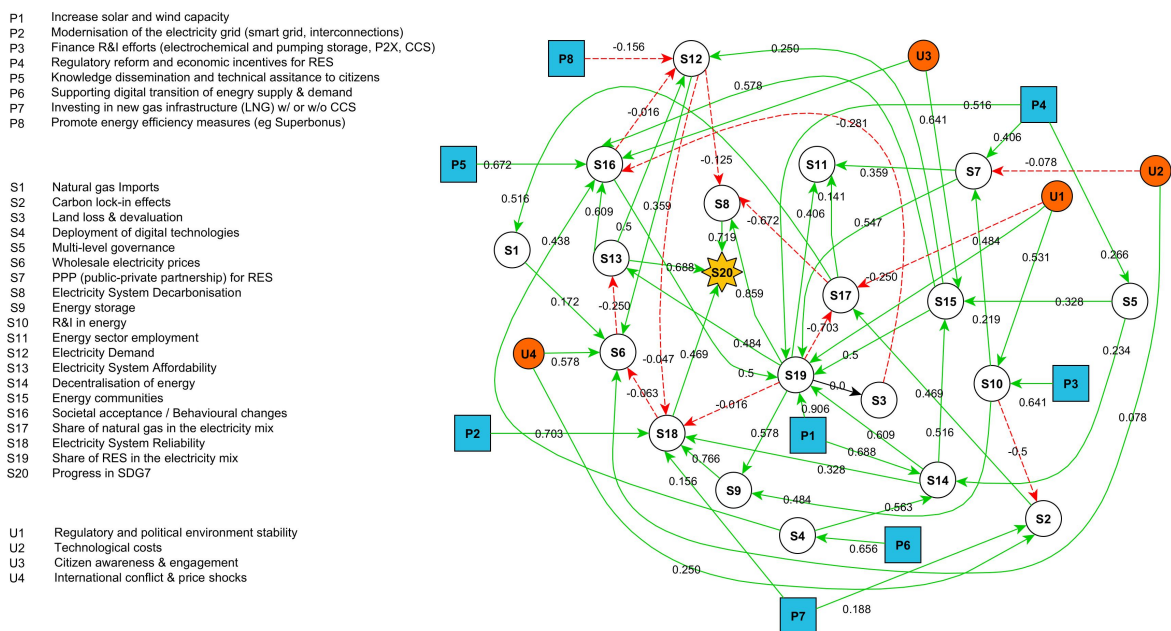


Figure 20: A simplified representation of the final FCM, as adapted from Figure 19 and populated to include the experts’ assessed weights of interactions.

On the left, the legend for all concepts is provided to facilitate readability.

It is noteworthy that, compared to the sign/direction of the impact assumed in the preliminary FCM design (Figure 19), experts’ responses highlighted three underestimated aspects, one concerning the overall effect of energy communities to electricity demand, one regarding the implications of RES expansion for land loss/devaluation, and a third highlighting the role of R&I in carbon lock-in. On the first point, experts seemingly believe that energy communities can have a negative impact (i.e., increase) on electricity demand; this finding was contested after the weight elicitation process, with experts defending their choice by pointing to possible rebound effects and/or misuse of the grid. To some extent, this is in line with insights from the literature on possible negative impacts of such communities, including rebound effects (Kazmi et al., 2021) and increased consumption yielding uneven



burdens across households (Nolden et al., 2020), considering the diversity of business models under current legislation in Italy (Cielo et al., 2021). On the second point, some experts appeared concerned that further diffusion of renewables may have negative impacts on landscapes and land value, unless mitigated by effective and targeted land-use planning with public consultation (Doukas et al., 2020); however, other participants seemingly consider that RES infrastructure may support the development of currently underdeveloped and/or low-impact areas (Fargione et al., 2012) and thus increase their land value. Such contested views, which in our case led to an overall (aggregated) negligible impact of renewables on land value, are largely acknowledged in the literature and demonstrated in various studies (e.g. Ioannidis and Koutsoyiannis, 2021)). On the third point, although experts underlined the role of CCS as an abating technology, most of them seemingly assume either that financing R&I will focus mainly on RES production & storage (Domínguez-Garabitos et al., 2022; Ministry of Development et al., 2019) and will not favour CCS, or that CCS is an essential part of a just transition (Janipour et al., 2021); regardless of the perspective, R&I was overall deemed not to further lock the country into carbon.

2.5 Simulation results and analysis

The scope of the FCM exercise is not to examine each policy instrument alone, but rather to follow a policy integration approach (Biesbroek, 2021) and develop thematic policy strategies that comprise these instruments, in order to simulate how their combination and synergistic effects can impact Italy's energy-sector sustainability, in light of the current challenges. Similar to Nikas et al. (2019b), we identify four policy strategies, each comprising two thematically close policies, based on the elicited stakeholders' knowledge and perspectives as well as our systemic view of the Italian electricity system dynamics.

The first strategy, *"large-scale RES diffusion"*, combines heavy prioritisation of investments in solar and wind power (P1), as well as regulatory reforms required to facilitate RES licensing and regional cooperation and various financing schemes for renewable energy production and storage (P4). This strategy is consistent with several studies highlighting the key role of RES in decarbonisation pathways (Gaeta et al., 2022; Bompard et al., 2020), the need for regulatory simplification in Italy (Di Nucci and Prontera, 2021), and the importance of targeted financial incentives (Prontera, 2021); it also reflects expert views on the imperative need to scale-up RES growth, despite concerns on unrealistic assumed growth rates (see Section 2.4).

The second strategy, *"grid enhancement"*, features policies that focus on upgrading the electricity grid (P2) and integrating interoperable technologies for its digitalisation (P6). In terms of electricity security and adequacy, these policies are considered interrelated and expected to play a critical role in Italy's energy transition (Borasio and Moret, 2022; Ministry of Development et al., 2019), while attesting to the recognised necessity for interconnections by the stakeholders.

Energy efficiency forms a central part of Italy's long-term roadmap and its key role in the green transition (Brugger et al., 2021), job creation (Anna, 2021) and energy poverty alleviation (Camboni et al., 2021) is widely acknowledged. Therefore, the third strategy, *"demand-side transformation"*, encompasses policies accelerating energy efficiency and promoting energy-saving practices (P8), as well as designing and implementing targeted information programmes and providing practical guidance to citizens (P5) to promote behavioural changes and sustainable energy profiles at home.

The final strategy, *"grey investments & innovation"*, includes controversial policies, in which both new natural gas investments are promoted for the diversification of gas imports (P7) and R&I financing is prioritised (P3), focusing not only on green technologies but also on CO₂ abating technologies like CCS, to overcome their technical and commercial barriers and untap their potential for wide-scale deployment. While Italian policymakers do not seem to favour CCS, its use in various mitigation scenarios is assessed as critical (IPCC, 2022), especially for hard-to-



abate sectors (Nikas et al., 2021a; Mapelli et al., 2022).

Having grouped the policies into four policy strategies, the FCM is initially simulated four times, once per strategy, to appreciate how experts qualitatively perceive the impacts of each strategy on the system, absent any negative effect stemming from the uncertainties. Acknowledging that SDG7 refers to clean, reliable, and affordable energy, Figure 21 illustrates the performance of each strategy on these three dimensions of energy sustainability: decarbonisation (S8), affordability (S13), and reliability (S18); the area covered in each triangle corresponds to the aggregated impact on SDG7 progress (S20).

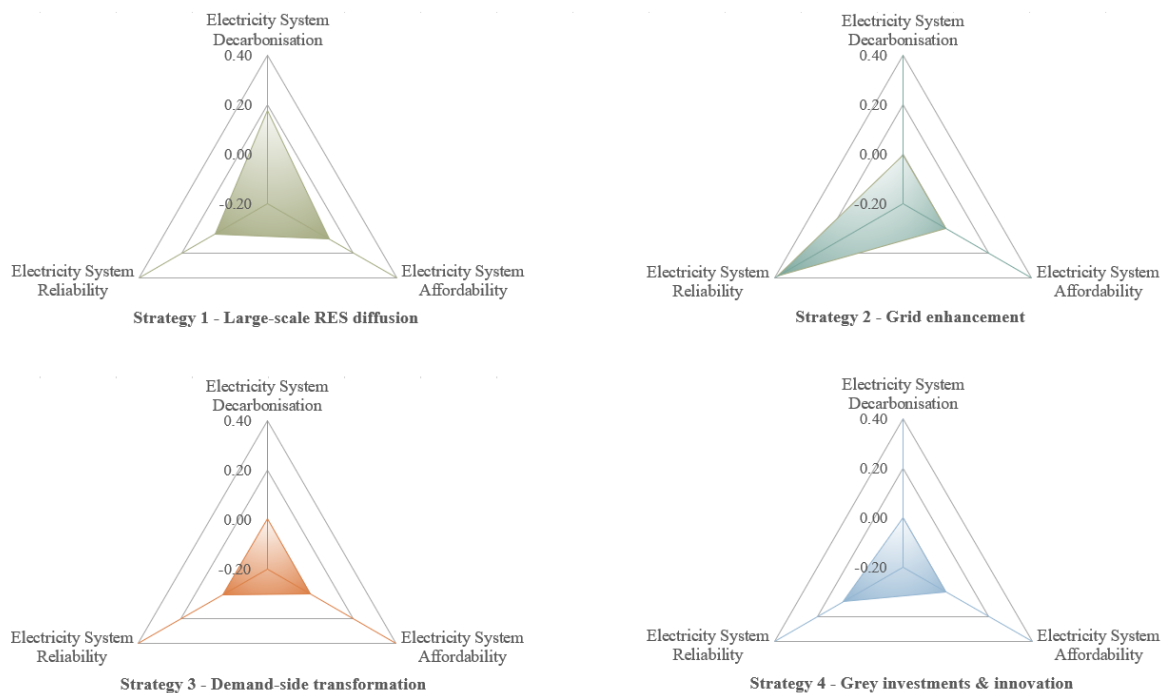


Figure 21: FCM results for the performance of the four policy strategies on the three key dimensions of SDG7 progress in Italy

A first observation is that electricity system decarbonisation is primarily promoted by Strategy 1 (*“large-scale RES diffusion”*), followed by Strategies 3 (*“grey investments & innovation”*) and 2 (*“demand-side transformation”*), although the latter to a much smaller extent. The fourth strategy can, according to our experts, perpetuate Italy’s reliance on fossil fuels (S2), thereby potentially even hindering the ‘clean’ part of the energy sector’s progress to sustainability.

With key affordability drivers being the increase in the share of RES in the electricity mix (S19) and lowered wholesale prices (S2), a considerable increase in energy affordability can only be attributed to Strategy 1, due to the potential for significant growth of renewable energy capacity through investments and regulatory reforms, despite this strategy showing limited effectiveness in driving wholesale electricity prices down. This indicates that RES expansion coupled with access to end-user financing and tax exemption schemes for RES could effectively lower electricity bills even in relatively stable (albeit currently high) wholesale prices. Still in terms of affordability, Figure 21 also highlights that a framework featuring policy instruments promoting energy efficiency and motivating citizens to commit to energy savings (Strategy 3) is perceived not to substantially boost affordability relative to the other three strategies explored, regardless of its potentially very high contribution to lowering energy demand and consequently wholesale prices. This is an interesting takeaway, especially as among the EU’s core responses to the 2022 energy crisis has been to encourage citizens to lower their demand to mitigate the

impact of fuel and electricity price spikes. From a different perspective, this finding indicates that affordability constitutes a much more forward-looking aspect of SDG7, encompassing concepts such as energy poverty and the 'right to energy' (Shyu, 2021), meaning that progress towards this dimension requires more effort than merely countering the negative impacts of the current crisis. Critically, this also stresses the perceived importance of renewables in eventually making energy affordable for Italian households. Nevertheless, the significance of demand-focused policies is showcased in terms of electricity demand (S12): this strategy seemingly is the only to potentially cut electricity demand, underlining that policy instruments solely targeting supply-side changes and improving grid stability may in fact yield electricity demand growth, as lower-cost electricity can lead to rebound effects.

Turning now to system reliability, *"grid enhancement"* is expectedly the most impactful strategy, as it explicitly aims to upgrade grid infrastructure, promote the deployment of digital technologies, and advance decentralisation (S14). Despite their intermittency, high deployment of renewables in Strategy 1 is not perceived to substantially risk stability, since energy storage (S9) and decentralisation are also supported. However, the fourth strategy on *"grey investments & innovation"* is considered more effective in ensuring reliability than the RES-heavy strategy.

Another critical insight can be gained into employment implications of these strategies. Although the overall effect on employment of a shrinking fossil-fuel market and an expanding RES market is often debated (see Section 2.3), experts participating in the FCM exercise assessed the renewable energy market as more labour-intensive: featuring by far the highest gap between an increasing RES share and a decreasing natural gas share, Strategy 1 is deemed to perform best in terms of new energy-sector employment gains (S11).

Ultimately, all four strategies are found to contribute to progress in SDG7, in the absence of critical uncertainties, with the *"large-scale RES diffusion"* (mainly through decarbonisation) and *"grid enhancement"* (mostly via reliability) strategies perceived as the most effective. Surprisingly, *"grey investments & innovation"* do not hinder SDG7 progress; on the contrary this strategy yields a positive impact, which is even higher than that of demand-oriented strategy, mainly via diffusing innovations also towards the green part of the technological spectrum as well as by ensuring supply reliability and diversification. In fact, although the Italian electricity system can become more affordable and less carbon-intensive via a *"demand-side transformation"*, such a strategy only marginally increases reliability, turning out to be the least potent in ensuring SDG7 progress.

Turning the attention to the four uncertainties signifying the unfolding energy crisis and key concerns on Italy's power-system sustainability, we simulate the system four times in the absence of policies, once for each uncertainty, to explore how negative developments can impact Italy's current progress and energy transition. Each uncertainty node was activated to reflect the maximum potential negative/non-desirable impact. Apart from overall SDG7 progress (S20), Figure 22 displays three other central concepts that can hinder the sustainable development of the energy sector, and upon which uncertainties displayed considerable impact: wholesale electricity prices (S6), behavioural changes (S16), and the share of natural gas in the country's power mix (S17).



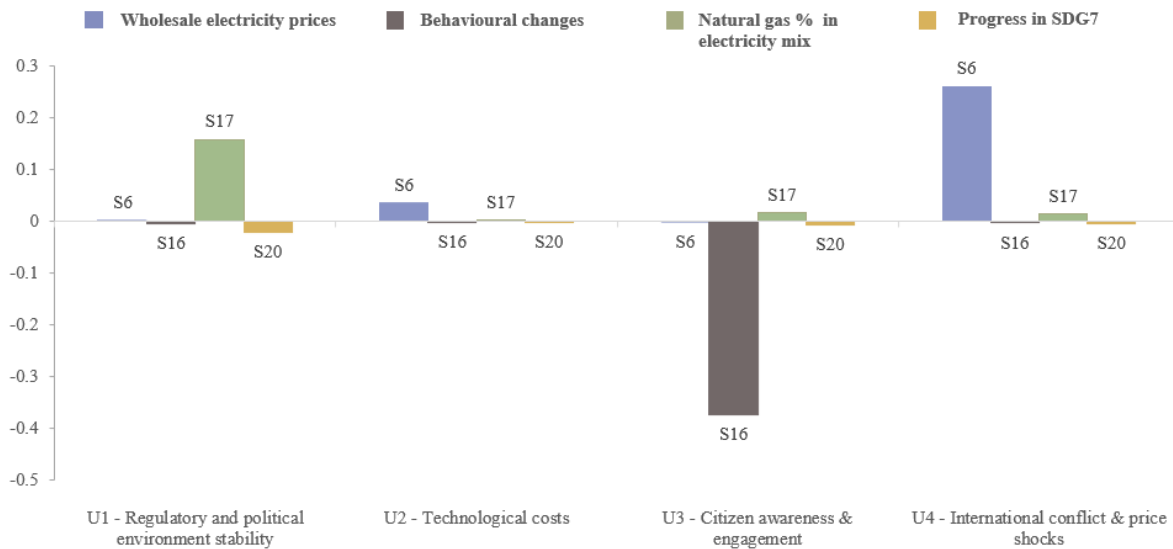


Figure 22: FCM results for the implications of the four uncertainties on wholesale electricity prices, behavioural changes, share of natural gas in the electricity mix, and progress on SDG7.

The most critical uncertainty in terms of progress to SDG7 appears to be a regulatory system with increased propensity to override its policies and limited ability to manage desirable changes and provide market signals (U1). This hints at experts' concerns over the lack of political cohesion and ownership in Italy, which can also be tied to the current political instability in the country. Such unstable regulatory framework may discourage RES investments and further expansion (Bellantuono, 2018), and thus drive an increased reliance on natural gas (S17).

Experts appear to have identified the share of renewables in the electricity mix (S19) as the main driver of affordability and decarbonisation, with its negative impact on reliability considered very low; affordability is also impacted by wholesale prices (S6), but—according to participants—this effect can be effectively offset by increased renewables. This can be contested by considerable international conflict and price volatility (U4) and high technological costs (U2): both uncertainties can foster negative conditions that may in turn mitigate the RES expansion potential while greatly increasing wholesale prices, and thus their overall impact on affordability and subsequent SDG7 progress is not very favourable, underpinning the perceived significance of RES growth in shielding consumers from rising electricity prices.

Lack of citizen participation in the electricity transition (U4) could undermine the necessary shifts in behavioural and consumption patterns (S16) as well as hinder the proliferation of, and active participation in, energy communities (S15). FCM results show that this renders the fourth uncertainty as the second most impactful in terms of RES expansion, with implications for decarbonisation, affordability, and SDG7 progress, despite the effect of the respective strategy (*"demand-side transformation"*) being deemed relatively low. This stresses stakeholders' expressed concern on the exclusion of behavioural aspects from core national energy scenarios (see Section 3.4).

Finally, each strategy is simulated against each uncertainty, to examine how uncertainties impact the performance of the different policy instruments on the core dimensions of SDG7—i.e., decarbonisation, affordability, and reliability (Figure 23). Results suggest that the most impactful uncertainty is regulatory instability, which can significantly hamper the effectiveness of all four strategies, and most notably of the *"demand-side transformation"* and *"grey investments and innovation"* strategies, where SDG7 progress not only drops but even becomes negative. In the case of *"demand-side transformations"*, the calculated negative impact is not a reflection on the widely accepted positive implications of pursuing demand-side policies such as energy efficiency (Rosenow and Eyre, 2022), but that this positive impact of the policies themselves is not enough to counterbalance the wider

negative impacts caused by the uncertainties in the regulatory framework. On the other end of the uncertainty spectrum, high technological costs (U2) appear to have negligible impact on any of the four policy strategies.

From a strategy perspective and despite the high uncertainty, heavy prioritisation of RES investments and targeted financial and regulatory incentives (*"large-scale RES diffusion"*) can be more robust, holistically achieving energy-sector sustainable development, since the impact of possible negative developments in terms of technological costs, levels of international cooperation, and active citizen participation are found limited. The same cannot be said for policies promoting energy demand reductions (*"demand-side transformation"*), especially in case of poor citizen engagement, where decarbonisation is hindered by the adverse effects on energy communities and behavioural changes, and implications on all key SDG 7 components become negative.



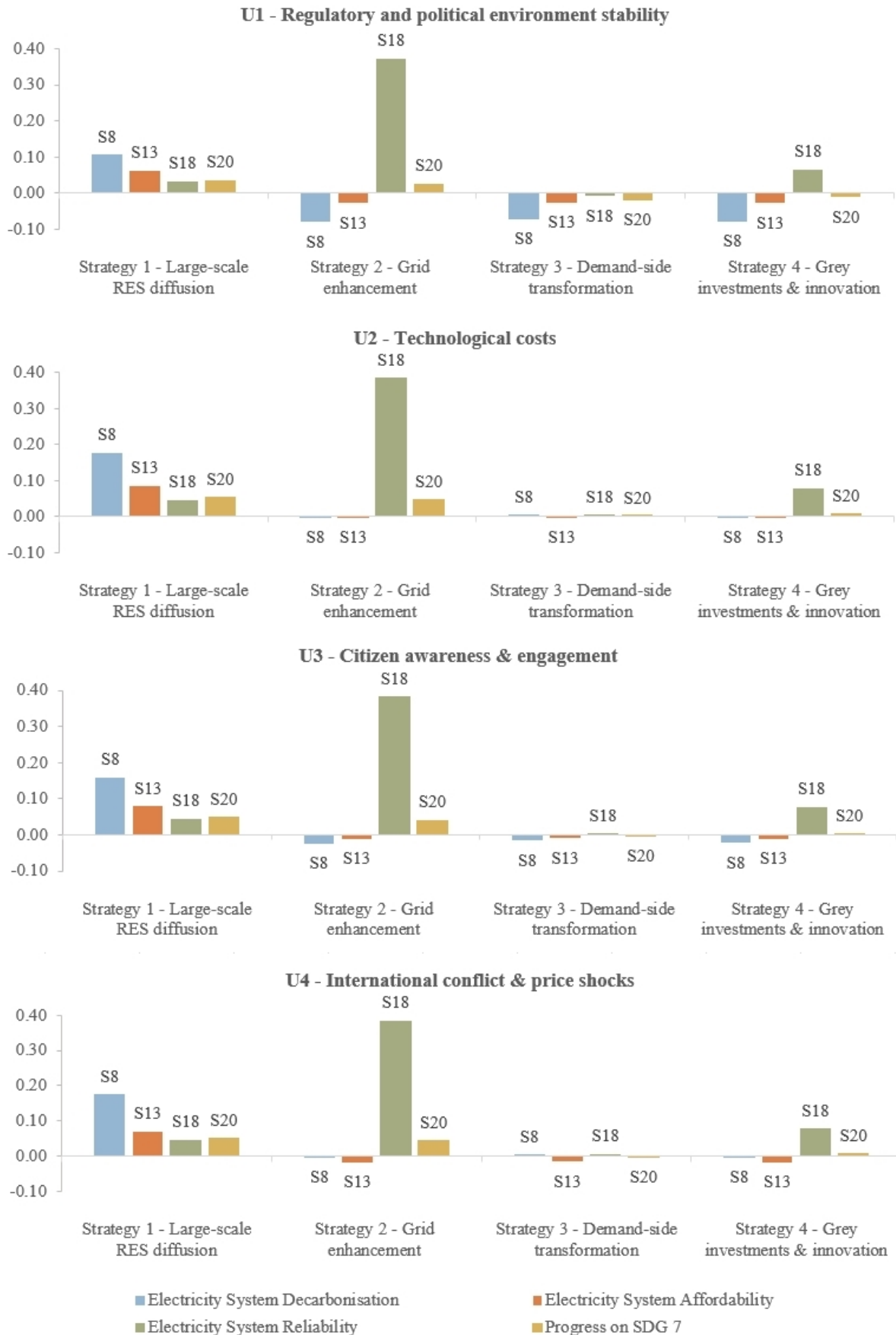


Figure 23: FCM results for the implementation of each policy strategy under uncertainty relative to a no policy – no uncertainty scenario



2.6 Conclusions

The unprecedented wave of crises, including a pandemic, early signs of an impending economic recession, high inflation rates, international conflict, and subsequent energy supply disruptions and price shocks, has brought many challenges for energy transitions and sustainable development worldwide. Among the first COVID-19 hotspots in the EU and highly dependent on Russian natural gas, Italy is particularly affected, with the current energy crisis and the country's response to it also impacting households and possibly its road to net-zero. Policymakers are forced to make high-level decisions, including large investments in natural gas infrastructure and/or renewables, which could divert pathways in unforeseen directions, with contrasting environmental implications in the long-run and fears of fossil-fuel lock-ins lurking. Modelling tools typically used to inform such decisions take time to produce meaningful scenarios, and real-world relevance of such scenarios amidst crises can be contestable owing to high uncertainty of underlying parameters. This research instead proposes the use of FCMs, offering a simplified representation of an energy system based on experts' perceptions, thus enabling informed policy support in a timely manner. The map of Italy's energy sector is constructed and discussed with Italian stakeholders with expertise in the sector's sustainability, which encompasses three dimensions: affordability, decarbonisation, and reliability.

Based on the elicited knowledge and after simulating the perceived impact of policies and uncertainties on the energy system, we find strong preference for policies revolving around RES diffusion, contrary to investments in natural gas, both as a response to the current situation and as a way to achieve progress towards SDG7. This is found consistently across the three dimensions of SDG7, with the policy strategy focusing on renewables decisively contributing to both decarbonisation and affordability—interestingly, with positive implications for reliability as well. According to experts, this strategy is outperformed on this dimension only by a policy mix targeting network enhancements and to a lesser extent by gas investments, which however would both fail to contribute to the other two dimensions. Efforts towards RES diffusion were also found more robust against uncertainties concerning tech costs, citizen participation, and conflict-related developments, further highlighting the preference over a gas-heavy roadmap.

Policies looking at demand-side transformations were also found beneficial, albeit to a lesser extent, but their perceived positive impacts were deemed inadequate to counterbalance potentially undesirable developments. Interestingly, this indicates that—from the engaged experts' perspective—a policy response focused solely on urging citizens to reduce their consumption may prove beneficial in the short run, but in the long run it could fail to have a strong impact on the progress towards energy-sector sustainability. More importantly, its sufficiency as a main response to the energy crisis may even be contested in the shorter term, should large system pressures from negative socioeconomic and technoeconomic developments persist. Focusing on uncertainties, experts stressed that the biggest risk for the Italian energy system—regardless of the strategy adopted—lies in regulatory and political instabilities. Italian policymakers should, thus, move swiftly and with determination towards cleaner transformations of the country's power sector, complementing or even replacing plans for promoting natural gas investments as a response to the current dynamic environment.

Although FCMs can be a very useful tool to timely assist decision makers based on expert perceptions, they should be considered additionally to, rather than instead of, conventional modelling approaches. FCM results are of semi-quantitative nature, meaning that they are not suitable for strictly defining investment mixes, levels of penetration for each technology, and/or concrete transition pathways. Results can, thus, inform high-level decision-making processes and fuel the debate on the examined strategies examined, but they must be interpreted qualitatively (i.e., comparatively between the impact of different strategies across a specific node), and only as a reflection of human perceptions rather than a quantitative system representation. In this respect, energy- and climate-economy modelling research can also extract expert preferences over technologies as well as plausible spectra of



highlighted uncertainties from this study. Finally, since SDG7 constitutes a much broader agenda and set of indicators for sustainable development, future studies can enhance the resolution of the FCM in each dimension considered, for example by explicitly integrating energy poverty as part of the affordability aspect. Future research could also benefit from a fully stakeholder-driven FCM process, entailing the design of the map with the experts rather than from the literature, thereby possibly highlighting different elements.



3 Expectations from and capabilities of climate-economy models for measuring the impact of crises on sustainability

This section has been submitted and is currently under review in *Applied Soft Computing*:

- Koasidis, K., Koutsellis, T., Xexakis, G., Nikas, A., & Doukas, H. (2022). Integrated assessment co-governance using Monte Carlo Fuzzy Cognitive Maps: expectations from and capabilities of climate-economy models for measuring the impact of crises on sustainability. *Applied Soft Computing*, under review.

3.1 Introduction

The way the climate crisis unfolds, with a marked increase of extreme and/or unusual weather and climatic conditions, poses a major threat to today's society and human development, with the world still far from on track to achieving the Paris Agreement goal of limiting global warming to well below 2°C (Peters et al., 2017; Sognaes et al., 2021). The road to delivering on this goal is challenging in terms of political feasibility (Jewell and Cherp, 2020). Despite the promises that current pledges and net-zero commitments may hold, possibly placing the 2°C milestone within grasp (Meinshausen et al., 2022), confidently meeting the Paris Agreement temperature goal means quickly and consistently ramping up climate ambition (Grant, 2022; Ou et al., 2021). The rapid decarbonisation required becomes even more challenging today in the light of a puzzling mix of global emergencies, including an unfolding economic recession, an ever-raging pandemic (COVID-19), and Russia's 2022 invasion of Ukraine, largely driving an energy prices crisis.

Towards facilitating decision-making and underpinning climate policy targets and efforts, integrated assessment models (IAMs) are typically employed as the 'best available science' (Peters, 2016). Forming a key part of major scientific assessment reports, such as the Intergovernmental Panel on Climate Change (IPCC) Sixth Assessment Report (Keppo et al., 2021), these modelling tools help to scientifically advance our understanding of what is needed to mitigate climate change, by offering a very detailed representation of the energy-environment-economy nexus, usually aiming to identify cost-optimal pathways to achieve specific targets. The unavoidable complexity owing to this level of detail, however, alongside high requirements in terms of input data and assumptions, may increase the uncertainty of the results and reduce the transparency of modelling processes—which remain key elements of criticisms to IAMs (Gambhir et al., 2019; Robertson, 2020). To partially address such criticisms, modelling scientists have called for and instigated stakeholder-informed processes, where scenarios are co-created with non-academic actors (Hamilton et al., 2015; Nikas et al., 2021b). However, only a handful of such exercises have managed to include stakeholders in the process (e.g., Nikas et al., 2021a; Ausseil et al., 2019; Rodrigues et al., 2022), with most IAMs still being considered "black boxes" outside the scientific community (Krey et al., 2019). Another critical next step for IAM modellers is to expand their scope to capture and assess interactions of climate with other sustainability dimensions: although the Paris Agreement is tightly intertwined with all of the United Nations' Sustainable Development Goals (SDGs) (von Stechow et al., 2016), the SDG action space of IAMs remains limited (van Vuuren et al., 2022). With the exception of a handful of applications (e.g., Soergel et al., 2021b) the focus of IAM applications remains narrow, targeting few proxy indicators of one (Poblete-Cazenave et al., 2021) or a small subset of SDGs (e.g., van de Ven et al., 2019). At the same time, stakeholder expectations from and capabilities of IAMs with regard to analysis of SDG interactions are not well aligned (van Soest et al., 2019).

To facilitate stakeholder engagement and bridge the gap between modelling scientists and non-experts, the use of Fuzzy Cognitive Maps (FCMs) (Kosko, 1986) has been proposed (van Vliet et al., 2010). Compared to quantitative systems models such as IAMs, FCMs offer a much more simplified representation of the causal relations and propagation within complex systems (Stylios and Groumpos, 2004), while incorporating human knowledge and



perception to make up for missing quantitative data (Papageorgiou et al., 2017), as they are usually constructed for as well as with stakeholders (Özesmi and Özesmi, 2004). Therefore, they constitute a useful tool for creating a comfortable space within the scientific process for non-experts, while also unlocking complex systems and offering a representation and visualisation that is comprehensible to all audiences, allowing them to draw useful results that they can trust and convert into practical action. Application areas in the broad energy-climate-environment-sustainability domain include inter alia building energy management systems (Mpelogianni and Groumpos, 2019), analysis of circular bioeconomy potentials (Kokkinos et al., 2020), temperature forecasting (Poczęta et al., 2018a), prediction of electricity consumption (Poczęta et al., 2018b), understanding of haze-fog formation (Peng et al., 2017), risk analysis for renewable energy sources (Rezaee et al., 2019; Nikas et al., 2020a), waste flow management (Morone et al., 2021), crop yield prediction and classification (Papageorgiou et al., 2013; Natarajan et al., 2016), urban sustainability (Assunção et al., 2020), and even progress assessment towards sustainable development goals in the light of COVID-19 (Ameli et al., 2022). Narrowing down to the energy and climate policy domain, applications have considerably increased recently (Doukas and Nikas, 2020), with FCMs being either coupled with (e.g., Antosiewicz et al., 2020; Nikas et al., 2020a), or intended to inform (e.g., Song et al., 2020), conventional modelling approaches such as energy system and integrated assessment models.

Despite their uncontested contribution to transparency and stakeholder engagement, including in integrated environmental assessments (Mourhir, 2021), FCMs have also received great criticisms over their capacity to handle uncertain information (Baykasoğlu and Gölcük, 2021). Key limitations revolve around their dependence on initial choices made by the analyst rather than the domain experts (Papageorgiou, 2010), such as the selection of the method for extracting stakeholder knowledge or the choice of transfer functions and parameters, as well as around the risks of non-convergence/-solution depending on the map structure and inputs (Nápoles et al., 2016). Common attempts to handle uncertainty include manual configurations and simulations based on a diversity of transfer functions and parameters to identify common patterns in the results (Knight et al., 2014). On the other hand, more elaborate attempts to introduce probabilistic uncertainty have resulted in optimisation requirements to avoid convergence issues (Sacchelli and Fabbrizzi, 2015), leading to losses of the cognitive information provided by the stakeholders. Recent research in the convergence of FCMs (Harmati et al., 2021) and selection of transfer function parameters (Koutsellis et al., 2022b) have paved the way for more concretely incorporating uncertainty in FCMs. Notably, Baykasoğlu and Gölcük (2021) drew on progress in calculating fixed points and introduced alpha-cuts from fuzzy logic in FCMs, to produce a range of output values for each node, allowing to represent part of the underlying uncertainty; however, as the left and right values of the fuzzy sets are not bound to appear at the same time across all inputs, part of the uncertainty remains unrepresented.

In this context, this study has a twofold objective. First, to extend the representation of uncertainty in FCMs, by introducing stochastic uncertainty based on Monte Carlo simulations to FCMs, an approach found promising in similar fields like fuzzy agent-based modelling (Raoufi and Fayek, 2020), multi-criteria decision making (Koasidis et al., 2022b) and portfolio analysis (Forouli et al., 2020), yet untested in FCMs (Nguyen and Fayek, 2022). Second, to inform IAMs on sustainable policy priorities, to increase their capacity to respond to broader sustainability questions and enhance their preparedness to tackle multi-faceted challenges. Drawing from calls to enhance the role of FCMs in integrated environmental assessment (Mourhir, 2021), we develop and employ a hybrid Monte Carlo-Fuzzy Cognitive Mapping (MCFCM) approach in a case study simulating the impact of financial crises (e.g., recession), health emergencies (e.g., pandemic), and international conflicts (e.g., war) resembling contemporary challenges that touch upon and jeopardise progress in several sustainable development goals (SDGs). With the crises constituting a major source of uncertainty, and the representation of sustainability dimensions on conventional quantitative modelling approaches only recently starting to unravel, this study draws from a global survey of modellers and experts over the importance of SDG interactions from an integrated assessment modelling perspective and over the current capabilities of IAMs to represent these interactions (van Soest et al., 2019).



Overall, the study aims to answer three research questions:

- What is the impact of a financial crisis, a health emergency, and an international conflict across the entire SDG landscape based on an FCM simulation of causal relationships among the SDGs?
- How do these causal relationships differ between experts and IAM modellers and how are their perceptions constrained by current modelling capabilities?
- What is the added value in terms of the provided uncertainty-induced information of an MCFCM approach contrary to the conventional FCM?

The rest of the study is organised as follows. Section 3.2 describes the methodology followed, introducing the integration of Monte Carlo in FCMs and presenting the construction of the SDG maps used. Section 3.3 reports the results of the FCM simulation, while Section 3.4 discusses these results aiming to address the study's research questions. Finally, Section 3.5 summarises the main outcomes and concludes with suggestions for future research.

3.2 Methods and tools

In this section, we present the MCFCM framework, including a brief introduction to FCM scope, structure, and mathematical background as well as a discussion on the selection and optimisation of the transfer function (Section 2.1), and a presentation of the proposed methodological novelty of integrating Monte Carlo simulations in FCMs (Section 2.2). Moreover, we discuss in detail the construction of the study's FCM and design the simulation scenarios (Section 2.3).

3.2.1 Fuzzy cognitive maps: concepts and mathematical formulation

An FCM consists of nodes and edges, with nodes representing concepts of a cognitive framework and edges how these concepts are interconnected, in terms of direction and degree (weight) of the influence among them. An initial value is provided to a subset of the nodes considered as exogenous nodes—also referred to as drivers and/or senders—of the system to activate the map. Then, the FCM is simulated to calculate the impact of the input on all system nodes, via the causal propagation of this input throughout the represented system, based on the following iterative expression:

$$A_i^{k+1} = f_h(x_i^k) = f_h\left(\sum_{j=1, j \neq i}^n (w_{ij}A_j^k + A_i^k)\right) \quad (64)$$

where $A_i^{(k+1)}$ is the value of concept i at the end of iteration k , A_i^k is the value of concept i at the beginning of iteration k , A_j^k is the value of concept j at the beginning of iteration k , n is the number of concepts included in the FCM, w_{ij} is the weight of the causal relationship between preceding concept j and following concept i , and f_h is a transfer function typically used to squash values within the FCM value domain.

Although there are several transfer functions used in the FCM literature, two are the most prominent: the S-shaped sigmoid function (Eq. 65) and the generalised version of the hyperbolic tangent function (Eq. 66) (Groumpos and Stylios, 2000):

$$f(x) = \frac{1}{1 + \exp(-\lambda x)} \quad (65)$$



$$f_h = \frac{\exp(\lambda x) - \exp(-\lambda x)}{\exp(\lambda x) + \exp(-\lambda x)} = \frac{\exp(2\lambda x) + 1}{\exp(2\lambda x) - 1} \quad (66)$$

Typically, the selection among the two follows the nature of the problem domain: the hyperbolic tangent transfer function squashes values in $[-1,1]$ and therefore allows negative concept values, while the sigmoid function works for positive values in $[0,1]$ and is therefore used in cases where the sign of causal propagation is irrelevant and/or all concept nodes and inputs are assumed *de facto* positive.

Eq. 1 eventually yields the final equilibrium state of FCMs, expecting a convergence of the FCM after $k = N$ iterations. However, said convergence is not always guaranteed (Harmati et al., 2018; Harmati and Kóczy, 2018; Koutsellis et al., 2022b), rendering the introduction of probabilistic uncertainty to FCMs difficult. To ensure convergence, bounding parameter $\hat{\lambda}$ of the transfer functions has been proposed (e.g., Lee and Kwon 2010; Knight et al. 2014). Extending on these research works, Koutsellis et al. (2022b) proposed a formula for parameter $\hat{\lambda}$ to operate within the “almost linear area”. This selection of parameter $\hat{\lambda}$ is derived from the combination of the Sigma and Frobenius norms in the case of the sigmoid transfer function, or from the combination of the Infinite and Frobenius norms in the case of the hyperbolic tangent transfer function. This value is related to the topology of the FCM, and thus is a function of the weight matrix, W . This means that parameter $\hat{\lambda}$ is application-specific.

3.2.2 Integrating Monte Carlo simulations into FCMs

The Monte Carlo simulation approach is a framework to allow assessing the impact of uncertainty propagation throughout a system. In practice, systems are not fully deterministic. Underlying variations or uncertainties may exist throughout a system, including its structure as well as assumed inputs. The Monte Carlo simulation is a brute force procedure to estimate this kind of uncertainty propagation, assuming certain statistical distributions for inputs and/or the parameters of a system, before deriving the corresponding distribution of the output. In the case of FCMs, where the represented system is governed by Eq. (64), we narrow our focus down on the w_{ij} values of the weight matrix and the driver node values A_i^0 , which constitute the key elements driving the FCM outputs, outside the system topology.

Introducing probabilistic uncertainty to weights via Monte Carlo simulations implies that each iteration would yield a different $\hat{\lambda}$, meaning that different weights lead to different $\hat{\lambda}$ and in turn to completely different FCM, which is counterintuitive to the purpose of the Monte Carlo approach. Therefore, we expand the selection of $\hat{\lambda}$ from Koutsellis et al. (2022b) to ensure that each iteration has a universal (constant) $\hat{\lambda}$ without jeopardizing the FCM's convergence, called $\hat{\lambda}_{MC}$, hereafter. To do so, we consider that parameter $\hat{\lambda}$ is a function of all w_{ij} values (except those equal to zero) and, by definition (Koutsellis et al., 2022b), the smallest and therefore safest possible $\hat{\lambda}_{MC}$ value to ensure that FCM simulation always yields results (i.e., does not yield chaotic behaviour) is calculated for $|w_{ij}| = 1, \forall i, j$, except for those referring to non-existent links (i.e., where $w_{ij} = 0$).

On the other hand, performing a Monte Carlo simulation for perturbations to the initial node values is straightforward because these have no impact on the $\hat{\lambda}$ value and therefore do not alter the FCM for each iteration.

The Monte Carlo Fuzzy Cognitive Map (MCFCM) process is illustrated in Figure 24.



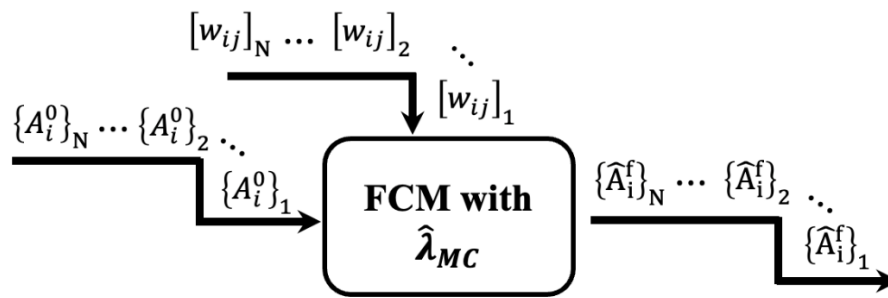


Figure 24: The proposed Monte Carlo FCM (MCFCM) method

To generate the samples of the random variables A_i^0 and w_{ij} based on the initial values, we choose the Beta distribution because it is supported on a bounded interval, as does the FCM input. The original Beta distribution support range is $[0,1]$, which is suitable for the A_i^0 values when the sigmoid transfer function is used (as in this study, see Section 3.2.3). It should be noted, this support range must be extended to $[-1,1]$ when the hyperbolic tangent transfer function is used as well as for the weights, in which case we divide the argument of the Beta distribution by 0.5 and then subtract 1 from the result.

3.2.3 Map construction and scenario design

To answer the research questions posed in Section 1, we employ both the FCM and MCFCM framework on a topology revolving around the sustainable development goals of the United Nations 2030 Agenda for Sustainable Development, introducing each SDG as a node, before adding three input 'crisis nodes', representing three different emergencies: financial crises (e.g., recession, inflation, etc.), health emergencies (e.g., pandemic), and international conflicts (e.g., war). The design of this topology aims to underpin the evaluation of direct and indirect impacts from the examined crises across the entire SDG landscape. The weights of the nodes are configured drawing from a global survey presented in van Soest et al. (2019), in which experts on the one hand and IAM modellers on the other were asked to evaluate the importance of each SDG interaction. Drawing from the expertise of the modellers participating in that study, indications were additionally provided on which interactions can currently or prospectively be represented in state-of-the-art IAMs. Based on this input, we construct four FCMs based on the typology presented in Figure 25, reflecting: (a) the importance of interactions among SDGs, according to experts, without considering modelling capabilities ("experts; no cut-off"); (b) the importance of interactions among SDGs, according to modellers, without considering modelling capabilities ("modellers; no cut-off"); (c) the importance of interactions among SDGs, according to experts but constrained based on modelling capabilities ("experts; cut-off"); and (d) the importance of interactions among SDGs, according to modellers but constrained based on modelling capabilities ("modellers; cut-off").

Considering both the multiple semi-linguistic scales used in van Soest et al. (2019) and the FCM requirements in terms of input, all values are normalised within $[0,1]$, to reflect the importance of the interactions (a very small subset of weights from the original survey are negative and are thus treated here as absolute values for consistency among the maps). To introduce the modelling capabilities, we establish thresholds based on whether an interaction is already represented in models, its representation is underway or planned (weighing differently each one of these options depending on the level of readiness of an interconnection in IAMs), as expressed in van Soest et al. (2019). If the representation is not planned in the foreseeable future, we discard the link from the weight matrix in the cut-off cases. The input 'crisis nodes' are connected to a subset of relevant SDGs, drawing from the recent context e.g., a health emergency is directly linked to SDG3 orbiting around good health and well-being

while, based on recent experience from COVID-19, it is expected to also have direct implications for the economy, which is reflected in SDG8 on sustainable economic growth). Considering the above, we select the sigmoid transfer function for the analysis, since the FCM output must be mapped within $[0,1]$. The complete input dataset used for the four maps can be found in the Supplementary Material (available in Zenodo: <https://doi.org/10.5281/zenodo.7071303>).



Figure 25: FCM typology forming the basis for the construction of the four maps used.

The connection of each SDG to the “Sustainable Development Goals” logo is used as a proxy to imply that all SDGs are in principle interconnected. The exact interconnections and their values in each map can be found in the Supplementary Material (available in Zenodo: <https://doi.org/10.5281/zenodo.7071303>).

For each map, three scenarios are designed. The first scenario introduces a “no crisis” baseline, where the three ‘crisis nodes’ are not activated; this is intended as a comparative basis for the remainder of the analysis. Exploiting the property of the sigmoid function to provide a non-zero solution of the map even without any input and essentially provide a reflection on weight interactions, this baseline is also intended to reflect the importance of each SDG interaction in the absence of any crisis based on perceptions of both expert stakeholders and modelling scientists, and how these are constrained by existing (or foreseen) modelling capacity.

The second scenario constitutes an evaluation of the impact of each crisis on each SDG, without considering any uncertainty. As a first step, each of the three crises is activated independently. We use an activation value of 0.75, representing a “fixed level of crisis” scenario, to allow enough margin for the fluctuations in the Monte Carlo uncertainty analysis at a later stage (third scenario), so as to simulate crises of both higher and lower impact. As a fourth variant of this scenario, the three input nodes are activated simultaneously (with the same activation level of 0.75), to simulate the impact of a combination of crises, resembling today’s conditions. The first two scenarios (“no crisis” and “fixed level of crisis”) are simulated using the original FCM framework, as described in Section 3.2.1.

In the third “crisis under uncertainty” scenario, the MCFCM framework is used to simulate the role of uncertainty on top of the impact of crises. This is performed in three steps:

- First, the activation levels of the crisis nodes are assumed to be of probabilistic nature, with a mean value of 0.75 (as in the no-uncertainty runs) and a standard deviation of 0.2, following the beta distribution as discussed in Section 3.2.2 and doing 1,000 Monte Carlo iterations. This parameterization enables the

simulation of a wide range of crisis levels, including shocks of higher and lower magnitude, intended to reflect the uncertainty of the contemporary environment (context-related uncertainty). For this reason, all crisis nodes are activated at the same time, with the Monte Carlo randomisation process deciding the exact level.

- Second, the Monte Carlo simulation is applied to the weights, keeping the original values of the weight matrix as a mean, and again using a standard deviation of 0.2, following a beta distribution (again, using 1,000 iterations). In this case, inputs are fixed as in the non-uncertainty runs, while once more all input nodes are activated at the same time. This step enables the simulation of the impact of uncertainty introduced by human bias (human-induced uncertainty) in terms of how they perceive the system (i.e., here, interactions/links among SDGs) to operate.
- Third, both the input and the weights are assumed to feature uncertainty simultaneously, and thus Monte Carlo iterations calculate the complete impact and full range of uncertainty propagation throughout the FCM. In this case, Monte Carlo iterations are increased to 10,000, acknowledging the higher complexity.

As discussed in Section 3.2.2, the MCFM in the case of underlying uncertainty of weights yields a different $\hat{\lambda}$ parameter compared to the non-uncertainty runs based on the selection process in Koutsellis et al. (2022b) and the introduced extension. To ensure comparability of the scenarios, the $\hat{\lambda}$ parameter is selected based on the third scenario with the Monte Carlo runs ($\hat{\lambda}_{MC}$), and then used across all three scenarios. The list of $\hat{\lambda}_{MC}$ parameters for each map is presented in the Supplementary Material (available in Zenodo: <https://doi.org/10.5281/zenodo.7071303>).

All simulations are performed using the In-Cognitive FCM simulation tool³, initially presented in Koutsellis et al. (2022b), and significantly expanded to incorporate the MCFM presented here. For more information on In-Cognitive and the theoretical background, please see Appendix 5.

3.3 Results

3.3.1 No-crisis baseline

To establish a benchmark and allow to evaluate the impact of the crises' propagation, the four maps discussed in Section 3.2 are initially simulated without activating the three input nodes corresponding to the crises (Figure 26), thereby representing a "no-crisis" baseline scenario—i.e., a balanced state of the system without disturbances. In the absence of initial input, the final state vector in this baseline scenario reflects the importance of the causal relationships of each node based on experts' and modellers' views and on whether these relationships are constrained by modelling capabilities. Thus, nodes with high values indicate SDGs that are perceived to be strongly affected by other SDGs and vice versa.

Experts appear to consider SDGs to be much more interconnected than modellers do, which is a direct result of the higher number of interactions and the respective weights of node interconnections. In the 'experts' map,

³ <https://github.com/ThemisKoutsellis/InCognitive>



SDG11 on city- and community-level sustainability emerges as the node with the highest level of importance in terms of interactions with the other SDGs, indicating a strong influence of other SDGs on the built environment. SDGs 17 and 16, on global partnerships as well as peace and strong institutions, closely follow SDG11; notably, these two SDGs are typically the most difficult to represent in climate change mitigation modelling (Soergel et al., 2021b). However, numerous other SDGs also feature high levels of importance, indicating that experts perceive most SDGs as well-interlinked across the whole SDG landscape. In contrast, the 'modellers' map features considerably lower evaluations, indicating poverty eradication (SDG1) as the goal that is most influenced by other SDGs—economic indicators of poverty are well-represented in IAMs (van Vuuren et al., 2022) and have been explored in the IAM literature (e.g., Fujimori et al., 2020; Soergel et al., 2021a). This is followed by economic growth (SDG8) and energy-sector sustainability (SDG7), which encompass aspects that are very familiar to the financial approach adopted by most models (Ackerman et al., 2009) and closely linked with the economy and energy modules of an IAM (Nikas et al., 2019a), and which therefore are much closer to the SDGs typically studied in climate-economy modelling practice.

Introducing cut-offs based on the modelling capabilities condenses the FCM results for the experts towards lower scales and better aligns experts' expectations with modellers' priorities, yielding the highest scores for those SDGs that models typically explore (e.g., SDGs 8, 13, 7). This indicates that the opinions, and thus expectations, of the experts are significantly restricted by modelling capabilities (i.e., experts have more ambitious goals/expectations from modelling exercises). On the other hand, the modellers' priorities are not largely dependent on restrictions according to perceived modelling capacity, indicating that their evaluations may be biased, driven by what their models can really study to begin with (i.e., modellers may have these restrictions already built into their thinking). Still, even in the modelling capacity-constrained case, there emerge some notable differences between experts and modellers (i.e., in the ordering), further highlighting the importance of exploiting expert knowledge to guide modelling studies.



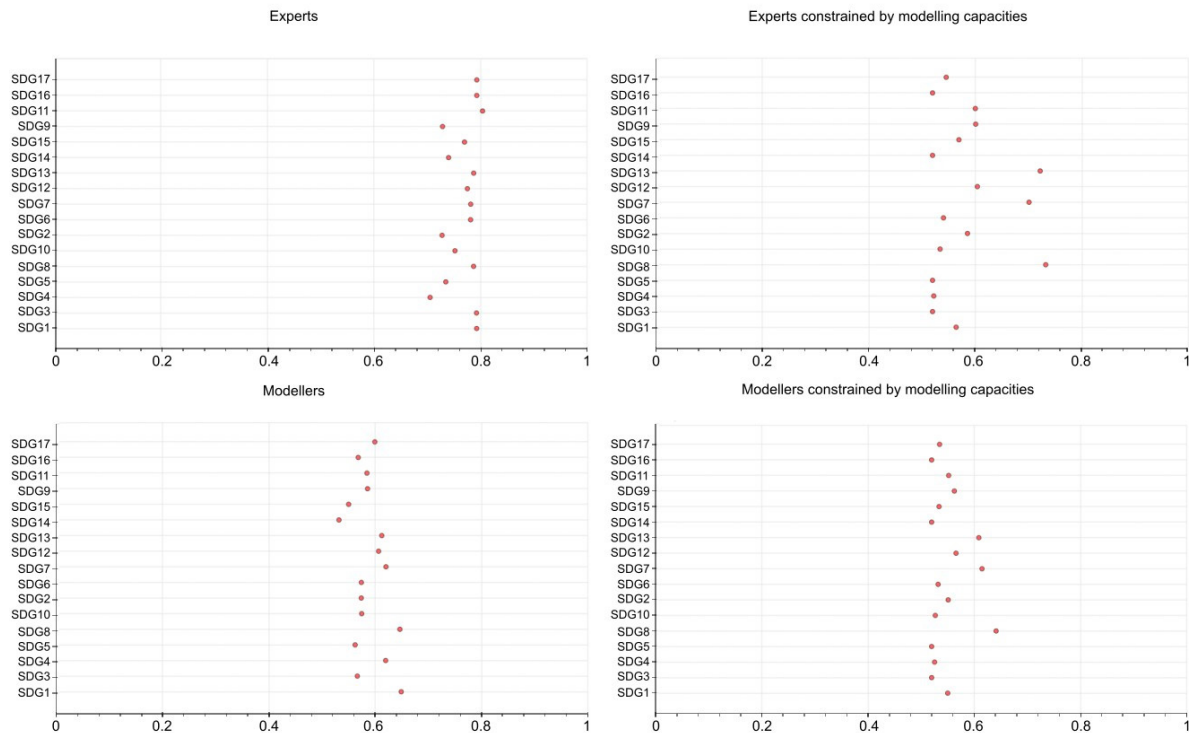


Figure 26: Causal Relationship Importance of each SDG in the “no-crisis” baseline scenario

3.3.2 Crisis propagation without uncertainty

Following the methodology described in Section 3.2.1, the three crisis nodes are initially activated independently in each map, using a fixed value of 0.75 (large enough to assess the impact, yet not too high allowing to later assess large uncertainty perturbations, in Section 3.3.3). A final run is performed by activating all three crisis nodes to also simulate the impact of a combination of crises similar to today’s landscape as a result of the pandemic, high inflation, and the international conflict with energy implications (Figures 27,28).

Across all four maps, SDG8 on economic growth sustainability is consistently affected by the crises activated independently and in tandem. Although SDGs linked directly with a crisis node expectedly experience the highest impact (e.g., the health emergency case primarily affects SDG3, see Figure 27), there are indirect impacts of these crises on almost all SDGs in both ‘experts’ and ‘modellers’ maps, which however appear heavily mitigated when modelling capabilities are considered, especially in the ‘modellers’ map. This may provide niche opportunities for model development and help expand the scope of analysis to better understand the impact of crises to dimensions that are seemingly irrelevant but essentially linked. It may also hint at a difficulty of FCMs constructed based on an optimal $\hat{\lambda}_{MC}$ selection to capture the impact of shocks on indirectly affected nodes, downplaying their importance as a result of potentially small λ values selected.

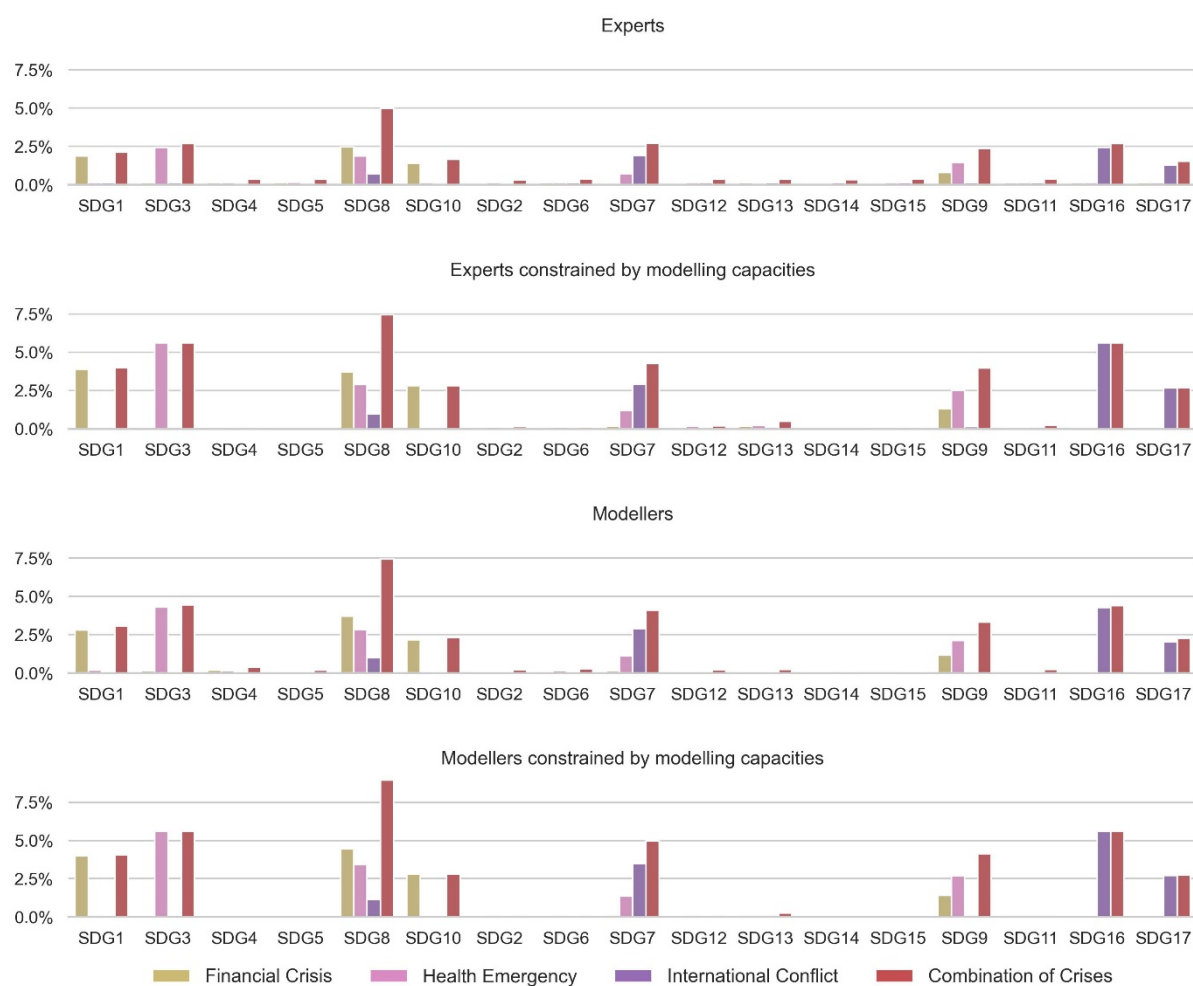


Figure 27: Impact of the crises on each SDG in the “fixed level of crisis” scenario expressed as a difference compared to the baseline (%) in each map. The impact is defined as a reflection of how the score of each SDG changes when the crises are introduced. Higher impact indicates that the relative importance of each SDG based on its interconnection increases as a result of the crisis activation.

In the absence of modelling capabilities, the ‘experts’ map shows that all SDGs are impacted in a similar way under the three crises (Figure 28). The weakest impact across almost all SDGs is found in the opposite end of the spectrum—i.e., modellers’ perceptions constrained by modelling capabilities—displaying similar trends as with the “no-crisis” baseline scenario. The only exception to this is quality education (SDG4), the impact of which experts consistently undervalued compared to modellers, expressing that this goal is less impacted in conjunction with these crises. Broadly, these two maps (experts unconstrained by model limitations and modellers considering actual modelling capacity) constitute two opposite sides.

The prioritisation stemming from the two maps in-between (experts accounting for modelling capabilities and modellers disregarding them) is much more dynamic, with each group showing different patterns (Figure 28). By delving into these two maps, we see experts (with cut-offs) prioritising not only SDGs 8, 7 and 13, but also food- (SDG2), innovation- (SDG9), community- (SDG11) and terrestrial ecosystem-related aspects (SDG15). Conversely, in the map from modellers without cut-offs, there are stronger impacts on all remaining SDGs, except for those on water-related sustainability (SDGs 6 and 14), which are nevertheless affected, albeit to a smaller extent. This hints that there are accumulated impacts from crises across a wide range of SDGs based on the modellers’ views of SDG interconnections, indicating that the affected SDGs should be further considered in future modelling improvements. In essence, these two maps highlight the actual differences in opinions among the two groups,



since experts' expectations are aligned with what models can realistically deliver, and unconstrained modellers' opinions reflect what capacities the modelling community should seek to develop.

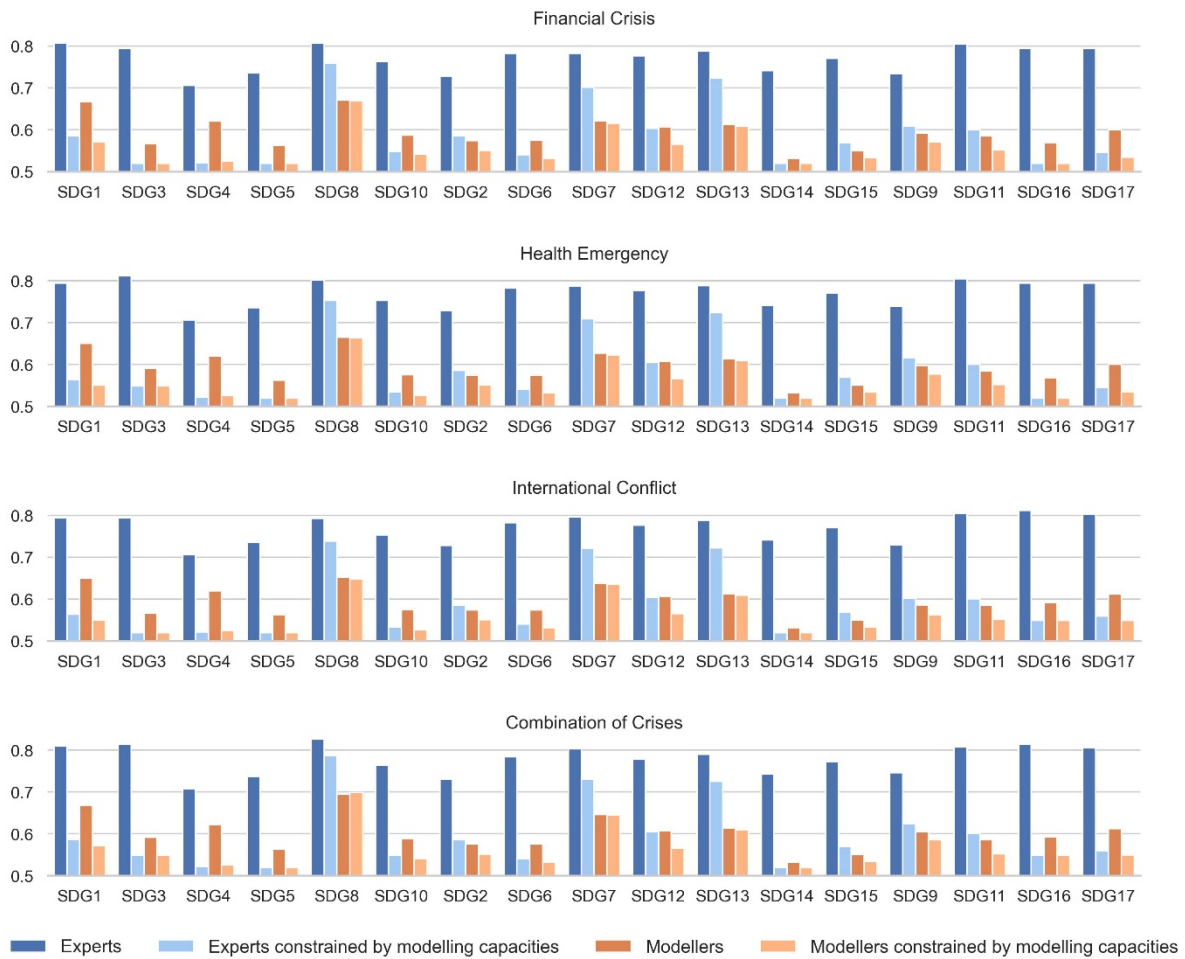


Figure 28: Impact of the crises on each SDG in the “fixed level of crisis” scenario expressed as absolute scores per crisis on each map

Narrowing down to SDG13 (climate action), which is the primary domain of IAMs, we observe that in all four maps the importance of this goal increases under crises, compared to the respective baselines (Figure 29), which indicates that the crises strengthen the need to analyse climate action in the sustainable development domain and not postpone it as a less contemporary priority. Similarly, in all maps, a combination of crises expectedly leads to accumulated impacts, meaning that the importance of climate action increases as diverse challenges pile up. In the absence of modelling capacity constraints, experts and modellers alike believe that the different crises have an almost similar impact on SDG13. When introducing modelling capabilities, the impact of a health emergency on SDG13 appears to outperform the other crises, possibly reflecting existing modelling capacity as well as considerable modelling work hitherto carried out related to health implications of climate change and action (e.g., Vandyck et al., 2018; McCollum et al., 2018; Reis et al., 2022). Contrary, the impact of international conflicts on climate action drops (most prominently from the experts' perspective), reflecting the limited capacity of many IAMs to endogenously account for geopolitical tensions (e.g., Soergel et al., 2021b) and realistically represent disruptions in international trade—except for, e.g., computable general equilibrium models. Although results and respective differences are small to drive conclusive outcomes (largely owing to small $\hat{\lambda}_{MC}$ values), these trends provide an estimation of the tendencies the crisis shocks introduce in the map and how they influence climate action.

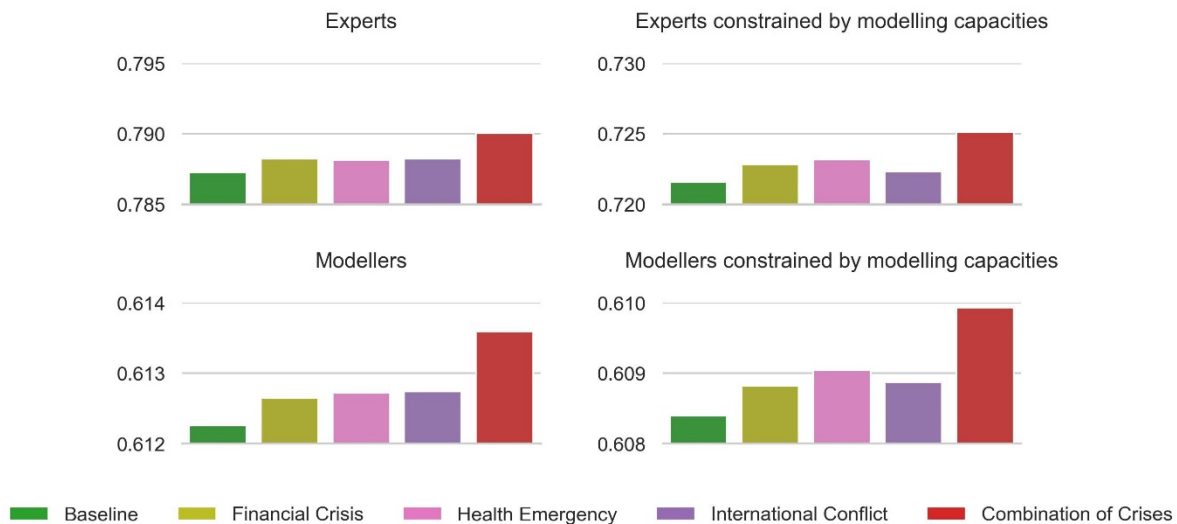


Figure 29: Impact of crises on SDG13 in the “fixed level of crisis” scenario

3.3.3 Crisis propagation under uncertainty

To simulate the impact of uncertainty, three runs are performed (Figures 30-32). The first run incorporates fluctuations on the input of the activation level of the three crisis nodes, aiming to represent combinations of different levels of emergencies, closely resembling real-world conditions rather than fixed assumptions. The second run introduces fluctuations to the weights of the links among nodes, aiming to represent underlying uncertainties in the causal relationships assumed, fleshing out biases among the experts and modellers providing these weights (in van Soest et al., 2020). As a supplement to these two independent runs for input and weight uncertainty (Figures 30.31), a third run introduces perturbations to both dimensions, aiming to capture the broad spectrum of uncertainty (Figure 32).

Overall, we observe that the uncertainty assumed in the FCM weights yields higher fluctuations in the output values compared to the uncertainty assumed in the FCM input nodes, with the impact of the former showing across all nodes, while that of the latter only in the nodes directly connected to an input node. This is an important finding from an FCM perspective: weights and structure are more influential than input node values—note that, although the small diffusion of uncertainty from the inputs could be a result of the small $\hat{\lambda}_{MC}$ parameter value, any change to the $\hat{\lambda}_{MC}$ parameter influences the effect of both types of uncertainty. But this finding is also important from a broader modelling perspective: apart from how a crisis is modelled (e.g., input assumptions, scenario protocol, etc.), better understanding of systemic interactions and underlying uncertainties is key to holistically assessing the true impact of disruptive events. This is especially true in the SDG domain, which remains far from accurately and extensively represented in IAMs.

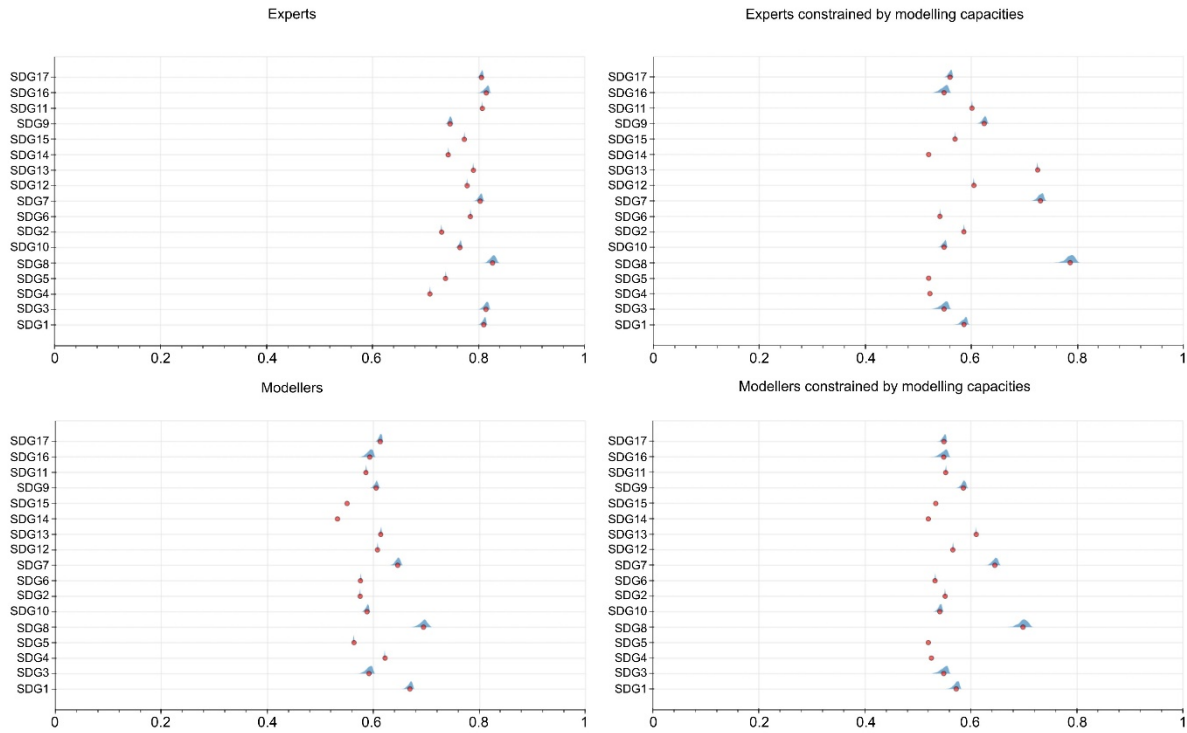


Figure 30: Impact of the crises on each SDG in the “crisis under uncertainty” scenario assuming uncertainty on inputs

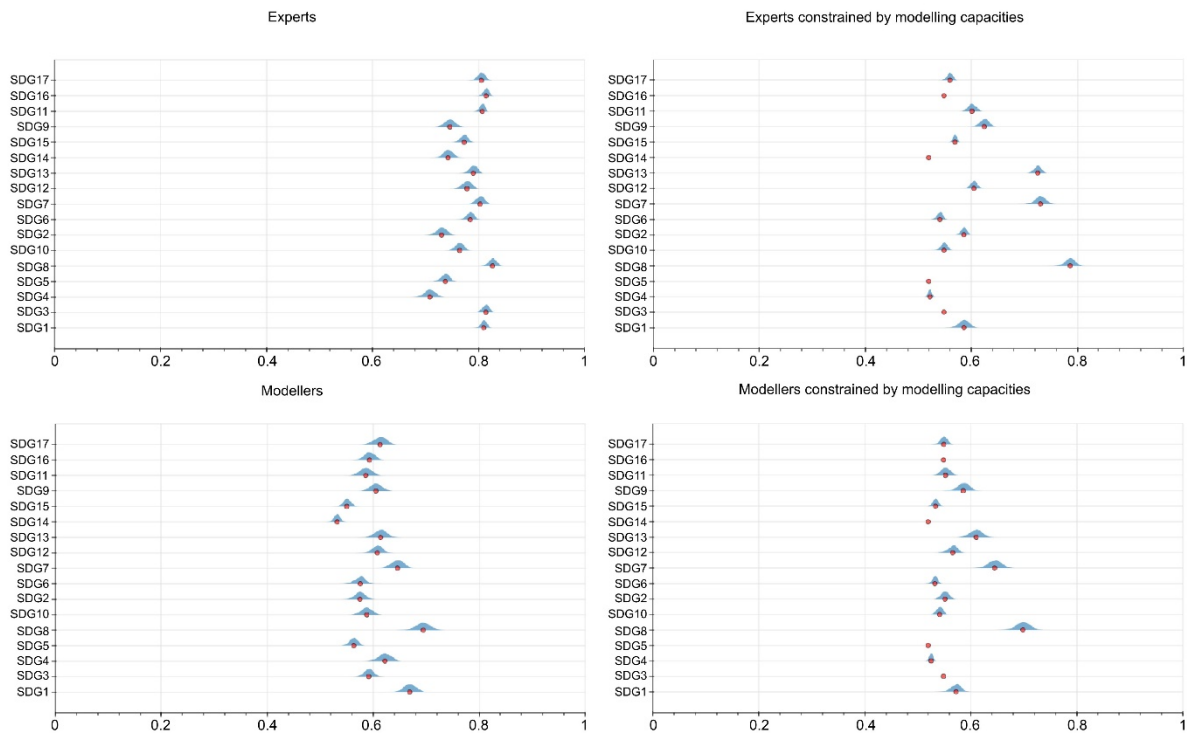


Figure 31: Impact of the crises on each SDG in the “crisis under uncertainty” scenario assuming uncertainty on weights



When introducing both types of uncertainty (input and weights), results are much less distinct and the final order of SDGs is harder to extract, compared to the case without uncertainty (Figures 27,28), especially when disregarding modelling capacities. Without cut-offs imposed to constrain within the IAM action space, all nodes end up interlinked, reflecting the truly intertwined nature of SDGs, thereby increasing uncertainty. Contrary, when modelling capabilities are considered, priorities are much clearer, pinpointing a higher impact on economic growth (SDG8), clean and affordable energy (SDG7), and climate action (SDG13) from the combined crises. This contradicts, for example, stakeholders' pre-COVID directly expressed priorities over broader planetary sustainability and environmental conservation (Koasidis et al., 2022a). Evidently, current challenges considered alongside state-of-the-art capacity of IAMs affect mostly human development as shown by the emphasis on SDG8 and SDG7, undermining broader environmental concerns outside the scope of SDG13.

The uncertainty runs shed light on the impacts on more SDGs: SDG2 (hunger elimination) and SDG1 (poverty eradication) in the 'experts' maps were among the SDGs with the highest uncertainty, eventually ranging from lower to higher ranks in the ordering. Similar insights were gained in the 'modellers' maps (e.g., for SDGs 9 and 11), although this was less evident because of their overall higher uncertainty. The latter justifies calls for considering expert opinions to inform and guide modelling studies, especially as dynamic and highly uncertain conditions significantly alter previously fixed socio- and techno-economic assumptions in models (Doukas and Nikas, 2022). To bring models much closer to experts'—and to some extent even to modelling scientists—perspectives, the representation of SDGs in the models must be significantly improved to better capture their trade-offs and co-benefits, as well as the uncertainties surrounding those, especially those standing out despite not being directly linked to the input nodes.



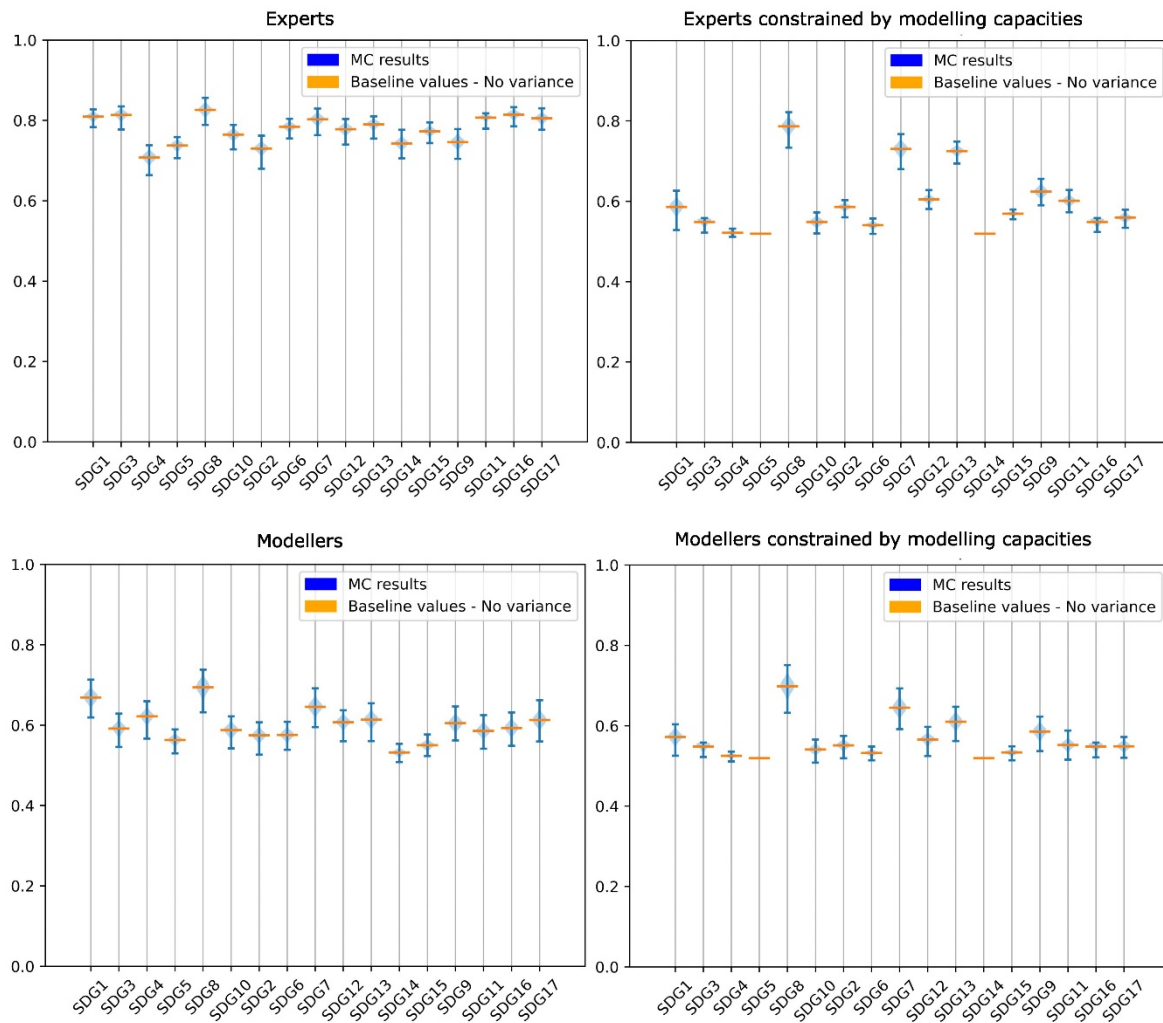


Figure 32: Impact of the crises on each SDG in the “crisis under uncertainty” scenario uncertainty on inputs and weights at the same time

3.4 Discussion

Among all maps, the SDGs that are most impacted by the three examined crises independently and in tandem with one another are SDGs 8 and 7, in most cases followed by SDGs that are directly linked to a crisis node. The strong effects found for SDG8 have been expected as this node is directly affected by every crisis and is also highly interconnected in all mental maps, reflecting the strong indirect impacts that many SDGs may have on the economy. These results persist even by taking actual modelling capabilities into account, as current IAM models traditionally by definition have a strong focus on the economy (Stoddard et al., 2021). Similarly, SDG7 is well interconnected and directly affected by the health emergency and international conflict shocks. However, not all SDG nodes that are directly connected with a crisis are heavily impacted. For instance, SDG16 (peace, justice, and strong institutions) and SDG17 (partnerships) are directly affected by international conflicts (Figure 26) but, overall, feature some of the lowest impact scores among all SDGs, especially in maps based on modellers’ perceptions and/or constrained by modelling capacities (Figure 26). This counter-intuitive finding underlines the importance of adequate representation of SDG interconnections in IAMs to correctly assess SDG impacts, especially in the international conflicts front, with our results hinting at IAMs being less adequate to incorporate such dimensions. SDG13 features the third highest impact in all maps underpinning the importance of climate change as a



cornerstone in the Sustainable Development Agenda, as well as echoing recent findings about the detrimental effects of the COVID-19 crisis and of the war on Ukraine on climate action (Zakeri et al., 2022)—including responses to them (Davis et al., 2022; Kemfert et al., 2022). However, the high scores across most SDGs especially from the experts' perspective hint at the importance of distributional impacts caused by the crises even on nodes that are not directly linked to a crisis node (e.g., SDG12) or where the impact of the crises is not obvious (e.g., SDG4).

Despite these broader and mostly universal trends across all maps, the impacts of the crises on SDGs largely depend on assumptions about the causal relationships among the SDGs, therefore on the difference between experts and modellers whose mental maps were examined, and the impact of perceived modelling capabilities. In other words, results show that impacts largely differ depending on whether these assumptions are based on the perceptions of IAM modellers or SDG experts and whether these perceptions are constrained by modelling capabilities. The map reflecting experts' input includes more interconnections among SDGs than the map based on modellers, thus increasing their overall importance, indicating that expert views can be helpful for improving SDG simulation in IAMs and echoing similar calls for making modelling more inter- and transdisciplinary (Trutnevyte et al., 2019; Voinov et al., 2016; van Voorn et al., 2016). While experts highlighted almost all SDGs as important, modellers presented clearer priorities and critically distinguished SDG8 (decent work and economic growth), SDG1 (no poverty), and SDG4 (quality education). However, introducing cut-offs based on modelling capabilities largely influenced the 'experts' map, as also hinted by van Soest et al. (2019). We highlight that modelling capabilities largely condense the perceived importance of SDGs from the experts' perspective, bringing it much closer to the modellers' map and respective resulting priorities. This finding has two important implications for IAM development. First, modellers' views about SDG interactions appear already constrained by the current or forthcoming capabilities of their models. As IAMs have been notoriously opaque in showing their inner workings (Bistline et al., 2021), the absence of detailed interactions among SDGs in IAMs may lead to the misinterpretation that these interactions do not exist or are insignificant. Second, while SDG experts can support modellers by providing a more holistic view of the interactions among SDGs, these views can be constrained by current modelling capacities. Tellingly, interconnections even in the 'experts' map with cut-offs remain relatively high only for SDG8, SDG13 (climate action), and SDG7 (affordable and clean energy), which are domains that most IAMs already cover sufficiently. Lately, many have pointed to the need to place expert and non-expert stakeholders at the heart of the modelling process (e.g., Peng et al., 2021; Doukas and Nikas, 2021), and even move from simple stakeholder consultation to co-creation and co-production of knowledge (Galende-Sánchez and Sorman, 2021)². Since modellers seemingly anchor their priorities to what their models can—or are planned to soon be able—do, the participation of experts is critical to open up new research considerations and viewpoints. Nonetheless, the large similarities found between the experts' and modellers' views, when constrained by modelling capabilities, indicate that, unless new modelling capacities are developed, it will be the models that drive future IAM studies forward instead of the experts' priorities and/or actual policy and societal needs—even with their participation in the process. Overall, results suggest that future development of SDG representation in IAMs can be enriched through transdisciplinarity, provided there are appropriate technical solutions to implement the experts' suggestions for model improvements.

From a methodological perspective, we also find significant added value in the proposed MCFCM framework, as reflected in the case of analysing the impacts of economic, health, and energy crises on SDGs. The introduced MCFCM method provides valuable additional insights on the robustness of the findings compared to a conventional FCM approach as well as on the variability of uncertainty among the different SDGs. Where differences between SDG nodes are already small, such as in maps based on expert and modeller views without modelling constraints, MCFCM shows that prioritisation of impacts is far from straightforward, as usually implied by purely ranking frameworks such as FCMs, since uncertainty ranges overlap among most SDGs. In maps where modelling capabilities constrained expert and modeller input, the highest impact is found for SDG8, SDG7, and



SDG13, even under uncertainty, which thus increases the robustness of this finding. Even in that case, however, prioritisation among them becomes less clear, as their uncertainty ranges also overlap. Additionally, SDG13 largely overlaps with SDG12 (responsible consumption and production) and SDG9 (industry, innovation, and infrastructure) in the modellers' mental map without cut-off, showing that these SDGs are also perceived by model developers and users to be highly prone to the crises. When model capacity cut-offs are introduced, we find some of the highest variability among SDGs in the case study: SDGs with the highest impacts have the widest uncertainty ranges and vice versa. Similar patterns were found in the expert-based map with cut-offs, while most SDGs had similar uncertainty ranges in the maps without cut-off. Also, despite their initial lower evaluation, the large uncertainty of specific SDGs (e.g., SDG2) can provide additional areas of interest since the impact of the crises in certain cases may be more substantial than initially anticipated, implying that a conventional FCM without Monte Carlo uncertainty analysis may overlook such cases. In summary, these results show that the MCFCM can be a powerful tool in the evaluation of FCM results providing additional insights compared to a conventional FCM approach on three fronts: (1) increasing the robustness of the calculated ranking and highlighting overlaps, (2) mitigating the bias of initial choices in the construction of a map, and (3) identifying nodes with high uncertainty and thus of interest irrespective of their conventional-FCM value (i.e., a small value in the non-Monte Carlo runs could shift focus away from some nodes that otherwise feature interesting response to uncertainty perturbations).

Among the types of uncertainties that were used in MCFCM—i.e., fluctuations on input parameters and on the weights of nodes describing the system—the former was shown to be less influential for the case study at hand. Fluctuations in the input parameters affected mostly nodes that were directly connected with them, while fluctuations on the weights led to uncertainty ranges in most of the system nodes and across all four maps. From an FCM point of view, results imply that the effects of uncertainty can vary based on the type of the node and/or system component that is stressed and may not always propagate across the map. From a modelling perspective, in turn, findings suggest that parametric uncertainties related to how (SDGs) interactions are modelled can have a large impact on the results. This interpretation agrees with suggestions that the choice of modelling approach in IAMs may have a stronger impact on the results than exogenous inputs (Sognaes et al., 2021). IAM modellers would thus need to be aware that choices on SDG simulation can strongly affect their results and use multi-model exercises to assess such effects across models with diverse modelling paradigms and structures (Duan et al., 2019).

3.5 Conclusions

The series of global crises within 2022, including the COVID-19 pandemic, the war in Ukraine, and the unfolding economic recession, have *inter alia* challenged climate action and the overall progress towards sustainable development (Zakeri et al., 2022). Integrated assessments modelling can potentially help to explore pathways out of these crises within the climate-economy nexus, and modellers aim to expand the scope of IAMs to assess impacts on broad sustainable development (van Vuuren et al., 2022). However, the modelling enhancements that are required for such assessments require a much more interdisciplinary approach in IAM development than what is commonly followed to date (Nikas et al., 2022), especially in the front of handling uncertainty and engaging experts and stakeholders in the modelling process. Fuzzy cognitive mapping approaches have the potential to enhance the dialogue between disciplines and enrich modelling development but, so far, they are also lacking a way to handle the uncertainties that are innate to climate-economy models and their inputs. In this study, drawing from two extensive surveys with IAM modellers and SDG experts (van Soest et al., 2019), we introduce uncertainty to FCMs by integrating them with Monte Carlo simulations (MCFCM) to evaluate the impacts of three types of crises (economic recession, health emergency, and international conflict) on the interconnected landscape of all 17 SDGs, to shed light on differences across experts and modellers opinions on the impact of the crises on SDGs, and to inform future IAM development.



Results show that all crises individually as well as their combination can have a significant impact across multiple SDGs, with SDG8 (decent work and economic growth), SDG7 (affordable and clean energy), and SDG13 (climate action) showcasing the highest priorities in an environment challenged by these crises. However, distributional impacts across most SDGs hint at broader implications of the crises that should be examined, with IAMs needing to expand their coverage of SDGs. Apart from similar overarching trends, results also point to large differences between experts and modellers in their perceptions with the former suggesting that the interconnections among SDGs are more impactful under the crises than assumed by the latter, but current modelling capabilities significantly constrain their viewpoint; modellers' perceptions, on the other hand, appear closer to what their models have to offer. As such, engaging with stakeholders in the modelling process is vital, but it should be accompanied by transcending current limitations and developing models based on expert preferences. Finally, the application of MCFCM provided valuable additional information compared to conventional FCMs enhancing the robustness of the aforementioned results by confirming the prioritisation of SDG8, SDG7, and SDG13 even when uncertainty is considered, while also shedding light on areas overlooked in the absence of the Monte Carlo analysis.

This study opens areas for future research that could build on the results presented here as well as overcome some of the limitations. Enabling the Monte Carlo integration in FCMs required the use of a small λ parameter to avoid non-convergence. Although this does not significantly influence the rigorousness of the results, it condenses the range of the output values, making knowledge extraction difficult. Future research can further analyse the use of this parameter in MCFCMs to enable parameterisation that would lead to more comprehensible results that are closer to their linguistic interpretation. Still, the introduced MCFCM framework can be a powerful tool for future applications that seek to evaluate uncertainty effects among different map structures and application domains. Furthermore, considering that the input data for our study originated in surveys with modellers and experts, it is possible that these surveys incorporate human biases as well as miss on latest developments in modelling, IAM improvements, and broader SDG-related research currently underway. Still, significant effort has been put to analyse these biases and mitigate them to a certain extent, based on the uncertainty framework presented. This way, the climate-economy modelling community could draw from the results presented to build models that are closer to the perception of relevant experts as well as increase the representation of SDGs and reduce uncertainties. Finally, future efforts can focus on expanding stakeholder engagement, by considering views from non-expert stakeholders, such as policymakers.



4 Enabling an energy transition in Greece following the Ukraine 2022 invasion

This section has been submitted and is currently under review in *Renewable & Sustainable Energy Transition*:

- Karamaneas, A, Koasidis, K., Frilingou, N., Xexakis, G., Nikas, A., & Doukas, H. (2022). A stakeholder-informed modelling study of Greece's energy transition amidst an energy crisis: the role of natural gas and climate ambition. *Renewable & Sustainable Energy Transition*, under review.

4.1 Introduction

Climate change is prominent on political agendas, notably since the Paris Agreement came into effect (Pickl et al., 2019). The European Union (EU) has been a world frontrunner in climate change mitigation efforts to meet the Paris temperature goals: after displaying early ambition in its initial Nationally Determined Contribution (NDC) aiming for a 40% and 80% reduction in greenhouse gas (GHG) emissions by 2030 and 2050 relative to 1990 levels respectively (Hirvonen et al., 2018), the bloc recently ramped this ambition up with its flagship European Green Deal and 'Fit for 55' policy package, upgrading the target to 55% in 2030 and net-zero by 2050 (Hainsch et al., 2022).

Among EU Member States, Greece has also pledged to reduce its emissions in line with EU targets. Following EU's first NDC, Greece submitted in 2018 and revised in 2019 its National Energy and Climate Plan (NECP) for 2030 and Long-Term Strategy (LTS) for 2050, aiming to reduce GHG emissions by 43% by 2030 relative to 1990 levels (Zervas et al., 2021; Hellenic Republic Ministry of the Environment and Energy, 2019) and by at least 75% by 2050 (Hellenic Republic Ministry of the Environment and Energy, 2020), respectively, in 2019. This year, the Greek parliament also legislated the Climate Law that, despite not setting specific emissions targets on top of the country's first NECP, proposed various mitigation measures, including for example deeper penetration of electric vehicles (EVs) (Hellenic Parliament, 2022). Finally, to align its climate targets with the EU's Green Deal, the Greek government has also proposed to further revise its NECP to eventually meet the Union's latest -55% GHG emissions reduction target for 2030 that is reflected in the Fit for 55 package (Serbia-energy.eu, 2022).

Among the most critical elements of the NECP is the delignitisation of Greece's electricity generation (Zervas et al., 2021) by 2028. Lignite has dominated the country's power sector for decades, although a series of initiatives as well as socioeconomic and technological developments during the past 30+ years have sharply reduced lignite use: by 2017, power generation from lignite had dropped to 34%, from 72% in 1990, with natural gas-powered electricity emerging from zero in 1990 to 31% in the same period, raising concerns over the prospect of following a gas-dependent trajectory (Nikas et al., 2020b). This trend has continued even faster since: the share of lignite-fired power generation reached 11% by the end of 2021, while natural gas rose to 43%, with the remainder covered by renewable energy sources (RES) (35%) and hydro (11%) (IPTO, 2022a).

Despite reducing power-sector emissions intensity (from 1,189 g CO_{2e}/kWh in 1990 to 479.2 g CO_{2e}/kWh in 2020) (European Environment Agency, 2022), this shift from lignite to gas and renewables significantly increased the country's energy dependence, since all gas is imported (Nikas et al., 2020b). EU-wide gas supply hurdles started in summer 2021: a considerable increase in EU electricity prices (Uribe et al., 2022), further deepened by Russia's invasion of Ukraine as well as the subsequent European response (Doukas and Nikas, 2022) and concerns over Russia weaponising fossil fuel supplies as in the past (Nikas et al., 2020c; Felkynina, 2012), led to a 24-fold increase in natural gas prices between summer 2020 and summer 2022 (Makholm, 2022). These developments inevitably affected Greece, which in 2020 imported almost 40% of its gas from Russia (Eurostat, 2022d). This unfolding energy crisis is increasingly evident in energy bills, in a country that has been dealing with high energy poverty levels for



a decade (Halkos and Gkampoura, 2021); so far, the several-fold increases in electricity retail prices are largely contained by government spending to subsidise a share of consumer bills (Climate Action Tracker, 2022), with fears over the long-term sustainability of subsidies, the flow of funds towards fossil fuels, and the implications for the available finance for the energy transition.

These gas price spikes and the subsequent energy crisis is hardly contained in the power sector, notably with consequent record-high inflation rates throughout Europe (e.g., (Oxford Analytica, 2022). Greece is facing a similar situation—a 10.5% inflation rate in May 2022, contrasted to -1.2% a year back, and an inflation index for energy products reaching 61%, making it the 5th highest among EU countries (Eurostat, 2022c). It was also in May 2022 that the EU, in its REPowerEU plan setting out how to eliminate its dependence on Russian fossil fuels (European Commission, 2022a), spelled out supply-side diversification, energy efficiency, and promotion of renewables. Nonetheless, most European countries have so far been active in pursuing grey alternatives, by mobilising every readily available fossil-fuel option [13]—which, for Greece, translates to lignite plants operating at maximum capacity, and expanding almost exclusively to new liquefied natural gas (LNG) investments (Inman et al., 2022). Although this strategy may help alleviate the situation in the short-term, critics fear it may lead to new fossil-fuel lock-ins, thereby hampering energy transition in the longer run (Kemfert et al., 2022).

In the absence of deep market interventions and by assuming continuously high gas prices (Reuters, 2022a), the increased European dependence on fossil-fuel imports can potentially lead to high risks of economic instability, fuel energy poverty, and jeopardise climate action for years to come. For Greece, this primarily highlights the need for a clear timeline towards phasing out gas imports and decarbonising the power sector, without overlooking socioeconomic burdens for citizens. In the constantly changing policy context of Greece, the aim of this study is to understand (a) the role of natural gas based on the current policy framework, and (b) the potential of pursuing a degasification pathway and high ambitious climate targets at the same time. Using two modelling tools, LEAP (Heaps, 2022) for energy demand and OSeMOSYS (Howells et al., 2011) for the power sector, we examine whether the Greek climate policy currently in place (i.e., the 2019 NECP and LTS, as well as the 2022 Climate Law) further anchors to or strays away from natural gas in the near-term and until 2035. Considering that many provisions of the NECP and the Climate Law are under constant revision in response to current events, an explorative scenario is also introduced, aiming for higher decarbonisation ambition with an explicit focus on phasing out all fossil fuels, including natural gas. Acknowledging the importance of expert input in timely defining the action space in the wake of the 2022 energy crisis (Frilingou et al., n.d.), this research then turns to stakeholder perceptions and employs fuzzy cognitive mapping (FCM), a widely established approach to eliciting expert knowledge in the energy and climate policy domain (Doukas and Nikas, 2020), to identify critical uncertainties and/or possible bottlenecks. Drawing from this participatory process, new modelling iterations of the original scenario analysis finally sheds light on the impact of these uncertainties.

Section 4.2 outlines the applied methods, by introducing the two modelling tools, the examined scenarios, and the fuzzy cognitive mapping framework. Section 4.3 presents and discusses model results based on the initial scenarios. Section 4.4 summarises the stakeholder engagement process and its outputs, highlighting the most important uncertainties stemming from it, while Section 4.5 explores how the results of the original modelling analysis change upon scenario modifications based on stakeholder feedback. Finally, Section 4.6 draws conclusions, discussing the policy implications of the study as well as prospects for future research.

4.2 Methods & Tools

4.2.1 The energy system modelling framework

We use two different modelling tools: the Low Emissions Analysis Platform (LEAP) (Heaps, 2022) is used to project



energy demand, and the Open Source Energy Modelling System (OSeMOSYS) (Howells et al., 2011) is then employed to optimise Greece's power-sector response to different policy strategies and to the energy demand trajectories from LEAP.

LEAP is a widely established model generation tool (Ben Amer et al., 2020), featuring flexible, easy-to-use data structure and capacity for representation of technologies and end-use specifications, and has been employed in several applications around the world to analyse policy impacts at different scales (Emodi et al., 2017). Although there exist applications for cities (e.g., (Ghanadan and Koomey, 2005)) and countries (e.g., (Nikolaev and Konidari, 2017)) around the world, including for Greece (Rionioti et al., 2012), it has been used extensively for capacity development activities in regions with limited in-house capacity in terms of sophisticated energy modelling tools—e.g., in Taiwan (Huang et al. (2011), Colombia (Nieves et al., 2019), Korea (Shin et al., 2005), Panama (McPherson and Karney, 2014), Malaysia (Azam et al., 2016), Pakistan (Mirjat et al., 2018). In this research, we develop a country-level implementation of the LEAP model for Greece to project energy demand for five sectors (households, transport, the tertiary sector, industry, and agriculture) in response to the different policy scenarios. Energy demand for these sectors comprises demand for electricity, fossil fuels (e.g., natural gas or oil products), biofuels, and renewables (e.g., solar thermal energy in the household sector), which are the main outputs of the model.

Likewise, OSeMOSYS is a widely established modelling framework used to develop capacities by creating dynamic, deterministic, technology-rich, energy system optimisation models for medium-to-long-term energy planning (Heaps, 2022). It is mainly used for national-level modelling—e.g., Tunisia (Dhakouani et al., 2017), Brazil (de Moura et al., 2018), Egypt (Rady et al., 2018) and Bangladesh (Olsson and Gardumi, 2021)—although regional model implementations also exist (e.g. for South America (Santos, 2021)). Drawing from existing work, we develop a national model implementation, OSeMOSYS-Greece (Koutsandreas et al., n.d.), to optimise the country's electricity generation trajectories, investment requirements by source, as well as CO₂ emissions.

While LEAP is a simulation-based accounting framework for the design of energy, the addition of OSeMOSYS enables an optimisation approach that minimises total system costs (García-Gusano and Iribarren, 2018). The two are commonly integrated (e.g., see implementations for Ghana (Awopone et al., 2017), Australia (Emodi et al., 2019) and Ireland (Rogan et al., 2013)), with LEAP including a power generation optimisation module using the GLPK solver of OSeMOSYS (Awopone et al., 2017). This research employs a slightly different approach: instead of using the built-in OSeMOSYS optimisation module included in LEAP, we use the two models separately by feeding LEAP's electricity demand trajectories into OSeMOSYS. We choose this approach because LEAP typically only applies a limited set of OSeMOSYS optimisation parameters regarding electricity generation plant expansion planning (Moksnes et al., 2015); therefore, using OSeMOSYS individually provides a wider choice of power generation constraints and parameters, leading to a higher-resolution framework.

The two models require different socioeconomic and technoeconomic inputs (see Table 8); to the extent there is overlap (e.g., policy assumptions and some technoeconomic parameters), input assumptions are fully harmonised between them.

Table 8: Input assumptions for LEAP and OSeMOSYS

LEAP	
Households	Fuel consumption data is drawn from Eurostat (Eurostat, 2022a) for 2020 and the Hellenic Statistical Authority (Hellenic Statistical Authority, 2013); the number of households was drawn from the Hellenic Statistical Authority (Hellenic Statistical Authority, 2012) and projected onwards based on Giarola et al. (2021).

Transport	Fuel consumption for transport passenger vehicles and freight trucks were adjusted (for LEAP) from Giarola et al. (2021) after transformation of vehicle-kilometres to passenger-kilometres and ton-kilometres, provided by WWF (2017), considering the occupancy rate for passenger cars in Greece (Politis et al., 2021), city (www.georgeyannis.gr, 2002) and intercity (Borken-Kleefeld et al., 2013) buses, as well as freight trucks (Kapros et al., 2014; Eurostat, 2022f). To disaggregate consumption by fuel for passenger cars, we retrieved data from ACEA (2021), adjusted to include LPG and CNG vehicles (Capital.gr, 2021) and biofuel consumption (Ministry of Environment and Energy, 2022); similar disaggregation was made for city and intercity buses using data from the Hellenic Statistical Authority (2022) and the Agency of Road Commuting (OS, 2022). For other means of transport, such as trains, planes, and passenger and freight boats, consumption data was retrieved solely from other sources (Dimoula et al., 2017; Prussi and Lonza, 2018; Prussi et al., 2021; worlddate.info, 2022), with transport work and fuel distribution also retrieved from WWF-Greece [56], except for trains for which data from Eurostat was used (Eurostat, 2022e).
Tertiary, industry, and agriculture	Energy consumption per gross value added (was obtained from the International Energy Agency's (IEA) energy consumption datasets (IEA, 2022a) and then disaggregated according to WWF (2017) and transformed based on Giarola et al. (2021)—from which we also got energy consumption data for specific technologies in the tertiary sector (e.g., heating).
OSeMOSYS	
Installed capacity	Installed capacity per plant type and technology is obtained from the Hellenic Electricity Distribution Network Operator (HEDNO, 2022), the Independent Power Transmission Operator (IPTO, 2022b) and the Renewable Energy Sources Operator & Guarantees of Origin (DAPEEP, 2022).
Costs	Capital (CAPEX) and operational (OPEX) costs come from the Greek LTS (Hellenic Republic Ministry of the Environment and Energy, 2020) as well as from IEA (2022b) and ETRI (Institute for Energy and Transport (JRC), 2014) data .
Lifecycle, factors, etc.	Lifecycle, efficiency rate, as well as availability and capacity factors were obtained from IEA [78] and Giarola et al. (2021).
Electricity demand profiles	Although LEAP runs provided electricity demand patterns, the daily electricity demand profile was drawn from Hirth et al.(2018).
CO ₂ emissions and prices	To accurately optimise electricity generation, we used CO ₂ emissions (and prices) per fuel based on the US Energy Information Administration (EIA, 2022) and the 2020 EU Reference Scenario (European Commission, 2022b) (adjusting the 2022 price with data from Ember Climate (2022)).
Fossil-fuel prices	IEA's 2021 World Energy Outlook (IEA, 2021), the latest available authoritative dataset.

4.2.2 Scenario design

The first policy scenario reflects the Greek NECP, originally introduced in 2018 and further revised in 2019 (Hellenic Republic Ministry of the Environment and Energy, 2019), which is extrapolated post-2030 by considering the provisions of the country's LTS (Hellenic Republic Ministry of the Environment and Energy, 2020) . This scenario is used as a baseline scenario, as it is deemed more accurate for modelling exercises to use mitigation policies in place as baseline scenarios instead of business-as-usual reference scenarios (Grant et al., 2020). All other scenarios are assessed against the NECP scenario, with any additional policies or enhanced targets added on top (e.g., different shares of RES, different rates of energy savings, etc.). The *Greek NECP* assumes that gas use increases in all sectors by substituting oil (50% increase in households) and that power generation from lignite is terminated by 2024, with the exception of the new Ptolemaida V lignite power plant (still under construction (Trachanas et al., 2022)) that remains operational until 2028. Current policy also aims for a 65% RES share in the electricity mix, as



well as increased EV penetration rate aiming for a 30% share, both by 2030. This baseline scenario further proposes that 1.1% of residential and tertiary buildings are deeply refurbished annually, until 2030. All scenarios assume that islands will be gradually interconnected to the mainland grid by 2030.

The 2022 Climate Law (Hellenic Parliament, 2022) proposed measures such as the ban on new oil boilers post-2025 and new oil-powered vehicles. Due to the absence of explicit upgrades to emissions, electricity mix, or energy mix targets, the legislation has been heavily criticised as inadequate to keep up with the bloc's ambitious vision and to address critical issues in the country, such as energy poverty and fossil-fuel dependence (WWF, 2022). The Climate Law is modelled as a separate scenario, adding two assumptions on top of the *Greek NECP* baseline scenario: first, it requires that all passenger cars registered post-2030 be electric; and, second, it assumes that no new oil boilers are sold after 2025, towards complete substitution of oil boilers by 2040, taking into consideration the life expectancy of a typical oil boiler (Hohne et al., 2019). Therefore, the Climate Law is understood to mainly affect the transport sector, introducing indirect changes to energy demand and electricity mix.

The implementation of specific provisions for the NECP and the Climate law is highly uncertain. In particular, the role of Ptolemaida V and the timeframe as envisaged in the NECP is constantly changing, while the role of oil boilers and the proposed ban post-2025 is also under discussions. To inform on this unstable Greek policy context and in the light of the EU's efforts to reduce carbon emissions and dependence on the Russian natural gas through the REPowerEU (building on the Fit for 55 package), we then introduce a third policy scenario (*High Ambition*), to examine to what extent Greece can realistically follow the EU's ambitious goals towards carbon neutrality and how it can stray away from its high fossil-fuel dependence, notably from Russian natural gas. This scenario examines various additional measures, including faster penetration of RES in power generation, faster penetration of EVs, higher rate of energy savings, and other measures for substituting oil and gas with electricity. Regarding electricity, the *High Ambition* scenario upgrades the RES penetration target to 80% by 2030 and 100% by 2035, leading to a carbon-neutral electricity sector by the middle of the next decade. In contrast to the *Greek NECP* and *Climate Law* scenarios, this entails smooth degasification of the power sector by 2035, by decreasing the use of gas plants by 10% annually from 2022 onwards and forbidding any new investment in natural gas infrastructure. The last electricity-sector component of this scenario is a mild prolongation of lignite use, by increasing the lifetime of the Ptolemaida V plant until 2030. Despite leading to a slight deviation from sectoral delignitisation, this is aligned with the current political debate (and extended mandates for lignite mining and use for power generation) (Naftemporiki, 2022) following Russia's invasion of Ukraine, in an effort to lower the country's dependence on Russian gas. Outside electricity, this scenario also examines several demand-side modifications, including double refurbishment rates in the built environment for the household and tertiary sectors, and faster deployment of EVs—double rate until 2030 and EV-only registrations in passenger transport post-2030, as in the *Climate Law* scenario but with faster withdrawal of existing oil-powered vehicles, aiming for a 100% EV passenger fleet in 2050. Finally, the *High Ambition* scenario completely substitutes oil and gas boilers by 2035 with heat pumps, shifting to solar water boilers by 2030, considering realistic potentials: for reference, solar water heater coverage in Greece increased from 30% in 2006 to 60% in 2015 despite the long-lasting recession (Martinopoulos and Tsalikis, 2018).

We explore power-sector implications of the three policy scenarios until 2035, aiming to cover the critical 2030 milestone as well as explore to what extent the country's power sector can realistically become carbon-neutral by mid-2030s.

Table 9 summarises the three policy scenario assumptions.

Table 9: Core policy assumptions across the three scenarios

Assumptions/targets	Greek NECP	Climate Law	Higher Ambition
---------------------	------------	-------------	-----------------



EV registration	30% registration rate by 2030	After 2030, 100% of registered cars are EVs. Until 2030, no difference in comparison with <i>Greek NECP</i>	Doubling the registration of EVs in comparison to the <i>Greek NECP</i> scenario; 100% passenger EVs by 2050
Lignite combustion	No lignite for electricity generation after 2028	No difference in comparison with <i>Greek NECP</i>	No lignite for electricity after 2030; slight prolongation of the Ptolemaida V plant lifetime
Natural gas combustion	Higher usage	Slightly higher usage in comparison with <i>Greek NECP</i>	Smooth natural gas phase-out by 2035 in electricity; no natural gas for heating purpose by 2035.
Oil combustion	Substitution with natural gas	Prohibition of oil boilers after 2025 (no oil in household heating after 2040). No further difference in comparison with <i>Greek NECP</i>	No oil for heating purpose by 2035.
Energy saving	1.1% annual rate of household and tertiary building	No difference in comparison with <i>Greek NECP</i>	Doubling the energy refurbishment rate of the <i>Greek NECP</i> scenario
RES target	65% by 2030	No difference in comparison with <i>Greek NECP</i>	80% by 2030 and 100% by 2035
Solar boilers	No specific provisions	No difference in comparison with <i>Greek NECP</i>	Hot water only from solar boilers by 2030 (electric and fossil-fuel boilers are substituted)

4.2.3 Fuzzy cognitive mapping

Fuzzy cognitive maps (FCMs) are widely used in energy (Doukas and Nikas, 2020), environmental (Mourhir, 2021), and climate (Nikas et al., 2019b) policymaking, owing to their flexibility to design and quasi-quantitatively simulate mental models of complex domains from the non-experts' and/or policymakers' perspective, even in cases of data unavailability (Gray et al., 2014b). Here, we follow the approach introduced in Antosiewicz et al. (2020): after carrying out the initial modelling analysis based on the policy scenarios of Section 4.2.2, we present the model results (discussed in detail in Section 4.3) to stakeholders aiming to elicit their feedback, co-design an FCM of the Greek power sector, explore the importance of relevant bottlenecks from their perspective, select the most critical among them, and then revisit our model scenarios accordingly.

The following FCM concept activation function is used:



$$A_i^{k+1} = f_h(x_i^k) = f_h\left(\sum_{j=1, j \neq i}^n (w_{ij}A_j^k + A_i^k)\right) \quad (67)$$

where A_i^{k+1} is the value of concept i at the end of iteration k , A_i^k is the value of concept i at the beginning of iteration k , A_j^k is the value of concept j at the beginning of iteration k , n is the number of concepts included in the FCM, w_{ij} is the weight of the causal relationship between preceding concept j and following concept i , and f_h is a threshold function typically used to squash values within the FCM value domain (Nikas et al., 2020c).

Here we use the hyperbolic tangent transfer function (Eq. 68), which is among the most widely used threshold functions in the FCM literature (Groumpos and Stylios, 2000). This function squashes values in $[-1,1]$, thereby allowing negative concept values, which is relevant to our research.

$$f_h = \frac{\exp(\lambda x) - \exp(-\lambda x)}{\exp(\lambda x) + \exp(-\lambda x)} = \frac{\exp(2\lambda x) - 1}{\exp(2\lambda x) + 1} \quad (68)$$

Upon FCM simulation, we optimise and normalise the value of parameter λ to ensure that the FCM simulation process converges, as shown in Koutsellis et al. (2022b). The FCM design and simulation process is presented in Section 4.4.

4.3 Initial energy-system modelling analysis

This section discusses the results of the modelling analysis based on the three scenarios outlined in Section 4.2.2: *Greek NECP*, *Climate Law*, and *High Ambition*. From an energy demand perspective (LEAP), results include: (a) total energy demand, (b) energy demand for the transport, household, and tertiary sectors, as well as (c) energy demand per fuel for transport and households. The industrial and agricultural sectors, although included in the LEAP model, are not presented as they are not impacted by the policy scenarios. Regarding power generation (OSEMOSYS), results include annual power generation by technology, total installed capacity per technology, CO₂ emissions from electricity generation, and cost of electricity generation per MWh. Although the timeframe of interest for power-sector decarbonisation is 2035, energy demand is projected to 2050, as demand-side trajectories are driven by several 2050 objectives with shorter-term implications (e.g., 100% EV fleet in 2050).

4.3.1 Energy demand

Figure 33 illustrates the different energy-demand trajectories for Greece until 2050. Regarding total demand (Figure 33a), the *Greek NECP* baseline demonstrates relative stability, with increased economic activity (Giarola et al., 2021) counterbalanced by mild EV penetration and a moderate rate of energy savings in buildings. The *Climate Law* scenario then hints at a decrease in total energy demand post-2030 (around -25 TWh by mid-century), mainly due to higher penetration of the more efficient EVs (Albatayneh et al., 2020). This trend is more evident in the *High Ambition* scenario (down by almost 30% or 55 TWh by 2050), where it is relatively smooth until 2030 due to refurbishments and fast EV registration and steeper onwards (even higher rates of EV registration and the consequent shift from gasoline/diesel to electricity). Transportation (Figure 33b) demonstrates the highest demand across scenarios and along the entire time horizon. EV penetration in the *Climate Law* and *High Ambition* scenarios alike leads to considerable energy demand cuts—about 30 TWh and 45 TWh, respectively. The second most energy-consuming sector is the residential sector (Figure 33c), showcasing almost identical trajectories for the *Greek NECP* and *Climate Law*, which differ in the rate of gas penetration for heating (Patiño-Cambeiro et al.,



2019). Instead, *High Ambition* demonstrates a 10 TWh additional decrease (i.e., approximately 20 TWh in total) until 2050, due to faster refurbishments and higher penetration of heat pumps (Wang, 2018). Similar insights can be gained for the tertiary sector (Figure 33d), although *Greek NECP* and *Climate Law* eventually boost sectoral demand by about 20% (4 TWh) due to increased economic activity, while High Ambition shows a decreasing tendency until 2030 and then a small rebound, overall yielding a negligible drop (~1 TWh) by 2050.



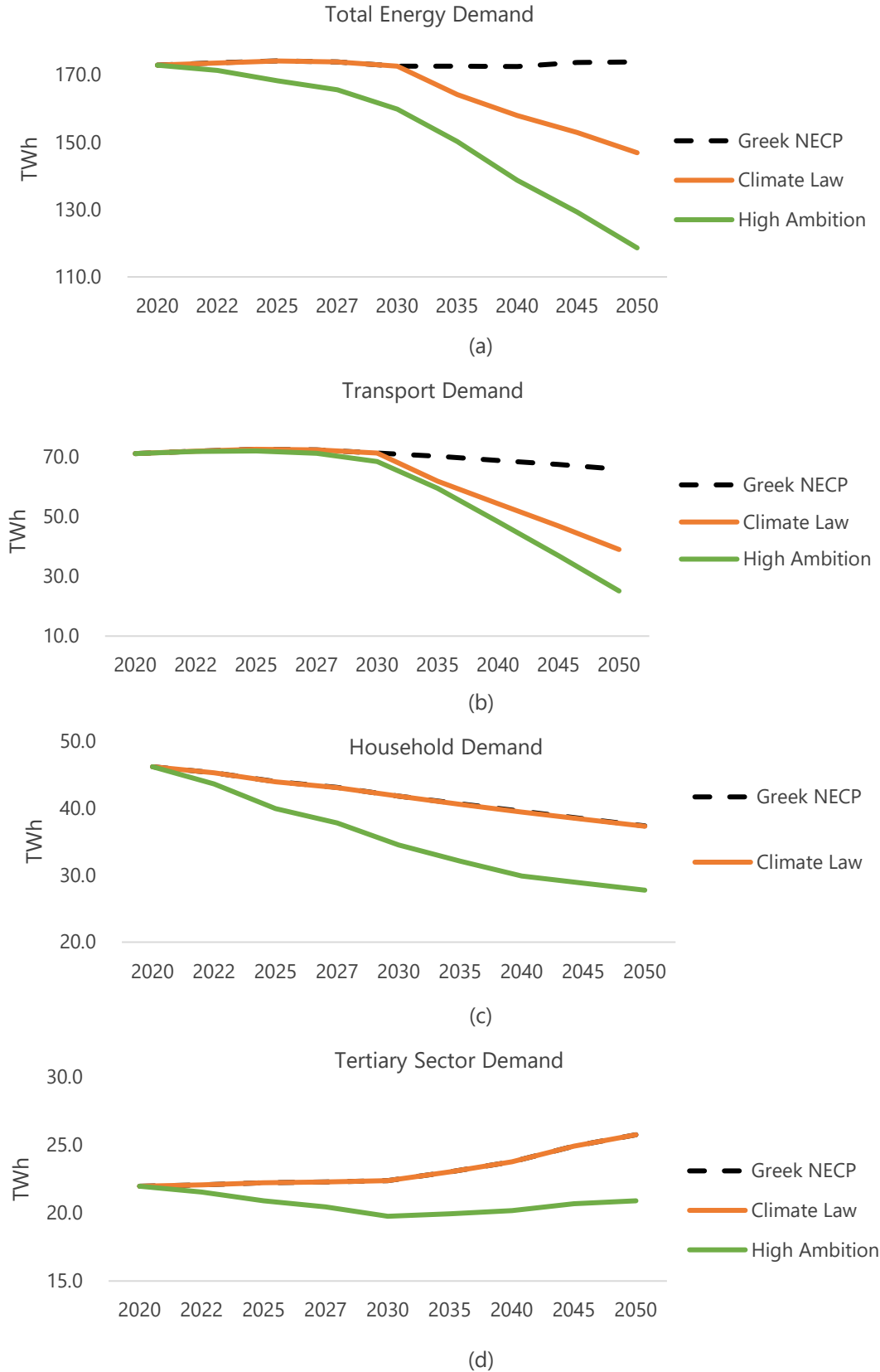


Figure 33: Projected energy demand (TWh) in Greece for the NECP, Climate Law, and High Ambition scenarios: (a) total demand (includes industry and agriculture), (b) the transport sector, (c) the household sector, and (d) the tertiary sector.

Source: LEAP. In panels (c) and (d) the "Greek NECP" and the "Climate Law" scenarios entail very small differences.



The transport fuel mix is dominated by gasoline, due to the high numbers of passenger vehicles (Spyropoulos et al., 2022). This trend continues until 2050 in the *Greek NECP* scenario (Figure 34a), which only aims for a 30% EV registration by 2030 and a constant rate of EV registration onwards, as well as for a moderate increase in biofuel shares (diesel and gasoline). We also observe that compressed natural gas (CNG) consumption is slightly increased since the Greek NECP aims to boost gas combustion in all sectors. The other two scenarios demonstrate quite different results. *Climate Law*, which proposes a 100% EV registration rate from 2030 onwards (maintaining the *Greek NECP* registration rate until 2030), leads to considerable cuts in transport energy demand (~32 TWh), a drop mainly related to the substitution of gasoline-powered cars with the more efficient EVs: gasoline demand drops by over 75% (almost 45 TWh), while demand for electricity rises by just 16 TWh. This scenario also demonstrates a slight boost in CNG use, drawing from the *Greek NECP* scenario. *High Ambition* demonstrates even higher gains in energy demand cuts (45 TWh), aiming for faster EV penetration until 2030 and a fully electric passenger fleet by 2050, and thus complete elimination of gasoline. In contrast, still used for freight transport (Fameli et al., 2020), diesel holds some ground—penetration of electric trucks is not examined in this case, since it remains uncompetitive, especially for long-haul trips (Guiliano et al., 2021). Much like *Climate Law*, biofuel consumption in the *High Ambition* scenario decreases post-2030 despite the higher biofuel share in diesel and gasoline, owing to wide-scale replacement of gasoline-powered cars by EVs.

Looking at household energy demand (Figure 35), we observe that the *Greek NECP* and *Climate Law* scenarios expectedly demonstrate almost identical performance, as the latter only differs in faster substitution of oil with gas (leading to zero diesel by 2040) for heating and in increased use of biofuels post-2030 ever since (i.e., a 30% mix of biofuels with heating oil (Hellenic Parliament, 2022)). Moreover, both scenarios demonstrate slight reduction in energy demand (9 TWh or ~20% relative to 2020). The *High Ambition* scenario, on the other hand, diverges: it leads to total elimination of oil and gas by 2035, by substituting them with heat pumps; it features an important increase in consumption of solar thermal energy (by 2.3 TWh, 75% up from 2020 values); and, although use of electricity increases, total electricity demand stabilises due to higher rates of energy savings in households—meaning that efficiency measures counterbalance the rising electricity demand. Therefore, this scenario is characterised by a significant drop in household energy demand (by almost 20 TWh, or 45% of total household energy demand in 2020) since oil and gas consumption becomes zero by 2035 without an equivalent increase in electricity demand.



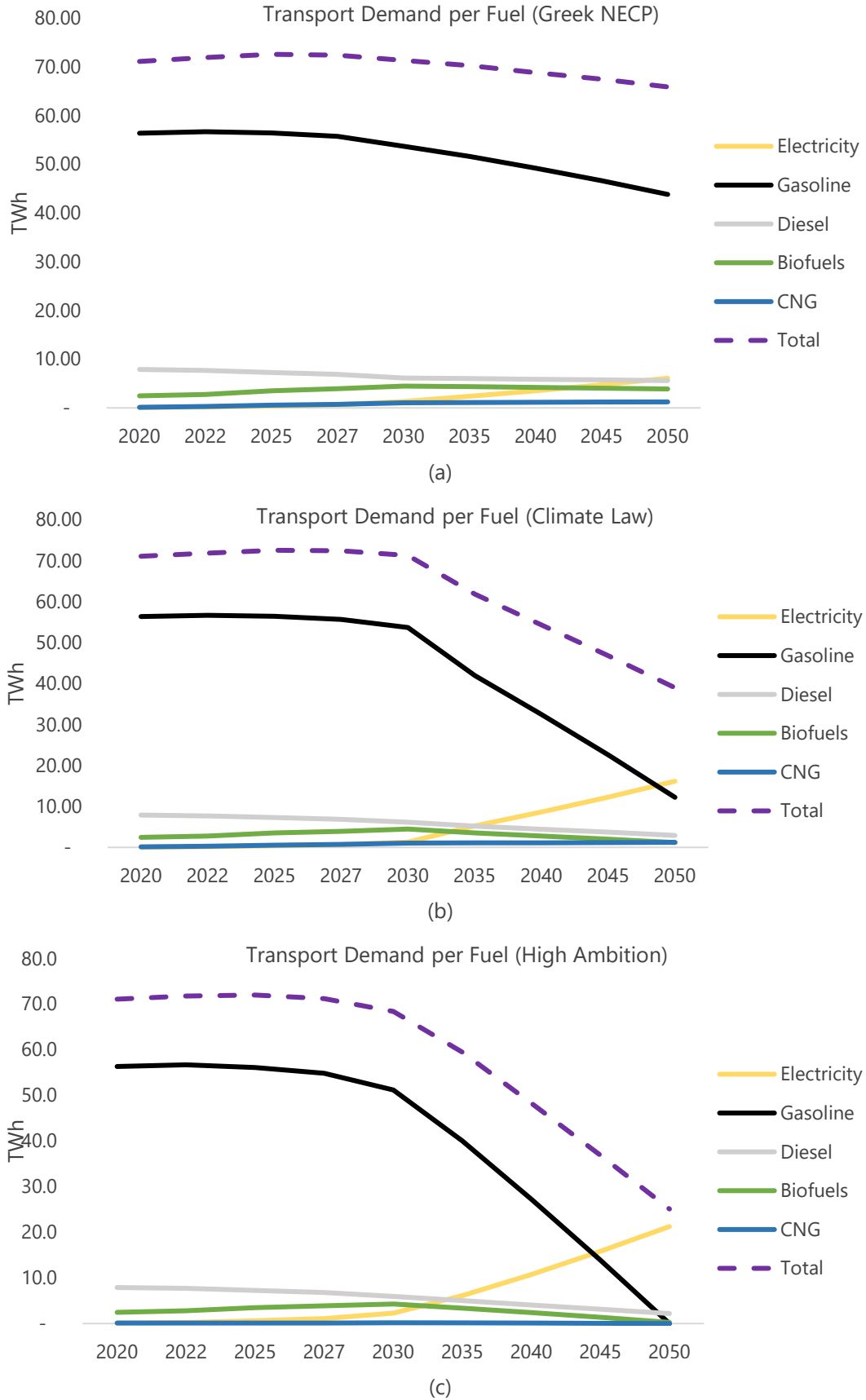


Figure 34: Transport energy demand per fuel (in TWh) for the: (a) Greek NECP, (b) Climate Law, and (c) High Ambition scenarios.

Source: LEAP.



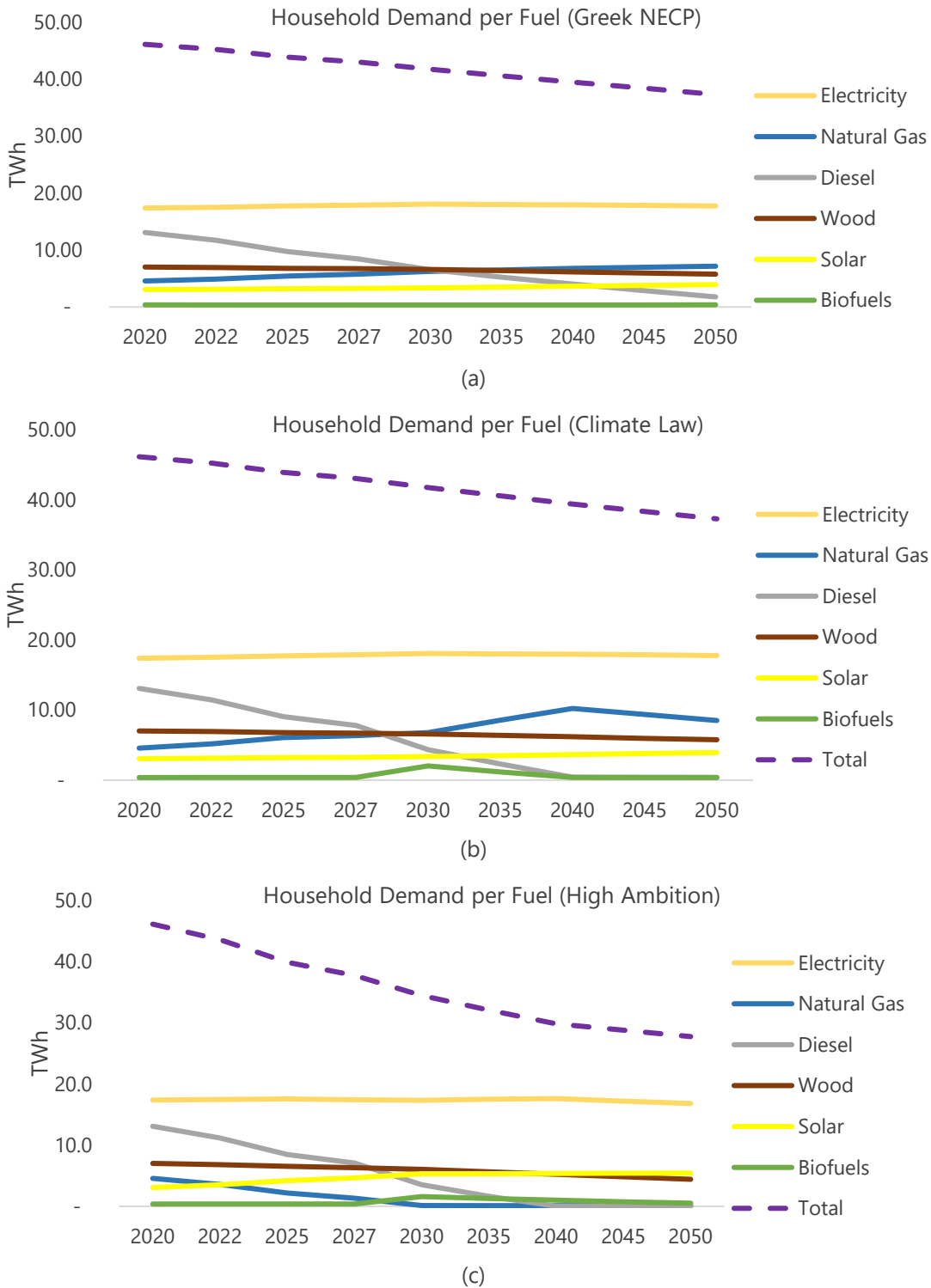


Figure 35: Household energy demand per fuel (in TWh) for the: (a) Greek NECP, (b) Climate Law, and (c) High Ambition scenarios.

Source: LEAP.

4.3.2 Electricity Generation

We then look at power-sector implications of the policy scenarios until 2035 using OSeMOSYS (Figure 36), drawing from the demand trajectories from LEAP. The *Greek NECP* demonstrates a slight increase (+12.5%) in power generation—expectedly owing to the increased demand, primarily for EVs (Figure 36a). The most important

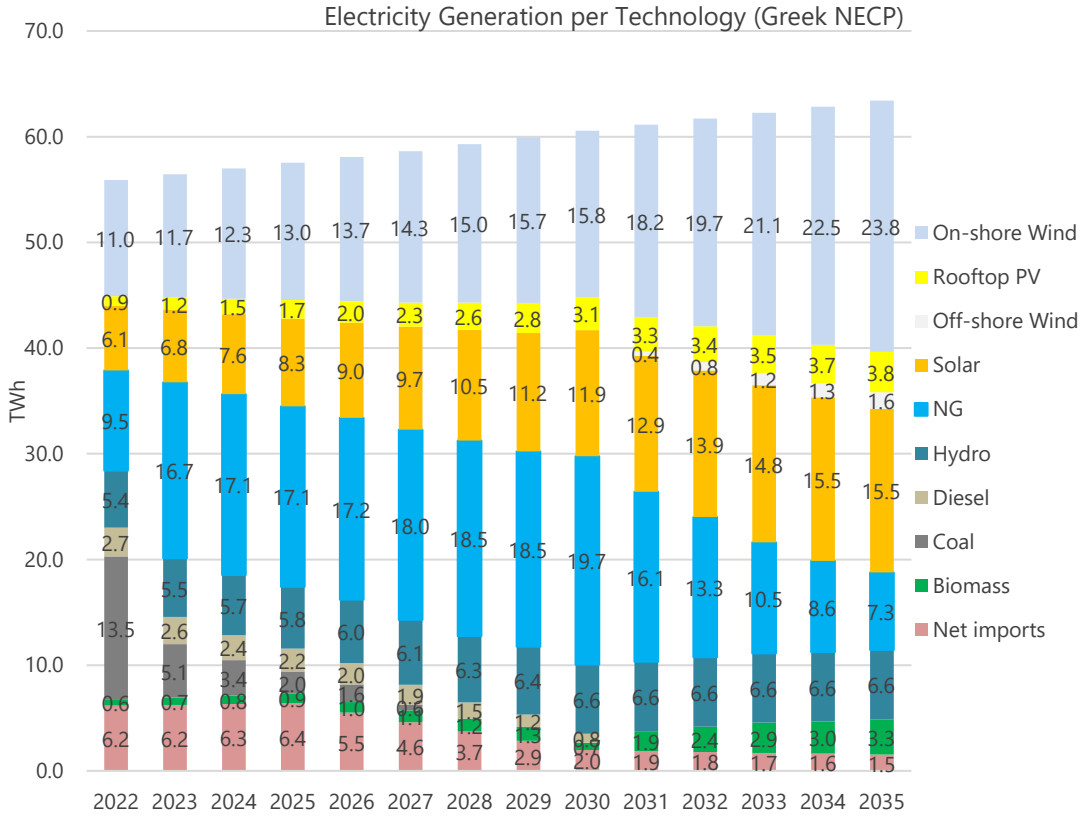


feature of this scenario is that gas-powered generation more than doubles by 2030, showing little clarity as to whether the NECP paved a concrete way out of gas as a transitional fuel (Koutsandreas et al., 2021). By definition, lignite phase-out is projected in 2028, after the shutdown of Ptolemaida V. Post-2030, the high use of gas slows down, mainly driven by LTS assumptions for wind and solar expansion and overall RES penetration in the electricity mix—again hinting at inconsistencies between the official NECP and LTS documents regarding the role of natural gas. Net imports sharply drop, since the Greek NECP explicitly aims to increase electricity independence. Diesel consumption monotonously decreases by the end of the decade, on the cross-scenario assumption that islands are interconnected to the mainland grid by 2030. Notably, offshore wind has a negligible role (outputting less than 2% of total electricity in 2035), a development largely attributed to their current and projected costs (almost double LCOE compared to onshore wind) (Ren et al., 2021). Similar results are drawn for *Climate Law* (Figure 36b), which almost anchors to the *Greek NECP* electricity provisions. Mild differences can be observed due to slightly increased electricity demand (an additional 3 TWh increase on top of the *Greek NECP*) from the higher EV penetration, leading to increased gas needs as well as a relative uptick in solar and (primarily small) hydro use.

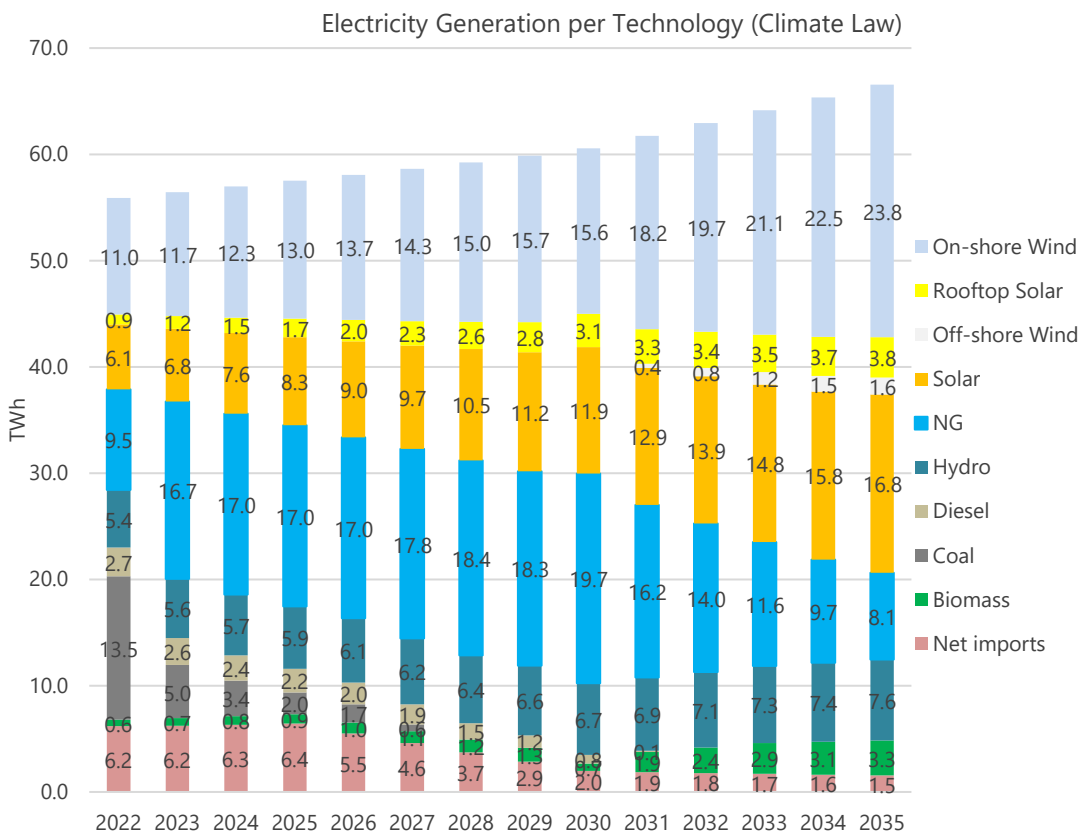
Again, the *High Ambition* policy scenario markedly differs (Figure 36c), aiming for smooth yet complete degasification by 2035. Similarly, lignite-fired generation also drops, albeit in a rockier route: despite the 2022 lignite use spike as a result of the immediate response to high fossil-fuel prices, delignitisation follows degasification and new RES flexibility renders Ptolemaida V idle, except for 2030, when it is put to use to meet growing electricity needs and complete gas phase-out goals. All other electricity is RES-powered, in line with the 80% and 100% RES targets. Solar and onshore wind plants expectedly demonstrate higher production in time, while technologies that are not widely used in the other two scenarios, such as geothermal, biomass, offshore wind, and small hydro, have a more significant role in this scenario, without hitting the maximum potentials outlined in the official LTS. Notably, geothermal produces around 2% of total electricity needed in 2035, despite its absence in the other two scenarios. This, however, hints that the *High Ambition* scenario target for 100% RES in 2035 can only be realistic if the country's outlined potentials (maximum capacity and speed of capacity expansion—key drivers in the OSeMOSYS framework) stand and there is provision for investments in costlier technologies (Giarola et al., 2021). It is also noteworthy that overall RES capacity is stressed until 2030; afterwards, power generation from biomass and offshore wind slightly drops as onwards more onshore wind can keep up with the 2035 target at lower costs.

A critical takeaway is that, as early as in 2026, total demand for natural gas can drop by 43% (including electricity generation and direct demand in the energy demand sector) relative to 2020 values—i.e., when 39% of gas imports were from Russia (Eurostat, 2022d). This means that the *High Ambition* scenario could achieve complete independence from Russian natural gas by 2026, without any new gas investments, and that includes LNG infrastructure (Balkan Green Energy News, 2022). As such, this rapid decline in natural gas demand also in line with current European trends (McWilliams et al., 2022) should be considered when planning new natural gas infrastructure. Afterwards, gas demand continues to decrease until 2030, before a rebound from the industrial sector, which is nevertheless contained and outperformed by rapid electricity-sector degasification.





(a)



(b)



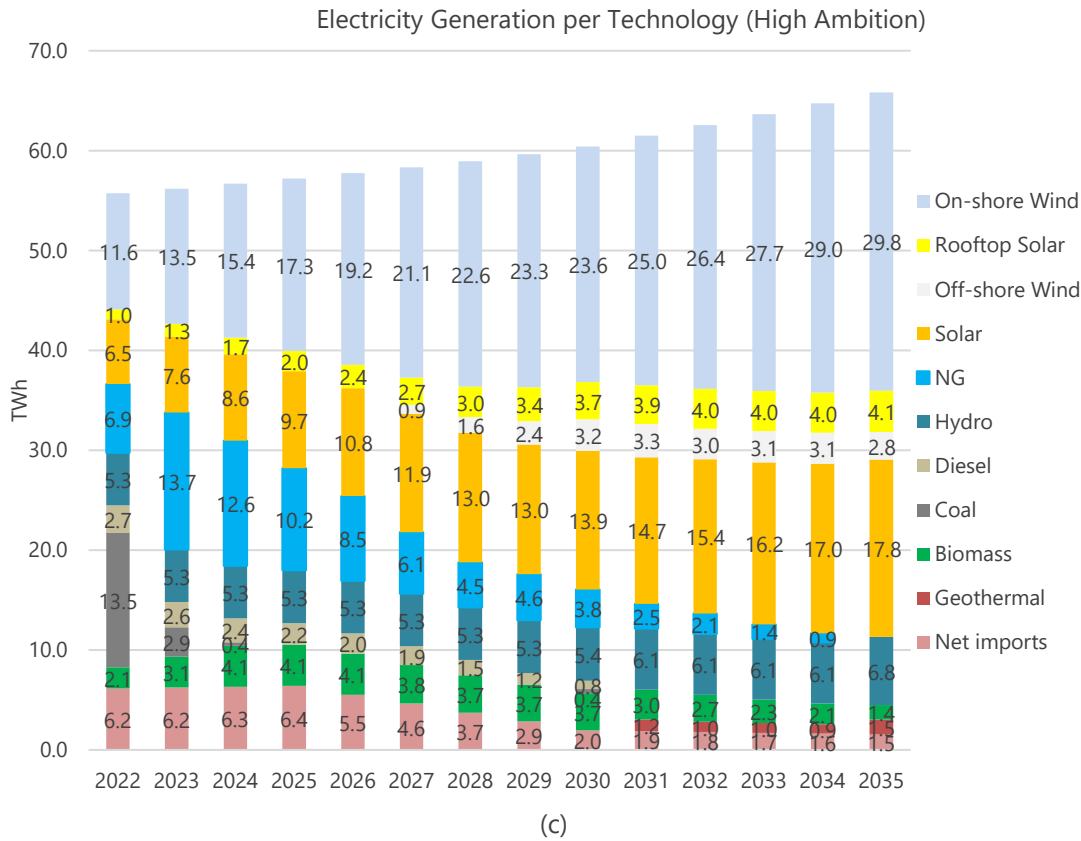


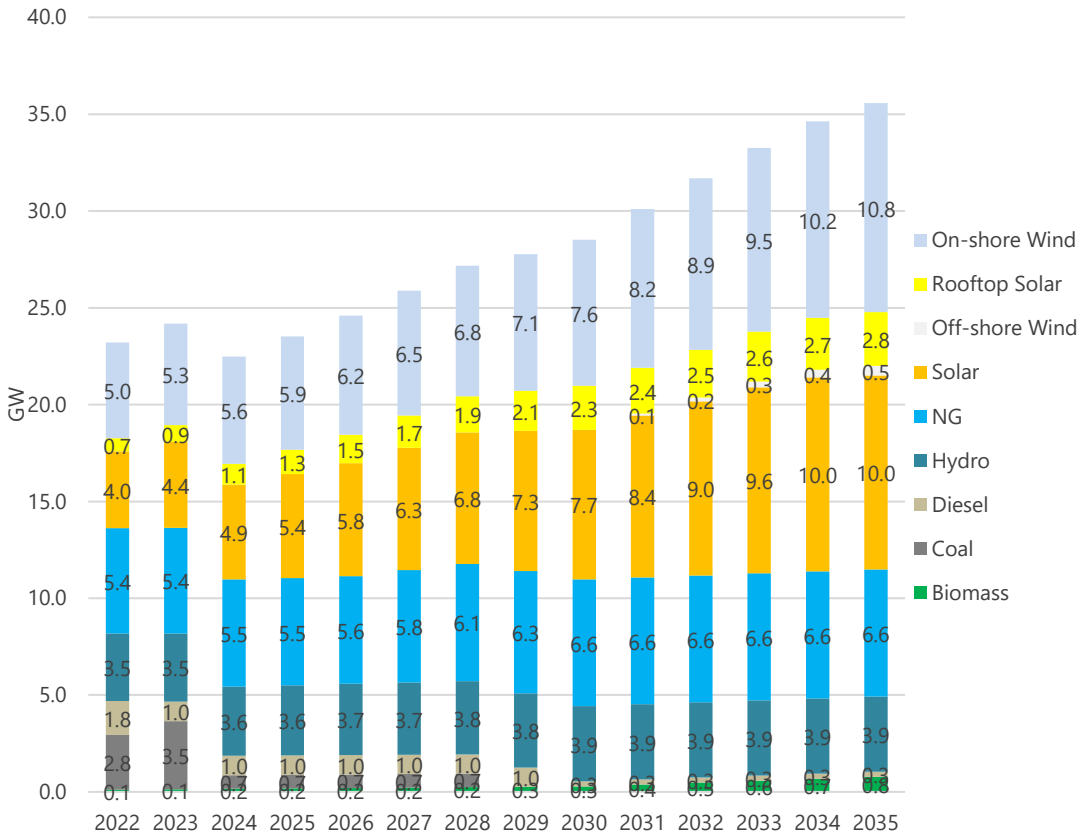
Figure 36: Electricity generation per technology (in TWh) for the: (a) Greek NECP, (b) Climate Law, and (c) High Ambition scenarios.

Source: OSeMOSYS.

A similar picture is drawn in installed capacities (Figure 37): the *Greek NECP* and *Climate Law* scenarios display similar patterns, except for (small) hydro, which is further boosted by *Climate Law*. In contrast, the *High Ambition* scenario leads to significant capacity increase in offshore wind, biomass, small hydro (even higher than the *Climate Law* boost), and geothermal, in fact closing in on the caps assumed in the official Greek NECP and LTS documents. Same potentials are assumed for the two first scenarios but never maxed out, due to higher costs compared to other alternatives that could get the lower RES target job done without limiting natural gas. A critical caveat is that only for onshore wind we define a slightly more flexible cap than assumed in the NECP, drawing from Enevoldsen et al. (2019) and the market’s willingness to support more ambitious rollout considering the total capacity of wind plant installation applications currently surpassing 35 GW (Kati et al., 2021)—we apply this flexibility to all three scenarios but it only comes into effect in *High Ambition*. It is noteworthy that higher RES capacity is linked to lower gas consumption and not higher electricity demand, which is not projected to increase compared to the two official policy scenarios, despite higher EV registration; this is because faster refurbishments in the household and tertiary sectors counterbalance the higher electricity demand in transport. Another important insight, however, is that this *High Ambition* scenario brings about energy security issues: fossil fuels and hydro are used for reserve margin, and only the latter remains post-2035. Therefore, considering the 5GW hydro potential, this scenario can best be implemented with further energy efficiency provisions to mitigate the hinted energy security risks (even if the 5GW cap is not reached), and it also highlights the indispensable role of energy efficiency in the feasibility of scenarios that respond to the current events but also pursue ambitious climate targets. Concerns over reserves are additional to the risk of nearing the assumed potentials for other key technologies (e.g., geothermal (Karytsas et al., 2018)), which gets close to 500 MW, with a technical limit assumed at 700 MW in the Greek NECP document (Hellenic Republic Ministry of the Environment and Energy, 2019)).

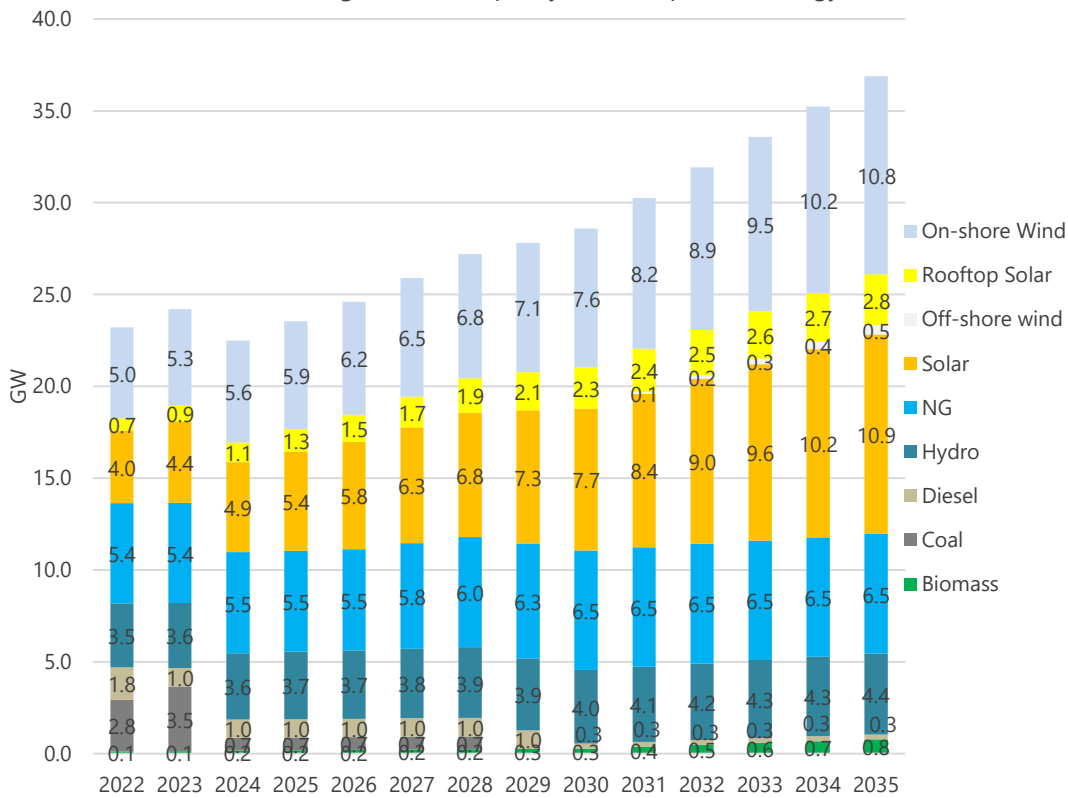


Power generation capacity installed per technology (Greek NECP)



(a)

Power generation capacity installed per technology (Climate Law)



(b)



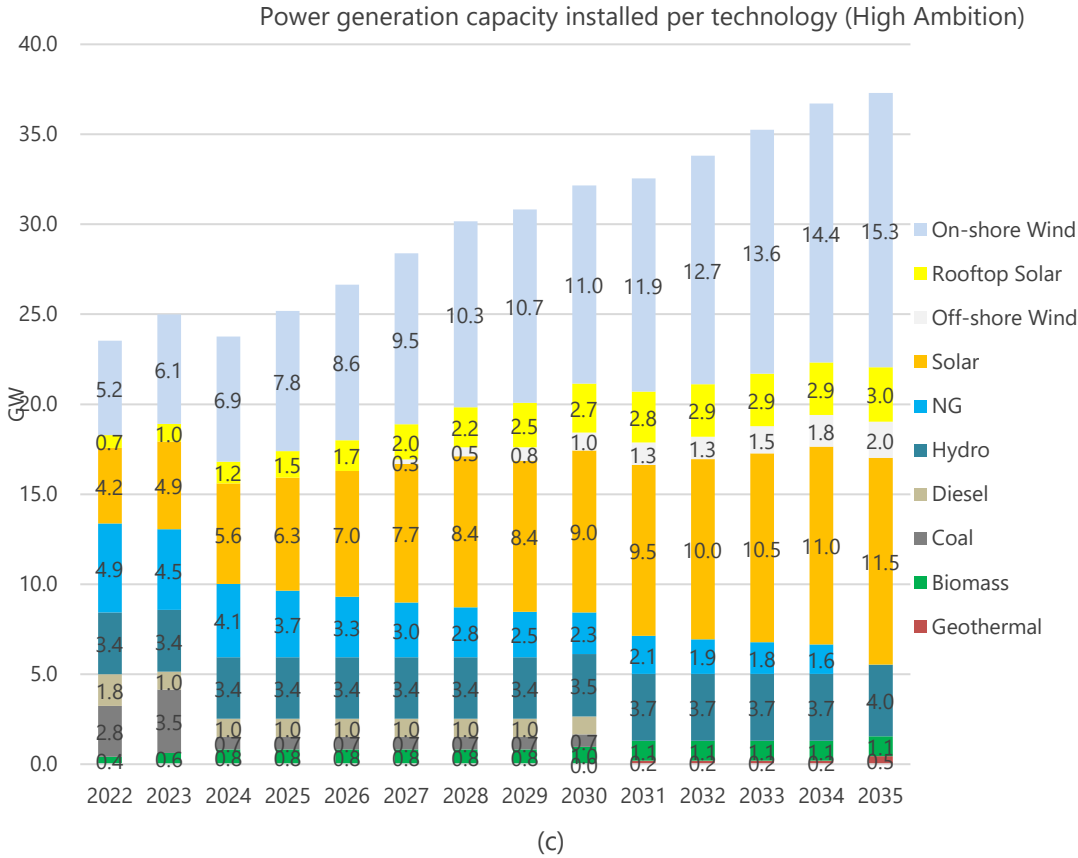


Figure 37: Power generation capacity installed per technology (in GW) for the: (a) Greek NECP, (b) Climate Law, and (c) High Ambition scenarios.

Source: OSeMOSYS.

We also extract electricity cost trajectories for the three scenarios, to investigate whether higher RES ambition dramatically increases the burden for end-users (Figure 38). In the two official policy scenarios, power generation costs constantly drop, due to RES penetration throughout the examined timeframe and thus a decrease in OPEX and costs associated with CO₂ emissions. Between the two scenarios, slight deviations occur post-2030, relevant to an increase in small hydro in *Climate Law*. *High Ambition*, on the other hand, displays significant divergence. First, costs remain considerably lower until 2030, mainly due to low operation and emissions costs originating from the higher RES penetration. By scenario definition, emissions costs totally diminish by 2035. In 2035, a spike can be observed (approximately 107 €/MWh, as opposed to 98 and 103 €/MWh for *Greek NECP* and *Climate Law*, respectively), reflecting that the required capacities from new technologies (geothermal, offshore wind, biomass) are costlier than solar and onshore wind. Therefore, from a purely cost viewpoint, initial model runs highlight trade-offs among the three scenarios, which are mainly attributed to the speed of degasification: the two official policy scenarios cost more in terms of operation and emissions but require little deployment of more expensive technologies until 2035. A critical question is whether the latter costs are only avoided in the short run, since gas phase-out must eventually occur and the more it is delayed the higher emissions from natural gas will cost; the other side of the coin, however, is the prospect of technological costs also dropping markedly in the near future (see, e.g., (Grant et al., 2021)). Benefits are further underpinned if we consider the significantly reduced energy demand for *High Ambition*: despite electricity demand remaining steady due to higher EV penetration, transport demand drops drastically; as such, the anticipated financial burden and total energy costs for households will also drop even if we consider the 2035 spike. However, this comes with the need to finance the necessary measures to support these demand reductions including high rate of refurbishments and increased EV penetration, as discussed in Section 4.2.2.



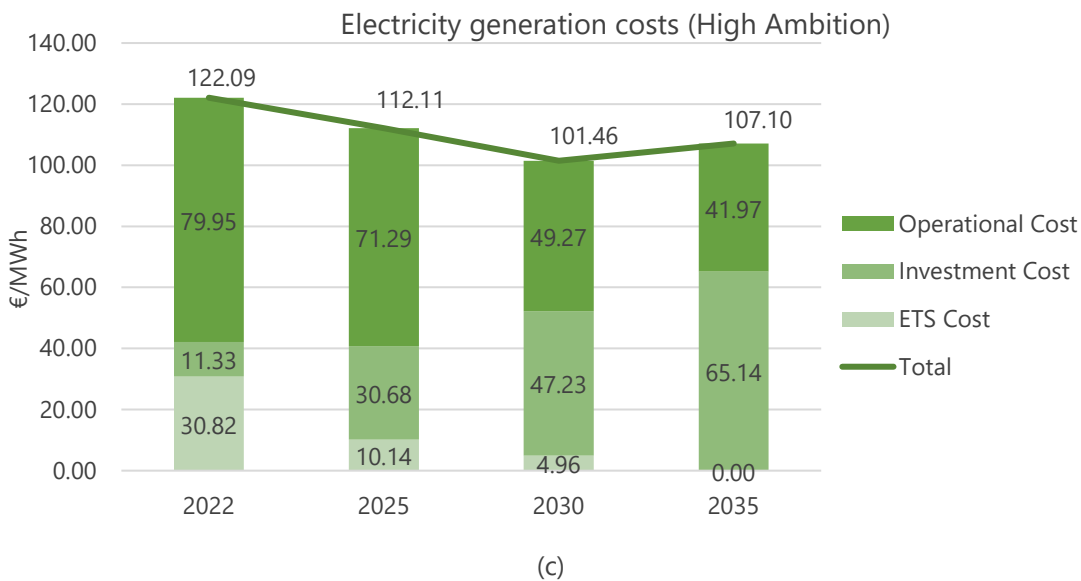
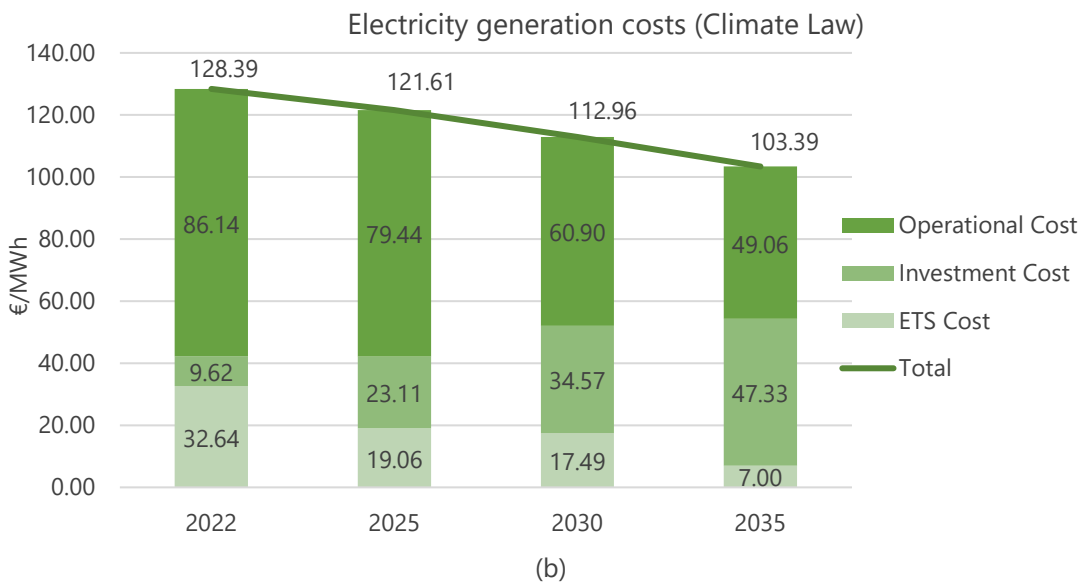
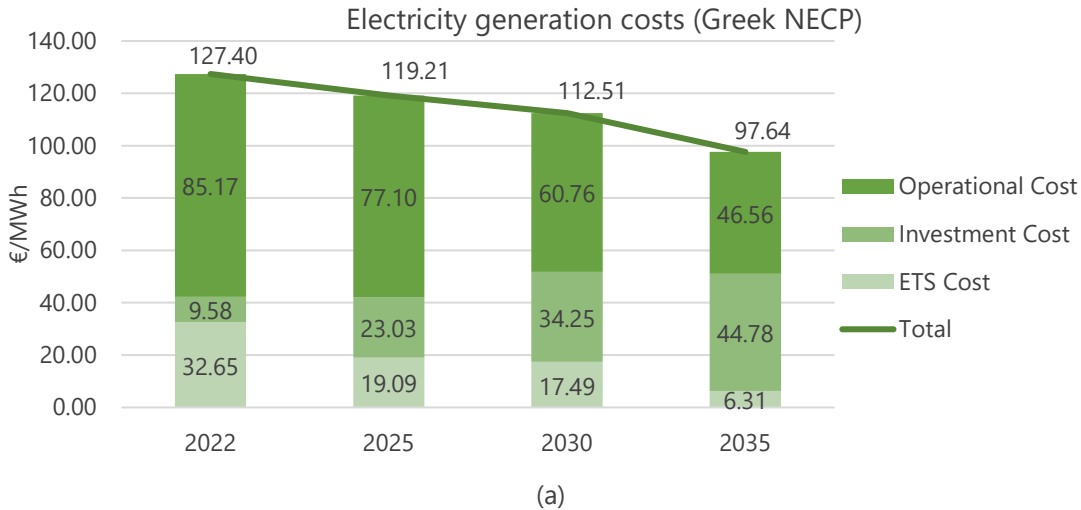


Figure 38: Electricity generation costs (in €/MWh) for the: (a) Greek NECP, (b) Climate Law, and (c) High Ambition scenarios.

Source: OSeMOSYS. ETS prices are drawn from the latest official EU Reference Scenario (European Commission, 2022b).



That said, the average annual cost of electricity generation for the entire horizon is lower in the *High Ambition* scenario (108 €/MWh, as opposed to 112 and 115 €/MWh for the *Greek NECP* and *Climate Law* scenarios, respectively), making the raised ambition lucrative. The largest caveat here lies in the assumption that mid-2022 price spikes (Makholm, 2022) return to normal levels soon: we use (and revise for 2021) the latest available authoritative database for fossil-fuel price projections—i.e., IEA’s 2021 World Energy Outlook (IEA, 2021); as such, OPEX for gas may be seriously underestimated. Constraints set by the model analysts should also factor in, when drawing conclusions from this cost analysis (Howells et al., 2011); these may heavily affect capacity additions and technologies included in the power mix to cover demand. Here, the upper deployment limits for each technology are obtained from the maximum potentials described in the official Greek NECP, except for onshore wind potential; nevertheless, we used the current solar and onshore wind deployment rate as maximum. Considering RES investments commonly face bureaucratic delays and/or societal opposition at the local level (Nikas et al., 2020b), the higher prices for the *High Ambition* scenario towards the end of the modelling timeframe may be perceived to reflect limited state capacity to overcome such barriers and preference of less cost-effective technologies.

Finally, Figure 39 illustrates CO₂ emissions trajectories per scenario. The *Greek NECP* and *Climate Law* cases demonstrate similar patterns, owing to their similar electricity mix, with a downward tendency towards a bolder-than-80% reduction by 2035, thanks to renewables and total delignitisation; their only—albeit notable—difference is that the *Climate Law* may in fact lead to slightly higher power-sector emissions due to higher transport electrification, although this increase in emissions may be outperformed by reduced consumption of gas and diesel and thus reduced transport-sector emissions, which is not reflected in the model. The *High Ambition* scenario demonstrates an emission trajectory that leads to zero (power-sector) emissions in 2035 by definition; what is important to note, however, is that this scenario achieves a very rapid reduction in the first years of the modelling timeframe, when lignite and natural gas are actively phased out of electricity generation—again, a small uptick in 2030 can be attributed to the need to use Ptolemaida V, which is otherwise left idle since 2025.

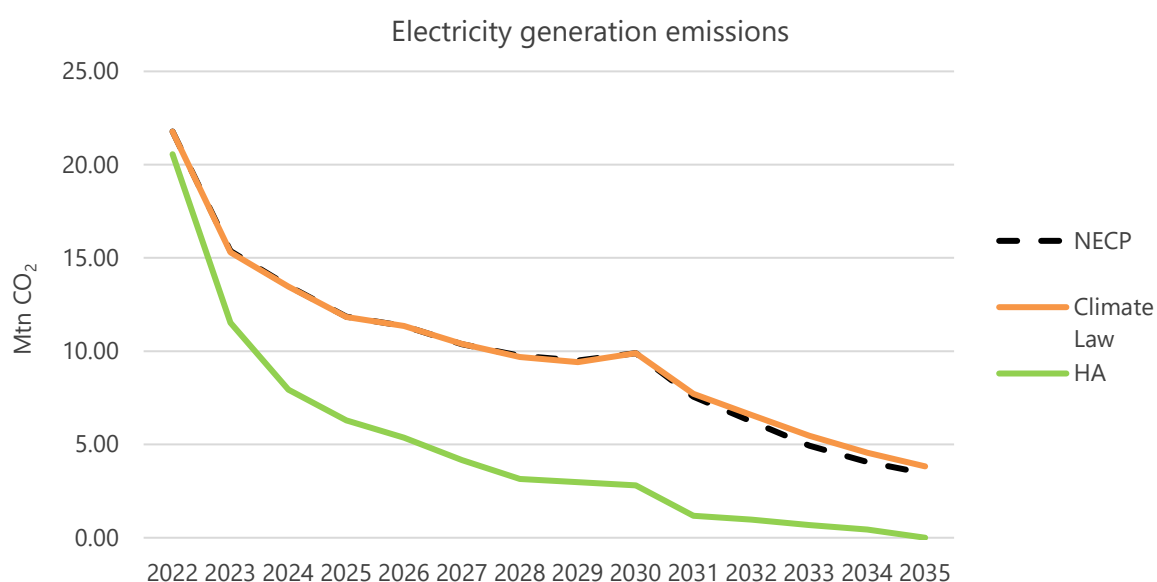


Figure 39: Electricity generation emissions (in Mtn CO₂) per scenario.

Source: OSeMOSYS.

4.4 Considerable risks from the stakeholders’ perspective

In June 2022, a physical workshop was held in Athens, Greece, to obtain feedback from stakeholders on the scenarios modelled, especially in the light of the unfolding energy crisis. Experts were identified and invited from



contacts of the National Technical University of Athens, based on their professional relevance to the country's energy-planning. Eventually, 36 people joined the workshop from 20 relevant institutions, including the ministry of environment and energy, the two largest electricity and gas companies, the regulatory authority for energy, the HEDNO and IPTO operators, the gas transmission operator, six renewable and fossil-fuel energy associations, two research centres, and two environmental NGOs. The workshop was followed up with a separate session dedicated to the FCM exercise, with a diverse subset of the stakeholder group attending the workshop (12 stakeholders). Participants were informed that both the workshop and the FCM session were held under the Chatham House Rule and that they were approved by the Ethics Mentor of the National Technical University of Athens.

The FCM design process was fuelled by the modelling results, as in Antosiewicz et al. (2020): it kicked off with a presentation of the model results, followed by group discussions, before eventually co-designing the map, following the sequential approach from Song et al. (2020). After co-designing the core body of the FCM (i.e., the system components of the Greek power sector, see Table 10), stakeholders were asked to voice their biggest concerns to today's energy crisis, in the form of possible bottlenecks to decarbonisation. Input was condensed into eight specific barriers and/or uncertainties (U_x), as shown in Table 11.

Table 10: System components of the Greek power sector FCM, as designed with the stakeholders

ID	Short description of selected system components
S1.	Natural Gas Imports
S2.	Decentralisation of Energy
S3.	Grid Stability
S4.	Energy Storage
S5.	Electricity Prices
S6.	Energy Poverty
S7.	Energy Security
S8.	Technological Lock-ins
S9.	RES Investments
S10.	RES Incentives
S11.	Electricity demand
S12.	RES Micro-generation
S13.	Large Scale RES Expansion
S14.	Energy Communities
S15.	Share of Lignite in the Electricity Mix
S16.	Share of RES in the Electricity Mix
S17.	Power System Decarbonisation

Table 11: Barriers/bottlenecks and/or uncertainties raised and discussed by the stakeholders

ID	Short description of selected barrier/uncertainty
U _{1.}	Societal opposition to new renewable energy projects, mainly driven by environmental concerns
U _{2.}	Bureaucracy and complexity of current regulatory framework (licensing, financing, etc.)
U _{3.}	Persisting energy crisis, with implications of gas price shocks for electricity system costs and energy bills
U _{4.}	Delayed take-off of (green) hydrogen technology, delaying energy storage diffusion and decarbonisation
U _{5.}	Fossil fuel lock-ins, notably due to new LNG infrastructure investments in response to current crisis
U _{6.}	National decarbonisation vision not shared among all stakeholders
U _{7.}	Challenges to interconnection between the mainland grid and the island systems



U8. Unavailability of geothermal for electricity (limited true potentials, concerns for costs, social opposition)

These bottlenecks were then linked to the FCM, with stakeholders discussing which FCM nodes are directly affected by negative developments, should each of these bottlenecks materialise. Finally, in a process of deliberation, participants altogether assigned one single weight to each of the identified interconnections of the map. The resulting FCM is illustrated in Figure 40.

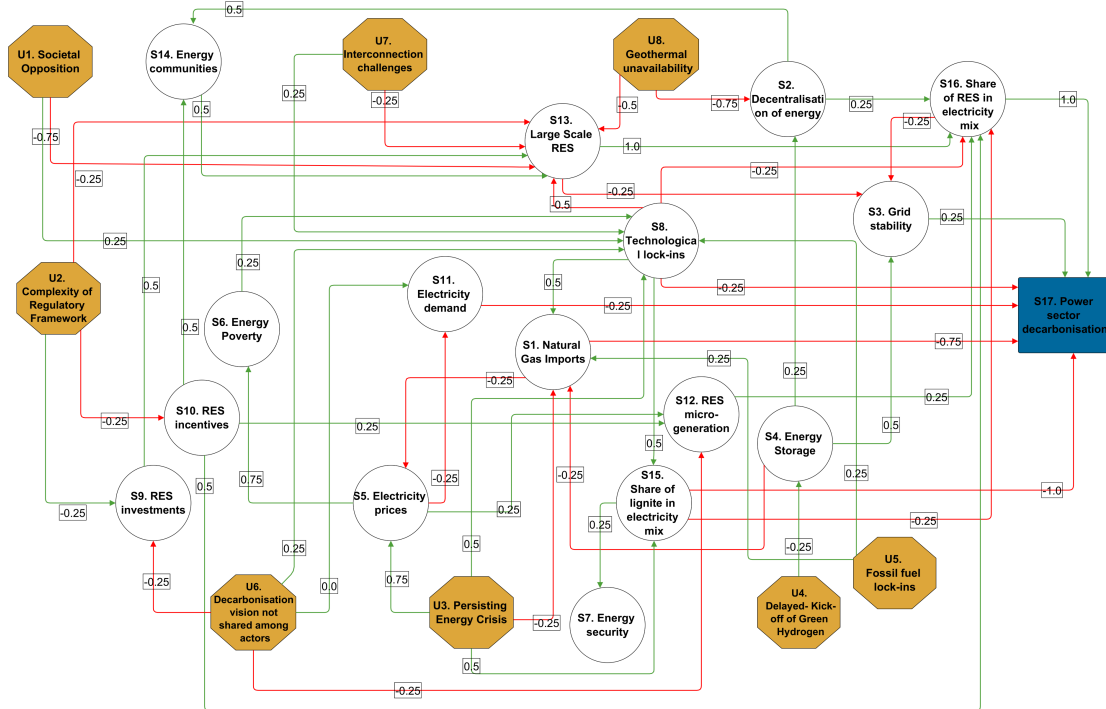


Figure 40: The resulting FCM for the Greek power sector, including the experts’ assessed weights of interconnections.

Yellow octagons are used for barriers/uncertainties (Ux), white ovals for system components (Sx) and blue rectangle for the end goal (S17). Positive cause-and-effect links are depicted with green arrows, while negative links are illustrated with red.

Contrary to common practice in FCM research, where FCMs are simulated for policy (strategy) shocks (e.g., (Nikas et al., 2020c; Nikas et al., 2019b; Song et al., 2020)), we instead stimulate the FCM explicitly based on uncertainty shocks, to explore which of the eight identified bottlenecks impact the system’s decarbonisation process the most. As discussed in Section 4.2.3, we use the tool and method discussed in Koutsellis et al. (2022b), by activating one bottleneck while keeping all others inactive (i.e., eight FCM simulations, one for each bottleneck). Results are presented in Figure 41.

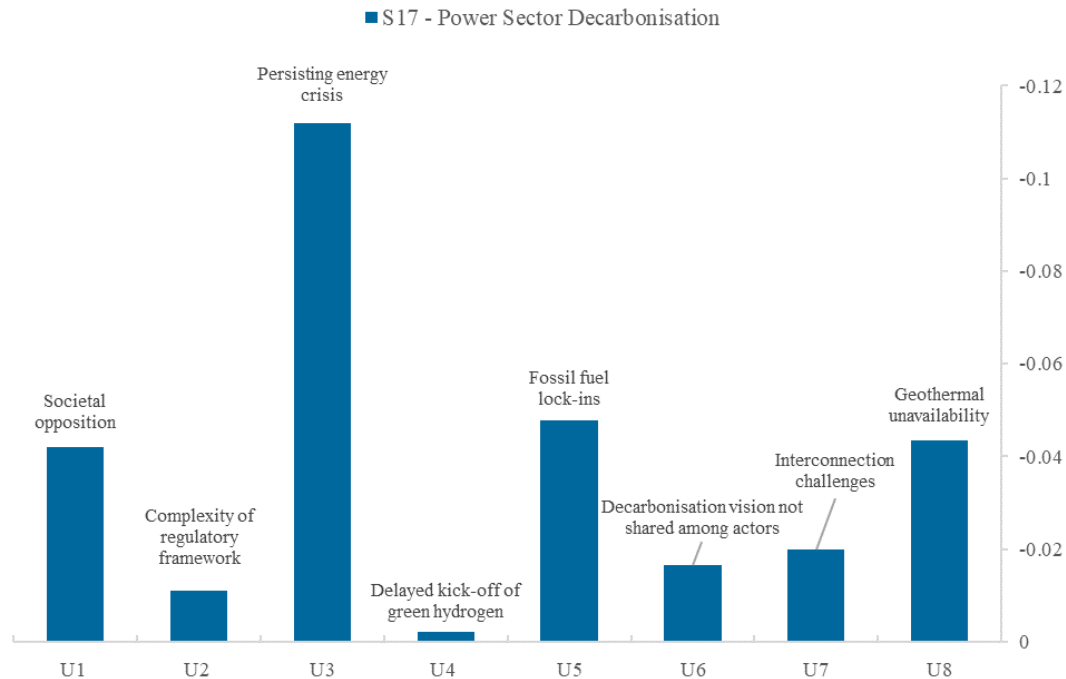


Figure 41: FCM results for the implications of each uncertainty (U_x) on Greek power sector decarbonisation (S17).

Each column presents the negative impact that the activation of the corresponding uncertainty/bottleneck has on the score of the decarbonisation (S17) node.

Evidently, participants' most pressing concern is the possibility of the energy crisis persisting, followed by fossil fuel lock-ins, lack of geothermal energy, and societal opposition to new RES projects. The already fragile energy supply due to the pandemic has suffered deeper disruptions following the Russian invasion of Ukraine and generated a surge in energy prices. Greece was shown to be particularly vulnerable to this surge, as wholesale electricity prices consistently remained among the highest in the EU since the start of the crisis and well into the second semester of 2022 (RAE, 2022), with stakeholders explicitly contesting our original assumption—and consequently the employed authoritative dataset—that prices soon return to normal levels. As the crisis persists, a prolonged phase-out of lignite has been increasingly viewed as a way to ensure supply-side flexibility (Reuters, 2022b). Throughout Europe, efforts to decrease Russian gas dependence have been focusing on four interrelated dimensions: diversifying supply, reducing demand, accelerating transitions, and improving interconnections (European Commission, 2022a). However, an extensive shut-off of Russian natural gas is likely to amplify the impact on energy prices, with persistent supply shocks deferring economic activity and a shift to lignite further undermining the goal of carbon neutrality (Di Bella et al., 2022). In terms of new energy infrastructure, even, Greece and Bulgaria jointly expect a new LNG terminal of 5.5 bcm capacity to be operational in 2023, an investment likely to perpetuate Greece's natural gas lock-in, in turn impairing its energy transition pathway, as indicated by the FCM results (Kemfert et al., 2022). Turning to the socio-political aspects of the transition, stakeholders seemingly perceive community opposition to renewable projects as more impactful in hindering decarbonisation than the current regulatory complexity or a lack of common vision among actors. The absence of community acceptance appears to be a substantial barrier to building new RES facilities (Sovacool et al., 2022), potentially hindering permit acquisition and leading to project delays or even cancellations (Susskind et al., 2022). Finally, the most significant technological uncertainty raised is the possible unavailability of geothermal resources attributed to community opposition, limited true potential, and high technological costs along the way. Geothermal utilisation in Greece is

rather limited even though its potential could considerably contribute to decarbonisation targets. The interest in exploiting geothermal energy is mainly focused on non-interconnected islands, where electricity is supplied by diesel-powered generators (Kavadias et al., 2019); however, past deficiencies (e.g., Milos power plant) have shaped local society opposition ever since, halting further development (Papachristou et al., 2019).

4.5 Stakeholder-informed sensitivity analysis

Following the participatory workshop and the bottlenecks/uncertainties that experts highlighted in the FCM analysis (Section 4.4), we select their four top concerns to introduce in the original modelling analysis and explore their implications. The most pressing concern orbits around the real risk of fossil-fuel prices remaining high in the near-term. The three following bottlenecks, which were found close to one another in Section 4.4 and are of similar (technological) nature, include limited technical capacity to achieve fast degasification by 2030, spatial constraints regarding the expansion of onshore wind plants in respect to the intertwined ecological (Natura 2000 areas) and societal (NIMBY) barriers, and absence of geothermal power.

Regarding fossil-fuel price projections and their consequent implications for technoeconomic model assumptions (Section 4.5.1), we design two sets of scenarios. The first set considers that the prices observed during the 1st half of 2022 (Tradingeconomics.com, 2022) remain as high throughout the year, before then linearly extrapolating them onwards to reach IEA's 2021 projections (IEA, 2021) by 2030. The second set assumes that these Q1-Q2 2022 prices remain steady until 2025, before then linearly extrapolating to gradually reach IEA's 2021 projections (IEA, 2021) by 2035. These assumptions are consistently considered for all three policy scenarios.

For all other three concerns, we design three variants of the *High Ambition* scenario (Section 4.5.2): the first one examines the inability to achieve fast degasification, by assuming that gas capacity remains steady until 2030 and no gas plants are shut down by 2030; the second variant assumes spatial constraints to further penetration of onshore wind due to environmental concerns for areas falling into the Natura 2000 network, setting a 10.7 GW cap of total onshore wind capacity (Kati et al., 2021); and the third variant blocks geothermal from power generation.

We finally run a *Combo* variant of all three policy scenarios to include all three bottlenecks, on top of the more pessimistic price scenario (Section 4.5.3).

Energy demand (Section 4.3.1) is assumed unimpacted throughout the sensitivity analysis.

4.5.1 Persistent price shocks from today's energy crisis

Despite higher fossil-fuel prices, evolution of the power generation mixes in *Greek NECP* and *Climate Law* remain similar to those of Figure 36, with the only important difference lying in 2023 power generation heavily relying on lignite instead of gas; the latter dominates afterwards once more. This pattern is also evident in the *High Ambition* scenario until 2025, at which point increased prices accelerate gas phase-out, supported by the active Ptolemaida V power plant, as well as hydro and biomass generation that considerably increases compared to the original *High Ambition* runs. Figure 42 inter alia shows that offshore wind is now introduced way earlier but attains a smaller share in 2035. Less significant deviations can be observed in installed power capacity, with the only changes observed in the *High Ambition* scenario: we see higher penetration of hydro (200 MW and 400 MW, if prices start returning to 'normal' between today and 2030 or between 2025 and 2035, respectively), and earlier penetration of geothermal and biomass. For the latter, however, the 2035 shares remain identical to the initial run. A similar behaviour can be observed for offshore wind, which eventually gets a small blow due to the larger share of the more cost-effective hydro.



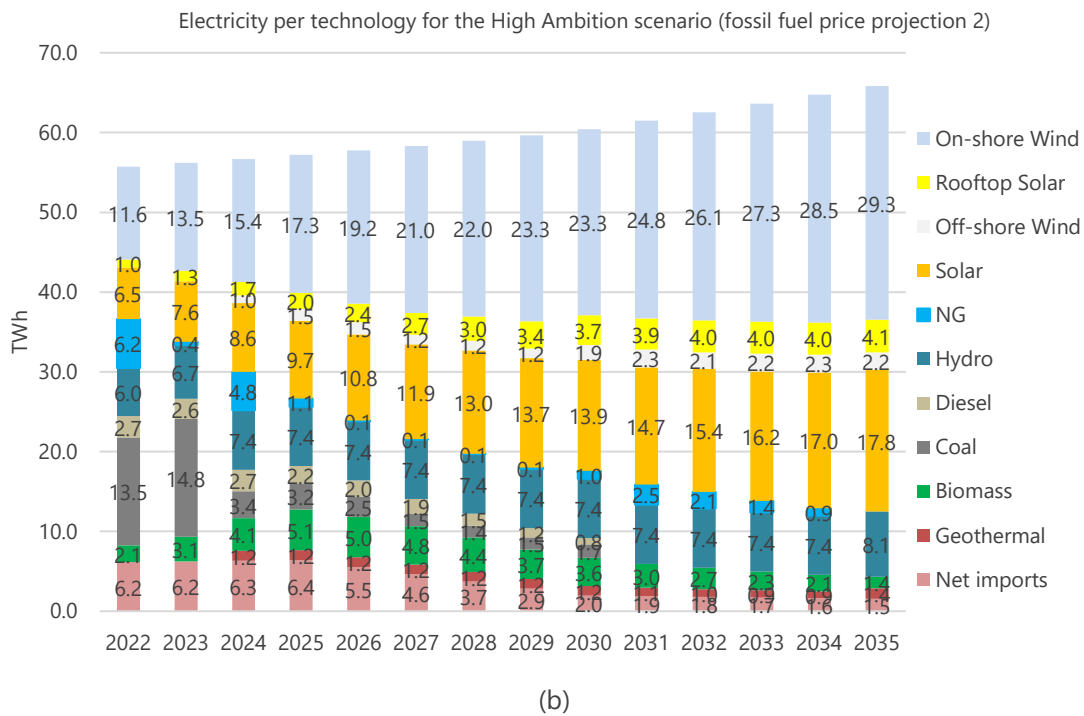
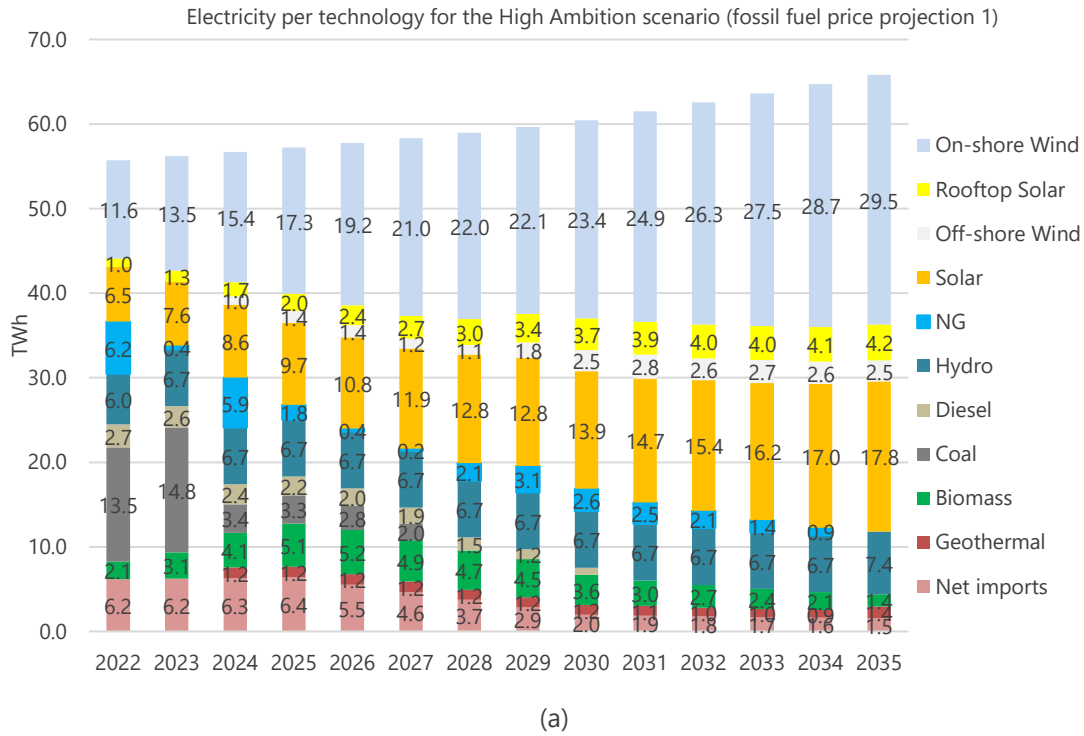


Figure 42: Electricity per technology (in TWh) in the High Ambition Scenario if current prices gradually align with IEA’s 2021 World Energy Outlook (IEA, 2021) projections (a) in 2023-2030 (fossil-fuel price projection 1) and (b) in 2025-2035 (fossil-fuel price projection 2).

Source: OSeMOSYS.

Expectedly, when looking at power-sector costs, electricity generation is significantly costlier since it is heavily based on persistently expensive gas. The effect of the new fossil-fuel price projections is more evident in the *Greek NECP* and *Climate Law* scenarios, since they set lower RES targets, leading to higher dependence on gas. Should prices return to what IEA had projected before the Ukraine conflict by 2030, the *Greek NECP* and *Climate Law* electricity generation costs begin at 148 €/MWh in 2022, stabilise until 2025 (140 €/MWh), and then drop to 113



€/MWh in 2030. This increase is reflected in the average generation costs for the entire horizon, which increase by almost 10% (122 €/MWh). Instead, *High Ambition* demonstrates a better response to the price shocks (139 €/MWh in 2022, before significantly dropping by 2025 to 118 €/MWh, leading to a total average of 114 €/MWh). This contrast is further amplified, if fossil-fuel price shocks are assumed to persist for the next three years before slowly aligning with IEA's projections by 2035. The two official policy scenarios reach 153 €/MWh in 2025, before dropping to 129 €/MWh in 2030 and finally aligning with Section 3 runs in 2035, leading to an average cost of approximately 130 €/MWh for the time horizon. On the other hand, *High Ambition* displays even higher robustness against the persistently high prices, with electricity costs remaining completely unaffected from this further delay of return-to-normal; in fact, from 2030 onwards costs are slightly reduced even, mainly due to lower diffusion of offshore wind.

4.5.2 The impact of underexplored technical constraints to the High Ambition scenario

In the case of slower degasification, despite the stable 5.4GW gas capacity until 2030, high RES targets still drive an important decrease in gas-powered electricity by 2030, yet not as steep as in the initial runs. This change mainly affects biomass and offshore wind, which now generate less electricity. Slower degasification also leads to complete delignitisation as early as in 2023, meaning that Ptolemaida V need not operate to make up for gas losses.

The spatial constraints variant, on the other hand, demonstrates larger deviations, limiting the penetration of onshore wind, which is the dominant source of renewable energy. This variant showcases an increase in the penetration of every other renewable technology, except for solar, which had already reached its cap. Offshore wind generates 3.6 TWh of electricity in 2035, compared to 2.8 TWh in the initial iteration (about +30%). Similar increase rates are found for hydro and biomass, while geothermal shares demonstrate even higher gains (more than doubling). Interestingly, a case for CSP is made for the first time, meaning that constraining onshore wind would require investing in all other (costlier) RES to deliver on the ambitious power-sector decarbonisation targets. This insight is even more visible in terms of capacity: geothermal and hydropower reach their maximum potential (700MW and 5.3 GW respectively), and even CSP maxes out its potential, thereby requiring 300MW-worth of investments, with all caps stemming from the official Greek NECP document. Although generation from offshore wind and biomass increases, their capacity remains unchanged.

Instead, should geothermal be considered off the table, results are similar to the initial *High Ambition* iteration, with few but insightful deviations in terms of technological dynamics in the model: onshore wind sees a non-negligible 6% reduction (1.7GWh), with hydro making up for both this drop and the absence of geothermal (around +44%) and rooftop solar power marking a 10% increase too. These are not reflected in total capacity installed other than hydro capacity further increasing by 25%, almost maxing out its officially prescribed potential.

Costs-wise, only negligible deviations can be observed: slower degasification leaves the *High Ambition* scenario unaffected (108 €/MWh), while the other two bottlenecks yield a negligible uptick of 1 €/MWh mainly due to the slightly bigger investments in costlier technologies (small hydro and CSP).

4.5.3 What happens if all goes sideways?

Assuming prices delay their return to their projected normal by more than a decade and applying all three technical bottlenecks means that *Greek NECP* and *Climate Law* are only affected by the fossil-fuel price shocks and the spatial constraints for onshore wind; the *High Ambition* scenario, in contrast, is affected by all four factors.

For *Greek NECP*, spatial constraints combined with the higher fossil-fuel prices would mean more hydropower (+18% capacity) to optimise electricity generation costs due to high gas prices, as well as slightly lower wind-



powered electricity. Spatial constraints also highlight the need for more solar in 2035. Cost-wise this deviation leads to a slight uptick in power-sector costs, due to new small hydro plants that are less cost-effective than onshore wind. The *Climate Law* scenario changes are similar, albeit smaller.

The most interesting takeaways lie in the *High Ambition* scenario, which now faces a series of critical constraints on top of the less troublesome, albeit otherwise game-changing, continuation of today's fossil fuel prices. To cost-optimally meet the 100% RES target for 2035 while counterbalancing the absence of geothermal and the significant reduction of onshore wind potential, biomass increases by 40%, hydropower increases by 30%, offshore wind more than doubles, while CSP is also introduced—this stresses that, from a modelling perspective, this higher ambition scenario is still doable, but the real-world implementation feasibility increases hinting at the need for effort and commitment. Slower degasification does not significantly affect the other sources since the slightly higher generation from gas mainly replaces the small chunks of geothermal electricity, without affecting the penetration of other renewables. These deviations are less evident in terms of generation capacity: apart from a new installation of 0.3 GW of CSP and the big drop of onshore wind (by 5GW compared to Section 4.5.1 results), all other RES are not much impacted: hydropower reaches its cap (5.3 GW) and offshore wind marks a 20% increase over Section 4.5.1 shares, demonstrating lower investment needs and capacity for better use of current power-sector infrastructure. This is also reflected cost-wise: this 'combined bottlenecks' case is the only variant, where costs continue to drop post-2030, as fewer investments are needed instead of spiking towards the end of the modelled timeframe.

4.6 Conclusions

By mid-2022, the evolving global energy crisis has led to soaring natural gas prices and rising inflation in Europe, which is threatened by energy shortages during the 2022-2023 winter (Sgaravatti et al., 2022). In response, most Member States are planning to diversify their natural gas supply to reduce their reliance on Russian gas, fuelling fears of a fresh gas lock-in that may jeopardise the ambitious climate action of the bloc (Climate Action Tracker, 2022). Among Member States, Greece is particularly affected by the current crisis: gas-fired power plants provided over 40% of generated electricity in 2021 and are now driving among the highest electricity prices in the EU, while further exacerbating energy poverty in the country. Nonetheless, gas is still assumed to be a pillar of the country's delignitisation effort based on the current energy policy, namely the Greek NECP (Hellenic Republic Ministry of the Environment and Energy, 2019) and the recently enacted Climate Law (Hellenic parliament, 2022). In an effort to quantify the reliance of existing policies on natural gas, we use an energy system modelling framework based on coupling the LEAP and OSeMOSYS models to assess the evolution of Greek energy demand and electricity generation mix until 2035 by simulating a *Greek NECP* and a *Climate Law* scenario. We contrast these scenarios with an alternative energy transition pathway (*High Ambition*), aiming for 100% decarbonisation by 2035 by assuming ambitious penetration of RES, rapid degasification, and electrification of heating and passenger transportation. Then, using an FCM model informed by a diverse group of 36 stakeholders from the Greek power sector, we elicit and model the impacts of diverse uncertainties that may affect the transition. This study is especially timely for Greece as measures for addressing the energy crisis in the short term, including plans for expanding the LNG infrastructure and re-activating lignite power plants, may push the country towards a fossil-fuel lock-in, jeopardising climate action in the long run.

Results show that electricity generation from natural gas almost doubles between 2022 and 2030 in both the *Greek NECP* and *Climate Law* scenarios, a finding that is especially troubling considering today's skyrocketing prices for natural gas and Greece's struggle to decrease reliance on Russian gas. In contrast, the *High Ambition* scenario achieves complete independence from Russian gas by 2026, avoiding any new gas infrastructure, including LNG terminals. This is mainly achieved by additionally investing in infrastructure for offshore wind, biomass, small hydro,



and geothermal, to make use of the potentials assumed as technically and socio-politically realistic in the Greek NECP and LTS on top of the large expansion in onshore wind and solar energy. Due to its focus on diverse renewable sources, the *High Ambition* scenario leads to deeper and faster CO₂ emissions cuts than in current national policies, but in line with the intentions from the European Commission to significantly decarbonise European power in this decade (European Commission, 2022a). While the proposed scenario is also cheaper on average over the entire horizon, its reliance on new and less cost-effective technologies (e.g., geothermal, small hydro, and offshore wind) requires new investments post-2030. Nonetheless, overall energy demand is projected to be much lower in this scenario due to faster electrification of the transport and residential sectors, reaching a 17% and 30% reduction compared to the *Greek NECP* and *Climate Law* scenario in 2050 and potentially leading to a less expensive energy system. Overall, results indicate that policy reactions to the energy crisis that promote a diversified renewable mix instead of insisting on natural gas can lead to a cleaner and cheaper energy system.

The *High Ambition* scenario also seems to be more robust than existing policies in case the currently high fossil-fuel prices continue post-2022, a concern highlighted the most in our stakeholder-informed FCM model of the Greek power-sector decarbonisation. While the *Greek NECP* and *Climate Law* scenarios clung on natural gas despite high fossil-fuel prices, these prices led to an even faster gas phase-out in 2025 in the *High Ambition* scenario, supported by slightly higher use of existing lignite plants, higher hydro and biomass generation, and faster introduction of offshore wind. High prices also affected the cost of electricity in existing policy scenarios, increasing the average cost over the entire horizon, especially in the short term. In contrast, the respective increase to the *High Ambition* scenario was relatively negligible, regardless of how long the sky-high prices remain high. However, stakeholders also pinpointed potential constraints to RES expansion that *High Ambition* requires, via lock-ins into fossil fuels due to current LNG expansion plans, community opposition to spatial expansion of onshore wind driven by environmental concerns, and likely unavailability of geothermal due to potential overestimation. Running these variants for the *High Ambition* scenario showed that, although minimal, cost-related effects stemming from these bottlenecks can all affect the electricity mix: community opposition can significantly limit penetration of onshore wind, unavailability of geothermal will increase hydropower needs to stabilise the grid, while slower degasification may slightly reduce investments for biomass and offshore wind despite yielding delignitisation already by 2023. These challenges emphasise that, while a diverse mix can help counteract uncertainties, this robustness comes with a slightly increased cost due to investments in less cost-effective technologies.

Despite our intention to reflect on the current energy crisis, one important caveat of our study is using pre-crisis fuel prices in our natural gas OPEX calculation, potentially underestimating the cost of electricity in the gas-rich electricity mixes of existing policy scenarios. Additionally, by calculating final electricity prices based on the current system of marginal-cost pricing (i.e., prices driven by the most expensive technology), the economic difference between existing policy scenarios and the *High Ambition* scenario would become even more apparent. On the other hand, large shares of renewable sources would also require a significant expansion of electricity storage as well as of transmission and distribution grids, concerns that have already been studied at a European level (Cebulla et al., 2018; Bruninx et al., 2015) but without offering detailed results for Greece. Additionally, the feasibility of the *High Ambition* scenario also entails large investments on the demand side for achieving high rates of EV penetration and increased energy efficiency. Costs for storage, grids and demand-side measures need to be holistically accounted in research building on the results presented here. Future studies could also evaluate these limitations to improve the technical realism of an ambitious turn to a renewable electricity mix in Greece and to provide even stronger evidence that such a turn can be beneficial to decarbonisation, affordability, and reliability of the Greek power sector while avoiding another fossil-fuel lock-in.



5 Key Takeaways

In this deliverable, the FCM framework was extended to evaluate different policy strategies from the stakeholders' point of view to inform, of be informed by, the modelling activities of PARIS REINFORCE. Most notably, this extension resulted in the development of In-Cognitive, an open webtool for interactive stakeholder engagement for FCM-based exercises that also considers uncertainties, by integrating Monte Carlo simulations to conventional FCMs.

The tool has been used in two national case studies (Italy and Greece) to assess policy mixes comprising multiple policy instruments and identify new pathway choices to decarbonisation. Producing feedback into modelling tasks, In-Cognitive has also been used to capture modellers' and experts' perceptions of the impacts of such crises on SDG progress, considering models' existing/planned capacity. As such, the results of this deliverable can be used to inform policymakers and modelling scientists alike, by helping formulate expert-driven decarbonisation and sustainability strategies as well as plan model advancements. These key insights by exercise are summarised below.

To inform the Italian context and the efforts towards decarbonisation (Section 2), we found that, according to our workshop participants:

- RES diffusion is preferred over new gas infrastructure and more robust against uncertainties
- Policies promoting renewables can also help tackle today's affordability challenges
- Solely urging citizens to reduce demand may not drive SDG7 progress in the longer run

By delving into the sustainable development domain and the experts'/modellers' expectations of models (Section 3), we found that:

- Expert perceptions of bigger and wider crisis propagation can inform model developments, although their perception is significantly restricted by modelling capabilities
- Modelers' perceptions may be biased based on their models' already existing and/or planned capacities
- Progress in SDGs 7, 8, 13 appears to be most prone to emergencies, such as pandemics, wars or recessions

In an iterative modelling and expert-consultation process for the Greek context (Section 4), we found that:

- The current policy framework in Greece is projected to double gas use between 2022 and 2030
- An ambitious but technically feasible RES strategy can lead to zero Russian gas imports before 2026
- A zero-carbon power-sector by 2035 would require the penetration of new, expensive technologies
- A diversified renewable mix is considerably more robust to uncertainties on several technical constraints and/or bottlenecks (e.g., availability of key technologies, socio-environmental concerns, and gas lock-ins) as well as on the duration of the energy crisis and the prices shocks – all of which were pointed out by experts



Appendix 1: Weight node interconnections

Nodes		Weight	Nodes		Weight
Source	Target		Source	Target	
C1	C15	-0.442	C14	C13	0.097
C1	C20	-0.375	C14	C23	0.11
C1	C23	-0.348	C15	C17	-0.852
C2	C12	0.594	C15	C18	0.902
C2	C25	0.706	C15	C24	0.226
C3	C14	-0.421	C15	C30	-0.852
C3	C16	-0.132	C16	C15	-0.719
C3	C23	-0.245	C16	C28	-0.274
C4	C15	-0.52	C17	C21	0.722
C4	C20	0.261	C17	C22	0.888
C4	C23	-0.29	C18	C19	-0.521
C5	C16	0.651	C19	C20	-0.311
C6	C15	0.487	C20	C26	-0.932
C7	C15	0.229	C20	C28	-0.419
C8	C10	0.776	C21	C27	0.322
C8	C12	0.319	C22	C29	0.21
C9	C23	0.792	C23	C19	0.9
C10	C11	0.319	C23	C24	0.189
C10	C13	0.391	C24	C29	0.196
C11	C26	-0.402	C25	C15	-0.311
C12	C14	-0.381	C28	C27	0.481
C13	C28	0.481	C29	C27	0.378



Appendix 2: Workshop questionnaire (in printed format)

Towards net-zero and SDGs: Challenges and opportunities from present turmoil – SDG7 & affordability – FCM session

Please fill in each white cell of the table, by indicating the type and level of impact that the row concept (on the left) has on the column concept (on the top) and disregarding all other cells. A positive impact means that a positive change on the row concept will have a positive effect on the column concept; a negative impact means that a positive change on the row concept will have a negative effect on the column concept.

	S1. Natural gas Imports	S2. Carbon lock-in effects	S3. Land loss and devaluation	S4. Deployment of digital technologies	S5. Multi-level governance	S6. Wholesale electricity prices	S7. Public-Partner Partnership (PPP) for RES	S8. Electricity system decarbonisation	S9. Energy storage	S10. R&I in energy	S11. Energy-sector employment	S12. Electricity demand	S13. Electricity system affordability	S14. Decentralisation of energy	S15. Energy communities	S16. Societal acceptance / Behavioural change	S17. Share of natural gas in electricity mix	S18. Electricity system reliability	S19. Share of RES in the electricity mix	S20. Progress in SDG7
P1. Increase solar & wind capacity																				
P2. Modernisation of the electricity grid																				
P3. Financing R&I																				
P4. Regulatory reform & economic incentives																				
P6. Information & tech. assistance to citizens																				
P7. Support digitalisation of supply & demand																				
P8. Investments in new gas infrastructure																				
P9. Promotion of energy efficiency measures																				
U1. Regulatory/political environment stability																				
U2. Technological costs																				
U3. Citizen awareness and engagement																				
U4. International conflict and price shocks																				
S1. Natural gas imports																				



Appendix 3: Mathematical framework of FCM simulations

The following FCM concept activation function is used:

$$A_i^{k+1} = f_h(x_i^k) = f_h\left(\sum_{j=1, j \neq i}^n (w_{ij}A_j^k + A_i^k)\right) \quad (\text{A3.1})$$

where $A_i^{(k+1)}$ is the value of concept i at the end of iteration k , A_i^k is the value of concept i at the beginning of iteration k , A_j^k is the value of concept j at the beginning of iteration k , n is the number of concepts included in the FCM, w_{ij} is the weight of the causal relationship between preceding concept j and following concept i , and f_h is a threshold function typically used to squash values within the FCM value domain (Nikas et al., 2020c).

Although there are several threshold functions used in the FCM literature, two are the most prominent: the simple S-shaped sigmoid function (Eq. 65) and the simple hyperbolic tangent function (Eq. A3.1) (Groumpos and Stylios, 2000).

$$f(x) = \frac{1}{1 + \exp(-x)} \quad (\text{A3.2})$$

$$f(x) = \tanh(x) \quad (\text{A3.3})$$

In our case, we use the hyperbolic tangent function, which squashes values in $[-1,1]$ and therefore allows negative concept values, which is relevant to our research (see Sections 2.3-2.4 above) as opposed to the sigmoid function that works only for positive values in $[0,1]$ (Nikas and Doukas, 2016). In particular, we use the generalised version of the hyperbolic tangent function (Eq. A3.2).

$$f_h = \frac{\exp(\lambda x) - \exp(-\lambda x)}{\exp(\lambda x) + \exp(-\lambda x)} = \frac{\exp(2\lambda x) + 1}{\exp(2\lambda x) - 1} \quad (\text{A3.4})$$

where Eq. (A3.4), for $\lambda = 1$, yields Eq. (A3.3).

The In-Cognitive FCM tool (Koutsellis et al., 2022b) used in this study is designed to optimise and then normalise the value of parameter λ to ensure that the FCM simulation process converges.



Appendix 4: Additional Material for Chapter 3

Figure A.1 elaborates on Figure 26 of the main text to enhance the comparability of the results per SDG.

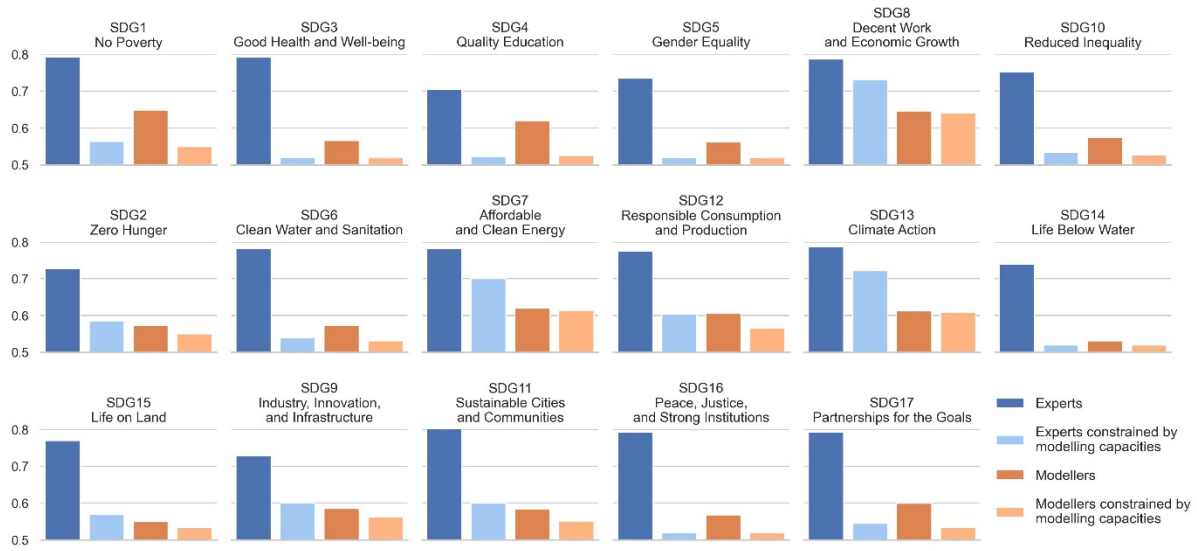


Figure A4.1: Causal Relationship Importance of each SDG in the “no-crisis” baseline scenario per SDG

Figure A.2 elaborates on Figures 27 and 28 of the main text to absolute values of the results per SDG and map.

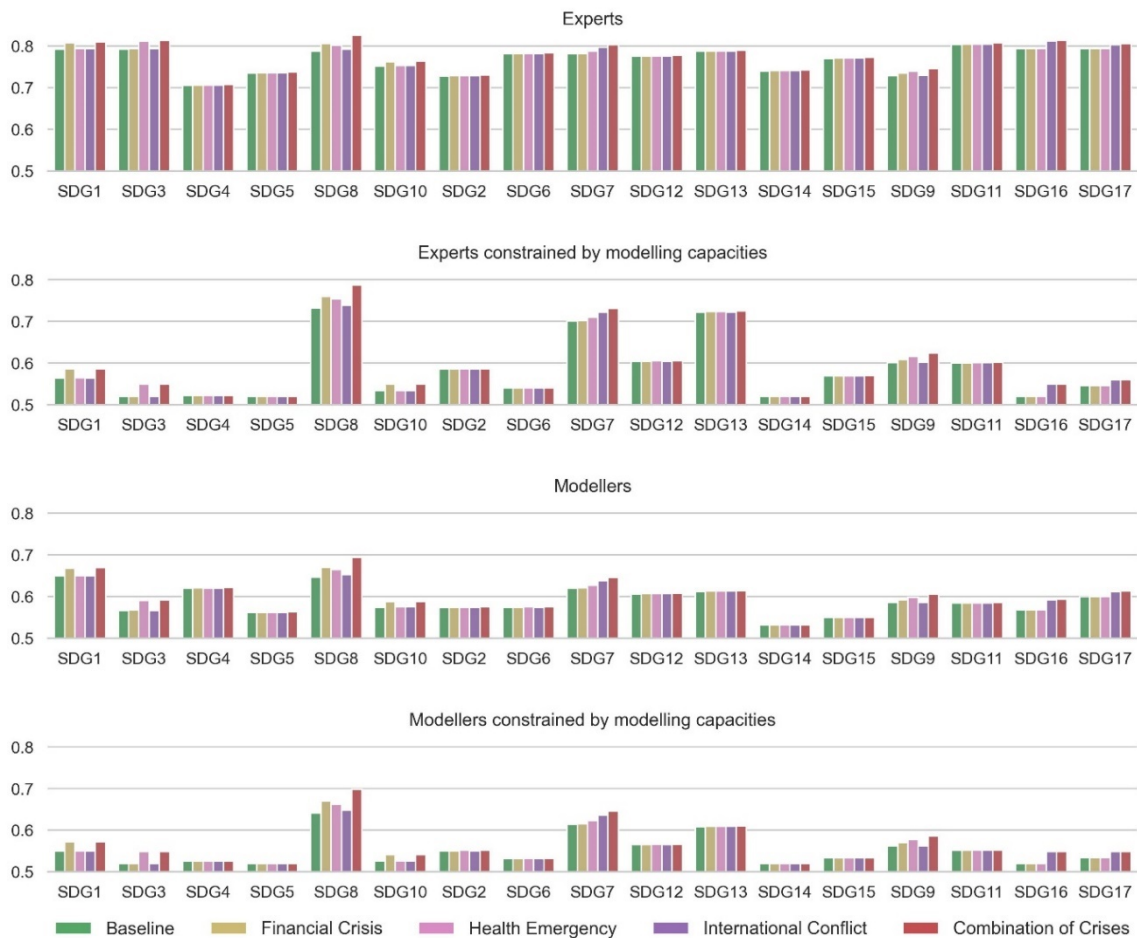


Figure A4.2: Impact of the crises on each SDG in the “fixed level of crisis” scenario per SDG



Appendix 5: In-Cognitive: a Python framework for Monte Carlo Fuzzy Cognitive Maps

The content of this section is currently under review in SoftwareX:

- Koutsellis, T., Koasidis, K., Xexakis, G., Frilingou, N., Karamaneas, A., Nikas, A., & Doukas, H. (2022). In-Cognitive: a Python framework for Monte Carlo Fuzzy Cognitive Maps. *SoftwareX*, under review.

A.5.1 Theoretical background

A Fuzzy Cognitive Mapping (FCM) network consists of *nodes* and *edges*. Each node is a pictorial representation of a cognitive concept, while edges describe how these concepts are interconnected. Each node can be connected with none, all, or a subset of the other nodes. Connections are defined by the degree of influence or *weight* between the interconnected nodes. If C_i and C_j are connected nodes, the weight w_{ij} indicates the influence of C_j over C_i . The ensemble of all weights is described through the FCM *weight matrix*, $\mathbf{W} = [w_{ij}]_{n \times n}$, where n is the number of nodes of the FCM. Note that the indexing order of w_{ij} is counterintuitively defined, as this order ensures that the i^{th} row of \mathbf{W} relates to the i^{th} node, C_i .

If A_j is the node value of C_j , the influence of C_j over C_i is $w_{ij}A_j$. Therefore, the overall influence of all nodes over the C_i node is equal to

$$x_i = \sum_{j=1, j \neq i}^n (w_{ij}A_j + d_iA_i) \tag{A5.1}$$

where d_iA_i is the influence of the C_i on itself (Figure A5.1). The last factor is used to indicate the dependence of C_i on its past values.

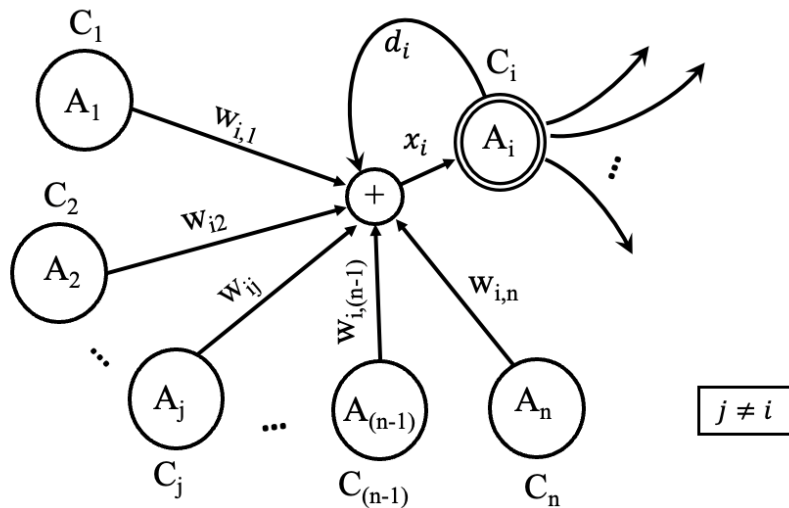


Figure A5.1: The summation of input values of a C_i node

In numerous FCM applications, the FCM nodes are divided into three categories: (a) sender (or input) nodes, (b) intermediate (or ordinary) nodes, and (c) receiver nodes. Input nodes are concepts, whose values affect the intermediate and output nodes without being affected by them. In mathematical formation, if the k^{th} node is an input node, then $w_{kj} = 0, \forall j \neq k$. To guarantee that the value A_k of an input node C_k is always constant, i.e., $A_k = c \in [-1, 1]$, the auto-weight value, d_i , should be also equal to one, i.e., $d_i = 1$. Therefore, for an input node, the following must hold: $w_{kj} = 0, \forall j \neq k$ and $d_i = 1$.

Receiver nodes are nodes, whose values are direct or indirect responses to the values of the input nodes, without affecting the values of any other node in the system. Nodes that are neither receiver nor sender nodes—i.e., whose values both are affected by and affect other nodes—are categorised as intermediate nodes. Note that the nodes, whose values represent desired results from the analysis of the system (hereafter defined as ‘output nodes’), typically contain receiver nodes, and possibly (depending on the application) a subset of the intermediate nodes.

The value of A_i is derived after passing an x_i argument to the *transfer function* (Figure A5.2). The transfer function maps the overall influence of x_i to the A_i value, aiming to ‘squash’ the value of a node after each simulation into the selected FCM domain. The shape and range of the transfer function is specified by the FCM designer based on the nature of the problem domain. Despite the diversity of FCM transfer functions in the literature, there are some generic principles for choosing one: a) the transfer function should be a monotonically increasing function and b) its smallest and largest values should be squashed to certain bounds to avoid indefinite values.

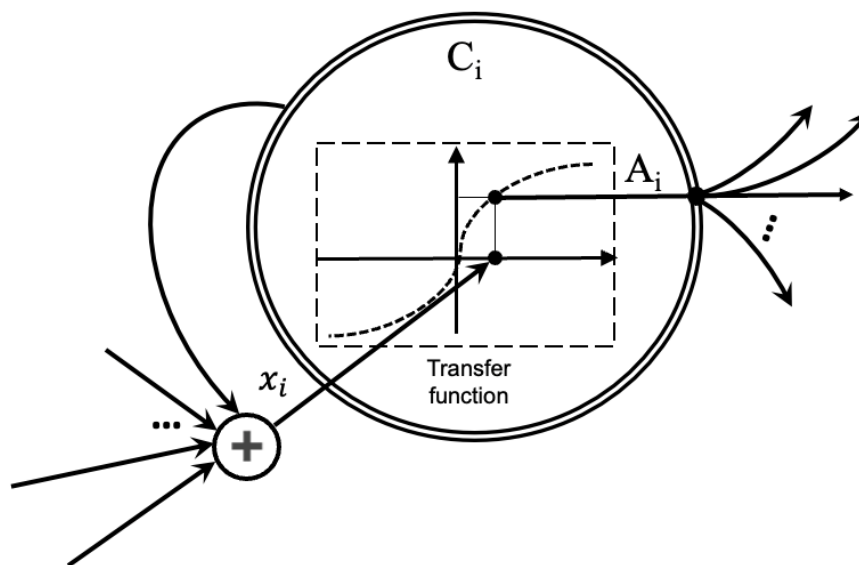


Figure A5.2: Pictorial representation of an FCM transfer function

It is common practice to use the sigmoid (f_s) or hyperbolic tangent (f_h) transfer function for FCM applications (Stylios and Groumos, 2004). The sigmoid and hyperbolic tangent functions are provided in Equations (A5.2) and (A5.3), respectively.

$$f_s = \frac{1}{1 + \exp(-\lambda x)} \quad (\text{A5.2})$$

$$f_h = \frac{\exp(\lambda x) - \exp(-\lambda x)}{\exp(\lambda x) + \exp(-\lambda x)} = \frac{\exp(2\lambda x) + 1}{\exp(2\lambda x) - 1} \quad (\text{A5.3})$$

The parameter λ is a design parameter and common to all nodes. The value range of the sigmoid function is the interval $[0,1]$ and that of the hyperbolic tangent function is $[-1, 1]$.

The mathematical formation of Figure A5.2 is:

$$A_i = f(x_i) = f\left(\sum_{j=1, j \neq i}^n (w_{ij}A_j + d_iA_i)\right) \quad (\text{A5.4})$$

where f is the transfer function.

During simulation, Eq. (A5. 4) is applied iteratively to each node, i.e.:

$$A_i^{k+1} = f(x_i^k) = f\left(\sum_{j=1, j \neq i}^n (w_{ij} A_j^k + d_i A_i^k)\right) \quad (\text{A5.5})$$

Eq. (A5.5) eventually yields the final equilibrium state of FCMs, expecting a convergence of the FCM after $k = N$ iterations. However, said convergence is not always guaranteed (Harmati et al., 2018; Koutsellis et al., 2022a; 2022b). To ensure convergence, the parameter λ of any FCM transfer function should lie within certain bounds (Harmati et al., 2018). Extending this research, Koutsellis et al. (2022a, 2022b) proposed a formula for the parameter λ , which provides the $\hat{\lambda}$ value, instead of bounds, to operate within the 'almost linear area' of the transfer functions.

The $\hat{\lambda}$ value, is related to the topology of the FCM and is thus a function of the weight matrix, \mathbf{W} . This further indicates that the parameter λ is application-specific and not a constant parameter. Parameter $\hat{\lambda}$ is derived from a combination of the Sigma and Forbenious norms of the weight matrix in the case of the sigmoid transfer function ($\|W\|_s$ and $\|W\|_{F,}$, respectively), or from the combination of the Infinite and Frobenius norms in the case of the hyperbolic tangent transfer function ($\|W\|_\infty$ and $\|W\|_{F,}$, respectively).

For most FCM applications, the parameter $\hat{\lambda}$ is small and, subsequently, yields small final A_i^{k+1} values [see Eq. (5)]. This hinders the process of extracting inferences from the FCM outcomes because it is hard to distinguish the order of the node values. The proposed $\hat{\lambda}$ parameter squashes all node values to the range of [0.211, 0.789] in the case of sigmoid function and to the range of [-0.577, 0.577] for the hyperbolic tangent transfer function. To bring the results back to the FCM domain, [0,1] and [-1,1] for sigmoid and hyperbolic tangent transfer function, respectively, a normalisation procedure takes place (Koutsellis et al., 2022a). If A_i^f is the final value of node C_j after applying Eq. (5) and \hat{A}_i^f is the final value of node C_i after normalisation, then

$$\hat{A}_i^f = A_i^f + (0.09\lambda_s) \cdot x_i^f \quad (\text{A5.6})$$

for the case of the sigmoid transfer function, where x_i^f the final value of Eq. (A5.1). When the hyperbolic tangent transfer function is used instead, the normalisation formula is

$$\hat{A}_i^f = 1.733 \cdot A_i^f \quad (\text{A5.7})$$

To conclude, the steps to derive the final equilibrium values of an FCM are illustrated in Figure A5.3 and can be summarised as follows:

- construct the weigh matrix, \mathbf{W} ;
- derive the parameter $\hat{\lambda}$ which guarantees the existence of solutions, based on the weight matrix;
- apply the iterative formula of Eq. (A5.5) until convergence;
- normalise the final values, A_i^f , of Eq. (A5.5) based on Eq. (A5.6) or Eq. (A5.7).

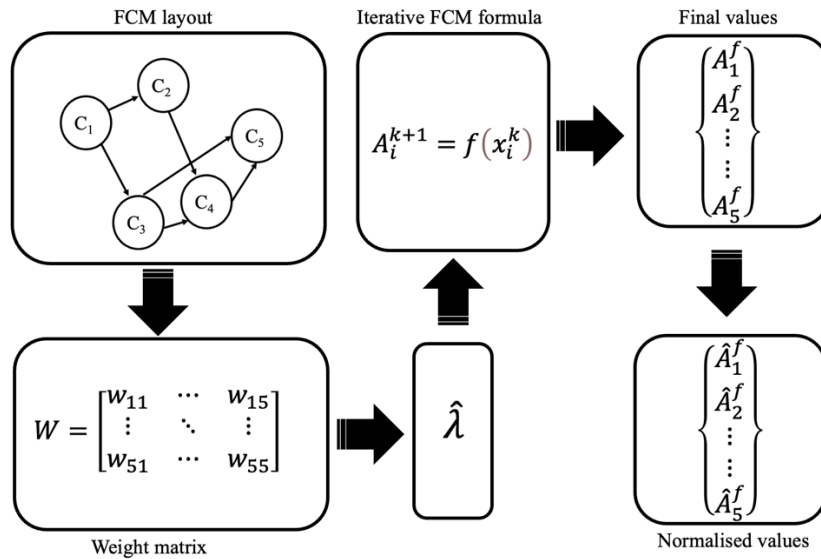


Figure A5.3: The FCM simulation procedure

The Monte Carlo (MC) simulation procedure assumes statistical distributions for the inputs variables and/or parameters of the FCM system. The procedure is based on a brute force iterative approach. In every iteration, the MC procedure generates samples of random variables for the input node values and/or the system node weights. After N iterations, N samples for each input variable and/or system’s parameter(s) are generated. The larger the number of iterations, the closer the histograms of the random variables are to the assumed statistical distributions. The generated samples of inputs and/or system parameters propagate to the system’s output variables and produce samples of values, which can then be used to reconstruct statistical distributions of the outputs.

Let $\{I\}$ be the vector of inputs variables, $\{P\}$ the vector of system’s parameters and $\{O\}$ the vector of output variables of the system. When the system acts deterministically, the vectors $\{I\}$ and $\{P\}$ pass through the system and generate a static output vector, $\{O\}$ (Figure A5.4a). When the system is statistically described instead of being deterministic, the vectors $\{I\}$, $\{P\}$, and $\{O\}$ consist of random variables. To derive the distribution of $\{O\}$, the Monte Carlo approach iteratively generates sample sets, $\{I\}_i$ and $\{P\}_i$, for $i = 1, 2, \dots, N$. The $\{I\}_i$ and $\{P\}_i$ are then generating the output sample set $\{O\}_i$ through the governing equations of the system. The final generated ensemble of N $\{O\}_i$ vectors provide the distribution of the random variables constituting the statistical $\{O\}$ (Figure A5.4b).

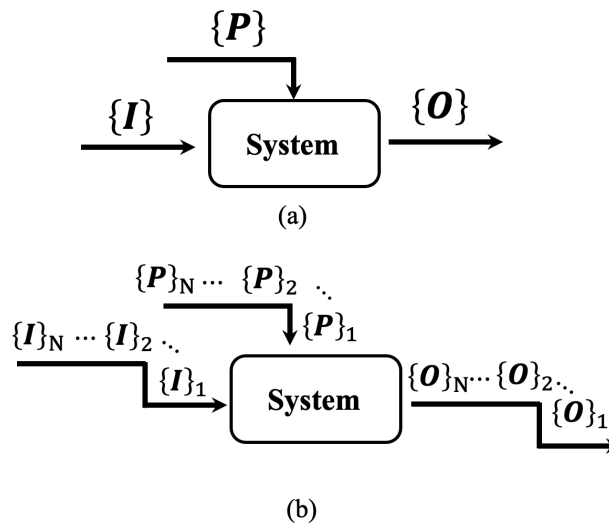


Figure A5.4: The Monte Carlo procedure

To integrate the MC procedure into an FCM simulation, it is necessary to perform a modification to the method that provides the parameter $\hat{\lambda}$. As discussed above, $\hat{\lambda}$ is a function of the weight matrix. However, the weight values, w_{ij} , are parameters of the FCM system and therefore are changing between iterations. This means that the parameter $\hat{\lambda}$ should change per iteration as well. However, if the $\hat{\lambda}$ parameter varies, the FCM system will not be the same for all iterations and this violates the fundamental principle of the MC approach that the system should be unchanged.

To tackle this issue, a constant parameter $\hat{\lambda}_{MC}$ is introduced for all iterations regardless of the weight matrix variation. However, this does not mean that the principle of choosing a parameter $\hat{\lambda}$ as a function of the weight matrix is violated. The $\hat{\lambda}_{MC}$ is chosen as a function of the weight matrix in the extreme case where all w_{ij} are equal to one ($|w_{ij}| = 1$), except for weights referring to non-existent FCM edges, for which $|w_{ij}| = 0$. This extreme case provides a $\hat{\lambda}_{MC}$ value that is the smallest among any other case, where the weight matrix varies. Therefore, we ensure that all iterations will provide stable outcomes, avoiding any indefinite or chaotic FCM behaviour that may cause the simulation to stop without giving any results.

To finalise the process of MC integration to the FCM framework, it is necessary to define the statistical distribution of the random variables (i.e., input nodes and the values of the weight matrix, w_{ij}). This statistical distribution should be a bounded interval in correspondence to the range of the weights, w_{ij} , and the node values, A_i . For that reason, the Beta distribution is used as a sample generator for the input node values and the weights. As the Beta distribution is bounded in $[0, 1]$, additional modification is needed in the case of hyperbolic transfer function as the weights should be in the $[-1, 1]$ interval. In this case, the value of the original Beta distribution should be divided by 0.5 before subtracting one from this value. No other modification is needed for the node values if the transfer function is sigmoid.

A.5.2 Software architecture

In-Cognitive is a web-based application⁴ that provides a user-friendly platform for designing, visualising, and simulating a Fuzzy Cognitive Mapping (FCM) network, with the option to add Monte Carlo (MC) uncertainty to the network's weights and inputs. The software is written in the Python programming language (version 3.8.11)⁵ and consists of a client-side Graphical User Interface (GUI or front-end system), which exchanges data with a web server (back-end system). Both front-end and back-end systems are developed through the Bokeh framework (version 2.4.0)⁶, which is a Python library that provides all the necessary tools to program interactions among the user, the GUI, and the back-end code (Figure A5.5). The application is open source and available on GitHub⁷.

⁴ <https://incognitive.paris-reinforce.epu.ntua.gr>

⁵ <https://www.python.org/downloads/release/python-3811/>

⁶ <https://bokeh.org>

⁷ <https://github.com/ThemisKoutsellis/InCognitiveApp>



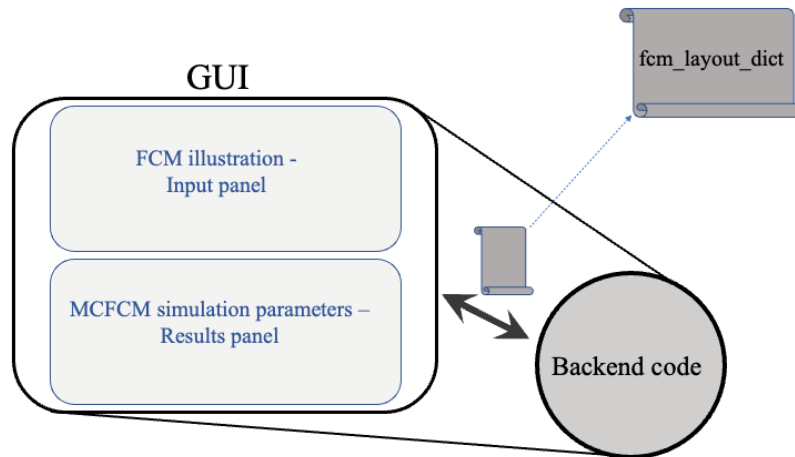


Figure A5.5: The In-Cognitive software architecture

A.5.3 Graphical User Interface (GUI)

The GUI is illustrated in Figure A5.6 and consists of two panels: the 'Inputs' panel on the left and top side of the GUI and the 'Results' panel on the right bottom side. In the first panel, the user can introduce a new FCM by uploading a Microsoft Excel file with a predefined format, which can be then edited using the two tables on the right-hand side of the panel. All information in these tables is then converted to an *'fcm_layout_dict'* dictionary, which is used as input for Bokeh's visualisation suite (Figure A5.6). The FCM display plot (left side of the Inputs panel) visualises the two tables. The display plot presents all FCM nodes in a circular layout, with the input nodes always positioning to the left of the plot and shown with a red colour. The lines connecting the nodes (edges) are coloured based on the values of the weights between the nodes they connect. The darker the colour of an edge line, the closer the weight is to the maximum weight of 1. The exact value of the weight is shown when the user hovers their mouse over the edge line (Figure A5.7).

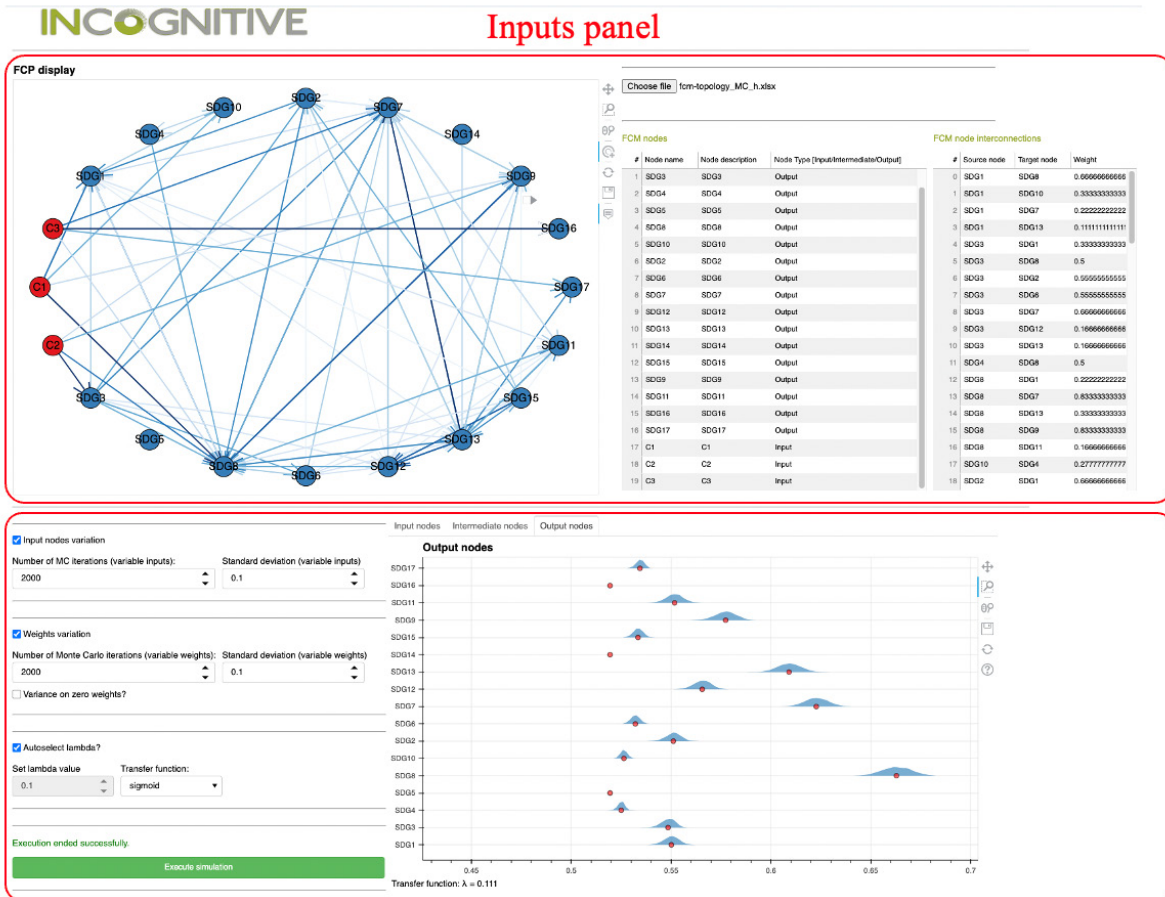


Figure A5.6: The In-Cognitive Graphical User Interface (GUI)

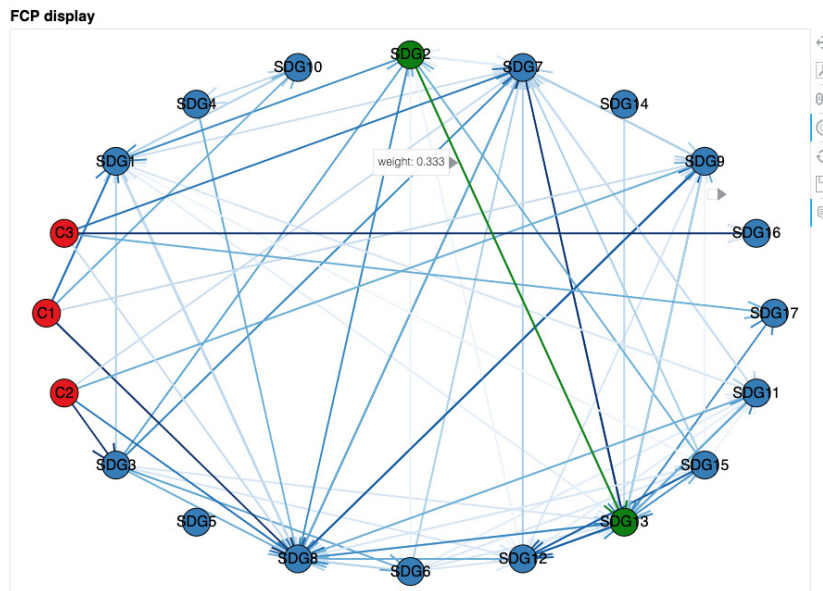


Figure A5.7: The hover functionality of FCM display plot

After editing the FCM topology, users can specify the MCFCM parameters (right and bottom side of the Inputs panel) and, specifically, whether they prefer to introduce variation on the input nodes and/or the weights. Users can also specify the standard deviation (SD) of this variation, which corresponds to the SD of the Beta distribution.



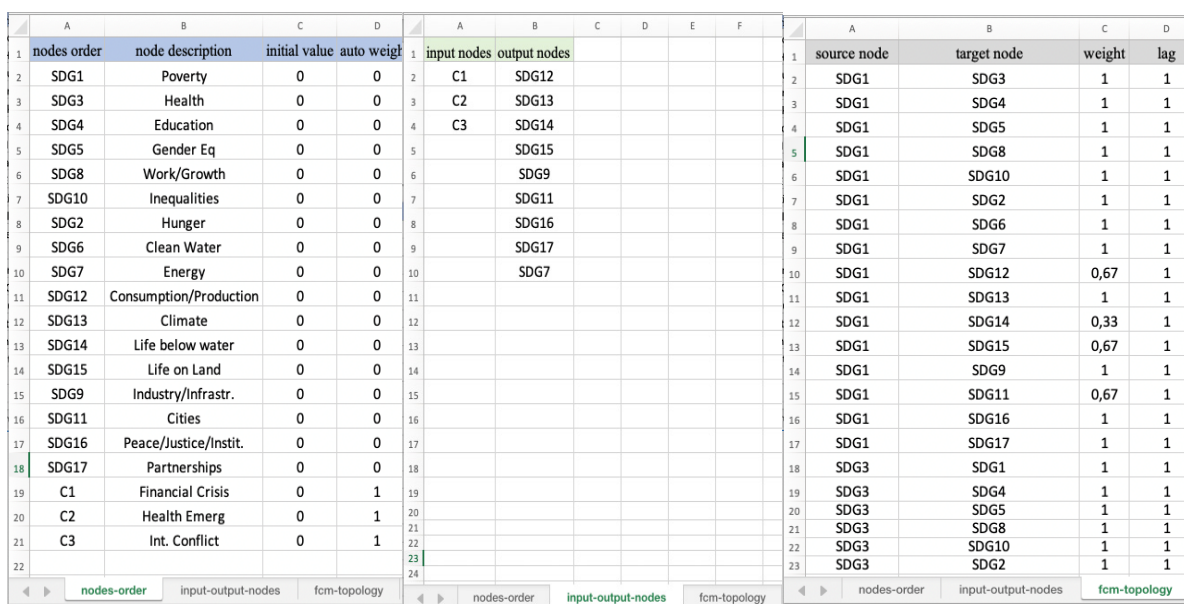
If the 'Weights variation' box is checked, the user can also specify whether zero weights (if any) are considered as random variables with zero mean by ticking the 'Variance on zero weights' box. If the box is left unchecked (default settings), then it is assumed that there is no connection between corresponding nodes. Next, the user can choose the parameter λ and the transfer function, which can be 'sigmoid' or 'hyperbolic'. By default, the parameter λ is automatically selected by the application (i.e., 'Autoselect lambda' is checked). Finally, users can submit their parameter preferences via the 'Execute simulation' button.

After the simulation is completed, the GUI alerts the user and presents the results on the plots of the Results panel (Figure A5.6). In these plots, the y-axis corresponds to the node names and the x-axis to the node values. The results of simulating the network without variation is presented with red dots. In case of a Monte Carlo simulation, the shape of distribution for each node is presented with a pale blue colour on top of the red dots (see Figure A5.6).

Finally, the HTML and CSS code required for generating the GUI is automatically created by the Bokeh library. However, it is possible for the user to change the default HTML and CSS code through the files stored in the 'static' and 'template' folders of the code repository.

A.5.4 Input data formatting and processing

To create an FCM network, the user can upload an input Excel file via a button on the top right side of the interface (featuring a 'Choose file' prompt). This Excel file must have a certain format, consisting of three sheets that must be named as: 1) 'nodes-order', 2) 'input-output-nodes', and 3) 'fcm-topology' (Figure A5.8).



nodes-order					input-output-nodes		fcm-topology				
A	B	C	D	E	F	A	B	C	D	E	F
1	nodes order	node description	initial value	auto weight	1	input nodes	output nodes				
2	SDG1	Poverty	0	0	2	C1	SDG12				
3	SDG3	Health	0	0	3	C2	SDG13				
4	SDG4	Education	0	0	4	C3	SDG14				
5	SDG5	Gender Eq	0	0	5		SDG15				
6	SDG8	Work/Growth	0	0	6		SDG9				
7	SDG10	Inequalities	0	0	7		SDG11				
8	SDG2	Hunger	0	0	8		SDG16				
9	SDG6	Clean Water	0	0	9		SDG17				
10	SDG7	Energy	0	0	10		SDG7				
11	SDG12	Consumption/Production	0	0	11						
12	SDG13	Climate	0	0	12						
13	SDG14	Life below water	0	0	13						
14	SDG15	Life on Land	0	0	14						
15	SDG9	Industry/Infrastr.	0	0	15						
16	SDG11	Cities	0	0	16						
17	SDG16	Peace/Justice/Instit.	0	0	17						
18	SDG17	Partnerships	0	0	18						
19	C1	Financial Crisis	0	1	19						
20	C2	Health Emerg	0	1	20						
21	C3	Int. Conflict	0	1	21						
22					22						
23					23						
24					24						

fcm-topology			
A	B	C	D
1	source node	target node	weight lag
2	SDG1	SDG3	1 1
3	SDG1	SDG4	1 1
4	SDG1	SDG5	1 1
5	SDG1	SDG8	1 1
6	SDG1	SDG10	1 1
7	SDG1	SDG2	1 1
8	SDG1	SDG6	1 1
9	SDG1	SDG7	1 1
10	SDG1	SDG12	0,67 1
11	SDG1	SDG13	1 1
12	SDG1	SDG14	0,33 1
13	SDG1	SDG15	0,67 1
14	SDG1	SDG9	1 1
15	SDG1	SDG11	0,67 1
16	SDG1	SDG16	1 1
17	SDG1	SDG17	1 1
18	SDG3	SDG1	1 1
19	SDG3	SDG4	1 1
20	SDG3	SDG5	1 1
21	SDG3	SDG8	1 1
22	SDG3	SDG10	1 1
23	SDG3	SDG2	1 1

Figure A5.8: The input Excel file

The first sheet contains information on all FCM nodes, including input, intermediate, and output nodes, and consists of five columns (left side of Figure A5.8). The first column features the names of the nodes in the desired order, the second column provides a brief description for each node, and the third column shows the initial value of each node before the FCM simulation. The fourth and fifth columns provide settings for the simulation. The 'auto weights' setting in the fourth column expresses the degree of correlation of the node's current value with its past value. The position of the past value in the time domain, t-lag, is defined by the lag parameter. If the auto-weight value is non-zero, the 'auto-lag' setting on the fifth column defines the lag between the node's current value and its corresponding past value, as defined in (Nikas et al., 2019b).



The second sheet is used to define the input and output nodes and consists of two columns (middle panel of Figure A5.8). The first column contains the names of input nodes, which should correspond to existing nodes provided in the first column of the first sheet. Similarly, the third column should include the names of output nodes. If there are no input or output nodes, the corresponding columns must remain empty.

The third sheet features specifications on the FCM edges (links). Each edge is characterised by its 'source' and 'target' node, i.e., the beginning and ending node, respectively. Next, there is a weight value assigned to each edge that indicates the correlation of the target node's value in time instance t with the source node's value in the time instance t -lag (again, based on Nikas et al., 2019b). The layout of the third sheet consists of four columns. The first and the second column specify the source node and the target node for each edge, while the third column gives the weight for each edge. Finally, the fourth column provides the correlation lag between the target and source node values.

The input data is then converted to an 'fcm_layout_dict' file, which is used for dynamic data exchange between the GUI and the web server (Figure A5.5). The 'fcm_layout_dict' is a Python dictionary, which contains all necessary information for the FCM layout and simulation. It consists of eleven key-value pairs with the following value types:

1. 'nodes_order': list of strings
2. 'node_discription': list of strings
3. 'auto_weights': list of floats
4. 'auto_lags': numpy array
5. 'initial_values': list of floats
6. 'input_nodes': list of strings
7. 'output_nodes': list of strings
8. 'source_nodes': list of strings
9. 'target_nodes': list of strings
10. 'weights': list of floats
11. 'lags': list of floats

A.5.5 Simulation and plotting

The core functionalities for simulating an FCM network and plotting the results are provided in the 'backendcode' folder in the application's code. It consists of seven modules that exchange information via the 'fcm_layout_dict' dictionary.

First, the 'xlparse' module parses the input Excel file and returns the 'fcm_layout_dict' dictionary. Based on this dictionary, the 'activation_function' module provides the specifications of the transfer function ('sigmoid', 'hyperbolic'), while the 'fcm_layout_parameters' module contains functions that return necessary parameters of the FCMs, i.e., the weight matrix (\mathbf{W}), the lag matrix (\mathbf{L}), and the lambda parameter of the transfer function (λ). The lambda parameter is estimated based on the methodology of Koutsellis et al. (2022b) in case of a conventional FCM simulation without Monte Carlo. In contrast, when there is MC variation on either input nodes or weights, the application calculates the parameter λ assuming $|w_{ij}| = 1$ (except when $|w_{ij}| = 0$), utilising the Sigma, Infinite, and Forbenious norms of the weight matrix.

After all FCM parameters are defined by the previous modules, their results are fed into the 'fcm_object'. This



module processes all data in a consistent 'FCMap' object that is then run by the 'fcm_simulator' module. Each value of the FCM nodes is derived by the iterative Eq. (A5.5). The simulation stops either right after the number of iterations is greater than the maximum iterations defined by the user in the GUI (Figure A5.1) or at an iteration where there is convergence for all nodes, i.e., the difference of two consecutive state vectors is smaller than an error threshold of 0.0001. In case of MC uncertainty, the 'fcmmc_object' and 'fcmmc_simulation' modules are used instead of the 'fcm_object' and 'fcm_simulator'. The 'fcmmc_simulation' module can handle the following four cases:

- variation on neither the weights nor the values of the input nodes;
- variation on input node values, with fixed weights;
- variation on weights, with fixed input node values;
- both weights and input node values are random variables.



References

- Abbaspour Onari, M., & Jahangoshai Rezaee, M. (2020). A fuzzy cognitive map based on Nash bargaining game for supplier selection problem: a case study on auto parts industry. *Operational Research*, 1-39.
- Ackerman, F., DeCanio, S. J., Howarth, R. B., & Sheeran, K. (2009). Limitations of integrated assessment models of climate change. *Climatic change*, 95(3), 297-315.
- Aguilar, J., & Contreras, J. (2010). The FCM designer tool. In *Fuzzy cognitive maps* (pp. 71-87). Springer, Berlin, Heidelberg.
- Akintoye, A., & Beck, Matthias Kumaraswamy, M. (2020). *Public Private Partnerships: A Global Review* (1st ed.). Routledge.
- Al kez, D., Foley, A. M., McIlwaine, N., Morrow, D. J., Hayes, B. P., Zehir, M. A., Mehigan, L., Papari, B., Edrington, C. S., & Baran, M. (2020). A critical evaluation of grid stability and codes, energy storage and smart loads in power systems with wind generation. *Energy*, 205, Article 117671.
- Albatayneh, A., Assaf, M. N., Alterman, D., & Jaradat, M. (2020). Comparison of the overall energy efficiency for internal combustion engine vehicles and electric vehicles. *Rigas Tehniskas Universitates Zinatniskie Raksti*, 24(1), 669-680.
- Ameli, M., Shams Esfandabadi, Z., Sadeghi, S., Ranjbari, M., & Zanetti, M. C. (2022). COVID-19 and Sustainable Development Goals (SDGs): Scenario analysis through fuzzy cognitive map modeling. *Gondwana Research*, xxxx.
- Amer, M., Daim, T. U., & Jetter, A. (2016). Technology roadmap through fuzzy cognitive map-based scenarios: the case of wind energy sector of a developing country. *Technology Analysis & Strategic Management*, 28(2), 131-155.
- Amer, S. B., Gregg, J. S., Sperling, K., & Drysdale, D. (2020). Too complicated and impractical? An exploratory study on the role of energy system models in municipal decision-making processes in Denmark. *Energy Research & Social Science*, 70, 101673.
- Amirkhani, A., Papageorgiou, E. I., Mohseni, A., & Mosavi, M. R. (2017). A review of fuzzy cognitive maps in medicine: Taxonomy, methods, and applications. *Computer methods and programs in biomedicine*, 142, 129-145.
- Amirkhani, A., Papageorgiou, E. I., Mosavi, M. R., & Mohammadi, K. (2018). A novel medical decision support system based on fuzzy cognitive maps enhanced by intuitive and learning capabilities for modeling uncertainty. *Applied Mathematics and Computation*, 337, 562-582.
- Anna, F. D. (2021). Green jobs and energy efficiency as strategies for economic growth and the reduction of environmental impacts. *Energy Policy*, 149, Article 112031.
- Antonelli, M., Desideri, U., & Franco, A. (2018). Effects of large scale penetration of renewables: The Italian case in the years 2008–2015. *Renewable and Sustainable Energy Reviews*, 81, 3090–3100.
- Antosiewicz, M., Nikas, A., Szpor, A., Witajewski-Baltvilks, J., & Doukas, H. (2020). Pathways for the transition of the Polish power sector and associated risks. *Environmental Innovation and Societal Transitions*, 35, 271-291.
- Antweiler, W., & Muesgens, F. (2021). On the long-term merit order effect of renewable energies. *Energy Economics*, 99.



- Apostolopoulos, I. D., Groumpos, P. P., & Apostolopoulos, D. I. (2017). A medical decision support system for the prediction of the coronary artery disease using fuzzy cognitive maps. In *Conference on Creativity in Intelligent Technologies and Data Science* (pp. 269-283). Springer, Cham.
- Assunção, E. R. G. T. R., Ferreira, F. A., Meidutė-Kavaliauskienė, I., Zopounidis, C., Pereira, L. F., & Correia, R. J. C. (2020). Rethinking urban sustainability using fuzzy cognitive mapping and system dynamics. *International Journal of Sustainable Development & World Ecology*, 27(3), 261-275.
- ASviS. (2021). Italy and the Sustainable Development Goals. Italian Alliance for Sustainable Development. https://asvis.it/public/asvis2/files/Rapporto_ASviS/Rapporto_2021/Report_ASviS_ENG_2021.pdf
- Ausseil, A. G. E., Daigneault, A. J., Frame, B., & Teixeira, E. I. (2019). Towards an integrated assessment of climate and socio-economic change impacts and implications in New Zealand. *Environmental Modelling & Software*, 119, 1-20.
- Awopone, A. K., Zobaa, A. F., & Banuenumah, W. (2017). Assessment of optimal pathways for power generation system in Ghana. *Cogent Engineering*, 4(1), 1314065.
- Axelrod, R. (Ed.). (2015). *Structure of decision: The cognitive maps of political elites*. Princeton university press.
- Azam, M., Othman, J., Begum, R. A., Abdullah, S. M. S., & Nor, N. G. M. (2016). Energy consumption and emission projection for the road transport sector in Malaysia: An application of the LEAP model. *Environment, development and sustainability*, 18(4), 1027-1047.
- Azevedo, A. R. S., & Ferreira, F. A. (2019). Analyzing the dynamics behind ethical banking practices using fuzzy cognitive mapping. *Operational Research*, 19(3), 679-700.
- Balkan Green Energy News. (2022). Launch of works on Alexandroupolis LNG terminal in Greece. <https://balkangreenenergynews.com/launch-of-works-on-alexandroupolis-lng-terminal-in-greece-heralds-reduced-dependence-on-russian-gas-for-the-balkans/>
- Bardazzi, R., Bortolotti, L., & Pazienza, M. G. (2021). To eat and not to heat? Energy poverty and income inequality in Italian regions. *Energy Research and Social Science*, 73, Article 101946.
- Baykasoğlu, A., & Gölcük, İ. (2021). Alpha-cut based fuzzy cognitive maps with applications in decision-making. *Computers & Industrial Engineering*, 152, 107007.
- Bellantuono, G. (2018). Regulatory Stability in the Energy Sector: The Italian Experience. *SSRN Electronic Journal*.
- Bertram, C., Johnson, N., Luderer, G., Riahi, K., Isaac, M., & Eom, J. (2015). Carbon lock-in through capital stock inertia associated with weak near-term climate policies. *Technological Forecasting and Social Change*, 90(PA), 62–72.
- Betakova, V., Vojar, J., & Sklenicka, P. (2015). Wind turbines location: How many and how far? *Applied Energy*, 151, 23–31.
- Bevilacqua, M., Ciarapica, F. E., & Mazzuto, G. (2018). Fuzzy cognitive maps for adverse drug event risk management. *Safety science*, 102, 194-210.
- Biermann, F., Hickmann, T., Sénit, C.-A., Beisheim, M., Bernstein, S., Chasek, P., Grob, L., Kim, R. E., Kotzé, L. J., Nilsson, M., Ordóñez Llanos, A., Okereke, C., Pradhan, P., Raven, R., Sun, Y., Vijge, M. J., van Vuuren, D., & Wicke, B. (2022). Scientific evidence on the political impact of the Sustainable Development Goals. *Nature Sustainability*.
- Biesbroek, R. (2021). Policy integration and climate change adaptation. *Current Opinion in Environmental*



Sustainability, 52, 75–81.

- Bistline, J., Budolfson, M., & Francis, B. (2021). Deepening transparency about value-laden assumptions in energy and environmental modelling: improving best practices for both modellers and non-modellers. *Climate Policy*, 21(1), 1-15.
- Bompard, E., Botterud, A., Corgnati, S., Huang, T., Jafari, M., Leone, P., Mauro, S., Montesano, G., Papa, C., & Profumo, F. (2020). An electricity triangle for energy transition: Application to Italy. *Applied Energy*, 277, Article 115525.
- Borasio, M., & Moret, S. (2022). Deep decarbonisation of regional energy systems: A novel modelling approach and its application to the Italian energy transition. *Renewable and Sustainable Energy Reviews*, 153.
- Borken-Kleefeld, J., Fuglestvedt, J., & Berntsen, T. (2013). Mode, load, and specific climate impact from passenger trips. *Environmental science & technology*, 47(14), 7608-7614.
- Boyle, A. D., Leggat, G., Morikawa, L., Pappas, Y., & Stephens, J. C. (2021). Green New Deal proposals: Comparing emerging transformational climate policies at multiple scales. *Energy Research and Social Science*, 81(August), 102259.
- Brauers, H., Braunger, I., & Jewell, J. (2021). Liquefied natural gas expansion plans in Germany: The risk of gas lock-in under energy transitions. *Energy Research and Social Science*, 76, Article 102059.
- Brisbois, M. C. (2020). Decentralised energy, decentralised accountability? Lessons on how to govern decentralised electricity transitions from multi-level natural resource governance. *Global Transitions*, 2, 16-25.
- Brugger, H., Eichhammer, W., Mikova, N., & Dönitz, E. (2021). Energy Efficiency Vision 2050: How will new societal trends influence future energy demand in the European countries? *Energy Policy*, 152.
- Bruninx, K., Orlic, D., Couckuyt, D., Grisey, N., Betraoui, B., Anderski, T., ... & Jankowski, R. (2015). Modular development plan of the Pan-European transmission system 2050: Data sets of scenarios for 2050. In Technical Report. The e-HIGHWAY 2050 Project. https://docs.entsoe.eu/baltic-conf/bites/www.e-highway2050.eu/fileadmin/documents/Results/D4.4-Modular_development_plan_from_2020_to_2050.pdf
- Cakmak, E. H., Dudu, H., Eruygur, O., Ger, M., Onurlu, S., & Tonguç, Ö. (2013). Participatory fuzzy cognitive mapping analysis to evaluate the future of water in the Seyhan Basin. *Journal of water and climate change*, 4(2), 131-145.
- Calvin, K., Wise, M., Kyle, P., Clarke, L., & Edmonds, J. (2017). A hindcast experiment using the GCAM 3.0 agriculture and land-use module. *Climate Change Economics*, 8(01), 1750005.
- Camboni, R., Corsini, A., Miniaci, R., & Valbonesi, P. (2021). Mapping fuel poverty risk at the municipal level. A small-scale analysis of Italian Energy Performance Certificate, census and survey data. *Energy Policy*, 155(May).
- Capital.gr. (2021). Low penetration of natural gas vehicles. <https://www.capital.gr/epixeiriseis/3538156/xamili-i-dieisdusi-ton-oximaton-fusikou-aeriou> (in Greek).
- Caporale, D., & De Lucia, C. (2015). Social acceptance of on-shore wind energy in Apulia Region (Southern Italy). *Renewable and Sustainable Energy Reviews*, 52(March 2010), 1378–1390.
- Carvalho, J. P., & Tomé, J. A. B. (2004). Qualitative modelling of an economic system using rule-based fuzzy cognitive maps. In 2004 IEEE International Conference on Fuzzy Systems (IEEE Cat. No. 04CH37542) (Vol. 2, pp. 659-664). IEEE.



- Castro, C. (2022). Systems-thinking for environmental policy coherence: Stakeholder knowledge , fuzzy logic , and causal reasoning. *Environmental Science and Policy*, 136(October 2021), 413–427.
- Cebulla, F., Haas, J., Eichman, J., Nowak, W., & Mancarella, P. (2018). How much electrical energy storage do we need? A synthesis for the US, Europe, and Germany. *Journal of Cleaner Production*, 181, 449-459.
- Ceccato, L. (2012). Three Essays on participatory processes and Integrated Water Resource Management in developing countries. Università Ca' Foscari Venezia
- Çelik, F. D., Ozesmi, U., & Akdogan, A. (2005). Participatory ecosystem management planning at Tuzla lake (Turkey) using fuzzy cognitive mapping. arXiv preprint q-bio/0510015.
- Cheah, W. P., Kim, Y. S., Kim, K. Y., & Yang, H. J. (2011). Systematic causal knowledge acquisition using FCM constructor for product design decision support. *Expert Systems with Applications*, 38(12), 15316-15331.
- Chiodi, A., Giannakidis, G., Labriet, M., Gallachóir, B. Ó., & Tosato, G. C. (2015). Informing Energy and Climate Policies Using Energy Systems Models. In *Lecture Notes in Energy* (Vol. 30, pp. 125–139).
- Cielo, A., Margiaria, P., Lazzeroni, P., Mariuzzo, I., & Repetto, M. (2021). Renewable Energy Communities business models under the 2020 Italian regulation. *Journal of Cleaner Production*, 316(July), 128217.
- Climate Action Tracker. (2022). Global reaction to energy crisis risks zero carbon transition. https://climateactiontracker.org/documents/1055/CAT_2022-06-08_Briefing_EnergyCrisisReaction.pdf
- Council of the EU. (2022). Member states commit to reducing gas demand by 15% next winter. Press Release 26 July 2022. <https://www.consilium.europa.eu/en/press/press-releases/2022/07/26/member-states-commit-to-reducing-gas-demand-by-15-next-winter/>
- D'Adamo, I., Gastaldi, M., Imbriani, C., & Morone, P. (2021). Assessing regional performance for the Sustainable Development Goals in Italy. *Scientific Reports*, 11(1), 1–10.
- DAPEEP. (2022). Monthly Special Account for RES & CHP - Renewable Energy Sources Operator & Guarantees of Origin S.A - DAPEEP S.A.. <https://www.dapeep.gr/dimosieuseis/miniaio-deltio-eidikou-logiasmoy/#1620887496946-a35db1f9-b7a9> (in Greek)
- Davis, S. J., Liu, Z., Deng, Z., Zhu, B., Ke, P., Sun, T., ... & Ciais, P. (2022). Emissions rebound from the COVID-19 pandemic. *Nature Climate Change*, 12(5), 412-414.
- De Laurentis, C., & Cowell, R. (2021). Reconfiguring energy flows: energy grid-lock and the role of regions in shaping electricity infrastructure networks. *Journal of Environmental Policy and Planning*, 24(4), 433–448.
- de Moura, G. N. P., Legey, L. F. L., & Howells, M. (2018). A Brazilian perspective of power systems integration using OSeMOSYS SAMBA–South America Model Base–and the bargaining power of neighbouring countries: A cooperative games approach. *Energy Policy*, 115, 470-485.
- Deane, J. P., Gracceva, F., Chiodi, A., Gargiulo, M., & Gallachóir, B. P. Ó. (2015). Assessing power system security. A framework and a multi model approach. *International Journal of Electrical Power and Energy Systems*, 73(2015), 283–297.
- Dhakouani, A., Gardumi, F., Znouda, E., Bouden, C., & Howells, M. (2017). Long-term optimisation model of the Tunisian power system. *Energy*, 141, 550-562.
- Di Bella, G., Flanagan, M. J., Foda, K., Maslova, S., Pienkowski, A., Stuermer, M., & Toscani, F. G. (2022). Natural Gas in Europe: The Potential Impact of Disruptions to Supply. *IMF Working Papers*, 2022(145).
- Di Nucci, M. R., & Prontera, A. (2021). The Italian energy transition in a multilevel system: between reinforcing



dynamics and institutional constraints. *Zeitschrift Für Politikwissenschaft*.

- Di Silvestre, M. L., Ippolito, M. G., Sanseverino, E. R., Sciumè, G., & Vasile, A. (2021). Energy self-consumers and renewable energy communities in Italy: New actors of the electric power systems. *Renewable and Sustainable Energy Reviews*, 151, Article 111565.
- Dimoula, V., Kehagia, F., & Tsakalidis, A. (2016). A holistic approach for estimating carbon emissions of road and rail transport systems. *Aerosol and air quality research*, 16(1), 61-68.
- Dinica, V. (2008). Initiating a sustained diffusion of wind power: The role of public-private partnerships in Spain. *Energy Policy*, 36(9), 3562–3571.
- Domínguez-Garabitos, M. A., Ocaña-Guevara, V. S., Santos-García, F., Arango-Manrique, A., & Aybar-Mejía, M. (2022). A Methodological Proposal for Implementing Demand-Shifting Strategies in the Wholesale Electricity Market. *Energies*, 15(4), 1–28.
- Doukas, H., & Nikas, A. (2020). Decision support models in climate policy. *European Journal of Operational Research*, 280(1), 1-24.
- Doukas, H., & Nikas, A. (2021). Involve citizens in climate-policy modelling. *Nature*, 590(7846), 389-389.
- Doukas, H., & Nikas, A. (2022). Europe's energy crisis -- climate community must speak up. *Nature*, 608, 472.
- Doukas, H., Nikas, A., Stamtsis, G., & Tsiouridis, I. (2020). The green versus green trap and away forward. *Energies*, 13(20), 1–6.
- Duan, H., Zhang, G., Wang, S., & Fan, Y. (2019). Robust climate change research: a review on multi-model analysis. *Environmental Research Letters*, 14(3), 033001.
- EIA. (2022). U.S. Energy Information Administration - EIA - Independent Statistics and Analysis, Eia.Gov. https://www.eia.gov/environment/emissions/co2_vol_mass.php
- Ember Climate. (2022). EU Carbon Price Tracker. <https://ember-climate.org/data/data-tools/carbon-price-viewer/>
- Emodi, N. V., Chaiechi, T., & Beg, A. R. A. (2019). Are emission reduction policies effective under climate change conditions? A backcasting and exploratory scenario approach using the LEAP-OSeMOSYS Model. *Applied Energy*, 236, 1183-1217.
- Emodi, N. V., Emodi, C. C., Murthy, G. P., & Emodi, A. S. A. (2017). Energy policy for low carbon development in Nigeria: A LEAP model application. *Renewable and Sustainable Energy Reviews*, 68, 247-261.
- Enevoldsen, P., Permien, F. H., Bakhtaoui, I., von Krauland, A. K., Jacobson, M. Z., Xydis, G., ... & Oxley, G. (2019). How much wind power potential does Europe have? Examining European wind power potential with an enhanced socio-technical atlas. *Energy Policy*, 132, 1092-1100.
- European Commission. (2018). Regulation (EU) 2018/1999 on the Governance of the Energy Union and Climate Action. *Official Journal of the European Union*, 328(1), 1–77. <https://eur-lex.europa.eu/legal-content/EN/TXT/PDF/?uri=CELEX:32018R1999&from=EN>
- European Commission. (2021). COM/2021/550: Fit for 55 - Delivering the EU's 2030 climate target on the way to climate neutrality. <https://eur-lex.europa.eu/legal-content/EN/TXT/?uri=CELEX:52021DC0550>
- European Commission. (2022a). COM/2022/230: REPowerEU Plan. https://ec.europa.eu/commission/presscorner/detail/en/IP_22_3131
- European Commission. (2022b) EU Reference Scenario 2020. <https://energy.ec.europa.eu/data-and->



analysis/energy-modelling/eu-reference-scenario-2020_en .

- European Environment Agency. (2022). Greenhouse gas emission intensity of electricity generation by country. https://www.eea.europa.eu/data-and-maps/daviz/co2-emission-intensity-9/#tab-googlechartid_googlechartid_googlechartid_chart_1111 .
- Eurostat. (2020a). Disaggregated final energy consumption in households - quantities. Online Data Code:T2020_RK200. https://ec.europa.eu/eurostat/databrowser/view/t2020_rk200/default/table?lang=en
- Eurostat. (2020b). Energy imports dependency. Online Data Code: NRG_IND_ID.. https://ec.europa.eu/eurostat/databrowser/view/NRG_IND_ID_custom_1851669/bookmark/table?lang=en&bookmarkId=381eaa9a-00a3-4e1d-bc6a-d155f6a9f8f6
- Eurostat. (2020c). Share of energy from renewable sources. Online Data Code: NRG_IND_REN.. https://ec.europa.eu/eurostat/databrowser/view/nrg_ind_ren/default/table?lang=en
- Eurostat. (2022a) Disaggregated final energy consumption in households - quantities. https://ec.europa.eu/eurostat/databrowser/view/NRG_D_HHQ_custom_2292550/default/table?lang=en
- Eurostat. (2022b). EU imports of energy products - recent developments. [https://ec.europa.eu/eurostat/statistics-explained/index.php?title=EU imports of energy products - recent developments#Trend in extra EU imports of energy products](https://ec.europa.eu/eurostat/statistics-explained/index.php?title=EU_imports_of_energy_products_-_recent_developments#Trend_in_extra_EU_imports_of_energy_products)
- Eurostat. (2022c). HICP - monthly data (annual rate of change). https://ec.europa.eu/eurostat/databrowser/view/PRC_HICP_MANR_custom_3056089/default/table?lang=en
- Eurostat. (2022d). Imports of natural gas by partner country. https://ec.europa.eu/eurostat/databrowser/view/NRG_TI_GAS_custom_3001996/default/table?lang=en
- Eurostat. (2022e). Number of locomotives and railcars, by source of power, Ec.Europa.Eu. https://ec.europa.eu/eurostat/databrowser/view/RAIL_EQ_LOCON_custom_1974861/default/table?lang=en
- Eurostat. (2022e). Number of locomotives and railcars, by source of power, Ec.Europa.Eu. https://ec.europa.eu/eurostat/databrowser/view/RAIL_EQ_LOCON_custom_1974861/default/table?lang=en
- Eurostat. (2022f). Road freight transport by maximum permissible laden weight of vehicle, 2019 and 2020 (million tonne-kilometres).png - Statistics Explained, Ec.Europa.Eu. [https://ec.europa.eu/eurostat/statistics-explained/index.php?title=File:Road_freight_transport_by_maximum_permmissible_laden_weight_of_vehicle,_2019_and_2020_\(million_tonne-kilometres\).png](https://ec.europa.eu/eurostat/statistics-explained/index.php?title=File:Road_freight_transport_by_maximum_permmissible_laden_weight_of_vehicle,_2019_and_2020_(million_tonne-kilometres).png)
- Eurostat. (2022f). Road freight transport by maximum permissible laden weight of vehicle, 2019 and 2020 (million tonne-kilometres).png - Statistics Explained, Ec.Europa.Eu. [https://ec.europa.eu/eurostat/statistics-explained/index.php?title=File:Road_freight_transport_by_maximum_permmissible_laden_weight_of_vehicle,_2019_and_2020_\(million_tonne-kilometres\).png](https://ec.europa.eu/eurostat/statistics-explained/index.php?title=File:Road_freight_transport_by_maximum_permmissible_laden_weight_of_vehicle,_2019_and_2020_(million_tonne-kilometres).png)
- Faiella, I., & Lavecchia, L. (2021). Energy poverty. How can you fight it, if you can't measure it? Energy and Buildings, 233, 1–11.
- Fameli, K. M., Kotrikla, A. M., Psanis, C., Biskos, G., & Polydoropoulou, A. (2020). Estimation of the emissions by transport in two port cities of the northeastern Mediterranean, Greece. Environmental Pollution, 257, 113598.



- Fargione, J., Kiesecker, J., Slaats, M. J., & Olimb, S. (2012). Wind and wildlife in the Northern Great Plains: Identifying low-impact areas for wind development. *PLoS ONE*, 7(7).
- Feklyunina, V. (2012). Russia's international images and its energy policy. An unreliable supplier?. *Europe-Asia Studies*, 64(3), 449-469.
- Felix, G., Nápoles, G., Falcon, R., Froelich, W., Vanhoof, K., & Bello, R. (2019). A review on methods and software for fuzzy cognitive maps. *Artificial intelligence review*, 52(3), 1707-1737.
- Fisch-Romito, V., Guivarch, C., Creutzig, F., Minx, J. C., & Callaghan, M. W. (2021). Systematic map of the literature on carbon lock-in induced by long-lived capital. *Environmental Research Letters*, 16(5), Article 053004.
- Fons, S., Achari, G., & Ross, T. (2004). A fuzzy cognitive mapping analysis of the impacts of an eco-industrial park. *Journal of Intelligent & Fuzzy Systems*, 15(2), 75-88.
- Forouli, A., Nikas, A., Van de Ven, D. J., Sampedro, J., & Doukas, H. (2020). A multiple-uncertainty analysis framework for integrated assessment modelling of several sustainable development goals. *Environmental Modelling & Software*, 131, 104795.
- Fragkos, P., & Paroussos, L. (2018). Employment creation in EU related to renewables expansion. *Applied Energy*, 230(August), 935-945.
- Franciscis, D. D. (2014). JFCM: a java library for FuzzyCognitive maps. In *Fuzzy cognitive maps for applied sciences and engineering* (pp. 199-220). Springer, Berlin, Heidelberg.
- Froelich, W., Papageorgiou, E. I., Samarinas, M., & Skriapas, K. (2012). Application of evolutionary fuzzy cognitive maps to the long-term prediction of prostate cancer. *Applied Soft Computing*, 12(12), 3810-3817.
- Fujimori, S., Hasegawa, T., & Oshiro, K. (2020). An assessment of the potential of using carbon tax revenue to tackle poverty. *Environmental Research Letters*, 15(11), 114063.
- Gaeta, M., Businge, C. N., & Gelmini, A. (2022). Achieving net zero emissions in Italy by 2050: Challenges and opportunities. *Energies*, 15(1), 46.
- Galende-Sánchez, E., & Sorman, A. H. (2021). From consultation toward co-production in science and policy: A critical systematic review of participatory climate and energy initiatives. *Energy Research & Social Science*, 73, 101907.
- Gambhir, A., Butnar, I., Li, P. H., Smith, P., & Strachan, N. (2019). A review of criticisms of integrated assessment models and proposed approaches to address these, through the lens of BECCS. *Energies*, 12(9), 1747.
- García-Gusano, D., & Iribarren, D. (2018). Prospective energy security scenarios in Spain: The future role of renewable power generation technologies and climate change implications. *Renewable energy*, 126, 202-209.
- Gencer, D., & Akcura, E. (2022). Amid energy price shocks, five lessons to remember on energy subsidies. *World Bank Blogs, Sustainable Energy for All*. <https://blogs.worldbank.org/energy/amid-energy-price-shocks-five-lessons-remember-energy-subsidies>
- Georgopoulos, V. C., Malandraki, G. A., & Stylios, C. D. (2003). A fuzzy cognitive map approach to differential diagnosis of specific language impairment. *Artificial intelligence in Medicine*, 29(3), 261-278.
- Ghaderi, S. F., Azadeh, A., Nokhandan, B. P., & Fathi, E. (2012). Behavioral simulation and optimization of generation companies in electricity markets by fuzzy cognitive map. *Expert systems with applications*, 39(5), 4635-4646.



- Ghanadan, R., & Koomey, J. G. (2005). Using energy scenarios to explore alternative energy pathways in California. *Energy Policy*, 33(9), 1117-1142.
- Giarola, S., Mittal, S., Vielle, M., Perdana, S., Campagnolo, L., Delpiazzi, E., ... & van de Ven, D. J. (2021). Challenges in the harmonisation of global integrated assessment models: A comprehensive methodology to reduce model response heterogeneity. *Science of the Total Environment*, 783, 146861.
- Giuliano, G., Dessouky, M., Dexter, S., Fang, J., Hu, S., & Miller, M. (2021). Heavy-duty trucks: The challenge of getting to zero. *Transportation Research Part D: Transport and Environment*, 93, 102742.
- Gjorgievski, V. Z., Cundeva, S., & Georghiou, G. E. (2021). Social arrangements, technical designs and impacts of energy communities: A review. *Renewable Energy*, 169, 1138-1156.
- Grant, N. (2022). The Paris Agreement's ratcheting mechanism needs strengthening 4-fold to keep 1.5° C alive. *Joule*, 6(4), 703-708.
- Grant, N., Hawkes, A., Napp, T., & Gambhir, A. (2020). The appropriate use of reference scenarios in mitigation analysis. *Nature Climate Change*, 10(7), 605-610.
- Grant, N., Hawkes, A., Napp, T., & Gambhir, A. (2021). Cost reductions in renewables can substantially erode the value of carbon capture and storage in mitigation pathways. *One Earth*, 4(11), 1588-1601.
- Gratton, G., Guiso, L., Michelacci, C., & Morelli, M. (2021). From weber to kafka: Political instability and the overproduction of laws. *American Economic Review*, 111(9), 2964-3003.
- Gray, S. A., Gray, S., Cox, L. J., & Henly-Shepard, S. (2013). Mental modeler: a fuzzy-logic cognitive mapping modeling tool for adaptive environmental management. In 2013 46th Hawaii International Conference on System Sciences (pp. 965-973). IEEE.
- Gray, S. A., Zanre, E., & Gray, S. R. (2014b). Fuzzy cognitive maps as representations of mental models and group beliefs. In *Fuzzy cognitive maps for applied sciences and engineering* (pp. 29-48). Springer, Berlin, Heidelberg.
- Gray, S. R. J., Gagnon, A. S., Gray, S. A., O'Dwyer, B., O'Mahony, C., Muir, D., Devoy, R. J. N., Falaleeva, M., & Gault, J. (2014a). Are coastal managers detecting the problem? Assessing stakeholder perception of climate vulnerability using Fuzzy Cognitive Mapping. *Ocean and Coastal Management*, 94, 74-89.
- Groumpos, P. P., & Stylios, C. D. (2000). Modelling supervisory control systems using fuzzy cognitive maps. *Chaos, Solitons and Fractals*, 11(1), 329-336.
- Hainsch, K., Löffler, K., Burandt, T., Auer, H., del Granado, P. C., Piscicella, P., & Zwickl-Bernhard, S. (2022). Energy transition scenarios: What policies, societal attitudes, and technology developments will realize the EU Green Deal?. *Energy*, 239, 122067.
- Halkos, G. E., & Gkampoura, E. C. (2021). Evaluating the effect of economic crisis on energy poverty in Europe. *Renewable and Sustainable Energy Reviews*, 144, 110981.
- Hamilton, S. H., ElSawah, S., Guillaume, J. H., Jakeman, A. J., & Pierce, S. A. (2015). Integrated assessment and modelling: overview and synthesis of salient dimensions. *Environmental Modelling & Software*, 64, 215-229.
- Harmati, I. Á., & Kóczy, L. T. (2018). On the existence and uniqueness of fixed points of fuzzy set valued sigmoid fuzzy cognitive maps. In 2018 IEEE International Conference on Fuzzy Systems (FUZZ-IEEE) (pp. 1-7). IEEE.
- Harmati, I. Á., Hatwágner, M. F., & Kóczy, L. T. (2018). On the existence and uniqueness of fixed points of fuzzy



- cognitive maps. In International conference on information processing and management of uncertainty in knowledge-based systems (pp. 490-500). Springer, Cham.
- Harmati, I. Á., Hatwágner, M. F., & Kóczy, L. T. (2021). Global stability of fuzzy cognitive maps. *Neural Computing and Applications*, 1-13.
- Heaps, C.G., 2022. LEAP: The Low Emissions Analysis Platform. [Software version: 2020.1.76] Stockholm Environment Institute. Somerville, MA, USA. <https://leap.sei.org>
- HEDNO. (2022). Monthly Reports for RES and thermal generation in non-interconnected islands | HEDNO, HEDNO. <https://deddie.gr/el/themata-tou-diaxeiristi-mi-diasundedemenwn-nisiwn/agora-mdn/stoixeia-ekkathariseon-kai-minaion-deltion-mdn/miniaia-deltia-ape-thermikis-paragogis/> (in Greek)
- Hellenic Parliament. (2022). Law 4936/2022 – National Climate Law. https://www.hellenicparliament.gr/Nomothetiko-Ergo/Anazitisi-Nomothetikou-Ergou?law_id=0b7f36df-2e5b-4d4b-b5f3-ae9900a07542 (in Greek)
- Hellenic Republic Ministry of the Environment and Energy. (2019). National Energy and Climate Plan. https://ec.europa.eu/energy/sites/ener/files/el_final_necp_main_en.pdf. (in Greek)
- Hellenic Republic Ministry of the Environment and Energy. (2020). Long-term Strategy for the Climate. https://ypen.gov.gr/wp-content/uploads/2020/11/lts_gr_el.pdf. (in Greek)
- Hellenic Statistical Authority. (2012). Characteristics of dwellings-households - ELSTAT. <https://www.statistics.gr/en/residential-household> (in Greek)
- Hellenic Statistical Authority. (2013). SURVEY ON ENERGY CONSUMPTION IN HOUSEHOLDS. https://www.statistics.gr/en/statistics?p_p_id=documents_WAR_publicationsportlet_INSTANCE_qDQ8fBKKo4IN&p_p_lifecycle=2&p_p_state=normal&p_p_mode=view&p_p_cacheability=cacheLevelPage&p_p_col_id=column-2&p_p_col_count=4&p_p_col_pos=1&_documents_WAR_publicationsportlet_INSTANCE_qDQ8fBKKo4IN_javax.faces.resource=document&_documents_WAR_publicationsportlet_INSTANCE_qDQ8fBKKo4IN_in=downloadResources&_documents_WAR_publicationsportlet_INSTANCE_qDQ8fBKKo4IN_documentID=105418&_documents_WAR_publicationsportlet_INSTANCE_qDQ8fBKKo4IN_locale=en
- Hirth, L., Mühlenpfordt, J., & Bulkeley, M. (2018). The ENTSO-E Transparency Platform—A review of Europe’s most ambitious electricity data platform. *Applied energy*, 225, 1054-1067.
- Hirvonen, J., Jokisalo, J., Heljo, J., & Kosonen, R. (2019). Towards the EU emissions targets of 2050: Optimal energy renovation measures of Finnish apartment buildings. *International journal of sustainable energy*, 38(7), 649-672.
- Hobbs, B. F., Ludsin, S. A., Knight, R. L., Ryan, P. A., Biberhofer, J., & Ciborowski, J. J. (2002). Fuzzy cognitive mapping as a tool to define management objectives for complex ecosystems. *Ecological Applications*, 12(5), 1548-1565.
- Hofbauer, L., McDowall, W., & Pye, S. (2022). Challenges and opportunities for energy system modelling to foster multi-level governance of energy transitions. *Renewable and Sustainable Energy Reviews*, 161, 112330.
- Höhne, N., Lui, S., Skribbe, R., Moisiu, M., Hare, B., Ramalope, D., Ancygier, A., & Heck, S. (2022). Global reaction to energy crisis risks zero carbon transition. *Climate Action Tracker*. https://climateactiontracker.org/documents/1055/CAT_2022-06-08_Briefing_EnergyCrisisReaction.pdf
- Hohne, P. A., Kusakana, K., & Numbi, B. P. (2019). A review of water heating technologies: An application to the



South African context. *Energy Reports*, 5, 1-19.

- Howells, M., Rogner, H., Strachan, N., Heaps, C., Huntington, H., Kypreos, S., ... & Roehrl, A. (2011). OSeMOSYS: the open source energy modeling system: an introduction to its ethos, structure and development. *Energy Policy*, 39(10), 5850-5870.
- Hsieh, E., & Anderson, R. (2017). Grid flexibility: The quiet revolution. *Electricity Journal*, 30(2), 1-8.
- Hsueh, S. L. (2015). Assessing the effectiveness of community-promoted environmental protection policy by using a Delphi-fuzzy method: A case study on solar power and plain afforestation in Taiwan. *Renewable and Sustainable Energy Reviews*, 49, 1286-1295.
- Hu, G., Chen, C., Lu, H. T., Wu, Y., Liu, C., Tao, L., Men, Y., He, G., & Li, K. G. (2020). A Review of Technical Advances, Barriers, and Solutions in the Power to Hydrogen (P2H) Roadmap. *Engineering*, 6(12), 1364-1380.
- Huang, S. C., Lo, S. L., & Lin, Y. C. (2013). Application of a fuzzy cognitive map based on a structural equation model for the identification of limitations to the development of wind power. *Energy policy*, 63, 851-861.
- Huang, Y., Bor, Y. J., & Peng, C. Y. (2011). The long-term forecast of Taiwan's energy supply and demand: LEAP model application. *Energy policy*, 39(11), 6790-6803.
- Huff, A. S. (1990). *Mapping strategic thought*. John Wiley & Sons Inc.
- IEA. (2021). *World Energy Outlook 2021 – Analysis* - IEA, IEA. <https://www.iea.org/reports/world-energy-outlook-2021>
- IEA. (2022a). *Energy Statistics Data Browser – Data Tools* - IEA. <https://www.iea.org/data-and-statistics/data-tools/energy-statistics-data-browser?country=GREECE&energy=Balances&year=2019>
- IEA; IRENA; UNSD; World Bank; WHO. (2022). *Tracking SDG 7: The Energy Progress Report*. https://trackingsdg7.esmap.org/data/files/download-documents/sdg7-report2022-full_report.pdf
- IMF. (2022). *World Economic Outlook Update*. International Monetary Fund. <https://www.imf.org/en/Publications/WEO/Issues/2022/07/26/world-economic-outlook-update-july-2022>
- Inman, M., Aitken, G., & Zimmerman, S. (2021). *Europe Gas Tracker Report*. <https://globalenergymonitor.org/wp-content/uploads/2021/03/GEM-Europe-Gas-Tracker-Report-2021-Embargoed.pdf>
- Institute for Energy and Transport (JRC). (2014). *Energy Technology Reference Indicator (ETRI) projections for 2010-2050.*, Op.Europa.Eu. <https://op.europa.eu/en/publication-detail/-/publication/79a2ddb5ba1-4380-93af-2ce274a840f0/language-en>
- Ioannidis, R., & Koutsoyiannis, D. (2020). A review of land use, visibility and public perception of renewable energy in the context of landscape impact. *Applied Energy*, 276(March), 115367.
- IPCC. (2022). *Climate Change 2022: Mitigation of Climate Change. Contribution of Working Group III to the Sixth Assessment Report of the Intergovernmental Panel on Climate Change*. <https://doi.org/10.1017/9781009157926>
- IPTO. (2022). *Monthly Energy Reports | IPTO, Admie.Gr*. <https://www.admie.gr/agora/enimerotika-deltia/miniaia-deltia-energeias> (in Greek)
- IRENA. (2020a). *Electricity Storage Valuation Framework: Assessing system value and ensuring project viability*. International Renewable Energy Agency. <https://irena.org/publications/2020/Mar/Electricity-Storage-Valuation-Framework-2020>



- IRENA. (2020b). Renewable Power Generation Costs in 2020. <https://www.irena.org/publications/2021/Jun/Renewable-Power-Costs-in-2020>
- Janipour, Z., Swennenhuis, F., Gooyert, V. De, & Coninck, H. De. (2021). Understanding contrasting narratives on carbon dioxide capture and storage for Dutch industry using system dynamics. *International Journal of Greenhouse Gas Control*, 105(February 2020), 103235.
- Jewell, J., & Cherp, A. (2020). On the political feasibility of climate change mitigation pathways: is it too late to keep warming below 1.5° C?. *Wiley Interdisciplinary Reviews: Climate Change*, 11(1), e621.
- Kapros, S., Panou, K., & Proios, G. (2014). Fast Screening Method for the Assessment of Freight Demand at the Initial Planning Stage of a New Transport and Logistics Centers. *Logistics and Transport*, 23.
- Karavas, C. S., Kyriakarakos, G., Arvanitis, K. G., & Papadakis, G. (2015). A multi-agent decentralized energy management system based on distributed intelligence for the design and control of autonomous polygeneration microgrids. *Energy Conversion and Management*, 103, 166-179.
- Karimi, F., & Rodi, M. (2022). *Energy Transition in the Baltic Sea Region: Understanding Stakeholder Engagement and Community Acceptance* (1st ed.). Routledge.
- Karytsas, S., Polyzou, O., & Karytsas, C. (2019). Social aspects of geothermal energy in Greece. In *Geothermal Energy and Society* (pp. 123-144). Springer, Cham.
- Kati, V., Kassara, C., Vrontisi, Z., & Moustakas, A. (2021). The biodiversity-wind energy-land use nexus in a global biodiversity hotspot. *Science of The Total Environment*, 768, 144471.
- Kavadias, K. A., Alexopoulos, P., & Charis, G. (2019). Techno-economic evaluation of geothermal-solar power plant in Nisyros island in Greece. *Energy Procedia*, 159, 136-141.
- Kazmi, H., Munné-Collado, Í., Mehmood, F., Syed, T. A., & Driesen, J. (2021). Towards data-driven energy communities: A review of open-source datasets, models and tools. *Renewable and Sustainable Energy Reviews*, 148(May), 111290.
- Kemfert, C., Präger, F., Braunger, I., Hoffart, F. M., & Brauers, H. (2022). The expansion of natural gas infrastructure puts energy transitions at risk. *Nature Energy*, 7(July), 582–587.
- Keppo, I., Butnar, I., Bauer, N., Caspani, M., Edelenbosch, O., Emmerling, J., ... & Wagner, F. (2021). Exploring the possibility space: taking stock of the diverse capabilities and gaps in integrated assessment models. *Environmental Research Letters*, 16(5), 053006.
- King, L., van den Bergh, J., & Kallis, G. (2022). Transparency crucial to Paris climate scenarios. *Science*, 375(6583), 827-828.
- Knight, C. J., Lloyd, D. J., & Penn, A. S. (2014). Linear and sigmoidal fuzzy cognitive maps: an analysis of fixed points. *Applied Soft Computing*, 15, 193-202.
- Koasidis, K., Karamaneas, A., Kanellou, E., Neofytou, H., Nikas, A., & Doukas, H. (2022a). Towards Sustainable Development and Climate Co-governance: A Multicriteria Stakeholders' Perspective. In *Multiple Criteria Decision Making for Sustainable Development* (pp. 39-74). Springer, Cham.
- Koasidis, K., Nikas, A., Daniil, V., Kanellou, E., & Doukas, H. (2022b). A multi-criteria decision support framework for assessing seaport sustainability planning: The case of Piraeus. *Maritime Policy & Management*, 1-27.
- Kok, K. (2009). The potential of Fuzzy Cognitive Maps for semi-quantitative scenario development, with an example from Brazil. *Global environmental change*, 19(1), 122-133.



- Kokkinos, K., Karayannis, V., & Moustakas, K. (2020). Circular bio-economy via energy transition supported by Fuzzy Cognitive Map modeling towards sustainable low-carbon environment. *Science of the Total Environment*, 721, 137754.
- Kokkinos, K., Lakioti, E., Papageorgiou, E., Moustakas, K., & Karayannis, V. (2018). Fuzzy cognitive map-based modeling of social acceptance to overcome uncertainties in establishing waste biorefinery facilities. *Frontiers in Energy Research*, 6(OCT), 1–17.
- Kosko, B. (1986). Fuzzy cognitive maps. *International journal of man-machine studies*, 24(1), 65-75.
- Kottas, T. L., Boutalis, Y. S., & Christodoulou, M. A. (2010). Fuzzy cognitive networks: Adaptive network estimation and control paradigms. In *Fuzzy cognitive maps* (pp. 89-134). Springer, Berlin, Heidelberg.
- Koulouriotis, D. E. (2004). Investment analysis & decision making in markets using adaptive fuzzy causal relationships. *Operational Research*, 4(2), 213-233.
- Koulouriotis, D. E., Diakoulakis, I. E., & Emiris, D. M. (2001). A fuzzy cognitive map-based stock market model: synthesis, analysis and experimental results. In *10th IEEE International Conference on Fuzzy Systems*.(Cat. No. 01CH37297) (Vol. 1, pp. 465-468). IEEE.
- Koutsandreas, D., Spiliotis, E., Doukas, H., & Psarras, J. (2021). What is the macroeconomic impact of higher decarbonization speeds? The case of Greece. *Energies*, 14(8), 2235.
- Koutsandreas, D., Trachanas, G., Pappis, I., Nikas, A., Doukas, H., Psarras, J. (n.d.). A multicriteria modeling approach for evaluating power generation scenarios under uncertainty: The case of green hydrogen in Greece, *Energy Strategy Reviews*. under review.
- Koutsellis, T., Nikas, A., Koasidis, K., Xexakis, G., Petkidis, C., Karamaneas, A., & Doukas, H. (2022a). Normalising the Output of Fuzzy Cognitive Maps. 2nd International Workshop on Big Data Analytics in the Energy. Thirteenth International Conference on Information, Intelligence, Systems and Applications (IISA 2022), Corfu, Greece.
- Koutsellis, T., Xexakis, G., Koasidis, K., Nikas, A., & Doukas, H. (2022b). Parameter analysis for sigmoid and hyperbolic transfer functions of fuzzy cognitive maps. *Operational Research*, in press.
- Krey, V., Guo, F., Kolp, P., Zhou, W., Schaeffer, R., Awasthy, A., ... & van Vuuren, D. P. (2019). Looking under the hood: a comparison of techno-economic assumptions across national and global integrated assessment models. *Energy*, 172, 1254-1267.
- Krug, M., Rosaria, M., Nucci, D., Caldera, M., & Luca, E. De. (2022). Mainstreaming Community Energy: Is the Renewable Energy Directive a Driver for Renewable Energy Communities in Germany and Italy? *Sustainability*, 14(12), Article 7181.
- Kyriakarakos, G., Dounis, A. I., Arvanitis, K. G., & Papadakis, G. (2012). A fuzzy cognitive maps–petri nets energy management system for autonomous polygeneration microgrids. *Applied Soft Computing*, 12(12), 3785-3797.
- Lee IK, Kwon SH (2010) Design of sigmoid activation functions for fuzzy cognitive maps via Lyapunov stability analysis. *IEICE Trans Inf Syst* 93:2883–2886
- Leiren, M. D., Aakre, S., Linnerud, K., Julsrud, T. E., Di Nucci, M. R., & Krug, M. (2020). Community acceptance of wind energy developments: Experience from wind energy scarce regions in Europe. *Sustainability (Switzerland)*, 12(5), 18–20.
- Liu, Z. Q., & Satur, R. (1999). Contextual fuzzy cognitive map for decision support in geographic information



- systems. *IEEE Transactions on Fuzzy Systems*, 7(5), 495-507.
- LNG Prime. (2022). Italy plans new LNG import terminals. <https://lngprime.com/europe/italy-plans-new-lng-import-terminals/45283/>
- Lowitzsch, J., Hoicka, C. E., & van Tulder, F. J. (2020). Renewable energy communities under the 2019 European Clean Energy Package – Governance model for the energy clusters of the future? *Renewable and Sustainable Energy Reviews*, 122.
- Makhholm, J. D. (2022). The 2021–2022 European Natural Gas Disaster: Was Reagan Right and Thatcher Wrong?. *Climate and Energy*, 38(10), 1-9.
- Mapelli, C., Osto, G. D., Mombelli, D., Barella, S., & Gruttadauria, A. (2022). Future Scenarios for Reducing Emissions and Consumption in the Italian Steelmaking Industry. 2100631.
- Markaki, O., & Askounis, D. (2021). Assessing the operational and economic efficiency benefits of dynamic manufacturing networks through fuzzy cognitive maps: a case study. *Operational Research*, 21(2), 925-950.
- Martinopoulos, G., & Tsalikis, G. (2018). Diffusion and adoption of solar energy conversion systems–The case of Greece. *Energy*, 144, 800-807.
- McCollum, D. L., Zhou, W., Bertram, C., De Boer, H. S., Bosetti, V., Busch, S., ... & Riahi, K. (2018). Energy investment needs for fulfilling the Paris Agreement and achieving the Sustainable Development Goals. *Nature Energy*, 3(7), 589-599.
- McPherson, M., & Karney, B. (2014). Long-term scenario alternatives and their implications: LEAP model application of Panama' s electricity sector. *Energy Policy*, 68, 146-157.
- McWilliams, B., G. Sgaravatti, S. Tagliapietra and G. Zachmann. (2022). A grand bargain to steer through the European Union's energy crisis. Policy Contribution 14/2022, Bruegel
- Meinshausen, M., Lewis, J., McGlade, C., Gütschow, J., Nicholls, Z., Burdon, R., ... & Hackmann, B. (2022). Realization of Paris Agreement pledges may limit warming just below 2° C. *Nature*, 604(7905), 304-309.
- Mendoza, G. A., & Prabhu, R. (2006). Participatory modeling and analysis for sustainable forest management: Overview of soft system dynamics models and applications. *Forest Policy and Economics*, 9(2), 179-196.
- Mihailova, D., Schubert, I., Burger, P., & Fritz, M. M. C. (2022). Exploring modes of sustainable value co-creation in renewable energy communities. *Journal of Cleaner Production*, 330(Article 129917).
- Miniaci, R., Scarpa, C., & Valbonesi, P. (2014). Energy affordability and the benefits system in Italy. *Energy Policy*, 75, 289–300.
- Ministry for Ecological Transition. (2022). Law Decree 17/2022: Energy Decree. <https://www.gazzettaufficiale.it/eli/id/2022/05/17/22G00059/sg>
- Ministry of Economic Development, Ministry of the Environment and Protection of Natural Resources and the Sea, & Ministry of Infrastructure and Transport. (2019). Integrated National Energy and Climate Plan. https://ec.europa.eu/energy/sites/ener/files/documents/it_final_necp_main_en.pdf
- Ministry of Economic Development. (2019). Ministerial Decree of 4 July 2019 (MD FER 1). <https://www.gazzettaufficiale.it/eli/id/2019/08/09/19A05099/sg>
- Ministry of Environment and Energy. (2022). Biofuels -, Ypen.Gov.Gr. <https://ypen.gov.gr/energeia/prasines-metafores/viokafsima/> (in Greek)



- Mirjat, N. H., Uqaili, M. A., Harijan, K., Walasai, G. D., Mondal, M. A. H., & Sahin, H. (2018). Long-term electricity demand forecast and supply side scenarios for Pakistan (2015–2050): A LEAP model application for policy analysis. *Energy*, 165, 512-526.
- Mizell, L., & Allain-Dupré, D. (2013). *Creating Conditions for Effective Public Investment*.
- Mohr, S. (1997). *Software design for a fuzzy cognitive map modeling tool*. Tensselaer Polytechnic Institute.
- Moksnes et al., 2015 Moksnes, N., Welsch, M., Gardumi, F., Shivakumar, A., Broad, O., Howells, M., ... & Sridharan, V. (2015). 2015 OSeMOSYS User Manual. KTH Royal Institute of Technology. http://www.osemosys.org/uploads/1/8/5/0/18504136/osemosys_manual_-_working_with_text_files_-_2015-11-05.pdf
- Morone, P., Yilan, G., & Imbert, E. (2021). Using fuzzy cognitive maps to identify better policy strategies to valorize organic waste flows: An Italian case study. *Journal of Cleaner Production*, 319, 128722.
- Mourhir, A. (2021). Scoping review of the potentials of fuzzy cognitive maps as a modeling approach for integrated environmental assessment and management. *Environmental Modelling and Software*, 135, 104891.
- Mpelogianni, V., & Groumpos, P. P. (2019). Building energy management system modelling via state fuzzy cognitive maps and learning algorithms. *IFAC-PapersOnLine*, 52(25), 513-518.
- N. Frilingou et al., (n.d.) Navigating through an energy crisis: challenges and progress towards electricity decarbonisation, reliability, and affordability in Italy. *Energy Research & Social Science*. under review.
- Naftemporiki. (2022). K.Mitsotakis: Energy generation from lignite is increased, M.Naftemporiki.Gr. <https://m.naftemporiki.gr/story/1850990/k-mitsotakis-auksanetai-i-paragogi-energeias-apo-ligniti> (in Greek).
- Nápoles, G., Leon Espinosa, M., Grau, I., Vanhoof, K., & Bello, R. (2018). Fuzzy cognitive maps based models for pattern classification: Advances and challenges. *Soft Computing Based Optimization and Decision Models*, 83-98.
- Nápoles, G., Leon, M., Grau, I., & Vanhoof, K. (2017). Fuzzy cognitive maps tool for scenario analysis and pattern classification. In 2017 IEEE 29th International Conference on Tools with Artificial Intelligence (ICTAI) (pp. 644-651). IEEE.
- Nápoles, G., Papageorgiou, E., Bello, R., & Vanhoof, K. (2016). On the convergence of sigmoid fuzzy cognitive maps. *Information Sciences*, 349, 154-171.
- Nasirzadeh, F., Ghayoumian, M., Khanzadi, M., & Rostamnezhad Cherati, M. (2020). Modelling the social dimension of sustainable development using fuzzy cognitive maps. *International Journal of Construction Management*, 20(3), 223–236.
- Natarajan, R., Subramanian, J., & Papageorgiou, E. I. (2016). Hybrid learning of fuzzy cognitive maps for sugarcane yield classification. *Computers and Electronics in Agriculture*, 127, 147-157.
- Nature. (2022). Europe must not backslide on climate action despite war in Ukraine. 607(8). <https://doi.org/https://doi.org/10.1038/d41586-022-01820-x>
- Neil, S. G. O. (2020). Community obstacles to large scale solar: NIMBY and renewables. *Journal of Environmental Studies and Sciences*, 11, 85–91.
- Nguyen, P. H., & Fayek, A. R. (2022). Applications of fuzzy hybrid techniques in construction engineering and management research. *Automation in Construction*, 134, 104064.



- Nieves, J. A., Aristizábal, A. J., Dyner, I., Báez, O., & Ospina, D. H. (2019). Energy demand and greenhouse gas emissions analysis in Colombia: A LEAP model application. *Energy*, 169, 380-397.
- Nikas, A., & Doukas, H. (2016). Developing robust climate policies: a fuzzy cognitive map approach. In *Robustness analysis in decision aiding, optimization, and analytics* (pp. 239-263). Springer, Cham.
- Nikas, A., Doukas, H., & Papandreou, A. (2019a). A Detailed Overview and Consistent Classification of Climate-Economy Models. In *Understanding Risks and Uncertainties in Energy and Climate Policy*. Springer, Cham.
- Nikas, A., Doukas, H., Lieu, J., Tinoco, R. A., Charisopoulos, V., & Van Der Gaast, W. (2017). Managing stakeholder knowledge for the evaluation of innovation systems in the face of climate change. *Journal of Knowledge Management*.
- Nikas, A., Doukas, H., van der Gaast, W., & Szendrei, K. (2018). Expert views on low-carbon transition strategies for the Dutch solar sector: A delay-based fuzzy cognitive mapping approach. *IFAC-PapersOnLine*, 51(30), 715-720.
- Nikas, A., Elia, A., Boitier, B., Koasidis, K., Doukas, H., Casseti, G., Anger-Kraavi, A., Bui, H., Campagnolo, L., De Miglio, R., Delpiazzi, E., Fougeyrollas, A., Gambhir, A., Gargiulo, M., Giarola, S., Grant, N., Hawkes, A., Herbst, A., Köberle, A. C., ... Chiodi, A. (2021a). Where is the EU headed given its current climate policy? A stakeholder-driven model inter-comparison. *Science of the Total Environment*, 793, 148549.
- Nikas, A., Gambhir, A., Trutnevvyte, E., Koasidis, K., Lund, H., Thellufsen, J. Z., ... & Doukas, H. (2021b). Perspective of comprehensive and comprehensible multi-model energy and climate science in Europe. *Energy*, 215, 119153.
- Nikas, A., Lieu, J., Sorman, A., Gambhir, A., Turhan, E., Baptista, B. V., & Doukas, H. (2020a). The desirability of transitions in demand: Incorporating behavioural and societal transformations into energy modelling. *Energy Research and Social Science*, 70(August 2020), 101780.
- Nikas, A., Neofytou, H., Karamaneas, A., Koasidis, K., & Psarras, J. (2020b). Sustainable and socially just transition to a post-lignite era in Greece: A multi-level perspective. *Energy Sources, Part B: Economics, Planning, and Policy*, 15(10-12), 513-544.
- Nikas, A., Ntanos, E., & Doukas, H. (2019b). A semi-quantitative modelling application for assessing energy efficiency strategies. *Applied Soft Computing*, 76, 140-155.
- Nikas, A., Stavrakas, V., Arsenopoulos, A., Doukas, H., Antosiewicz, M., Witajewski-Baltvilks, J., & Flamos, A. (2020c). Barriers to and consequences of a solar-based energy transition in Greece. *Environmental Innovation and Societal Transitions*, 35, 383-399.
- Nikas, A., Xexakis, G., Koasidis, K., Acosta-Fernández, J., Arto, I., Calzadilla, A., ... & Doukas, H. (2022). Coupling circularity performance and climate action: From disciplinary silos to transdisciplinary modelling science. *Sustainable Production and Consumption*, 30, 269-277.
- Nikolaev, A., & Konidari, P. (2017). Development and assessment of renewable energy policy scenarios by 2030 for Bulgaria. *Renewable energy*, 111, 792-802.
- Nolden, C., Barnes, J., & Nicholls, J. (2020). Community energy business model evolution: A review of solar photovoltaic developments in England. *Renewable and Sustainable Energy Reviews*, 122(May 2019), 109722.
- Offshore Technology. (2022). Snam acquires \$350m floating LNG regasification terminal from Golar LNG. Retrieved 1 September 2022, from <https://www.offshore-technology.com/news/snam-floating-lng-golar>.



- Olazabal, M., & Pascual, U. (2016). Use of fuzzy cognitive maps to study urban resilience and transformation. *Environmental Innovation and Societal Transitions*, 18, 18-40.
- Olsson, J. M., & Gardumi, F. (2021). Modelling least cost electricity system scenarios for Bangladesh using OSeMOSYS. *Energy Strategy Reviews*, 38, 100705.
- OSY. (2022). The Fleet - OSY -OSY S.A. <https://www.osy.gr/%ce%b7-%ce%bf%cf%83%cf%85-%ce%b1%ce%b5/%cf%83%cf%84%cf%8c%ce%bb%ce%bf%cf%82/> (in Greek)
- Ou, Y., Iyer, G., Clarke, L., Edmonds, J., Fawcett, A. A., Hultman, N., ... & McJeon, H. (2021). Can updated climate pledges limit warming well below 2° C?. *Science*, 374(6568), 693-695.
- Oxford Analytica. (2022). High inflation will curb Baltic growth rates in 2022. *Emerald Expert Briefings*, (oxan-db).
- Özesmi, U., & Özesmi, S. L. (2004). Ecological models based on people's knowledge: a multi-step fuzzy cognitive mapping approach. *Ecological modelling*, 176(1-2), 43-64.
- Papachristou, M., Arvanitis, A., Mendrinou, D., Dalabakis, P., Karytsas, C., & Andritsos, N. (2019). Geothermal Energy Use, Country Update for Greece (2016-2019). *Transport*, 1, 1-68.
- Papada, L., Katsoulakos, N., Doulos, I., Kaliampakos, D., & Damigos, D. (2019). Analyzing energy poverty with Fuzzy Cognitive Maps: A step-forward towards a more holistic approach. *Energy Sources, Part B: Economics, Planning and Policy*, 14(5), 159-182.
- Papaefthymiou, G., Haesen, E., & Sach, T. (2018). Power System Flexibility Tracker: Indicators to track flexibility progress towards high-RES systems. *Renewable Energy*, 127, 1026-1035.
- Papageorgiou, E. I. (2010). A novel approach on constructed dynamic fuzzy cognitive maps using fuzzified decision trees and knowledge-extraction techniques. In *Fuzzy Cognitive Maps* (pp. 43-70). Springer, Berlin, Heidelberg.
- Papageorgiou, E. I., Aggelopoulou, K. D., Gemtos, T. A., & Nanos, G. D. (2013). Yield prediction in apples using Fuzzy Cognitive Map learning approach. *Computers and electronics in agriculture*, 91, 19-29.
- Papageorgiou, E. I., Hatwagner, M. F., Buruzs, A., & Kóczy, L. T. (2017). A concept reduction approach for fuzzy cognitive map models in decision making and management. *Neurocomputing*, 232, 16-33.
- Papageorgiou, E. I., Stylios, C. D., & Groumpos, P. P. (2004). Active Hebbian learning algorithm to train fuzzy cognitive maps. *International Journal of Approximate Reasoning*, 37(3), 219-249.
- Papaioannou, M., Neocleous, C., Sofokleous, A., Mateou, N., Andreou, A., & Schizas, C. N. (2010, October). A generic tool for building fuzzy cognitive map systems. In *IFIP International Conference on Artificial Intelligence Applications and Innovations* (pp. 45-52). Springer, Berlin, Heidelberg.
- Papakostas, G. A., Boutalis, Y. S., Koulouriotis, D. E., & Mertzios, B. G. (2008). Fuzzy cognitive maps for pattern recognition applications. *International Journal of Pattern Recognition and Artificial Intelligence*, 22(08), 1461-1486.
- Papakostas, G., Boutalis, Y., Koulouriotis, D., & Mertzios, B. (2006). A first study of pattern classification using fuzzy cognitive maps. In *International conference on systems, signals and image processing-INSSIP* (Vol. 6, pp. 369-374).
- Patiño-Cambeiro, F., Armesto, J., Bastos, G., Prieto-López, J. I., & Patiño-Barbeito, F. (2019). Economic appraisal of energy efficiency renovations in tertiary buildings. *Sustainable Cities and Society*, 47, 101503.
- Pedersen, T. T., Kyhl, E., Dvorak, A., Andresen, B., Victoria, M., Pedersen, T. T., Gøtske, E. K., Dvorak, A., & Andresen,



- G. B. (2022). Long-term implications of reduced gas imports on the decarbonization of the European energy system Long-term implications of reduced gas imports on the decarbonization of the European energy system. In *Joule* (Vol. 6, Issue 7). Elsevier Inc.
- Pellizzone, A., Allansdottir, A., De Franco, R., Muttoni, G., & Manzella, A. (2015). Exploring public engagement with geothermal energy in southern Italy: A case study. *Energy Policy*, 85(2015), 1–11.
- Peng, W., Iyer, G., Bosetti, V., Chaturvedi, V., Edmonds, J., Fawcett, A. A., ... & Weyant, J. (2021). Climate policy models need to get real about people—here’s how. *Nature*, 594, 174-176.
- Peng, Z., & Wu, L. (2017). A new perspective on formation of haze-fog: The fuzzy cognitive map and its approaches to data mining. *Sustainability*, 9(3), 352.
- Penn, A. S., Knight, C. J., Lloyd, D. J., Avitabile, D., Kok, K., Schiller, F., ... & Basson, L. (2013). Participatory development and analysis of a fuzzy cognitive map of the establishment of a bio-based economy in the Humber region. *PloS one*, 8(11), e78319.
- Peters, G. P., Andrew, R. M., Canadell, J. G., Fuss, S., Jackson, R. B., Korsbakken, J. I., ... & Nakicenovic, N. (2017). Key indicators to track current progress and future ambition of the Paris Agreement. *Nature Climate Change*, 7(2), 118-122.
- Pickl, M. J. (2019). The renewable energy strategies of oil majors—From oil to energy?. *Energy Strategy Reviews*, 26, 100370.
- Pierro, M., Perez, R., Perez, M., Prina, M. G., Moser, D., & Cornaro, C. (2021). Italian protocol for massive solar integration: From solar imbalance regulation to firm 24/365 solar generation. *Renewable Energy*, 169.
- Poblete-Cazenave, M., Pachauri, S., Byers, E., Mastrucci, A., & van Ruijven, B. (2021). Global scenarios of household access to modern energy services under climate mitigation policy. *Nature Energy*, 6(8), 824-833.
- Poczeta, K., Kubuś, Ł., Yastrebov, A., & Papageorgiou, E. I. (2018a). Temperature forecasting for energy saving in smart buildings based on fuzzy cognitive map. In *Conference on Automation* (pp. 93-103). Springer, Cham.
- Poczeta, K., Papageorgiou, E. I., & Yastrebov, A. (2018b). Application of fuzzy cognitive maps to multi-step ahead prediction of electricity consumption. In *2018 Conference on Electrotechnology: Processes, Models, Control and Computer Science (EPMCCS)* (pp. 1-5). IEEE.
- Poczeta, K., Yastrebov, A., & Papageorgiou, E. I. (2015). Learning fuzzy cognitive maps using structure optimization genetic algorithm. In *2015 federated conference on computer science and information systems (FedCSIS)* (pp. 547-554). IEEE.
- Politis, I., Georgiadis, G., Papadopoulos, E., Fyrogenis, I., Nikolaidou, A., Kopsacheilis, A., ... & Verani, E. (2021). COVID-19 lockdown measures and travel behavior: The case of Thessaloniki, Greece. *Transportation research interdisciplinary perspectives*, 10, 100345.
- Polzin, F., Sanders, M., Steffen, B., Egli, F., Schmidt, T. S., Karkatsoulis, P., Fragkos, P., & Paroussos, L. (2021). The effect of differentiating costs of capital by country and technology on the European energy transition. *Climatic Change*, 167(1–2), 1–21.
- Prontera, A. (2021). The dismantling of renewable energy policy in Italy. *Environmental Politics*, 30(7), 1196–1216.
- Prussi, M., & Lonza, L. (2018). Passenger aviation and high speed rail: a comparison of emissions profiles on selected European routes. *Journal of Advanced Transportation*, 2018.
- Prussi, M., Scarlat, N., Acciaro, M., & Kosmas, V. (2021). Potential and limiting factors in the use of alternative fuels



- in the European maritime sector. *Journal of cleaner production*, 291, 125849.
- Puerto, E., Aguilar, J., López, C., & Chávez, D. (2019). Using multilayer fuzzy cognitive maps to diagnose autism spectrum disorder. *Applied soft computing*, 75, 58-71.
- Rady, Y. Y., Rocco, M. V., Serag-Eldin, M. A., & Colombo, E. (2018). Modelling for power generation sector in Developing Countries: Case of Egypt. *Energy*, 165, 198-209.
- RAE. (2022) Average Day-Ahead Market Prices (Year-to-Date). <https://www.rae.gr/map-graph/>.
- Raoufi, M., & Fayek, A. R. (2020). Fuzzy Monte Carlo agent-based simulation of construction crew performance. *Journal of Construction Engineering and Management*, 146(5), 04020041.
- Reckien, D. (2014). Weather extremes and street life in India—Implications of Fuzzy Cognitive Mapping as a new tool for semi-quantitative impact assessment and ranking of adaptation measures. *Global Environmental Change*, 26, 1-13.
- Reis, I. F., Gonçalves, I., Lopes, M. A., & Antunes, C. H. (2021). Business models for energy communities: A review of key issues and trends. *Renewable and Sustainable Energy Reviews*, 144, 111013.
- Reis, L. A., Drouet, L., & Tavoni, M. (2022). Internalising health-economic impacts of air pollution into climate policy: a global modelling study. *The Lancet Planetary Health*, 6(1), e40-e48.
- Ren, Z., Verma, A. S., Li, Y., Teuwen, J. J., & Jiang, Z. (2021). Offshore wind turbine operations and maintenance: A state-of-the-art review. *Renewable and Sustainable Energy Reviews*, 144, 110886.
- Reuters. (2022a). Goldman sees strong case for higher oil prices despite negative shocks. <https://www.reuters.com/markets/commodities/goldman-sees-strong-case-higher-oil-prices-despite-negative-shocks-2022-08-08/#:~:text=The%20investment%20bank%20forecast%20U.S.,%244.40%20and%20%245.25%20in%202023>
- Reuters. (2022b). Greece will keep coal-fired plants running for longer amid gas crisis. <https://www.reuters.com/business/energy/greece-will-keep-coal-fired-plants-running-longer-amid-gas-crisis-2022-09-05/>.
- Rezaee, M. J., Yousefi, S., & Hayati, J. (2019). Root barriers management in development of renewable energy resources in Iran: An interpretative structural modeling approach. *Energy Policy*, 129, 292-306.
- Ritchie, H., Roser, M., & Rosado, P. (2020). Italy: Energy Country Profile. <https://ourworldindata.org/energy/country/italy>
- Robertson, S. (2021). Transparency, trust, and integrated assessment models: An ethical consideration for the Intergovernmental Panel on Climate Change. *Wiley Interdisciplinary Reviews: Climate Change*, 12(1), e679.
- Rodrigues, R., Pietzcker, R., Fragkos, P., Price, J., McDowall, W., Siskos, P., ... & Capros, P. (2022). Narrative-driven alternative roads to achieve mid-century CO2 net neutrality in Europe. *Energy*, 239, 121908.
- Rogan, F., Cahill, C. J., Daly, H. E., Dineen, D., Deane, J. P., Heaps, C., ... & Ó Gallachóir, B. P. (2014). LEAPs and bounds—an energy demand and constraint optimised model of the Irish energy system. *Energy Efficiency*, 7(3), 441-466.
- Roinioti, A., Koroneos, C., & Wangensteen, I. (2012). Modeling the Greek energy system: Scenarios of clean energy use and their implications. *Energy Policy*, 50, 711-722.
- Rosenow, J., & Eyre, N. (2022). Reinventing energy efficiency for net zero. *Energy Research and Social Science*,



90(March), 102602.

- Sacchelli, S., & Fabbrizzi, S. (2015). Minimisation of uncertainty in decision-making processes using optimised probabilistic Fuzzy Cognitive Maps: A case study for a rural sector. *Socio-Economic Planning Sciences*, 52, 31-40.
- Sareen, S. (2021). Digitalisation and social inclusion in multi-scalar smart energy transitions. *Energy Research and Social Science*, 81, 102251.
- Sarrica, M., Biddau, F., Brondi, S., Cottone, P., & Mazzara, B. M. (2018). A multi-scale examination of public discourse on energy sustainability in Italy: Empirical evidence and policy implications. *Energy Policy*, 114(June 2017), 444–454.
- Satur, R., & Liu, Z. Q. (1999a). A contextual fuzzy cognitive map framework for geographic information systems. *IEEE transactions on fuzzy systems*, 7(5), 481-494.
- Satur, R., & Liu, Z. Q. (1999b). Contextual fuzzy cognitive maps for geographic information systems. In *FUZZ-IEEE'99. 1999 IEEE International Fuzzy Systems. Conference Proceedings (Cat. No. 99CH36315) (Vol. 2, pp. 1165-1169)*. IEEE.
- Serbia-energy.eu. (2022). Greece, Revised NECP envisages storage capacity at 3 GW by 2030. <https://serbia-energy.eu/greece-revised-necp-envisages-storage-capacity-at-3-gw-by-2030/>.
- Sgaravatti, G., Tagliapietra, S., & Zachmann, G. (2021). National policies to shield consumers from rising energy prices. *Bruegel Datasets*. <https://www.bruegel.org/publications/datasets/national-policies-to-shield-consumers-from-rising-energy-prices/>
- Sgaravatti, G., Tagliapietra, S., & Zachmann, G. (2022). National policies to shield consumers from rising energy prices. *Bruegel*. <https://www.bruegel.org/dataset/national-policies-shield-consumers-rising-energy-price>
- Shin, H. C., Park, J. W., Kim, H. S., & Shin, E. S. (2005). Environmental and economic assessment of landfill gas electricity generation in Korea using LEAP model. *Energy policy*, 33(10), 1261-1270.
- Shyu, C. W. (2021). A framework for 'right to energy' to meet UN SDG7: Policy implications to meet basic human energy needs, eradicate energy poverty, enhance energy justice, and uphold energy democracy. *Energy Research and Social Science*, 79(June), 102199.
- Siksnyte-Butkiene, I. (2022). Combating Energy Poverty in the Face of the COVID-19 Pandemic and the Global Economic Uncertainty. *Energies*, 15(10), 3649.
- Silva, P. C. (1995). Fuzzy cognitive maps over possible worlds. In *Proceedings of 1995 IEEE International Conference on Fuzzy Systems. (Vol. 2, pp. 555-560)*. IEEE.
- Soergel, B., Kriegler, E., Bodirsky, B. L., Bauer, N., Leimbach, M., & Popp, A. (2021a). Combining ambitious climate policies with efforts to eradicate poverty. *Nature communications*, 12(1), 1-12.
- Soergel, B., Kriegler, E., Weindl, I., Rauner, S., Dirnaichner, A., Ruhe, C., Hofmann, M., Bauer, N., Bertram, C., Bodirsky, B. L., Leimbach, M., Leininger, J., Levesque, A., Luderer, G., Pehl, M., Wingens, C., Baumstark, L., Beier, F., Dietrich, J. P., ... Popp, A. (2021b). A sustainable development pathway for climate action within the UN 2030 Agenda. *Nature Climate Change*, 11(8), 656–664.
- Sognaes, I., Gambhir, A., van de Ven, D. J., Nikas, A., Anger-Kraavi, A., Bui, H., Campagnolo, L., Delpiazzi, E., Doukas, H., Giarola, S., Grant, N., Hawkes, A., Köberle, A. C., Kolpakov, A., Mittal, S., Moreno, J., Perdana, S., Rogelj, J., Vielle, M., & Peters, G. P. (2021). A multi-model analysis of long-term emissions and warming implications of current mitigation efforts. *Nature Climate Change*, 11(12), 1055–1062.



- Soler, L. S., Kok, K., Camara, G., & Veldkamp, A. (2012). Using fuzzy cognitive maps to describe current system dynamics and develop land cover scenarios: a case study in the Brazilian Amazon. *Journal of Land Use Science*, 7(2), 149-175.
- Song, L., Lieu, J., Nikas, A., Arsenopoulos, A., Vasileiou, G., & Doukas, H. (2020). Contested energy futures, conflicted rewards? Examining low-carbon transition risks and governance dynamics in China's built environment. *Energy Research and Social Science*, 59(September 2019), 101306.
- Sorrell, S. (2015). Reducing energy demand: A review of issues, challenges and approaches. *Renewable and Sustainable Energy Reviews*, 47, 74–82.
- Sovacool, B. K., Hess, D. J., Cantoni, R., Lee, D., Brisbois, M. C., Walnum, H. J., ... & Goel, S. (2022). Conflicted transitions: Exploring the actors, tactics, and outcomes of social opposition against energy infrastructure. *Global environmental change*, 73, 102473.
- Spandagos, C., Tovar Reaños, M. A., & Lynch, M. (2022). Public acceptance of sustainable energy innovations in the European Union: A multidimensional comparative framework for national policy. *Journal of Cleaner Production*, 340, Article 130721.
- Spyropoulos, G. C., Nastos, P. T., Moustiris, K. P., & Chalvatzis, K. J. (2022). Transportation and air quality perspectives and projections in a mediterranean country, the case of Greece. *Land*, 11(2), 152.
- Stach, W., Kurgan, L. A., & Pedrycz, W. (2008). Numerical and linguistic prediction of time series with the use of fuzzy cognitive maps. *IEEE transactions on fuzzy systems*, 16(1), 61-72.
- Stoddard, I., Anderson, K., Capstick, S., Carton, W., Depledge, J., Facer, K., ... & Williams, M. (2021). Three decades of climate mitigation: why haven't we bent the global emissions curve?. *Annual Review of Environment and Resources*, 46(1), 653-689.
- Stylios, C. D., & Groumpos, P. P. (2004). Modeling complex systems using fuzzy cognitive maps. *IEEE Transactions on Systems, Man, and Cybernetics-Part A: Systems and Humans*, 34(1), 155-162.
- Susskind, L., Chun, J., Gant, A., Hodgkins, C., Cohen, J., & Lohmar, S. (2022). Sources of opposition to renewable energy projects in the United States. *Energy Policy*, 165, 112922.
- Thimet, P. J., & Mavromatidis, G. (2022). Review of model-based electricity system transition scenarios: An analysis for Switzerland, Germany, France, and Italy. *Renewable and Sustainable Energy Reviews*, 159, Article 112102.
- Trachanas, G. P., Mantzaris, N., Marinakis, V., & Doukas, H. (2022). Multi-criteria evaluation of power generation alternatives towards lignite phase-out: the case of Ptolemaida V1. https://www.researchgate.net/profile/Georgios-Trachanas-2/publication/358043507_Multi-criteria_evaluation_of_power_generation_alternatives_towards_lignite_phase-out_the_case_of_Ptolemaida_V/links/61edb77edafcdb25fd476c2c/Multi-criteria-evaluation-of-power-generation-alternatives-towards-lignite-phase-out-the-case-of-Ptolemaida-V.pdf
- Tradingeconomics.com. (2022). Commodities - Live Quote Price Trading Data. <https://tradingeconomics.com/commodities>
- Trutnevyte, E., Hirt, L. F., Bauer, N., Cherp, A., Hawkes, A., Edelenbosch, O. Y., ... & van Vuuren, D. P. (2019). Societal transformations in models for energy and climate policy: the ambitious next step. *One Earth*, 1(4), 423-433.
- Tsadiras, A. K. (2008). Comparing the inference capabilities of binary, trivalent and sigmoid fuzzy cognitive maps.



- Information Sciences, 178(20), 3880-3894.
- Tsadiras, A. K., & Kouskouvelis, I. (2005). Using fuzzy cognitive maps as a decision support system for political decisions: The case of Turkey's integration into the European Union. In Panhellenic Conference on Informatics (pp. 371-381). Springer, Berlin, Heidelberg.
- Tsadiras, A., Pempetzoglou, M., & Viktoratos, I. (2021). Making predictions of global warming impacts using a semantic web tool that simulates fuzzy cognitive maps. *Computational Economics*, 58(3), 715-745.
- UN. (2015). Sustainable Development Goal 7. <https://sdgs.un.org/goals/goal7>
- Unruh, G. C., & Carrillo-Hermosilla, J. (2006). Globalizing carbon lock-in. *Energy Policy*, 34(10), 1185–1197.
- Uribe, J. M., Mosquera-López, S., & Arenas, O. J. (2022). Assessing the relationship between electricity and natural gas prices in European markets in times of distress. *Energy Policy*, 166, 113018.
- Vagliasindi, M. (2012). The role of policy driven incentives to attract PPPs in renewable-based energy in developing countries: a cross-country analysis. Policy Research Working Paper; No. WPS 6120. <http://documents.worldbank.org/curated/en/2012/07/16481342/role-policy-driven-incentives-attract-ppps-renewable-based-energy-developing-countries-cross-country-analysis>
- Van de Ven, D. J., Sampedro, J., Johnson, F. X., Bailis, R., Forouli, A., Nikas, A., ... & Doukas, H. (2019). Integrated policy assessment and optimisation over multiple sustainable development goals in Eastern Africa. *Environmental Research Letters*, 14(9), 094001.
- van Soest, H. L., van Vuuren, D. P., Hilaire, J., Minx, J. C., Harmsen, M. J. H. M., Krey, V., Popp, A., Riahi, K., & Luderer, G. (2019). Analysing interactions among Sustainable Development Goals with Integrated Assessment Models. *Global Transitions*, 1, 210–225.
- van Vliet, M., Kok, K., & Veldkamp, T. (2010). Linking stakeholders and modellers in scenario studies: The use of Fuzzy Cognitive Maps as a communication and learning tool. *Futures*, 42(1), 1-14.
- van Vliet, O., Hanger-Kopp, S., Nikas, A., Spijker, E., Carlsen, H., Doukas, H., & Lieu, J. (2020). The importance of stakeholders in scoping risk assessments—Lessons from low-carbon transitions. *Environmental Innovation and Societal Transitions*, 35(September 2018), 400–413.
- Van Voorn, G. A. K., Verburg, R. W., Kunseler, E. M., Vader, J., & Janssen, P. H. (2016). A checklist for model credibility, salience, and legitimacy to improve information transfer in environmental policy assessments. *Environmental Modelling & Software*, 83, 224-236.
- van Vuuren, D. P., Zimm, C., Busch, S., Kriegler, E., Leininger, J., Messner, D., ... & Soergel, B. (2022). Defining a sustainable development target space for 2030 and 2050. *One Earth*.
- Vandyck, T., Keramidas, K., Kitous, A., Spadaro, J. V., Van Dingenen, R., Holland, M., & Saveyn, B. (2018). Air quality co-benefits for human health and agriculture counterbalance costs to meet Paris Agreement pledges. *Nature communications*, 9(1), 1-11.
- Villavicencio Calzadilla, P., & Mauger, R. (2018). The UN's new sustainable development agenda and renewable energy: the challenge to reach SDG7 while achieving energy justice. *Journal of Energy and Natural Resources Law*, 36(2), 233–254.
- Voinov, A., Kolagani, N., McCall, M. K., Glynn, P. D., Kragt, M. E., Ostermann, F. O., ... & Ramu, P. (2016). Modelling with stakeholders—next generation. *Environmental Modelling & Software*, 77, 196-220.
- Von Stechow, C., Minx, J. C., Riahi, K., Jewell, J., McCollum, D. L., Callaghan, M. W., Bertram, C., Luderer, G., &



- Baiocchi, G. (2016). 2°C and SDGs: United they stand, divided they fall? *Environmental Research Letters*, 11(3).
- Wagner, O., & Götz, T. (2021). Presentation of the 5ds in energy policy: A policy paper to show how germany can regain its role as a pioneer in energy policy. *Energies*, 14(20).
- Wang, Z. (2018). Heat pumps with district heating for the UK's domestic heating: Individual versus district level. *Energy Procedia*, 149, 354-362.
- Wilson, C., Pettifor, H., Cassar, E., Kerr, L., & Wilson, M. (2019). The potential contribution of disruptive low-carbon innovations to 1.5 °C climate mitigation. *Energy Efficiency*, 12(2), 423-440.
- worlddata.info. (2022). Average height and weight by country. <https://www.worlddata.info/average-bodyheight.php>
- WWF. (2017). Long Term energy plan for the Greek Energy System. Contentarchive.Wwf.Gr. https://www.contentarchive.wwf.gr/images/pdfs/Long_Term_Energy_Plan4Greece.pdf (in Greek)
- WWF. (2022). Greek climate law: One small step, while giant leaps are needed towards climate neutrality. <https://www.wwf.gr/en/news/?uNewsID=6718391>.
- www.georgeyannis.gr. (2002). Four ministries scuttle bus lanes. <https://www.georgeyannis.gr/%CF%84%CE%AD%CF%83%CF%83%CE%B5%CF%81%CE%B1-%CF%85%CF%80%CE%BF%CF%85%CF%81%CE%B3%CE%B5%CE%AF%CE%B1-%CF%84%CE%BF%CF%81%CF%80%CE%B9%CE%BB%CE%AF%CE%B6%CE%BF%CF%85%CE%BD-%CF%84%CE%B9%CF%82-%CE%BB%CE%B5/> (in Greek)
- Xirogiannis, G., Stefanou, J., & Glykas, M. (2004). A fuzzy cognitive map approach to support urban design. *Expert Systems with Applications*, 26(2), 257-268.
- Yenneti, K., Day, R., & Golubchikov, O. (2016). Spatial justice and the land politics of renewables: Dispossessing vulnerable communities through solar energy mega-projects. *Geoforum*, 76, 90-99.
- Zakeri, B., Paulavets, K., Barreto-Gomez, L., Echeverri, L. G., Pachauri, S., Boza-Kiss, B., ... & Pouya, S. (2022). Pandemic, War, and Global Energy Transitions. *Energies*, 15(17), 6114.
- Zervas, E., Vatikiotis, L., Gareiou, Z., Manika, S., & Herrero-Martin, R. (2021). Assessment of the Greek National Plan of Energy and Climate Change—Critical remarks. *Sustainability*, 13(23), 13143.
- Zhang, W. R., Chen, S. S., & Bezdek, J. C. (1989). Pool2: A generic system for cognitive map development and decision analysis. *IEEE Transactions on Systems, Man, and Cybernetics*, 19(1), 31-39.
- Zhang, W. R., Chen, S. S., Wang, W., & King, R. S. (1992). A cognitive-map-based approach to the coordination of distributed cooperative agents. *IEEE Transactions on systems, man, and cybernetics*, 22(1), 103-114.
- IEA. (2022b) World Energy Outlook 2022 – Data product – IEA. <https://www.iea.org/data-and-statistics/data-product/world-energy-outlook-2022>
- Craiger, P., & Covert, M. D. (1994, June). Modeling dynamic social and psychological processes with fuzzy cognitive maps. In *Proceedings of 1994 IEEE 3rd International Fuzzy Systems Conference* (pp. 1873-1877). IEEE.
- Margaritis, M., Stylios, C., & Groumos, P. (2002, October). Fuzzy cognitive map software. In *10th international conference on software, telecommunications and computer networks SoftCom* (Vol. 2002, pp. 8-11).
- Boutalis, Y., Kottas, T., & Christodoulou, M. (2008, December). On the existence and uniqueness of solutions for



the concept values in fuzzy cognitive maps. In 2008 47th IEEE conference on decision and control (pp. 98-104). IEEE.

ACEA. (2021). Vehicles in use Europe January 2021, Acea.Auto. <https://www.acea.auto/files/report-vehicles-in-use-europe-january-2021-1.pdf>

IPTO. (2022a). Monthly Energy Report December 2021. Admie.gr. 2022, from https://www.admie.gr/sites/default/files/attached-files/type-file/2022/02/Energy_Report_202112_v2.pdf. (in Greek)

Hellenic Statistics Authority. (2022). Vehicle fleet / January 2020, Statistics.Gr. <https://www.statistics.gr/en/statistics/-/publication/SME18/-> (in Greek)

Peters, G. P. (2016). The “best available science” to inform 1.5 °C policy choices. *Nature Clim Change*, 6, 646–649.



